NOVEL pH-SENSITIVE HYDROGELS FROM HYDROXYETHYLACRYL CHITOSAN/SODIUM ALGINATE FOR SITE-SPECIFIC DRUG DELIVERY

PITCHAYA TREENATE

A THESIS SUBMITTED IN PARTIAL FULFILLMENT OF THE REQUIREMENT FOR
THE DEGREE OF DOCTOR OF PHILOSOPHY IN APPLIED CHEMISTRY
DEPARTMENT OF CHEMISTRY
FACULTY OF SCIENCE
KING MONGKUT'S INSTITUTE OF TECHNOLOGY LADKRABANG
2017

KMITL-2017-SC-D-010-013

Faculty of Science
King Mongkut's Institute of Technology Ladkrabang
Thesis Certification

Thesis Title	"NOVEL pH-SENSITIVE HYDROGELS FROM HYDROXYETHYLACRYL CHITOSAN/SODIUM ALGINATE FOR SITE-SPECIFIC DRUG DELIVERY"
Student Name	Miss Pitchaya Treenate
Student ID	52650301
Degree	Doctor of Philosophy (Applied Chemistry)
Department	Chemistry
Thesis Advisor	Asst.Prof.Dr. Pathavuth Monvisade
Thesis Co-advisor	-

Thesis Committee	Signatures
Assoc.Prof.Dr. Ittipol Jangchud Chairperson	
Asst.Prof.Dr. Chonlada Ritvirulh Examiner	
Asst.Prof.Dr. Suparat Rukchonlatee Examiner	
Assoc.Prof.Dr. Taweechai Amornsakchai External Examiner	
Asst.Prof.Dr. Pathavuth Monvisade Thesis Advisor	

Examination Date 13th June 2017 **Time** 09.00-12.00 a.m.
Place Faculty of Science room 305

Approved by Faculty of Science

(Assoc.Prof.Dr. Dusanee Thanaboripat)
Dean
Date 14 July 2017

หัวข้อวิทยานิพนธ์	ไฮโดรเจลชนิดใหม่ที่ว่องไวต่อพีเอชจากไฮดรอกซีเอทิลอะคริลไคโตซาน/โซเดียมอัลจิเนต สำหรับการนำส่งยาเฉพาะที่
ชื่อนักศึกษา	นางสาวพิชญา ตรีเนตร
รหัสประจำตัว	52650301
ปริญญา	ปรัชญาดุษฎีบัณฑิต (เคมีประยุกต์)
ภาควิชา	เคมี
พ.ศ.	2560
อาจารย์ที่ปรึกษาวิทยานิพนธ์	ผศ. ดร.ภัทธาวุธ มนต์วิเศษ

บทคัดย่อ

งานวิจัยนี้มุ่งพัฒนาไฮโดรเจลที่ว่องไวต่อพีเอชโดยเตรียมจากไฮดรอกซีเอทิลอะคริลไคโตซาน (Hydroxyethylacryl chitosan, HC) และโซเดียมอัลจิเนต (Sodium alginate, SA) เชื่อมโยงด้วยไอออนของโลหะชนิดต่าง ๆ ได้แก่ แคลเซียมไอออน (Ca^{2+}), ซิงค์ไอออน (Zn^{2+}) และคอปเปอร์ (II) ไอออน (Cu^{2+}) โดยเริ่มจากการเตรียม HC ด้วยปฏิกิริยาการเติมแบบไมเคิล (Michael addition reaction) ระหว่างไคโตซานและไฮดรอกซีเอทิลอะคริเลต HC ที่สังเคราะห์ได้นำไปเตรียมเป็นฟิล์มร่วมกับ SA โดยวิธีหล่อด้วยตัวทำละลาย โดยปรับเปลี่ยนอัตราส่วนของ HC:SA ที่ใช้เป็น 100:0, 75:25, 50:50, 25:75 และ 0:100 โดยน้ำหนัก จากผลการทดสอบโดย DMA และ FT-IR พบว่า HC และ SA มีความเข้ากันได้ในทุกอัตราส่วนผสม จากนั้นแช่ฟิล์มที่เตรียมได้ในสารละลายไอออนของโลหะชนิดต่าง ๆ ได้แก่ สารละลายแคลเซียมคลอไรด์ความเข้มข้น 0.01, 0.05, 0.1, 0.25 และ 0.5 M สารละลายซิงค์ซัลเฟตความเข้มข้น 0.5 M และ สารละลายคอปเปอร์ (II) ซัลเฟตความเข้มข้น 0.5 M เพื่อเตรียมเป็นฟิล์มไฮโดรเจลสูตรเชื่อมโยง จากนั้นนำฟิล์มไฮโดรเจลที่เตรียมได้ไปตรวจพิสูจน์เอกลักษณ์ด้วยเทคนิค FT-IR และ SEM-EDS ผลของ FT-IR แสดงให้เห็นว่าแคลเซียมไอออนสามารถเชื่อมโยงเฉพาะ SA ด้วยพันธะไอออนิก ในขณะที่ซิงค์ไอออนและคอปเปอร์ (II) ไอออนสามารถเชื่อมโยงได้ทั้ง HC ด้วยพันธะโคออร์ดิเนตและ SA ด้วยพันธะไอออนิกและ/หรือพันธะโคออร์ดิเนต นอกจากนี้พบว่ารูปแบบการกระจายตัวของไอออนของโลหะในฟิล์มไฮโดรเจลมีการกระจายตัวดี จากนั้นทดสอบพฤติกรรมการบวมตัวและปริมาณเจลของฟิล์มไฮโดรเจลที่อุณหภูมิ 37 องศาเซลเซียส ในของเหลวชนิดต่าง ๆ ได้แก่ น้ำกลั่น, สารละลายจำลองของเหลวในกระเพาะอาหาร (Simulated gastric fluid, SGF, pH 1.2), สารละลายจำลองของเหลวในลำไส้เล็ก (Simulated intestinal fluid, SIF, pH 7.4) และสารละลายจำลองของเหลวในระบบทางเดินอาหาร (Simulated gastrointestinal fluid, SGF ตามด้วย SIF) เพื่อวิเคราะห์ปัจจัยในการเตรียมที่มีผลต่อสมบัติของฟิล์มไฮโดรเจล พบว่าฟิล์มไฮโดรเจลที่เตรียมได้มีสมบัติว่องไวต่อพีเอชต่างกัน โดยฟิล์มไฮโดรเจลระหว่าง HC และ SA มีเสถียรภาพในสารละลาย SGF แต่สลายตัวได้ในสารละลาย SIF การผสมกันระหว่าง HC และ SA ทำให้อัตราการสลายตัวของฟิล์มไฮโดรเจลในสารละลายจำลองของเหลวในระบบทางเดินอาหารลดลง เนื่องจากการเกิดสารประกอบเชิงซ้อนพอลิอิเล็กโทรไลต์ระหว่าง HC และ SA ขณะย้ายฟิล์มไฮโดรเจลจาก SGF ไป SIF นอกจากนี้พบว่าฟิล์มไฮโดรเจลที่มีการเชื่อมโยงด้วยแคลเซียมไอออนมีปริมาณเจลในสารละลายจำลองของเหลวในระบบทางเดินอาหาร

มากกว่าฟิล์มไฮโดรเจลที่มีการเชื่อมโยงด้วยซิงค์ไอออนหรือคอปเปอร์ (II) ไอออน เนื่องจากการเกิดสารประกอบเชิงซ้อนระหว่าง HC กับซิงค์ไอออนหรือคอปเปอร์ (II) ไอออนขัดขวางการเกิดสารประกอบเชิงซ้อนพอลิอิเล็กโทรไลต์ระหว่าง HC และ SA การศึกษาพฤติกรรมการปลดปล่อยยาในสภาวะจำลองระบบทางเดินอาหารทำโดยใช้พาราเซตามอลเป็นยาต้นแบบ โดยวิเคราะห์ปริมาณพาราเซตามอลที่ถูกปลดปล่อยออกมาจากถุงที่ถูกปิดผนึกที่ทำจากฟิล์มไฮโดรเจลระหว่าง HC และ SA ด้วยเทคนิค UV-Vis พบว่าอัตราในการปลดปล่อยพาราเซตามอลจากไฮโดรเจลระหว่าง HC และ SA ทุกสูตรในสารละลาย SGF มีค่าต่ำ โดยมีค่าน้อยกว่า 20 เปอร์เซ็นต์ พฤติกรรมการปลดปล่อยแบบระเบิดออก (Burst release) ของพาราเซตามอลลดลงได้โดยการเพิ่มปริมาณ HC และ/หรือการเชื่อมโยง สูตร HC75SA25 มีพฤติกรรมการปลดปล่อยยาแบบเชิงเส้นตรงและพาราเซตามอลเกือบทั้งหมดเกิดการปลดปล่อยในสารละลาย SIF ผลการศึกษาแสดงให้เห็นว่าสูตร HC75SA25 เป็นตัวเลือกที่ดีสำหรับใช้ในการปลดปล่อยยาในลำไส้เล็ก สูตร HC50SA50 ที่มีการเชื่อมโยงด้วยแคลเซียมไอออนความเข้มข้น 0.5 M มีการปลดปล่อยยาในสารละลายจำลองของเหลวในระบบทางเดินอาหารต่ำ โดยมีค่าน้อยกว่า 20 เปอร์เซ็นต์ แสดงถึงศักยภาพในการใช้เป็นตัวนำส่งยาเฉพาะที่ที่ลำไส้ใหญ่ นอกจากนี้ได้เตรียมแคปซูลไฮโดรเจลระหว่าง HC และ SA โดยกระบวนการจุ่ม โดยใช้คาร์ราจีแนนและกลีเซอรอลเป็นสารที่ทำให้เกิดเจลและพลาสติไซเซอร์ตามลำดับ จากการศึกษาพฤติกรรมการปลดปล่อยยาจากแคปซูล พบว่าแคปซูลสูตร HC50SA50 ที่มีการเชื่อมโยงด้วยแคลเซียมไอออนความเข้มข้น 0.5 M มีพฤติกรรมการปลดปล่อยยาแบบเชิงเส้นตรงและพาราเซตามอลทั้งหมดเกิดการปลดปล่อยในสารละลาย SIF ผลการศึกษาแสดงให้เห็นถึงศักยภาพในการใช้ควบคุมการปลดปล่อยยาในลำไส้เล็ก

คำสำคัญ : การปลดปล่อยยา ความว่องไวต่อพีเอช โซเดียมอัลจิเนต ไฮดรอกซีเอทิลอะไครลิไคโตซาน ไฮโดรเจล

Thesis Title	Novel pH-sensitive hydrogels from hydroxyethylacryl chitosan/sodium alginate for site-specific drug delivery
Student Name	Miss Pitchaya Treenate
Student ID	52650301
Degree	Doctor of Philosophy (Applied Chemistry)
Department	Chemistry
Year	2017
Thesis Advisor	Asst. Prof. Dr. Pathavuth Monvisade

Abstract

This thesis aims to develop pH-sensitive hydrogels from hydroxyethylacryl chitosan (HC)/sodium alginate (SA) crosslinked by various metal ions (i.e., Ca^{2+}, Zn^{2+} and Cu^{2+}). HC was synthesized by the Michael addition reaction of chitosan (CS) and hydroxyethylacrylate (HEA). The synthesized HC was blended with SA to form film by solvent casting method. The weight ratios of HC to SA were varied at 100:0, 75:25, 50:50, 25:75 and 0:100. It was found that HC and SA were compatible for all blend compositions examined by DMA and FT-IR. The prepared films were subsequently soaked into various metal ion solutions, i.e., 0.01, 0.05, 0.1, 0.25 and 0.5 M of calcium chloride, 0.5 M of zinc sulfate and 0.5 M of copper(II) sulfate solutions, to form crosslinked hydrogel films. The obtained hydrogel films were then characterized by FT-IR and SEM-EDS. FT-IR results demonstrated that calcium ions could crosslink only SA through the formation of ionic bonds while zinc and copper ions could crosslink both HC through the formation of coordinate bonds and SA through the formation of partially ionic and/or coordinate bonds. In addition, it was found that the distribution patterns of metal ions were well-dispersed within the hydrogel films. Swelling behavior and gel content of the hydrogel films at 37 °C in various fluids, i.e., distilled water, simulated gastric fluid (SGF, pH 1.2), simulated intestinal fluid (SIF, pH 7.4) and simulated gastrointestinal fluid (SGF followed by SIF), were also evaluated in order to investigate the effects of preparation parameters on the properties of the hydrogel films. It was found that the prepared hydrogel films possessed pH-sensitive properties. The HC/SA hydrogel films were stable in SGF but degraded in SIF. In addition, the combination between HC and SA could delay the degradation rate of the hydrogel films in simulated gastrointestinal fluid due to the formation of polyelectrolyte complexes between HC and SA during the transfer of the hydrogel film from SGF to SIF. Additionally, the calcium crosslinked film showed higher gel content in simulated gastrointestinal fluid than that of zinc or copper

crosslinked film because the complexation of HC by zinc or copper ions impeded the formation of polyelectrolyte complexes between HC and SA. Furthermore, *in vitro* drug release profiles in simulated gastrointestinal tract were investigated using paracetamol as a model drug. The amount of released paracetamol from the sealed bag formed by HC/SA hydrogel films was determined by UV-Vis. In SGF, the release rate of paracetamol from all HC/SA hydrogel formulations was relatively low (< 20%). The burst release of paracetamol in SIF was depressed by increasing HC content and/or applying crosslink. The HC75SA25 formulation demonstrated the linearity of drug release profile and most of paracetamol was released from the hydrogel in SIF. It was suggested that the HC75SA25 formulation could be a good candidate to be used for controlling drug release in the small intestine. Interestingly, the 0.5 M calcium crosslinked HC50SA50 formulation exhibited the relatively low drug release in simulated gastrointestinal fluid (< 20%). It was suggested that this formulation could be a potential candidate for a site-specific drug delivery in the colon. Moreover, the HC/SA hydrogel capsules were also prepared by dipping process using carrageenan and glycerol as gelling agent and plasticizer, respectively. *In vitro* drug release profiles from the capsules were carried out. It was found that the 0.5 M calcium crosslinked HC50SA50 capsule showed the linearity of drug release profile and paracetamol was completely released in SIF. The results suggested its potential in controlled drug release in small intestine.

Keywords : Drug release, pH-sensitivity, Sodium alginate, Hydroxyethylacryl chitosan, Hydrogel

ACKNOWLEDGEMENTS

The author would like to take this opportunity to express deep gratitude to her advisor, Asst. Prof. Dr. Pathavuth Monvisade, for valuable guidance, attention and encouragement throughout this thesis. The grateful thanks also go to the thesis committees, Assoc. Prof. Dr. Ittipol Jangchud, Asst. Prof. Dr. Chonlada Ritvirulh, Asst. Prof. Dr. Suparat Rukchonlatee and Assoc. Prof. Dr. Taweechai Amornsakchai, for reading and criticizing the manuscript.

The author would like to express her very great appreciation to Prof. Dr. Masayuki Yamaguchi for his suggestions while doing research at Japan Advanced Institute of Science and Technology (JAIST) in Japan.

The author greatly appreciates the entire professors who provided invaluable knowledge while studying in the Department of Chemistry, Faculty of Science, King Mongkut's Institute of Technology Ladkrabang.

Special thanks go to Scientific Instruments Service Center at Faculty of Science at King Mongkut's Institute of Technology Ladkrabang, Scientific and Technological Research Equipment Centre at Chulalongkorn University and National Metal and Materials Technology Center (MTEC) for helping in analysis with special instruments. In addition, the thanks also go to Faculty of Science, King Mongkut's Institute of Technology Ladkrabang and School of Materials Science, Japan Advanced Institute of Science and Technology for laboratory instruments and instrument analysis.

The author deeply appreciates the Royal Golden Jubilee Ph.D. Program, Thailand Research Fund (RGJ 11) for financial support.

The author also would like to give the special thanks to all of her friends who have been helping and encouraging her while studying the Ph.D. program.

Last but not least, the author would like to express her appreciation to her beloved family for love, care and encouragement, which enabled her to complete this thesis.

Pitchaya Treenate

Contents

Contents (cont.)

Contents (cont.)

Contents (cont.)

List of Tables

List of Tables (cont.)

List of Tables (cont.)

List of Figures

List of Figures (cont.)

List of Figures (cont.)

List of Figures (cont.)

List of Figures (cont.)

Abbreviations

CS	Chitosan
HEA	Hydroxyethylacrylate
HC	Hydroxyethylacryl chitosan
SA	Sodium alginate
DSC	Differential scanning calorimeter
NMR	Nuclear magnetic resonance spectrometer
GPC	Gel permeation chromatograph
FT-IR	Fourier transform infrared spectrophotometer
SEM-EDS	Scanning electron microscope-energy dispersive X-ray spectrometer
XRD	X-ray diffractometer
DMA	Dynamic mechanical analyzer
UV-Vis	UV-Vis spectrophotometer
GI tract	Gastrointestinal tract
SGF	Simulated gastric fluid
SIF	Simulated intestinal fluid
MIC	Minimal inhibitory concentration
E. coli	*Escherichia coli*
S. aureus	*Staphylococcus aureus*
DD	Deacetylation degree
DS	Degree of substitution
M_w	Weight average molecular weight
Mw_{unit}	Average molecular weight per repeating unit
T_g	Glass transition temperature
E′	Dynamic storage modulus
E″	Dynamic loss modulus
tan δ	Damping
ESD	Equilibrium swelling degree
W_e	Equilibrium water content
W_f	Freezing water content
W_{nf}	Non-freezing bound water content
Semi-IPN	Semi-interpenetrating polymer network

Chapter 1
Introduction

1.1 Research motivation

Drug delivery system is defined as a device that enables the introduction of a therapeutic agent in the body and improves its effectiveness and safety by controlling the rate, time and place of release of drugs in the body [1]. Oral administration of drugs has been the most convenient and comfortable route for delivery of most therapeutic agents. It provides patients less pain, greater convenience and reduced risk of cross-infection. In recent years, pH-sensitive hydrogels have been attracted attentions for the design of controlled oral drug delivery systems [2]. This is because the fact that the pH range of fluids in various segments of the gastrointestinal (GI) tract can provide environmental stimuli for responsive drug release (Fig. 1.1) [3]. The pH-sensitive hydrogel can be prepared from a variety of synthetic and natural polymers [4-5]. Compared to synthetic polymers, natural polymers offer a range of advantages. Natural polymers are usually biocompatible, on the contrary, synthetic polymers often induce local inflammation and toxicity from trace chemicals. Among various kinds of the natural polymers, one which can attract our interest is chitosan (CS).

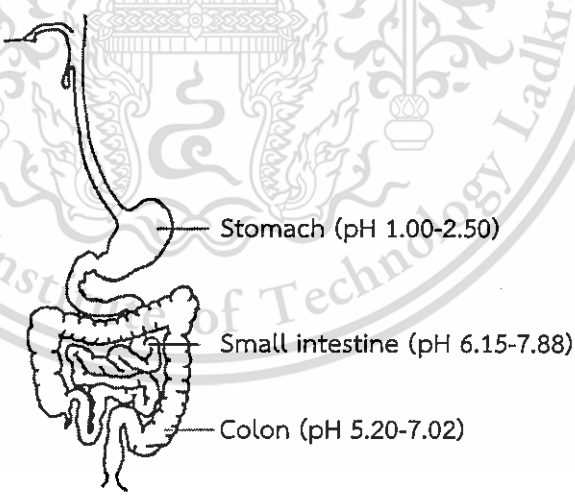

Figure 1.1 Schematic illustration of GI tract. Adapted from Ref. [3].

CS is a cationic natural polymers obtained from the deacetylation of chitin, the second most abundant natural polymer. CS is a copolymer consisting of *N*-acetyl-*D*-glucosamine and *D*-glucosamine units. CS shows excellent biological properties such as biocompatibility, non-toxicity and biodegradability [6-7]. In addition, CS exhibits pH-sensitive behavior which easily dissolves at low pH while

being insoluble at high pH [8]. Regarding to those reasons, CS has been widely used for controlled release [9-10]. However, acetic acid or other acids applied to dissolution of CS in water can cause cytotoxic to the final product [11]. To overcome this problem, CS was modified by introducing hydrophilic groups to its reactive amino groups. Many CS derivatives have been prepared, among the others; hydroxyethylacryl chitosan (HC) was interesting. HC is easily prepared by the Michael addition reaction of CS and hydroxyethylacrylate. It was reported that HC is able to dissolve in distilled water and to enzymatic degradation [12]. However, the applications of CS or CS derivatives in oral drug delivery are restricted because they are easily dissolved at low pH leading to the rapid drug release in gastric environment [13].

Sodium alginate (SA) is a non-toxic biodegradable anionic natural polymer, extracted from brown seaweed. SA consists of different proportions of β-*D*-mannuronic acid (M) and α-*L*-guluronic acid (G) units. It has been used for controlled drug release because it easily forms into three-dimensional networks in the presence of multivalent metal cations, e.g., Ca^{2+}, Zn^{2+}, Cu^{2+}, etc. [14-16]. Furthermore, it has pH-sensitive property; negative charges allow the SA to shrink in acidic pH but to swell when it is in neutral or basic pH [17]. It was reported that hydrogels based on SA show the slow drug release in gastric environment [18-19]. However, the use of SA alone for oral drug delivery leads to burst release of drug in intestinal environment [20-21].

The various hydrogels based on the combination of CS derivative and SA have been developed for controlled release of drug such as carboxymethyl chitosan/SA [22-24], methoxy poly(ethylene glycol) grafted carboxymethyl chitosan/SA [25], *N*-α-glutaric acid chitosan /SA [26] and *N*-trimethyl chitosan/SA [27]. However, there was no previous report about the combination of HC and SA in drug delivery field. Moreover, the prepared hydrogels in all of above examples exhibited relatively high drug release in an intestinal environment. Therefore, it was interesting to find an alternative drug delivery system with better prolonging drug release to colon environment.

In this work, the hydrogel based on the combination between HC and SA was prepared to make a new drug delivery material which incorporates the retarding drug release property of HC at high pH and of SA at low pH. Additionally, it was expected that HC could form polyelectrolyte complexation with SA in simulated gastrointestinal fluid like CS which would extend drug release ability [28].

The various kinds of crosslinkers, i.e., Ca^{2+}, Zn^{2+} and Cu^{2+}, would be applied to improve properties of the HC/SA hydrogels. In case of calcium crosslinking system, it was expected that the new type of hydrogels could be developed *via*

semi-IPN technique (crosslinked only SA part). In case of zinc and copper crosslinking systems, it was expected that zinc and copper ions could crosslink both HC and SA unlike calcium ion. The drug release profiles from the HC/SA hydrogels in simulated gastrointestinal fluid were explored using paracetamol as a soluble model drug. Paracetamol was selected as a soluble model drug (class 1) according to the biopharmaceutics drug classification [29].

Furthermore, pH-sensitive HC/SA hydrogel capsule was prepared using carrageenan and glycerol as gelling agent and plasticizer, respectively. The drug release profiles from the capsules were also evaluated.

1.2 Objectives of the study

1. To prepare the novel pH-sensitive hydrogel films and capsules composed of HC and SA for site-specific oral drug delivery.

2. To have a better understanding the crosslink structures of the pH-sensitive HC/SA hydrogels crosslinked by different types of metal ions (Ca^{2+}, Zn^{2+} and Cu^{2+} ions).

3. To investigate effects of preparation parameters on swelling behavior, gel content and *in vitro* drug release profile of the pH-sensitive HC/SA hydrogel films.

4. To investigate effects of preparation parameters on *in vitro* drug release profile of the pH-sensitive HC/SA hydrogel capsules.

1.3 Scopes of the study

1. The HCs were synthesized using various conditions as follows:

- Reaction temperature, i.e., 60, 80 and 90 °C.
- Reaction time, i.e., 24 and 48 h.

2. The HCs were characterized by GPC, FT-IR, ^{1}H-NMR and XRD, and were tested solubility and antibacterial activity in order to find suitable HC.

3. The HC/SA films were prepared using various weight ratios of HC:SA, i.e., 100:0, 75:25, 50:50, 25:75 and 0:100.

4. Characterization of the HC/SA films by DMA and FT-IR techniques was carried out in order to estimate miscibility of the HC/SA blends.

5. The HC/SA hydrogel films were prepared by soaking the prepared HC/SA films into crosslinking metal ion solutions as follows:

- 0.01, 0.05, 0.1, 0.25 and 0.5 M of calcium chloride solutions
- 0.5 M of zinc sulfate solution
- 0.5 M of copper(II) sulfate solution

6. Characterization of the HC/SA hydrogel films by various techniques, i.e., FT-IR, SEM-EDS, swelling behavior and gel content in water, were performed in order to determine crosslink structure of the hydrogel.

7. Swelling behavior and gel content in various fluids, i.e., simulated gastric fluid (SGF), simulated intestinal fluid (SIF) and SGF followed by SIF and *in vitro* drug release profile of the hydrogel films were evaluated in order to find suitable drug carriers for different parts of the body.

8. The HC/SA (1:1 weight ratio) and SA hydrogel capsules were prepared by dipping process using carrageenan and glycerol as gelling agent and plasticizer, respectively.

9. *In vitro* drug release profile of the HC/SA hydrogel capsules was investigated.

1.4 Benefits of the study

1. Obtain new types of pH-sensitive hydrogel films and capsules from HC and SA with varying drug release profiles for site-specific drug delivery in different parts of the body.

2. Understand the crosslink structures of the pH-sensitive HC/SA hydrogels crosslinked by different types of metal ions (Ca^{2+}, Zn^{2+} and Cu^{2+} ions).

3. Understand the relationship between preparation parameters and properties of the pH-sensitive HC/SA hydrogels.

Chapter 2
Theory and Literature Reviews

2.1 Drug delivery systems [30]

Drug delivery systems can be defined as devices that enable the introduction of a therapeutic substance in the body [1]. The major advantages in developing drug delivery systems are described in Fig. 2.1, which illustrates change in drug concentration levels in the blood plasma following a single dose of a therapeutic agent. As shown in Fig. 2.1, the drug concentration levels in the blood plasma rapidly rises and then exponentially decays as the drug is excreted and/or metabolized. The figure also shows concentrations above which the drug produces undesirable side effects and below which it is not therapeutically effective. The difference between these two levels is known as the therapeutic index. Using a single dose, the time during which the drug concentration is above the minimum effective level can only be extended by increasing the size of the dose. However, drug concentration levels in the blood plasma might extend into the toxic level. For this reason, developing drug delivery systems that can maintain a desired drug concentration levels in the blood plasma for long periods without reaching a toxic level or dropping below the minimum effective level is important. In addition, drug delivery systems can be used to achieve protection of drugs having a very short half-life, solution of the drug stability problem, elimination of side-effects and reduction in the frequency of the drug admiration [31]. Drug delivery systems can be classified according to the mechanism controlling the drug release as shown in Table 2.1.

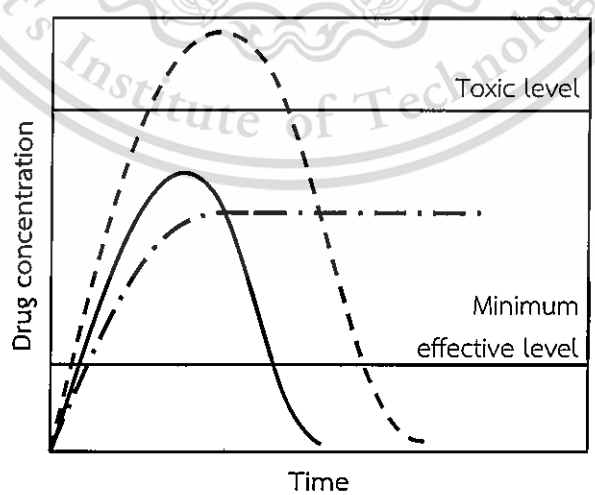

Figure 2.1 Drug concentration levels in the blood plasma as a function of time. (——) safe dose, (- - - -) unsafe dose and (—·—) controlled release [32].

Table 2.1 Classification of controlled release systems [30].

Type of system	Rate controlled mechanism
Diffusion controlled	
- Monolithic devices	- Diffusion through bulk polymer
- Reservoir devices	- Diffusion through membrane
Water penetration controlled	
- Swelling systems	- Water penetration into glassy polymer
- Osmotic systems	- Osmotic transport of water through semipermeable membrane
Chemically controlled	
- Bioerodible systems	- Either pure polymer erosion (surface erosion) or combination of erosion and diffusion (bulk erosion)
- Pendant chain systems	- Combination of hydrolysis of pendant group and diffusion from bulk polymer
Regulated systems	
- Magnetic or ultrasound	- External application of magnetic field or ultrasound to device
- Chemical	- Use of competitive desorption or enzyme substrate reaction

2.2 Hydrogels

According to the Polymer Science Dictionary, hydrogels can be defined as "an insoluble slightly crosslinked polymer which is highly swollen by water of solvation" [33]. Peppas defined hydrogels to be "hydrogels are water-swollen, crosslinked polymeric structures produced by the simple reaction of one of more monomers or by association bonds such as hydrogen bonds and strong Van der Waals interactions between chains" [30]. Another definition of hydrogel recommended by Hoffman is "hydrogels are hydrophilic polymer networks which may absorb from 10-20% (an arbitrary lower limit) up to thousands of times their dry weight in water" [24]. Hydrogel can be defined in many different ways. From above definition, it can be concluded that hydrogels are any hydrophilic polymer that are able to absorb water. On the other hand, they are insoluble in water because of the

presence of a three-dimensional network structure. Hydrogels have received considerable attention in the last few decades, owing to their exceptional promise in wide range of applications.

2.2.1 Classification of hydrogels

There are various methods of classifying hydrogels. Generally, they are grouped into six categories as detailed below:

- Classification based on the method of crosslink formation [35]

Hydrogels can be divided into two categories based on the chemical or physical crosslinks. Chemical crosslinked networks have permanent junctions, while physical networks have temporary junctions that occur from either polymer chain entanglements or physical interactions such as ionic interactions, hydrogen bonds, or hydrophobic interactions. Generally, hydrogels formed by chemical bonding are called irreversible hydrogels because they cannot be dissolved again. While, physical hydrogels can be reversed by changes in temperature, composition of solvent and pH, therefore, they are called reversible hydrogels. It will be discussed in detail in section 2.2.2.

- Classification based on polymer that forms hydrogel [36]

Hydrogels can be classified into natural, synthetic and semi-synthetic according to their origin. Most of synthetic hydrogels are synthesized by traditional polymerization of vinyl-activated monomers. The synthetic hydrogels are widely used because they have precise chemical structure and can be designed at molecular level. However, many of the synthetic hydrogels are not biodegradable and often induce local inflammation and toxicity from trace chemicals. The natural hydrogels based on natural polymers can be obtained from different natural sources. For instance, collagen is derived from mammals whereas chitin and chitosan are obtained from the exoskeleton of shellfish. Generally, natural polymers show inherent biocompatibility, biodegradability and biological moieties that support cellular activities. However, they usually do not provide sufficient mechanical properties and may contain pathogens or evoke immune/inflammatory responses. Table 2.2 shows some examples of different types of polymer used in the preparation of hydrogels.

Table 2.2 Examples of different types of polymers used in the preparation of hydrogels.

Polymer category	Examples	Reference
Synthetic polymer	Poly(vinyl alcohol) poly(*N*-isopropyl acrylamide) poly(ethylene glycol)	[37] [38] [39]
Natural polymer	Chitosan Alginate Cellulose	[40] [41] [42]
Semi-synthetic polymer	Poly(vinyl alcohol)/alginate Poly(2-hydroxyethyl methylacrylate)/dextrin Polyester/alginate	[43] [44] [45]

- Classification based on electric charge [46]

Hydrogels are also classified as non-ionic and ionic (anionic, cationic and ampholytic), as shown in Fig. 2.2. Non-ionic hydrogels, such as dextran and agarose, swell in aqueous medium due to water-polymer interaction. In case of hydrogel based on ionic polymers the swelling is dependent on the pH of aqueous medium. Cationic hydrogels, such as chitosan, show superior swelling at acidic media since the pendant groups of cationic hydrogels are ionized at low pH, and non-ionized at neutral and higher pH values. On the contrary, anionic hydrogels, such as alginate and xanthan gum, display superior swelling in neutral to basic media. The pendant groups of anionic hydrogels are non-ionized at low pH and ionized at pH above the pK_a of the polymeric network. Ampholytic hydrogels, such as gelatin and carboxymethyl chitosan, possess both positive and negative charges. Ampholytic hydrogels exist as cationic hydrogels at low pH values and as anionic hydrogels at high pH values. At intermediate pH-values, they display a point where the ratio of positive to negative charge is the unity, called the isoelectric point (IP). The IP is identified as a minimum of chain expansion in solution.

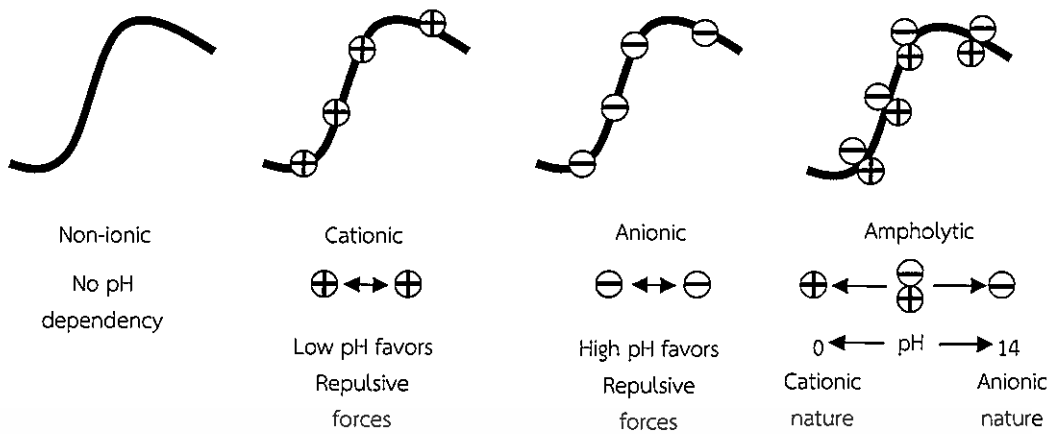

Figure 2.2 Classification based on electric charge [46].

- Classification based on response to external effect

Hydrogels can stimuli sensitive as to shrink or expand by changing in external environment. This class is called smart hydrogel. The physical stimuli include temperature, electric or magnetic field, light, pressure and sound, while the chemical stimuli include pH, solvent composition, ionic strength and molecular species (Fig. 2.3).

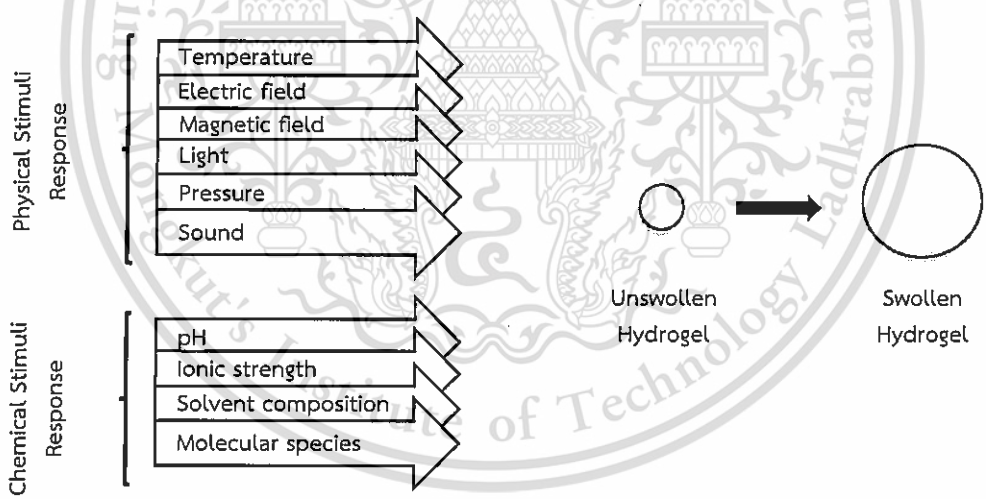

Figure 2.3 Stimuli response swelling hydrogel [47].

For example, poly(*N*-isopropyl acrylamide) hydrogel, a temperature sensitive hydrogel, has a reversible hydrophilic/hydrophobic phase transition at the lower critical solution temperature (LCST) of approximately 32 °C, where the polymer chain undergoes a transition from a swollen (hydrophilic state) to a collapsed (hydrophobic state) [38]. Another example, the UV light sensitive hydrogel was synthesized by introducing bis(4-dimethylamino) phenylmethyl leucocyanide into the polymer network. This hydrogel swells in response to UV light but shrinks when the UV light

is removed. The swelling is due to an increase in osmotic pressure within the hydrogel owing to the appearance of cyanide ions formed by UV light [48]. Other examples of stimuli responsive hydrogels are shown in Table 2.3.

Table 2.3 Examples of stimuli responsive hydrogels.

Stimuli	Hydrogel	Reference
Temperature	- Poly(*N*-isopropyl acrylamide)/carboxymethyl chitosan - Kappa-carrageenan - poly(ethylene glycol) grafted chitosan	[49] [50] [51]
pH	- *N*-succinyl chitosan grafted polyacrylamide - Sodium alginate grafted polyglycidyl methacrylate	[52] [53]
Electric field	- Kappa-carrageenan/carboxymethyl chitosan/ nano-Fe_3O_4 - Poly(vinyl alcohol)/hydroxyapatite/Fe_2O_3	[54] [55]
Light	- β-cyclodextrin-grafted alginate/diazobenzene-modified poly(ethylene glycol)	[56]

- Classification based on the hydrogel durability [57]

Hydrogels can be classified into durable and biodegradable depending on their stability in physiological environment. Recently, biodegradable hydrogels have been applied as carriers for controlled delivery or as tissue engineering. In drug delivery systems, degradation rate of hydrogel can be used to determine drug availability and pharmacokinetic effects on surrounding cells and tissues. For tissue engineering applications, it is usually desirable to have biodegradable scaffolding to promote cell infiltration and tissue growth. It is commonly believed that the degradation rates of tissue scaffold must be matched to the rate of various cellular processes in order to optimize tissue regeneration.

- Classification based on physical appearance

Hydrogels have many different physical appearances, including films [41], fibers [58], microparticles [59], nanoparticles [60], scaffolds [61], and liquids [62]. Physical appearances of hydrogels depend on the technique of polymerization involved in the preparation process.

2.2.2 Hydrogel preparation

2.2.2.1 Chemical or irreversible hydrogels

Chemical crosslinking is a method to produce irreversible hydrogel networks using covalent bonding between polymer chains. Covalent bonding is much stronger than non-covalent, providing excellent mechanical stability. The following sections describe the different ways of making irreversible hydrogels.

- Small molecule crosslinker [35]

Many bifunctional small molecules have been used to prepare hydrogels by the crosslinking of hydrophilic polymers. The hydrophilic polymer should have a suitable functionality that is able to react with the crosslinking agent. Examples of a crosslinking agent in relation to a functional group of polymer are shown in Table 2.4. The main disadvantage of this method is that many crosslinkers have been found to be relatively toxic. To prevent trace amounts of unreacted crosslinker agents *in vivo*, synthesized hydrogels must be purified before administration.

Table 2.4 Examples of a crosslinking agent in relation to a functional group of polymer [35].

Crosslinking agent	Type of polymer
- Dialdehyde compound	- Polymer with amino and hydroxyl group
- Amine compound	- Halogen-type polymer, carboxylic polymer ester, isocyanate, epoxy base and polymer with methylol base
- Aziridine compound	- Polymer with carboxyl base
- Di or polymethylol phenolic resin	- Polymer with nitril base, mercapto base and carboxyl base
- Halogen compound	- Polymer with amine, diene
- Di or polyisocyanate compound	- Polymer with active hydrogen like –OH, -SH, $-NH_2$ and –COOH
- Alcohol like diol, polyol, bisphenol	- Polymer and cellulose chlorosulfonate base and isocyanate base
- Diepoxy compound	- Polymer with carboxyl base, hydroxide base, mercapto base and chlorosulfonate base

- Polymer-polymer crosslinking

In order to eliminate the use of crosslinkers during gelation, many efforts have been pre-functionalized polymer chains with reactive functional groups. For example, a hydrogel based on *N*-succinylated chitosan and aldehyde-terminated hyaluronic acid could be formed *via in situ* crosslinking by Schiff's base reaction [63]. Chitosan hydrogels have also exploited Michael addition reactions to form polymer-polymer crosslinking. Amino groups of chitosan can react with the vinyl group on another polymer [64]. This approach has been popular for hydrogel preparation due to its rapid reaction time and ability to form different types of bonds. Although polymer-polymer systems have many advantages, they require multi-step preparation and purification processes.

- Photo-crosslinking

Like polymer-polymer crosslinking, researchers have been developed polymer that can form hydrogels *in situ* using photo-sensitive functional groups. By adding these reactive moieties to polymer, the polymer can form crosslinkages upon irradiation with UV light. For example, a photo-crosslinked chitosan hydrogel has been developed by K. Ono et al. [65]. They were able to prepare a photosensitive chitosan hydrogel that could be formed *in situ* by functionalizing the polymer with azide groups. After UV irradiation, the azide is converted into a reactive nitrene group that binds chitosan's free amino groups, causing gelation within 60 s. Another example, an oxidized methacrylated alginate/poly(ethylene glycol) (OMA/PEG) hydrogel was also produced by UV photo-crosslinking [66]. Alginate was chemically functionalized with aldehyde groups by oxidation to react with amine groups of PEG and then a fraction of the alginic acids were further modified with 2-aminoethylmethacrylate (AEMA) *via* carbodiimide chemistry to allow photo-crosslinking of the methacrylate groups by UV light.

- Free-radical polymerization crosslinking [36]

Free-radical polymerization crosslinking is the preferred method used to prepare hydrogels from the class of acrylates and vinyl lactams. It can also be applied to prepare hydrogels based on natural polymers, which the polymer backbone or chain end of the natural polymers has been functionalized with a radically polymerizable group. Preparation of hydrogel by this method involves the chemistry of typical free-radical polymerizations, which includes initiation, propagation, chain transfer, and termination steps. Initiation step, a wide variety of thermal, visible light, ultraviolet and redox initiators can be used to generate radicals. Then the radicals react with the monomers converting them into active forms. After

that, these active monomers react with more monomers and so on in the propagation step. The resulting long chain radicals undergo termination either through chain transfer or through radical combination. For example, sorbitan methacrylate (SMA) hydrogel was synthesized following conditions: SMA as monomer, α, α′-azo-bis(isobutyronitrile) as thermal initiator and ethylene glycol dimethacrylate as crossliking agent [67]. Another example is sodium 2-acrylamido-2-methylpropanesulfonate (Na-AMPS) hydrogel. This hydrogel was prepared by redox initiation *via* free radical polymerization in aqueous solution. At room temperature, potassium persulfate as the free radical initiator and potassium metabisulfite and ferrous sulfate as coinitiators were added into the Na-AMPS solution to form hydrogel [68].

- **Irradiation crosslinking** [36]

Hydrogels can also be obtained by ionizing radiation techniques. This route can be employed for both the synthetic and natural polymers. Ionizing radiation is a radiation that possesses enough energy to ionize molecules either in air or water. Types of irradiation include both electron beam irradiation and γ–radiation. During irradiation, many reactive sites are generated along the polymer backbone. Upon combination of these radicals, the crosslink is formed. Examples of polymers crosslinked by the radiation method are poly(vinyl alcohol)/ carboxymethylate chitosan/honey hydrogel [69] and gelatin/carboxymethyl chitosan [70]. Irradiation crosslinking has been widely used since it does not involve the use of chemical additives or catalysts. However, irradiation is not recommended for preparation of hydrogels from some polymer that can degrade under the ionizing irradiation [71].

2.2.2.2 Physical or reversible hydrogels

Hydrogels can be formed through a physical interaction. The hydrogels obtained by this technique are usually prepared under mild conditions. The gelation does not require any toxic covalent linker molecules. However, their widespread application is limited due to the weak mechanical strength and uncontrolled dissolution. The following sections describe the different ways of making reversible hydrogels.

- **Crosslinking by hydrogen bonding**

Hydrogels can be formed through the hydrogen bonding of polymer chain. A hydrogen bond is formed through the association of electron-deficient hydrogen atom and functional groups of high electron density [36]. For instance, carboxymethyl cellulose (CMC) network can be formed by dispersing CMC into 0.1 M HCl [72]. The mechanism involves replacing the sodium in CMC with hydrogen in the

acid solution to promote hydrogen bonding (Fig. 2.4). The hydrogen bonds induce a decrease of CMC solubility in water and result in the formation of an elastic hydrogel. Another example is hydrogen-bonded complex of poly(acrylic acid) and poly(*N*-vinylpyrrolidone) [73]. This complex is affected by a variety of factors such as the molar ratio of each polymer, the solution temperature, polymer concentration, type of solvent and polymer structure.

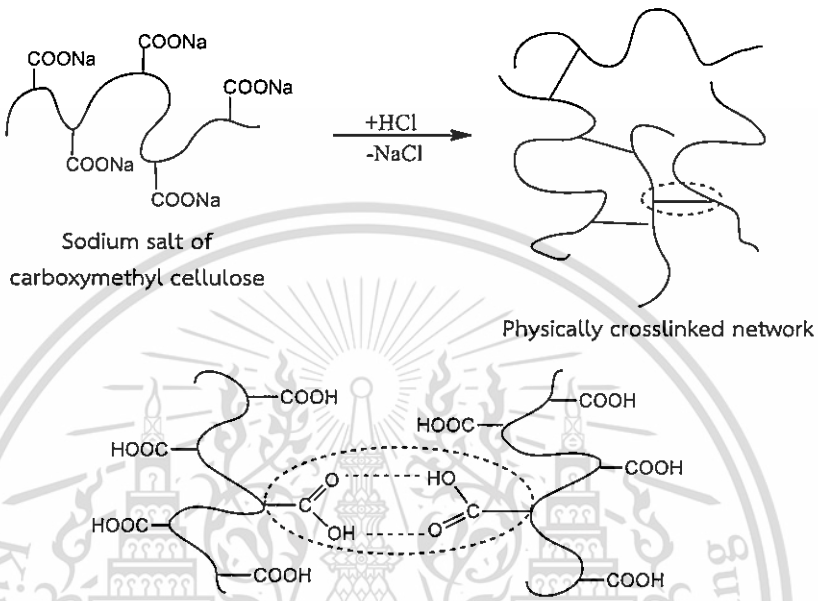

Figure 2.4 Hydrogel network formation due to intermolecular H-bonding in CMC at low pH [72].

- Crosslinking *via* ionic bonding

Mixing two types of polyelectrolyte solutions of opposite charges leads to a polyelectrolyte complex hydrogel (Fig. 2.5a). The hydrogels formed through electrolytic complexation are insoluble in water and the electrolytic bonds can be very stable depending on the pH of the system [74]. In order to prepare an ionically crosslinked polymeric network, an ionic polymer (e.g., sodium alginate and chitosan) and charged counterion (also known as ionic crosslinker) (e.g., calcium chloride) having an opposite charge are dispersed in a solvent, after that ionic interaction occurs (Fig. 2.5b). Some examples are calcium-alginate [75] and tripolyphosphate-chitosan [76]. In addition, the polyelectrolyte complex can also be formed between two oppositely charged polymers (Fig. 2.5c). Some examples are chitosan-xanthan [77], sodium alginate-chitosan [78], and chitosan-pectin [79].

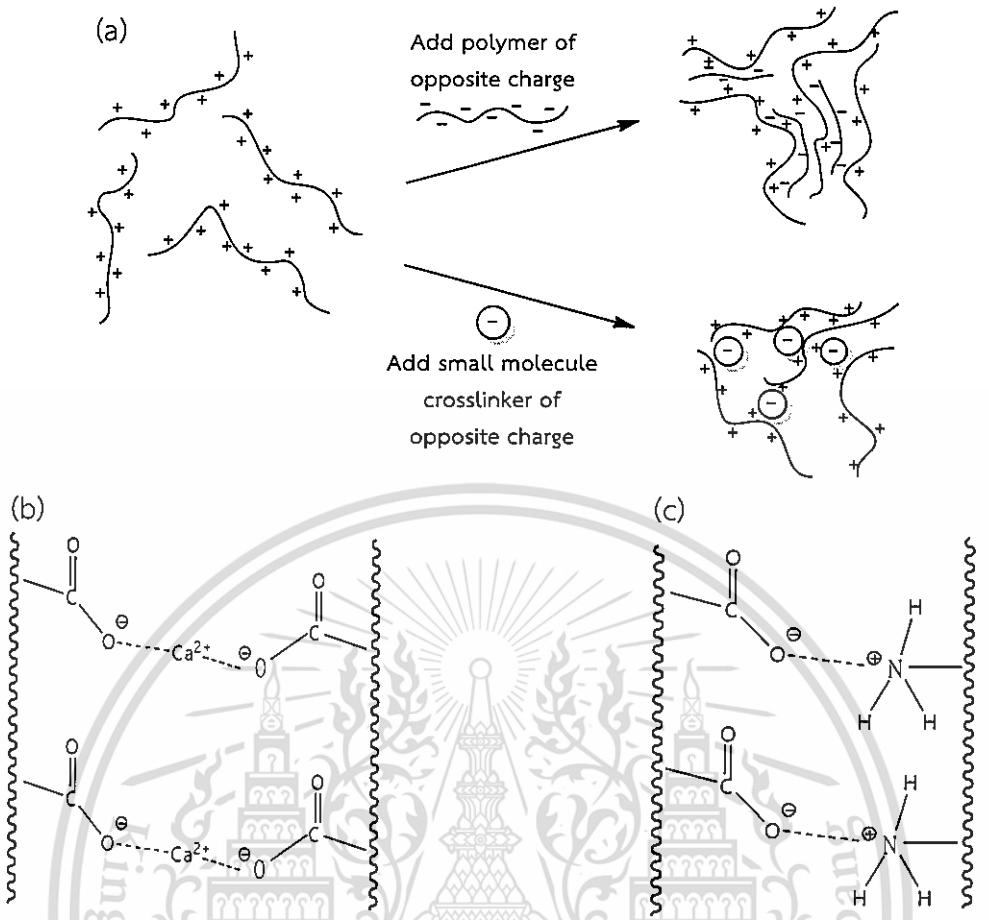

Figure 2.5 (a) physical crosslink driven by charge interaction, (b) hydrogel formation using a polyelectrolyte and an ionic crosslinker and (c) hydrogel formation using polyelectrolytes with opposite charges [74].

- Crosslinking by coordination bonding

This is the method for forming hydrogels by bonding between the metal cation and functional groups on polymer chains such as carboxylic acid or amino groups [35]. A wide variety of metal ions can be used for the formation of hydrogel such as Ag^{+} [80], Cu^{2+} [81], Zn^{2+} [82] and Fe^{3+} [83]. This bond is stronger than that found between a polyelectrolyte and an ionic crosslinker [7]. In addition, this bonding is formed *via* hydrating water molecules rather than direct bonding between the metal ions and chelates. There is a correlation between the radius of the hydrating ions and the bonding strength. The smaller radius of hydration, the easier the gel forms due to the increased static interaction. Gelation also depends on the molecular weight of polymer, concentration and type of solution that cause crosslinking reactions and salt concentrations.

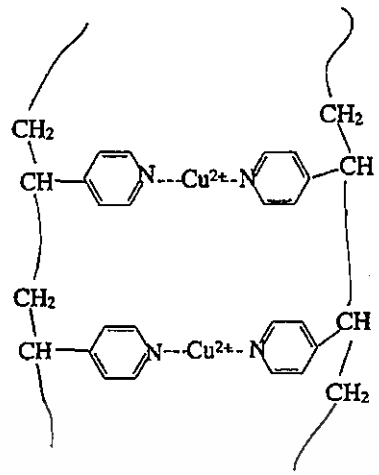

Figure 2.6 Chelation in copper-poly(4-vinyl pyridine) complex [35].

- Crosslinking caused by helix formation

Hydrogels of agar (from agarose and agaropectin), gelatin and carrageenan can be formed by helix formation [35]. The gelation caused by heat induced sol-gel transition. For example, kappa carrageenan in hot solution above the melting transition temperature is in the random coil conformation. By cooling hot solution of kappa carrageenan, the double helices are formed at a certain temperature. In the presence of potassium ions, the double helices of kappa carrageenan cluster together into bigger units that are called helices aggregates. Potassium can act as intramolecular glue, forming electrostatic interactions with the sulfate esters and anhydro-oxygen atom of kappa carrageenan (Fig. 2.7) [84].

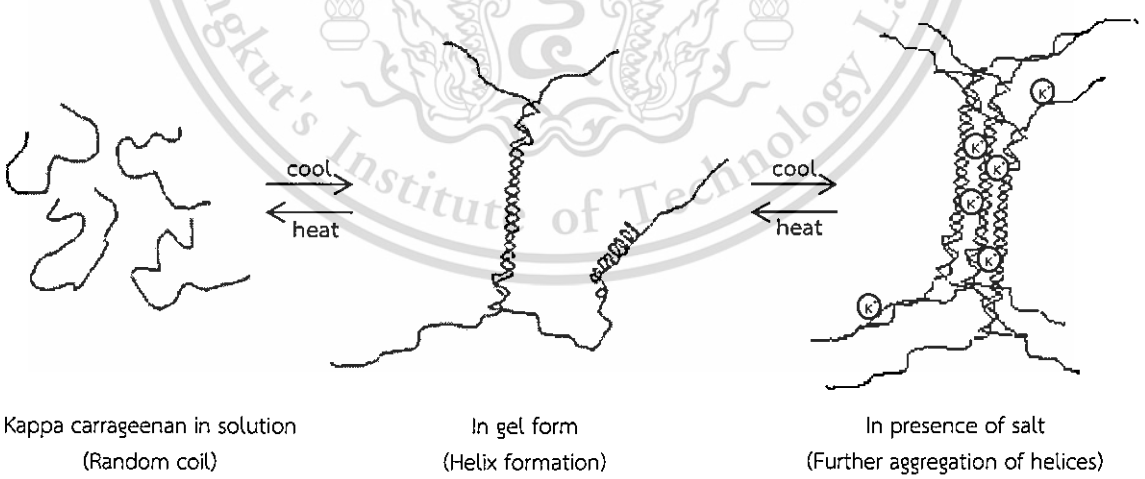

Figure 2.7 Gel formation due to aggregation of helix upon cooling a hot solution of kappa carrageenan [84].

- Crosslinking by hydrophobic bonding

Hydrogels can be formed through hydrophobic associations. Polymer systems such as block copolymers, graft copolymers and polymer blends can form microphase/microdomain separated structures. The hydrophobic domains in these structures behave as associated crosslink sites. These polymers combine hydrophobic segments that form unique hydrophobic phases dispersed by hydrophilic water absorbing regions. An example of hydrophobic associated hydrogel is poly(ethylene glycol) grafted chitosan hydrogel. Graft copolymer of chitosan and poly(ethylene glycol) was produced by chemically grafting monohydroxy poly(ethylene glycol) on the chitosan backbone using Schiff base and sodium cyanoborohydride chemistry [85]. It was reported that this copolymer underwent a thermoreversible transition from an injectable solution at room temperature to a gel at body temperature (Fig. 2.8). It was believed that at low temperatures, the hydrogen bonding between the poly(ethylene glycol) and water molecules dominates. While, at high temperatures, the hydrophobic interactions between the polymer chains prevail resulting in the hydrogel formation.

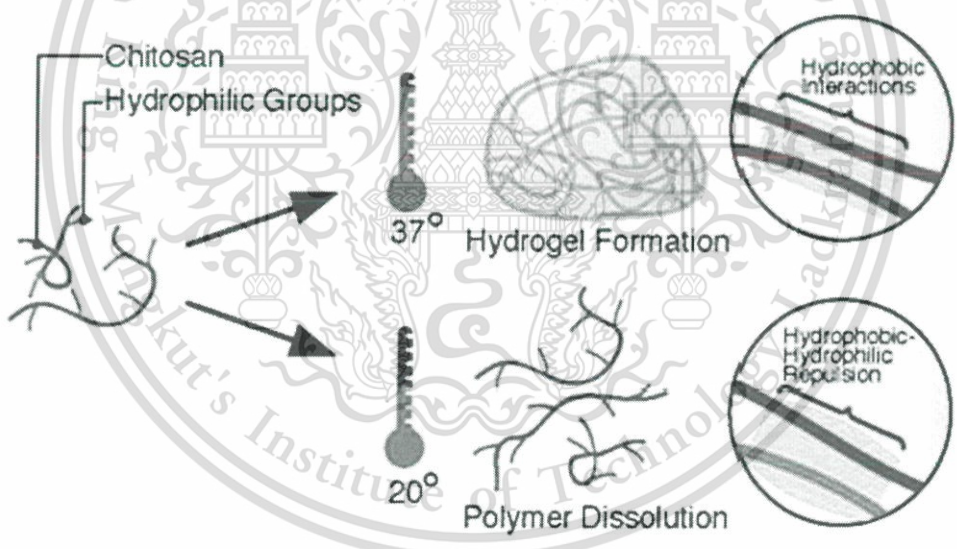

Figure 2.8 Networks of chitosan graft copolymer resulting semi solid gel at body temperature and liquid below room temperature [7].

- Crosslinking by freeze-thawing

Hydrogels can be achieved by using freeze-thaw method. The mechanism involves the formation of microcrystals in the structure due to freeze-thawing. An example of this type of gelation is poly(vinyl alcohol) hydrogel [86].

2.2.2.3 Interpenetrating polymer networks (IPNs)

The performance of hydrogels can be enhanced by the formation of interpenetrating polymer networks (IPNs). The IUPAC definition of IPNs is "a polymer comprising two or more networks which are at least partially interlaced on a molecular scale but not covalently bonded to each other and cannot be separated unless chemical bonds are broken" [87]. If only one component is crosslinked, the resulting network is defined as semi-IPNs. The IUPAC definition of semi-IPNs is "a polymer comprising one or more networks and one or more linear or branched polymer(s) characterized by the penetration on a molecular scale of at least one of the networks by at least some of the linear or branched macromolecules" [87]. An illustration of semi-IPNs and IPNs is presented in Fig. 2.9.

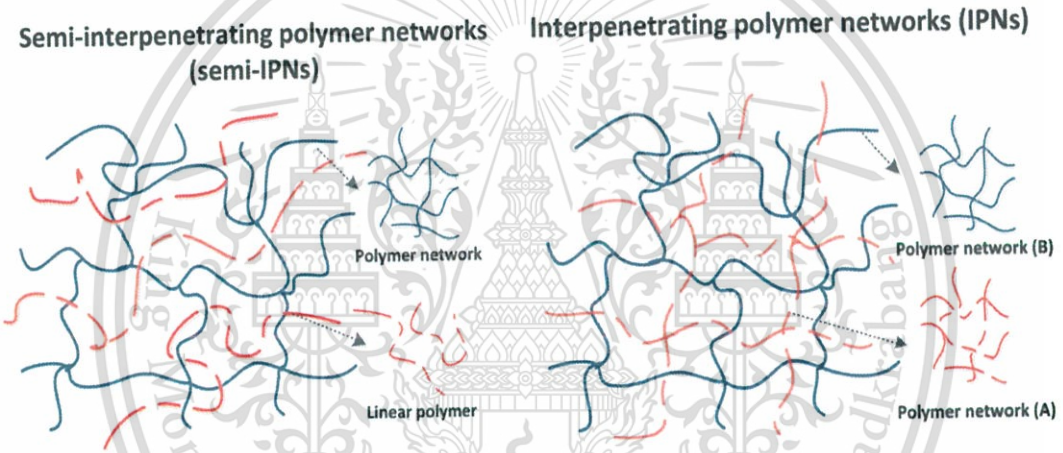

Figure 2.9 Schematic representation of semi-IPNs and IPNs [88].

The most commonly used procedure to form IPNs is by an *in situ* preparation where the reactants (monomers or polymers) are mixed in a solution before crosslinking is performed, as shown in Fig. 2.10. In the case of IPNs, the two networks can be formed either simultaneously or sequentially. In the case of the simultaneous pathway, the reactions leading to the two networks must be orthogonally because otherwise cross reactions (i.e., copolymer formation) probably occur. An alternative procedure is based on the sequential formation of the semi-IPNs. Firstly, a polymer network is prepared and subsequently the monomers or the second polymer are loaded into the swollen network, thus, leading to semi-IPNs. When the loaded polymer is crosslinked to form the second network, the semi-IPNs are converted into IPNs [89].

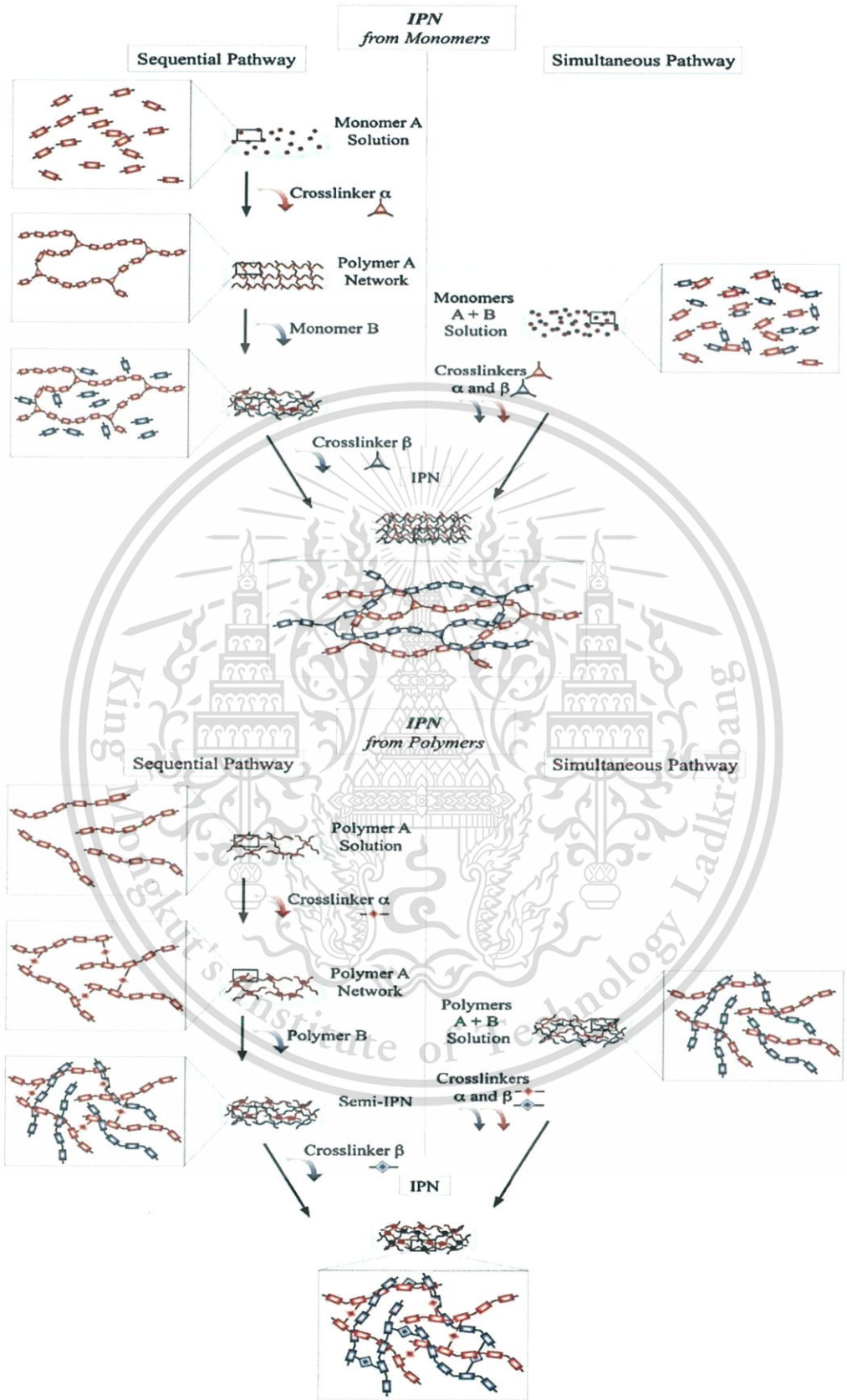

Figure 2.10 Schematic representation of the semi-IPN and IPN formation [89].

The advantage of IPNs is that the combination of favourable properties of each constituent polymer of the IPNs leads to new systems with improved properties, which are different from those of the individual polymers. In addition, synergism of properties is also observed in several systems [90-91]. The combination and synergism of properties can be used to modify and tailor the characteristics of the resulting material to meet specific needs.

Examples of IPN hydrogels are pH-responsive silk sericin/ poly(methacrylic acid) IPN hydrogel [92] and cyclodextrin/carbopol micro-scale IPN hydrogel [93]. Examples of semi-IPN hydrogels are pH/temperature-responsive carboxymethyl chitosan/poly(*N*-isopropyl acrylamide) semi-IPN hydrogel [94] and thermo-sensitive poly(*N*-isopropyl acrylamide-co-vinyl pyrrolidone)/chitosan semi-IPN hydrogel [95].

2.2.3 Properties of hydrogels [36]

Hydrogel is a crosslinked polymer that swells in water to an equilibrium value. The amount of water that a material needs to absorb to be classified as a hydrogel remains undefined, but most researchers generally agree that if a material absorbs at least 10% water and is insoluble in water, it can be classified as a hydrogel. The swollen equilibrated state of a hydrogel results from a balance between the osmotic driving forces that cause the water to enter the hydrophilic polymer and the cohesive forces exerted by the polymer chains in resisting expansion. It can be concluded that an equilibrium swelling state depends on the osmotic driving forces and the crosslink density. The degree of hydration (water content) can be expressed using the following equation:

$$\%\text{Water (weight)} = \frac{\text{hydrated weight} - \text{dry weight}}{\text{hydrated weight}} \times 100 \qquad (2.1)$$

The degree of water absorption related to the dry state of the polymer is called percent hydration. This is calculated using the following equation:

$$\%\text{Hydration} = \frac{\text{hydrated weight} - \text{dry weight}}{\text{dry weight}} \times 100 \qquad (2.2)$$

The more hydrophilicity of polymer used to prepare the hydrogel, the higher the degree of hydration. This hydration can also be controlled by crosslink density. The higher the degree of crosslinking results in a corresponding decrease in water content.

2.2.4 Water in hydrogels [34, 96-97]

The water in hydrogels is classified into three categories, i.e., free water, freezing bound water and non-freezing bound water. When a dry hydrogel begins to absorb water, the hydrophilic groups along the polymer chain are hydrated first. After that, water forms a hydration sphere around these hydrophilic groups leading to non-freezing bound water. This type of water is tightly held in the hydrogel through interactions such as hydrogen bonding and cannot freeze or melt at normal temperature range of pure water. As the polar groups are hydrated, the network swells and exposes hydrophobic groups, which also interact with water molecules leading to freezing bound water. This type of water interacts weakly with the polymer and can freeze or melt at temperature shifted with respect to that of free water. Freezing and non-freezing bound water are often combined and called the total bound water. After the polar and hydrophobic sites have interacted with bound water molecules, the network will absorb additional water. The additional water that is imbibed after the ionic, polar, and hydrophobic groups become saturated with bound water is called free water. This water is assumed to fill the space between the network chains.

The major method used to determine the relative amounts of free and bound water as fractions of the total water content is differential scanning calorimetry (DSC) [98]. Because only the free water and the freezing bound water can be frozen, it is assumed that the endothermic peak measured when warming the frozen hydrogel represents the melting of the free water and the freezing bound water. The amount of free water and freezing bound water in the sample can be calculated by the area under the corresponding endothermic peak. Then non-freezing bound water is obtained by difference of the measured total water content of sample before DSC experiment and the calculated free water and freezing bound water.

The amount and type of water contained in the hydrogels can be used to determine diffusion and transport characteristics of the hydrogel. This is important for drug delivery application. It has been found that the population of non-freezable bound water plays an important role in drug delivery behavior [99].

2.2.5 Hydrogels in controlled drug delivery systems

In recent years, the hydrogels have been attracted attentions for the design of controlled drug delivery systems [100-101]. The soft and hydrophilic nature of hydrogels makes them particularly suitable as drug delivery systems. The control of swelling properties of hydrogel can be used to trigger drug release. Through proper

design, hydrogels can be used in a variety of applications including sustained, targeted and stealth biomolecule delivery.

Oral administration of drugs has been the most convenient and comfortable route for delivery of most therapeutic agents. The smart hydrogels that swell and shrink in response to external pH have been investigated to create controlled oral drug delivery systems [2, 102]. This is because the fact that the pH range of fluids in various segments of the gastrointestinal (GI) tract (Fig. 2.11) can provide environmental stimuli for responsive drug release. After ingestion, food passes quickly through the oesophagus (taking around 10-14 s [103]) and reaches the stomach. The pH values of the stomach have been reported to lie within pH 1.00-2.50 [104]. Gastric emptying time is highly variable [105], and is often reported as between 5 min and 2 h. However, the half gastric emptying time is around 80.5 min [106]. After passage through the stomach, food enters the small intestine. Transit times for small intestine are about 3-6 h [3]. The pH of the small intestine has been estimated to lie in the range of pH 6.15-7.35 in the proximal region, rising to pH 6.80-7.88 in the distal small intestine [107]. After passage through the small intestine, food reaches the colon at which point the pH lowers slightly to pH 5.26-6.72 in the ascending colon, and pH 5.20-7.02 in the descending colon [108]. The transit time in colon is highly variable, with a range of 6-32 h [109]. Examples of pH-sensitive hydrogels for oral drug delivery are poly(acrylic acid) [110], chitosan [6] and sodium alginate [18].

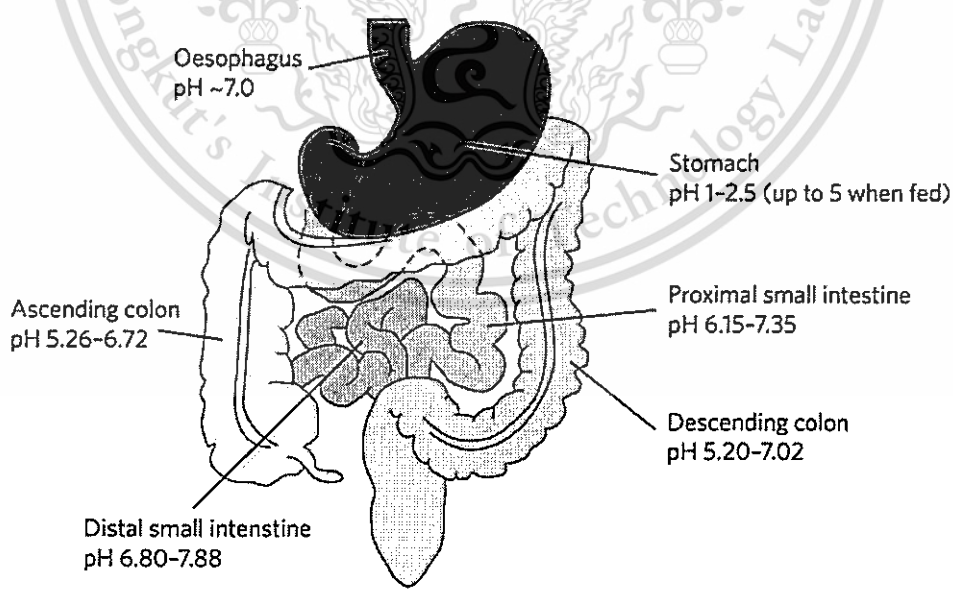

Figure 2.11 Characteristics of the GI tract showing the pH at the different parts [107].

The drug release from pH-sensitive hydrogels depends on many factors. The main factor is based on the structure of the polymers used in the preparation of the hydrogels. Thus, it is important to choose the proper polymers upon designing hydrogels for drug delivery. In this work, chitosan was selected as the base polymer to develop the novel pH-sensitive hydrogels for site-specific drug delivery to different parts of gastrointestinal tract.

2.3 Chitosan

2.3.1 Chemical structure of chitosan [8]

Chitosan (CS) is a copolymer composed of *N*-acetyl-*D*-glucosamine and *D*-glucosamine units. It is a polycationic polymer that has one amino group and two hydroxyl groups in the repeating glucosidic residue. The carbohydrate backbone is very similar to cellulose, which consists of β-1,4-linked *D*-glucosamine with a variable degree of *N*-acetylation, except that the acetylamino group replaces the hydroxyl group on the C_2 position. Thus, chitosan is a copolymer consisting of *N*-acetyl-2-amino-2-deoxy-*D*-glucopyranose and 2-amino-2-deoxy-*D*-glucopyranose, where the two types of repeating units are linked by (1⟶4)-β-glycosidic bonds. The structure of this polymer is depicted in Fig. 2.12a. Chitosan is derived from the deacetylation of chitin (Fig. 2.12b). Chitin is found in the shells of crustaceans, exoskeletons of insects and cell walls of fungi. Commercially, chitin is mainly isolated from shells of crabs and shrimps that are waste products of the seafood industry. The manufacturing methods for chitosan are illustrated in Fig. 2.13. The deacetylation degree (DD) of chitosan, giving indication of the number of amino groups along the chains, is calculated as the ratio of *D*-glucosamine to the sum of *D*-glucosamine and *N*-acetyl-*D*-glucosamine. To be classified as chitosan, the deacetylated chitin should contain at least 60% of *D*-glucosamine residues (which corresponds to a deacetylation degree of 60) [111].

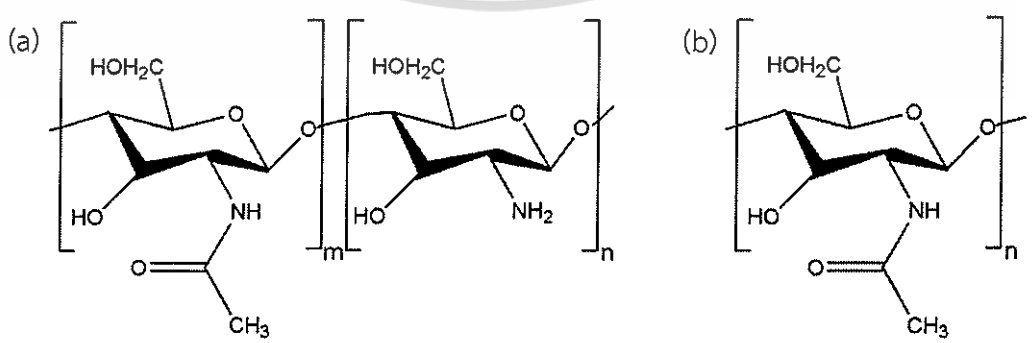

Figure 2.12 Chemical structures of (a) chitosan and (b) chitin [111].

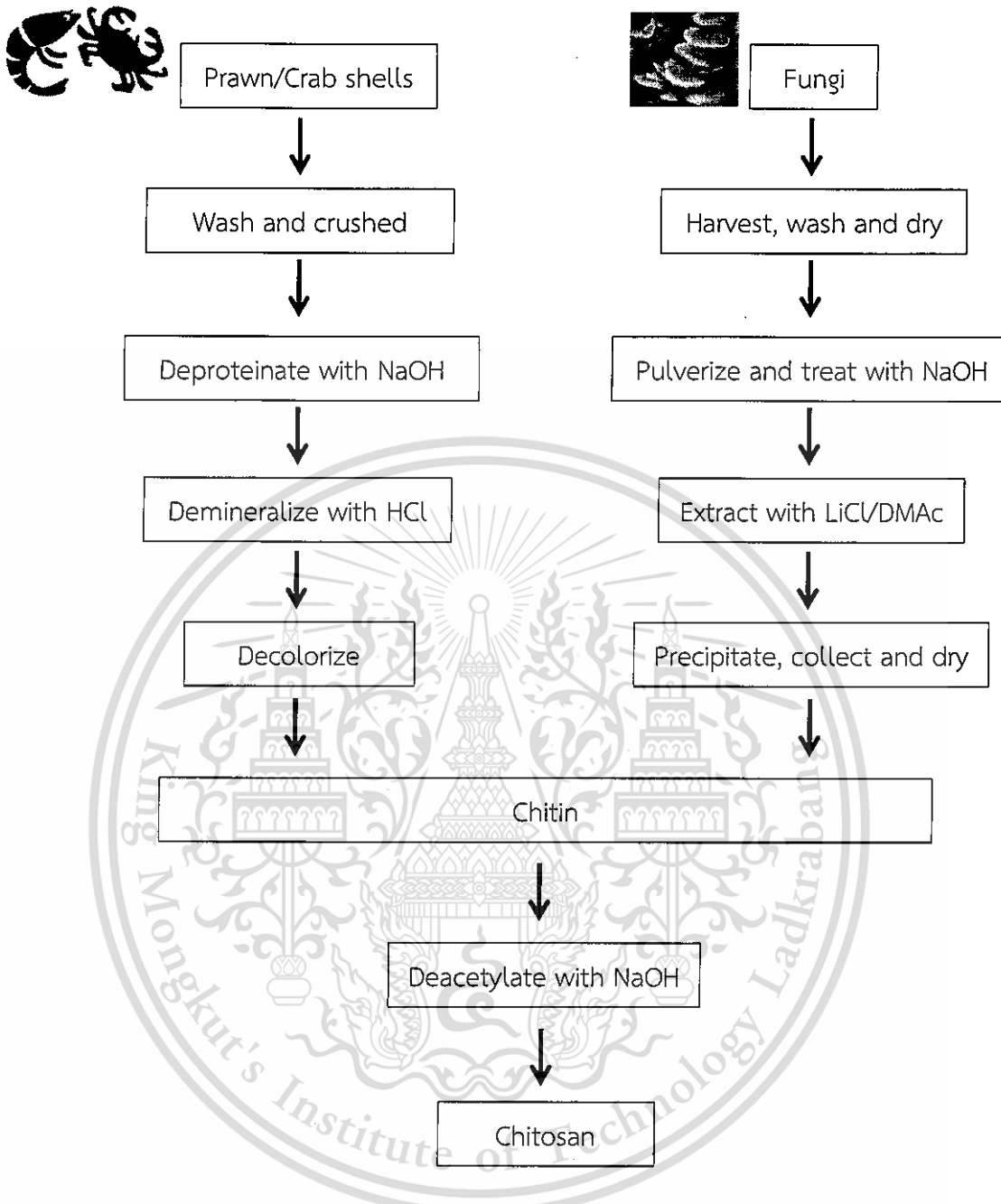

Figure 2.13 Schematic of manufacturing methods for chitosan. Adapted from Ref. [112].

2.3.2 Properties of chitosan

The properties (i.e., solubility, crystallinity, biodegradability, viscosity and biocompatibility) and the biological properties (i.e., mucoadhesion, analgesic, antimicrobial, permeation enhancing effect, antioxidant and hemostatic) of chitosan are directly related to its DD and the molecular weight (Table 2.5).

Table 2.5 Relationship between structural parameters and properties [8].

Property	Structural characteristics[a]
- Solubility	↑DD
- Crystallinity	↓DD
- Biodegradability	↓DD, ↓Molecular weight
- Viscosity	↑DD
- Biocompatibility	↑DD
Biological	
- Mucoadhesion	↑DD, ↑Molecular weight
- Analgesic	↑DD
- Antimicrobial	↑DD, ↑Molecular weight
- Permeation enhancing effect	↑DD
- Antioxidant	↑DD, ↓Molecular weight
- Hemostatic	↑DD

[a] ↑ Directly proportional to property, ↓ inversely proportional to property.

- **Solubility** [8]

While the parent chitin is insoluble in most organic solvents, chitosan is readily soluble in dilute acidic solutions below pH 6.0 due to the quaternization of the amino groups that have a pK_a value of 6.3. At low pH, these amino groups are protonated and become positively charged making chitosan a water-soluble cationic polyelectrolyte. On the other hand, when the pH increases above 6, amino groups of chitosan become deprotonated and chitosan is insoluble. The soluble-insoluble transition occurs at its pK_a value around pH between 6 and 6.5. The solubility of chitosan is related to the DD because the pK_a value is highly dependent on the degree of *N*-acetylation [113]. Apart from the DD, the molecular weight is also an important parameter that significantly affects the solubility [114-115].

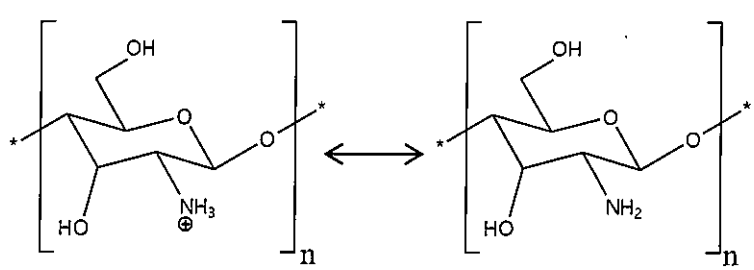

Figure 2.14 Schematic illustration of chitosan's versatility [8].

- Biodegradability [96]

Chitosan can be degraded *in vivo* by several proteases and mainly lysozyme [8, 116]. The biodegradation of chitosan leads to the formation of non-toxic oligosaccharides of variable length. These oligosaccharides can be incorporated in metabolic pathways or be further excreted [117]. The degradation rate of chitosan is mainly related to its molecular weight and DD [118]. Smaller chitosan chains are more rapidly degraded into oligosaccharides than chitosan with higher molecular weight. The relationship between biodegradation of chitosan and its DD can be explained by its semi-crystalline nature. Crystallinity is maximum for a DD equal to 0 or 100% (chitin or fully deacetylated chitosan, respectively), and decreases for intermediate DD. When DD of chitosan decreases (close to 60%), the crystallinity also decreases resulting in an increase of the biodegradation rate. Besides, the distribution of acetyl residues along chitosan chain also affects its crystallinity and consequently the biodegradation rate.

- pH-sensitivity [8]

Chitosan exhibits a pH-sensitive behavior due to the amino groups on its chain. The mechanism of pH-sensitive swelling involves the protonation of amino groups of chitosan under low pH conditions. This protonation leads to chain repulsion, diffusion of proton and counter ions together with water inside the hydrogel and dissociation of secondary interactions. This pH-sensitive property makes chitosan to be used in the delivery of drugs to the stomach. However, the applications of chitosan in drug delivery to the small intestine are restricted because chitosan is easily dissolved at low pH leading to the rapid drug release in the stomach [13].

- Biocompatibility [119]

Chitosan has been widely used in food industry and it is approved by the Food and Drug Administration (FDA) for use in wound dressings [120]. Chitosan has also been promoted as a component in non-medical products (a fat binder in cholesterol-lowering and slimming formulations). It has also been studied in biomedical field and has been found to be highly biocompatible.

- Biological property [111]

The presence of the amino groups along chitosan chains allows explaining the most of chitosan properties. The mucoadhesion of chitosan can be explained by the presence of negatively charged residues (sialic acid) in the mucin (the glycoprotein that composes the mucus) which can interact with positive charges of

chitosan generated in acidic medium. This mucoadhesion is directly related to the DD of chitosan. If DD increases, the number of positive charges also increases leading to the improvement of mucoadhesive properties [121].

The haemostatic activity of chitosan can also be related to the presence of positive charges on chitosan backbone. The positive charges of chitosan can interact with negative charges on red blood cell. Besides, chitin shows less effective haemostatic activity than chitosan, which tends to confirm this explanation [122-123].

The permeation enhancing property of chitosan can be described by the presence of positive charges of chitosan which can interact with the negative part of cells membrane leading to reorganization and an opening of the tight junction proteins. Like mucoadhesion, if DD of chitosan increases, the permeation ability also increases [124].

The case of antimicrobial activity of chitosan is slightly more complicated to explain. There are two main mechanisms proposed to elucidate chitosan antibacterial and antifungal activities. In the first proposed mechanism, positively charged chitosan can interact with negatively charged groups at the cell surface resulting in the change of its permeability. This would prevent important materials to enter the cells and/or lead to the leaking of primary solutes out of the cell. The second mechanism involves the binding ability of chitosan with the cell DNA, which would lead to the inhibition of the microbial RNA synthesis [125-126].

The polycationic behavior of chitosan also allows elucidating the analgesic effects of chitosan. The amino groups of chitosan can be protonated in the presence of proton ions that are released in the inflammatory area leading to an analgesic effect [127].

Considering all the aforementioned properties, it is not surprising that chitosan has been widely used in various biomedical applications and drug delivery systems.

2.3.3 Gelation

Chitosan hydrogels have been prepared with a variety of different shapes, geometries and formulations including liquid gels, powders, beads, films, tablets, capsules, microspheres, microparticles, sponges, nanofibrils, textile fibers and inorganic composites. The main method of preparation chitosan hydrogels is covalent crosslinking. The most common crosslinkers used for preparation of covalently crosslinked chitosan hydrogel are dialdehydes such as glyoxal and glutaraldehyde [128-129]. Their reaction with chitosan is well-documented; the aldehyde groups form covalent imine bonds with the amino groups of chitosan due to the resonance established with adjacent double ethylenic bonds *via* a

Schiff reaction [130]. Dialdehydes allow direct reaction in aqueous media, under mild conditions and without the addition of auxiliary molecules such as reducers. However, the main drawback of dialdehydes is that they are generally considered to be toxic. For example, glutaraldehyde and glyoxal are known to be neurotoxic and mutagenic, respectively [131-132]. Therefore, a new alternative covalent crosslinker for chitosan is required. There have been attempts to use genipin as a crosslinker for chitosan. Genipin is a naturally occurring material, which is commonly used in herbal medicine and as a food dye [133]. The biocompatibility of genipin in the human body has not been evaluated yet, but it is not cytotoxic *in vitro* and has been shown to be biocompatible after injection in rats [133-134]. However, genepin is expensive.

To avoid toxic crosslinking agent, many researches have played a role on photo-crosslink [135-136] and radiation crosslink [137-138] systems. However, these hydrogels are not pH-sensitive and not effectively used as drug controlled release. The formation of hydrogels by reversible ionic crosslinking is an alternative route to overcome these limitations. Small anionic molecules such as sulfates, citrates and phosphates can interact with cationic amino groups of chitosan [76, 139]. Anionic molecules with a high charge density should be chosen to ensure strong ionic interactions. In addition, anionic ions with the smaller ionic radii may translate to smaller impedance in their diffusion throughout the polymer matrix and quickly form electrostatic bonds compared to the larger ones.

Besides, the amino and hydroxyl groups of chitosan can form coordinate bonds to various metal ions such as Ag^{+} [80], Cu^{2+} [81], Zn^{2+} [82] and Fe^{3+} [83]. This type of bond is stronger than the electrostatic interactions formed by the anionic molecules used as crosslinker [7]. The nature of the metal ions is very important in the mechanism of interaction. The affinity of chitosan for various metal ions is in the following order: $Cu^{2+} >> Hg^{2+} > Zn^{2+} > Cd^{2+} > Ni^{2+} > Co^{2+} \sim Ca^{2+}$, $Eu^{3+} > Nd^{3+} > Cr^{3+} \sim Pr^{3+}$ [140].

In addition, larger negatively charge molecules, natural and synthetic polyanions can also form gels with chitosan. Chitosan-based polyelectrolyte complex networks have been prepared with DNA, anionic polysaccharides (e.g., alginate, glucosamineglycans, chondroitin sulfate, hyaluronic acid, heparin, carboxymethyl cellulose, pectin, dextran sulfate, and xanthan), proteins (e.g., gelatin, albumin, fibroin, keratin, and collagen) and synthetic anionic polymers (e.g., polyacrylic acid). The stability of these polyelectrolyte complexes depends on charge density, solvent, ionic strength, pH, and temperature [8].

Furthermore, it should be noted that electrostatic interactions can occur with other secondary interactions (e.g., hydrogen bonding). These interactions can

enhance the properties of the chitosan hydrogel and can be modulated to express unique material properties, such as pH-sensitivity [111].

2.3.4 Water-soluble chitosan

Although chitosan have many favourable characteristics such as good biocompatibility and low toxicity, the poor solubility of chitosan at the physiological pH 7.4 is the major limiting factor in its utilization. This restricts the use of chitosan in oral drug delivery systems. In addition, acetic acid or other acids would be commonly applied for dissolution of chitosan in water, which would cause cytotoxic issue to the final product [11]. To improve solubility of chitosan, many efforts have been made to prepare a water-soluble chitosan.

High molecular weight is responsible for the low solubility of chitosan in water. Therefore, it is interesting to improve the solubility of chitosan by decreasing the molecular weight. Low molecular weight (LMW) chitosan can be prepared by various methods as follows:

C. Qin et al. [141] synthesized water-soluble LMW chitosan from enzymatic hydrolysis with efficient hemicellulase. The hydrolysates were separated into three fractions by ultrafiltration membranes. A separated fraction with molecular weight more than $5x10^3$ and with a degree of deacetylation of 58% was water-soluble in the free amine form.

J. Li et al. [142] also prepared LMW chitosan and chito-oligomers from enzymatic hydrolysis. Firstly, chitosan with a degree of deacetylation of 91.7% was hydrolyzed by a commercially available and efficient neutral protease. The optimum temperature was 50 °C and the optimum pH was 5.4. IR spectra confirmed that the chemical structures of residues were not modified. Different reaction times gave chitosan with different molecular weights. Mn^{2+} was the most efficient activator of the enzymatic reaction. The degree of deacetylation of the main hydrolysis products decreased compared with the initial chitosan. The decrease of molecular weight of the resulting chitosan led to transformation of crystal structure and the increase of water solubility.

Besides the use of enzymatic hydrolysis, hydrogen peroxide (H_2O_2) was used to hydrolyze chitosan because it is easy to handle, readily available and environmentally friendly [143]. This technique is based on the formation of free radicals, which can attack the glucosidic linkages of chitosan [144]. The literature reviews related about the preparation of LMW chitosan by hydrolysis using H_2O_2 are shown as follows:

Z. Xia et al. [145] prepared water-soluble chitosan by hydrolyzing chitosan using H_2O_2 under the catalysis of phosphotungstic acid. Water-soluble chitosan could be obtained under optimum conditions of H_2O_2 2% (v/v), phosphotungstic acid 0.1% (w/v), 65 °C and 40 min. The water-soluble chitosan content of the product and the yield were 94.7% and 92.3% (w/w), respectively. All products were white powders and soluble in water.

Y. Du et al. [146] also prepared water-soluble chitosan by hydrolyzing chitosan using H_2O_2. Firstly, crude chitosan was prepared from shrimp shell by HCl, NaOH and ethanol solution successively. After that, H_2O_2 was used to degrade the crude chitosan into water-soluble chitosan. The optimal conditions to obtain the highest recovery of water-soluble chitosan were 5.5% of H_2O_2 level, 3.5 h of time and 42.8 °C of temperature. The predicted recovery was 93.5%.

Furthermore, the presence of amino groups on chitosan chains allows modifications under mild conditions. In an attempt to improve the water solubility of chitosan, many efforts have been made to introduce hydrophilic groups by covalent attachment to reactive amino groups at the C_2 position. Various kinds of modification of chitosan have been investigated in recent years and examples reported using alkylation [147], carboxymethylation [148], and quaternarization [149] reaction. Michael addition reaction is one of favored methods to modify chitosan because it is an environmentally mild chemical modification process. The literature reviews related about the preparation of water-soluble chitosan by Michael addition reaction are shown as follows:

M. Jiang et al. [150] synthesized water-soluble chitosan by Michael addition reaction by introducing sodium allylsulfonate into the chitosan. The chemical structure of the chitosan derivative was characterized by FT-IR, ^{1}H-NMR and elemental analysis. The degree of substitution was calculated by elemental analysis. The increase of sodium allylsulfonate to chitosan increased the sulfur content in the chitosan derivative. The chitosan derivative showed an excellent solubility in the distilled water. The XRD study suggested that the crystallinity of chitosan derivative decreased. The thermal analysis exhibited that chitosan derivative had lower thermal stability than the unmodified chitosan.

G. Ma et al. [12] synthesized *N*-alkylated chitosan derivative by Michael addition reaction of chitosan and hydroxyethylacrylate. The chemical structure and physical properties of the chitosan derivatives were characterized by FT-IR, ^{1}H-NMR, XRD and DSC. The ^{1}H-NMR results indicated that the degree of substitution was from

0.18 to 1.2. The chitosan derivatives showed an excellent solubility in distilled water. XRD analysis exhibited that the derivatives were amorphous. DSC results demonstrated that thermal stability of the derivatives was lower than that of unmodified chitosan. The chitosan derivatives had the ability to enzymatic degradation and the initial degradation rate of the chitosan derivatives depended on its molecular weight. The antimicrobial activity of the chitosan derivatives decreased compared with that of chitosan.

In this work, water-soluble chitosan was prepared by partially referring to the procedure of G. Ma et al. [12]. Michael addition reaction of chitosan and hydroxyethylacrylate was carried out to synthesize hydroxyethylacryl chitosan (HC), a water-soluble chitosan.

2.3.5 Chitosan-based hydrogels in controlled drug delivery

Chitosan and its derivatives show excellent biological properties such as biocompatibility, non-toxicity and biodegradability. In addition, they possess pH-sensitive behavior which easily dissolves at low pH while being insoluble at high pH. Regarding to those reasons, Chitosan and its derivatives have been widely used for controlled release. The utilization of chitosan and its derivatives based hydrogels in controlled drug delivery is shown as follows:

X.Z. Shu et al. [151] prepared a pH-sensitive citrate crosslinked chitosan film for drug controlled release. Citrate crosslinked chitosan film was prepared by dipping chitosan film into sodium citrate solution. The swelling ratio of crosslinked film was sensitive to pH. In acidic conditions, the crosslinked film swelled and dissociated in the pH less than 3.5, and the model drugs (brilliant blue and riboflavin) incorporated in the film were quickly released (within 2 h released completely in simulated gastric fluid at 37 °C). While in neutral conditions, the swelling ratio of the crosslinked film was less significant and the release rate of brilliant blue and riboflavin was low (less than 40% released in simulated intestinal fluid in 24 h). The parameters of film preparation, i.e., citrate concentration and solution pH, affect the film swelling and drug release profiles. The lower concentration and the higher pH of citrate solution resulted in a larger swelling ratio and quicker riboflavin release. To improve the drug controlled release properties of citrate crosslinked chitosan film, heparin, pectin and alginate were further coated on the film surface. Among them only the coating of alginate prolonged riboflavin release in SGF significantly, while the coating of heparin and pectin only retarded drug release slightly. The results indicated that the pH-sensitive citrate crosslinked chitosan film was useful in drug delivery such as for the site-specific drug controlled release in stomach.

S. Das et al. [152] developed zinc–pectin–chitosan composite particles for drug delivery to the colon. Resveratrol was used as model drug due to its potential activity on colon diseases. Formulations were spherical with 920.48-1107.56 μm size and 21.19-24.27 mg weight of 50 particles. Encapsulation efficiency of the formulations was very high (96.95-98.85%) and the drug was stable within the formulation during their storage due to poor aqueous solubility of the drug and quick formation of the crosslinked matrix. Crosslinking time, pH of crosslinking solution, chitosan concentration and drug concentration exhibited major influence on drug release pattern. Formulation prepared at pH 1.5, 1% chitosan, 120 min crosslinking time and pectin:drug at 3:1 ratio demonstrated colon-specific drug release. Hence, Zn-pectin-chitosan composite particles could be considered as colon-specific formulation.

L.N.M. Ribeiro et al. [153] prepared chitosan/layered double hydroxide (LDH) biohybrid beads coated with pectin for controlled release in the treatment of colon diseases. These systems were designed in order to combine advantages from the three components: (i) the external pectin coating protects the drug delivery system in low pH ambient, as that found in the stomach; (ii) the chitosan matrix in which the drug is incorporated presents mucoadhesive properties of interest for specific adsorption in the intestinal tract; and (iii) the immobilization of the drug in the LDH host solid offers the possibility to control the kinetics of the drug release. These systems were tested using 5-aminosalicylic acid (5ASA) as model drug. The resulting composite beads presenting the pectin coating are stable to water swelling and procure a controlled release of the drug along their passage through the simulated gastrointestinal tract in *in vitro* experiments, due to their resistance to pH changes. Moreover, the kinetics of the drug release can be also tuned by changing the thickness of the pectin coating. Based on these results, these drug delivery systems could be proposed as promising candidates for the colon-targeted delivery of 5ASA.

A. Islam et al. [154] developed pH-sensitive chitosan (CS)/poly(vinyl alcohol) (PVA) hydrogel crosslinked with tetraethoxysilane (TEOS) for controlled release. IR results confirmed the presence of the incorporated components and the existence of siloxane linkages between CS and PVA. All hydrogels exhibited low swelling in acidic and basic pH media, whereas maximum swelling was showed at neutral pH. This pH sensitivity of the hydrogel has been investigated as enteric coating for commercial aspirin tablets. The dissolution test of enteric-coated aspirin tablet in simulated gastric fluid (pH 1.2) showed 7.11% aspirin release over a period of 2 h, whereas a sustained release of remaining aspirin (83.25%) was found in simulated

intestinal fluid (pH 6.8). This release profile of the enteric-coated aspirin in SGF and SIF fulfilled the U.S. Pharmacopeia specification (USP XXIV). According to this, a maximum release of 10% is acceptable at the acidic stage (SGF), and a minimum of 80% is acceptable at buffer stage (SIF).

Z. Liu et al. [155] prepared carboxymethyl chitosan (CMCS) hydrogel beads by ionically crosslinking with calcium ion. The pH-sensitive characteristics of the beads were investigated by simulating gastrointestinal pH conditions. Bovine serum albumin (BSA) was used as a model protein. The entrapment efficiency of BSA in beads was greatly improved (from 44.4 to 73.2%) when the beads were coated with a chitosan/CMCS polyelectrolyte complex (PEC) membrane. The maximum swelling ratios of the beads at pH 7.4 were much higher than those at pH 1.2. The prepared membrane limited the BSA release, while the final disintegration of beads at pH 7.4 still led to a full BSA release. Therefore, the chitosan-coated calcium-CMCS hydrogel beads with higher entrapment efficiency and proper protein release properties were a promising protein drug carrier for the site-specific release in the small intestine.

From the literature reviews, it should be noted that the applications of chitosan or chitosan derivatives in oral drug delivery are restricted because they are easily dissolved at low pH leading to the rapid drug release in gastric environment. Thus, chitosan and its derivatives have usually been blended with other polysaccharides in order to improve their stability in low pH environment and the subsequent controlled delivery of drugs in the small intestine and colon. Among various kinds of polysaccharides, one which can attract our interest is alginate.

2.4 Alginate

2.4.1 Chemical structure of alginate [156]

The extraction of brown seaweed with alkali and its subsequent treatment with mineral acids yields alginic acid. Alginic acid can be converted into various salts, e.g., sodium alginate. A few bacteria, e.g., Azotobacter and Pseudomonas species, are also capable of synthesizing alginate in and *O*-acetylated form. Alginate consists of (1⟶4) linked β-*D*-mannuronic acid (M) and α-*L*-guluronic acid (G) residues (Fig. 2.15a and 2.15b) of widely varying composition and sequence. By partial acid hydrolysis, alginate was separated into three fractions. Two of these contain almost homopolymeric molecules of G and M, respectively, while a third fraction consists of nearly equal proportions of both monomers. It was concluded that alginate could be regarded as true block copolymer composed of sequences of M (M blocks) and G (G blocks) residues interspersed with MG sequences (MG blocks) (Fig. 2.15c). The M/G

composition differs not only between one species of brown algae to another, but also between different parts of the same plant. The alginate monomer composition (i.e., M/G ratio) affects the physical properties of alginate and its resultant hydrogels. Alginate with a high M content is suited for thickening applications whereas that with a high G content is suited for gelation. The mechanism of gelation will be discussed in more detail in section 2.4.3.

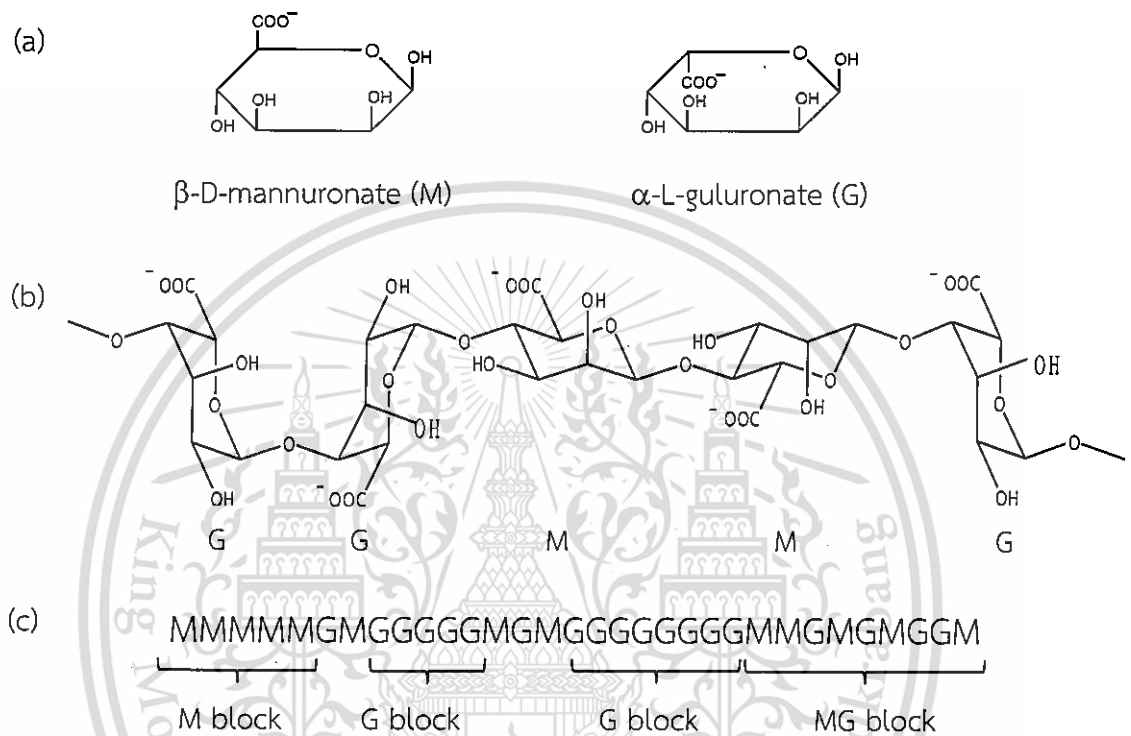

Figure 2.15 Structural characteristics of alginate: (a) alginate monomers, (b) chain conformation and (c) block distribution [156].

2.4.2 Properties of alginate

- Solubility [156]

The solubility of alginate in water is influenced by three parameters, i.e., pH of the solvent, ionic strength of the medium and the presence of gelling ions in the solvent [157]. To make alginate soluble, it is necessary that the pH has to be above a certain critical value and the carboxylic acid groups are deprotonated. It was reported that the dissociation constants for mannuronic and guluronic acid monomers are 3.38 and 3.65, respectively [158]. The pK_a value of the alginate differs only slightly from those of the monomeric residues. In addition, the change of ionic strength in an alginate solution has a profound effect, especially on polymer chain extension and solution viscosity. At high ionic strengths, the solubility is also affected. Alginate may be precipitated by high concentrations of inorganic salts like

potassium chloride [159]. Moreover, alginate can form gel in the presence of multivalent cations such as Ca^{2+}, Sr^{2+}, and Ba^{2+} ions. Therefore, it is essential to have an aqueous solvent free of crosslinking ions to enable dissolution.

- pH-sensitivity

The presence of carboxylic groups in alginate structure provides the alginate a remarkable sensitivity to external pH stimuli. The pH-sensitive behavior of alginate has been exploited to develop drug delivery system. It was reported that the release of drugs from alginate beads in low pH solutions was relatively low which could be a good candidate for an oral delivery system [160-161]. This is because alginate shrinks at low pH (gastric environment) and the encapsulated drugs are not released [162]. At low pH, the carboxylic acid groups of alginate are in the non-ionized form leading to an insoluble structure so-called alginic acid. When transfer into the higher pH of the intestinal tract, the carboxylic groups become ionized resulting in an increase of electrostatic repulsion of these negative charges causing polymer chain expansion and subsequently dissolution. However, the rapid dissolution of alginate in the higher pH ranges may result in burst release of drugs [163]. Thus, many modifications in the physicochemical properties are required for the prolonged controlled release of drugs.

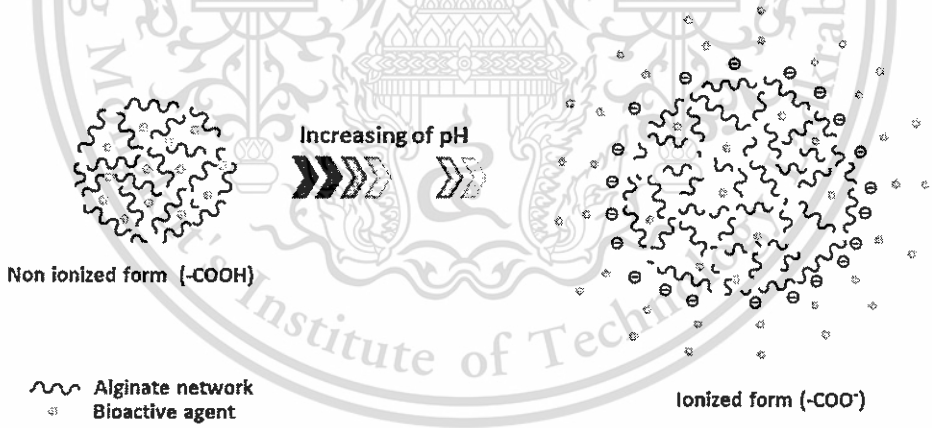

Figure 2.16 Schematic illustration of pH stimuli-responsiveness of alginate hydrogels [164].

- Biocompatibility [165]

Alginate is considered to be biocompatible, non-toxic, non-thrombogenic, and non-immunogenic. It has been approved by the Food and Drug Administration (FDA) for various medical applications (e.g., gel forming for dental impression materials and wound dressings). Moreover, alginate has been studied clinically for several applications, such as β-cell islet encapsulation for the treatment of type I diabetes

(DIABECELL® (Living Cell Technologies) ClinicalTrials.gov Identifiers NCT00940173, NCT01736228, NCT01739829), choroid plexus cell encapsulation for Parkinson's disease (NTCELL® (Living Cell Technologies), ClinicalTrials.gov Identifier NCT01734733) and glucagon peptide-1 (GLP-1)-transfected mesenchymal cell encapsulation for the treatment of space-occupying intracerebral hemorrhage (GLP-1 CellBeads® (CellMed AG, BTG), ClinicalTrials.gov Identifier NCT01298830).

- Biological property [165]

Mucoadhesive drug delivery systems work by increasing the drug residence time at the site of activity or resorption. It has been reported that polymers with charge density can serve as good mucoadhesive agents. An increased charge density provides better adhesion. It has also been reported that polyanion polymers are more effective as bioadhesives than polycation polymers or nonionic polymers. Alginate, being an anionic polymer, is a good mucoadhesive agent. Studies have shown that alginate has higher mucoadhesive strength as compared to polymers such as polystyrene, chitosan, carboxymethyl cellulose and poly(lactic acid) [166-167].

2.4.3 Gelation

Alginate hydrogels can be prepared by chemical and/or physical crosslinking of the polymer chains. The properties of the alginate hydrogels depend on the type of crosslinking, crosslinking density and molecular weight and composition of the alginate. The most common method for the formation of alginate gels is by crosslinking with multivalent cations. This method can take place under mild conditions, making it ideal for the entrapment of sensitive materials. The gelation of alginate occurs by an exchange of sodium ions from guluronic acid units with multivalent cations, and the stacking of these G blocks to form a characteristic "egg-box" structure (Fig. 2.17) [168]. Each chain can be linked with many other chains leading to the formation of a three dimensional network. Generally, divalent cations (e.g., Cd^{2+}, Co^{2+}, Cu^{2+}, Mn^{2+}, Ni^{2+}, Pb^{2+} and Zn^{2+}) are suitable crosslinking agents but not monovalent cations or Mg^{2+} [169].

The crosslinking metal ions show different affinities for alginate. Divalent alkaline ions (e.g., Ca^{2+}, Ba^{2+} and Sr^{2+}) bound mainly to GG segments while trivalent lanthanide ions (e.g., La^{3+}, Pr^{3+}, and Nd^{3+}) exhibit affinity for both GG and MM segments [170]. The differences in binding affinity are related to the ionic radius, coordination number of crosslinking ions and the presence of water of hydration surrounding ions [170]. It has been reported that divalent ions of larger ionic radii (e.g., Ba^{2+} and Sr^{2+}) produced stronger alginate hydrogels than Ca^{2+} ions [171].

In contrast, C.M. DeRamos et al. reported that the presence of water molecules surrounding Eu^{3+} ions may disrupt coordination binding in alginate cavities, thereby affecting effective crosslinking [170]. Furthermore, it has also been reported that alginate with high M content showed lower affinity to calcium than the alginate with high G content in a sodium-calcium ion exchange process [172]. Thus, hydrogels prepared from alginate with a high G content tend to form stronger, stiffer, more brittle and more porous gels. On the other hand, high M content results in gels which are more elastic and weaker [173]. The affinity of alginate towards divalent ions decreases in the following order: $Pb^{2+} > Cu^{2+} > Cd^{2+} > Ba^{2+} > Sr^{2+} > Ca^{2+} > Co^{2+} \sim Ni^{2+} \sim Zn^{2+} > Mn^{2+}$ [174].

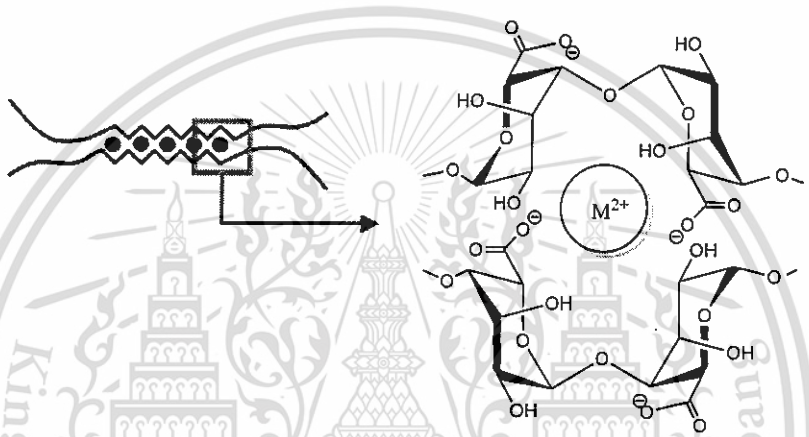

Figure 2.17 Formation of an alginate gel by multivalent cations, resulting in "egg-box" structure. Adapted from Ref. [168].

The gelation of alginate solutions with multivalent cations can be performed by two methods, i.e., external gelation and internal gelation [168]. For external gelation method, alginate is often dripped into a bath containing cations, such as a calcium chloride solution. The cations diffuse from the outside to the interior of the alginate droplets, and form an alginate hydrogel. This method is referred to as diffusion method. For internal gelation method, an insoluble calcium salt (e.g., calcium carbonate) is first mixed with the alginate solution. Calcium ions are subsequently released from the interior of the alginate phase by lowering the pH of the system and/or increasing the solubility of the calcium source, resulting in the formation of an alginate hydrogel.

In addition, when the pH of alginate solutions is lowered below the pK_a value, alginic acid gels are formed. This type of gels is stabilized by an intermolecular hydrogen bonding network. Two methods are generally used to produce alginic acid gels [175]. For the first method, a slowly hydrolyzing lactone such as glucono delta lactone (GDL) is added to a solution of sodium alginate. For

the second method, calcium alginate gels are converted to alginic acid gels by proton exchange.

2.4.4 Alginate-based hydrogels in controlled drug delivery

Alginate has been wieldy used for controlled drug release because it easily forms into three-dimensional networks in the presence of multivalent metal cations. Furthermore, alginate has pH-sensitive property; negative charges allow it to shrink in acidic pH but to swell when they are in neutral or basic pH. However, the use of SA alone for oral drug delivery leads to burst release of drug in intestinal environment, as mentioned in section 2.4.2. The most commonly used strategy to overcome this limitation is incorporation of alginate with other polymers. The literature reviews related about the utilization of alginate-based hydrogels in controlled drug delivery are shown as follows:

S. Hua et al. [20] developed pH-sensitive sodium alginate/poly(vinyl alcohol) (SA/PVA) hydrogel beads by combined Ca^{2+} crosslinking and freeze-thawing (FT) cycles in order to enhance the drug entrapment efficiency and improve the swelling behaviors of drug delivery system. The mixture solution of SA and PVA was firstly crosslinked with Ca^{2+} to form beads and then subjected to freezing–thawing cycles for further crosslinking. The swelling and pH-sensitive properties of the beads were investigated, and the drug loading and controlled release properties of the beads were also evaluated using diclofenac sodium (DS) as a model drug. The results indicated that the new DS-loaded dual crosslinked SA/PVA hydrogel beads were obtained with high encapsulation efficiency and sustained drug release profiles as compared to conventional calcium alginate beads. With increased content of PVA, these beads show decreased swelling capacity but increased stability in PBS of pH 7.4. The degradation of calcium alginate matrix in simulated intestinal fluid (SIF) was prevented by the incorporation of PVA and FT treatment. It was found that the release of diclofenac sodium was higher in SIF compared to simulated gastric fluid (SGF), indicating that the drug delivery system could be used as a release system for small intestine specific drug delivery.

T. Agarwal et al. [176] prepared calcium alginate (CA)-carboxymethyl cellulose (CMC) beads for colon-specific oral drug delivery. The CA-CMC beads were prepared by ionic gelation method. The swelling and mucoadhesivity of the beads were found higher at the simulated colonic environment. The CA-CMC beads degraded slowly in simulated colonic fluid, however the degradation rate increased drastically in the presence of colonic microflora. *In vitro* release study of anticancer drug 5-fluorouracil (5-FU) exhibited a release (> 90%) in the presence of colonic enzymes.

All results indicated that these beads could effectively protect the therapeutics from the harsh lytic environment of the stomach during its transit through the gastrointestinal tract and could preferentially deliver the drug at colon under the influence of colonic pH and microflora. It could be concluded that CA-CMC beads could be used for colon-specific drug delivery.

The hydrogels from the combination of chitosan and alginate have also been reported as follows:

M.A. Azevedo et al. [60] developed alginate/chitosan nanoparticles using a pre-gelation ionotropic method for encapsulation and controlled release of vitamin B_2. Firstly, vitamin B_2 and calcium chloride solution were added in the alginate solution. Then, chitosan solution was added dropwise into the previous solution to obtain B_2-loaded alginate/chitosan nanoparticles. Nanoparticles were characterized in terms of average size, polydispersity index (PDI), zeta potential and vitamin entrapment efficiency. The average size for alginate/chitosan nanoparticles was 119.5±49.9 nm for samples without vitamin B_2 and 104.0±67.2 nm with the encapsulation of vitamin B_2, presenting a PDI of 0.454±0.066 and 0.319±0.068, respectively. The nanoparticles showed encapsulation efficiency and loading capacity values of 55.9±5.6% and 2.2±0.6%, respectively. Release profiles were evaluated at different conditions showing that the polymeric relaxation was the most influent phenomenon in vitamin B_2 release. In order to study their stability, nanoparticles were stored at 4 °C and then their particles sizes and PDI were evaluated. It was found that this system was stable for at least five months.

L. Li et al. [28] studied the drug release characteristics from chitosan-alginate (CS-SA) matrix tablets containing different types of drugs. Theophylline, paracetamol, metformin hydrochloride and trimetazidine hydrochloride were used as model drugs exhibiting different solubilities (12, 16, 346 and > 1000 mg/mL at 37 °C in water). The concept of this work was that drugs were released from chitosan-alginate matrix tablets based on the theory of a self-assembled film-controlled release system. Tablets containing chitosan and alginate as polymer matrix were prepared by direct compression method. DSC studies demonstrated that *in situ* self-assembled film could be formed on CS-SA matrix based tablets surface in the simulated gastrointestinal tract. CS-SA matrix tablet was a combination of film coating and hydrophilic gel system. The formed film could limit polymer swelling and erosion. The release mechanisms of the four types of drugs were all anomalous non-Fickian diffusion transport and drug release occurred through diffusion in the hydrated matrix and polymer relaxation, but with different release kinetics. The effects of polymer

level and initial drug loading on release were dependent on drug properties. Drug release was influenced by the change of pH. On the other hand, the impact of ionic strength of the release medium was insignificant within the physiological range. Importantly, hydrodynamic conditions showed a key factor determining the superiority of the self-assembled film in controlling drug release compared with conventional matrix tablets. Thus, the new insight into chitosan-alginate matrix tablets could help to facilitate the optimization of this type of dosage forms.

The hydrogels based on the combination between chitosan and alginate exhibited significant potential for controlled drug delivery. These hydrogels incorporated the retarding drug release property of chitosan at high pH and of alginate at low pH. Furthermore, chitosan could form polyelectrolyte complexation with alginate in simulated gastrointestinal tract which would extend drug release ability. However, chitosan could not homogeneously blend with alginate since they immediately formed gel by ionic crosslinking between protonated amino groups of chitosan and carboxylate groups of alginate. As this point, water-soluble chitosan was usually replaced. The literature reviews related about the utilization of water-soluble chitosan/alginate hydrogels for controlled drug delivery are shown as follows:

S.C. Chena et al. [162] developed a novel pH-sensitive hydrogel system composed of *N,O*-carboxymethyl chitosan (NOCC) and alginate crosslinked by genipin for controlling protein drug delivery. The NOCC/alginate hydrogels were fabricated using a casting/solvent evaporation technique. Swelling characteristics of these hydrogels as a function of pH values were studied. In addition, release profiles of a model protein drug (bovine serum albumin, BSA) from test hydrogels were investigated in simulated gastric and intestinal media. At pH 1.2, the swelling ratio of the genipin-crosslinked NOCC/alginate hydrogel was limited due to the formation of hydrogen bonds between NOCC and alginate. At pH 7.4, the carboxylic acid groups on the genipin-crosslinked NOCC/alginate hydrogel became progressively ionized. In this case, the hydrogel swelled more significantly due to a large swelling force created by the electrostatic repulsion between the ionized acid groups. The amount of BSA released at pH 1.2 was relatively low (20%), while that released at pH 7.4 increased significantly (80%). The results suggested that the genipin-crosslinked NOCC/alginate hydrogel could be a potential candidate for site-specific protein drug delivery in the small intestine.

Y.H. Lin et al. [177] developed physically crosslinked alginate/ *N,O*-carboxymethyl chitosan (NOCC) hydrogels with calcium for oral delivery of

protein drugs. The microencapsulated beads were formed by dropping the mixture of alginate and NOCC into a $CaCl_2$ solution. These microencapsulated beads were evaluated as a pH-sensitive system for delivery of a model protein drug (bovine serum albumin, BSA). The main advantage of this system was that all processes used were carried out in aqueous medium at neutral environment, which may preserve the bioactivity of protein drugs. The swelling characteristics of these hydrogel beads at distinct compositions as a function of pH values were studied. It was found that the test beads with an alginate to NOCC weight ratio of 1:1 had a better swelling characteristic among all studied groups. With increasing the total concentration of the mixture of alginate and NOCC, the effective crosslinking density of test beads increased significantly and a greater amount of drug was entrapped in the polymer chains (up to 77%). The swelling ratios of all test groups were approximately the same at pH 1.2. In contrast, the swelling ratios of test beads at pH 7.4 increased significantly with increasing the total concentration of the mixture of alginate and NOCC, due to a larger swelling force created by the electrostatic repulsion between the ionized acid groups. It was observed that BSA was uniformly distributed in all test beads. At pH 1.2, retention of BSA in hydrogels could be improved by rinsing test beads with acetone (the amount of BSA released was below 15%). At pH 7.4, the amounts of BSA released increased significantly (~80%) as compared to those released at pH 1.2. With increasing the total concentration of the mixture of alginate and NOCC, the release of encapsulated proteins was slower. Thus, the calcium-alginate-NOCC beads with distinct total concentrations developed in the study could be used as a potential system for oral delivery of protein drugs to different regions of the intestinal tract.

I.M. El-Sherbiny [23] developed pH-responsive carrier system based on alginate and chemically modified carboxymethyl chitosan for oral delivery of protein drugs. Firstly, the microspheres were formed based on ionotropically-crosslinked mixture of sodium alginate and chemically modified carboxymethyl chitosan and then were coated through polyelectrolyte complexation with chitosan grafted with poly(ethylene glycol). The goal of the developed microspheres was to survive the harsh acidity of stomach and preferably release peptide and protein drugs in small intestine. Both ionotropic gelation and coating process were performed under mild aqueous conditions, which should be appropriate for retention of biological activity of protein drugs. The swelling studies of the developed hydrogel microspheres at 37 °C in both simulated gastric fluid (SGF) and simulated intestinal fluid (SIF) exhibited their pH-responsive nature. The *in vitro* biodegradation study of the microspheres was carried out in SIF at 37 °C in presence of lysozyme and showed

promising degradation rates. Bovine serum albumin (BSA) was entrapped in microspheres as a model for protein drugs and the *in vitro* release profiles were investigated at 37 °C in both SGF and SIF. The preliminary investigation of the hydrogel microspheres developed in this study exhibited a consistent swelling pattern, high entrapment efficiency and promising sustained release profiles of the model protein drug.

M. Tavakol et al. [24] studied sulfasalazine (SA) release from calcium crosslinked *N,O*-carboxymethyl chitosan (NOCC)/alginate beads coated by chitosan. The beads were sphere-like and had dense structure. At pH 1.2, the swelling degree of the beads was limited. On the contrary, at pH 6.8, the swelling degree of beads reached to a maximum and then decreased due to disintegration and dissolution of hydrogel network. The effect of coating, as well as drying procedure, on the swelling behavior of unloaded beads and SA release of drug loaded ones were investigated in simulated gastrointestinal tract fluid. The rate of swelling and drug release were decreased for air-dried and coated beads in comparison with freeze-dried and uncoated ones, respectively. No burst release of drug was observed from whole tested beads. Chitosan coated beads released approximately 40% of encapsulated drug in simulated gastric and small intestine tract fluid. Based on these results, the calcium crosslinked NOCC/alginate beads coated by chitosan could be used as potential polymeric carrier for colon-specific delivery of sulfasalazine.

J. Yang et al. [25] prepared pH-sensitive interpenetrating network hydrogels based on methoxy poly(ethylene glycol) grafted carboxymethyl chitosan (mPEG-*g*-CMCS) and alginate for oral drug delivery. The hydrogel beads without mPEG addition and those with PEG added by two different methods (physical mixing and chemical grafting) were prepared and studied. Bovine serum albumin (BSA) as a model for a protein drug was encapsulated in the hydrogel network, and the drug release properties were investigated. The results showed that the swelling ratio of mPEG-g-CMCS/alginate hydrogel beads was decreased in comparison with those without the addition of mPEG and those with mPEG added by physical mixing method, while the drug release behavior was increased. The loading capacity of the mPEG-g-CMCS/alginate hydrogel was enhanced in comparison with the one prepared by physical mixing method. The burst release of the protein was slightly decreased at pH 1.2, while the release at pH 7.4 was improved. All results suggested that the mPEG-g-CMCS/alginate pH-sensitive hydrogel was promising for site-specific protein drug delivery in the small intestine.

R. Gong et al. [26] developed a novel pH-sensitive hydrogel based on dual crosslinked alginate/*N*-α-glutaric acid chitosan (GAC). The homogeneous mixture of alginate and GAC was dropped into calcium chloride solution to form calcium crosslinked beads. Sequentially, the crosslinked beads were suspended in sodium sulfate solution for forming dual crosslinked beads. The swelling behaviors of dual crosslinked beads in simulated gastric fluid (SGF), simulated intestinal fluid (SIF) and simulated colonic fluid (SCF) were studied. Bovine serum albumin (BSA) was loaded into the beads by physical incorporation. The results showed that the gel beads swelled slightly at pH 1.2 and the BSA released is less than 18%, however, they swelled more at pH 6.8 and 7.4 and almost 100% of BSA was released from different weight ratios of alginate/GAC gel beads within 3 h. The results suggested that the dual crosslinked alginate/GAC hydrogel could be a good candidate of polymeric carrier for oral delivery of bioactive protein drugs.

A.F. Martins et al. [27] prepared *N*-trimethyl chitosan/alginate complexes. Firstly, *N*-trimethyl chitosan (TMC) of two quaternization degrees, DQ = 20 and 80 mol% and labeled as TMC20 and TMC80, were prepared. After that, polyelectrolyte complexes (PECs) of TMC/alginate were formed at pHs 2, 7 and 10 by mixing the aqueous solutions of unlike polymers. Using the TMC of DQ = 20 mol% and following the same methodology for preparing the PECs, beads of TMC20/ALG were obtained at pH 2 and loaded with curcumin (CUR) at pH 6.0-6.5. Studies *in vitro* of the controlled release of CUR from beads were investigated in simulated intestinal fluid (SIF) and simulated gastric fluid (SGF). Results suggested that the beads based on TMC20 and ALG presented potential as drug-carrier to improve the solubility and biological activity of CUR at pH close to physiological one.

From the literature reviews, among various types of water-soluble chitosan, carboxymethyl chitosan has been used the most in the combination with alginate. No attempt at using hydroxyethylacryl chitosan (HC) has been made. In this work, it was expected that the new drug delivery hydrogel materials could be developed by the effective combination of HC with alginate.

2.5 Crosslinking systems

It is well known that chitosan, chitosan derivatives and alginate demonstrate the affinity towards many metal cations. Therefore, in this work, hydrogel from HC and alginate was prepared using various metal cations, i.e., Ca^{2+}, Zn^{2+} and Cu^{2+} as crosslinkers.

2.5.1 Calcium ion

Calcium ion is the most frequently used as a crosslinking agent in alginate based hydrogels for drug delivery applications. This preference could be the acceptability of calcium by human organism because of its role as major component of the skeletal system as well as in the regulation of several physiological processes [164]. Calcium ions bind preferentially to the G blocks in the alginate resulting in the formation of an egg-box structure [178]. The formation of alginate gel by calcium ions are shown in Fig. 2.18.

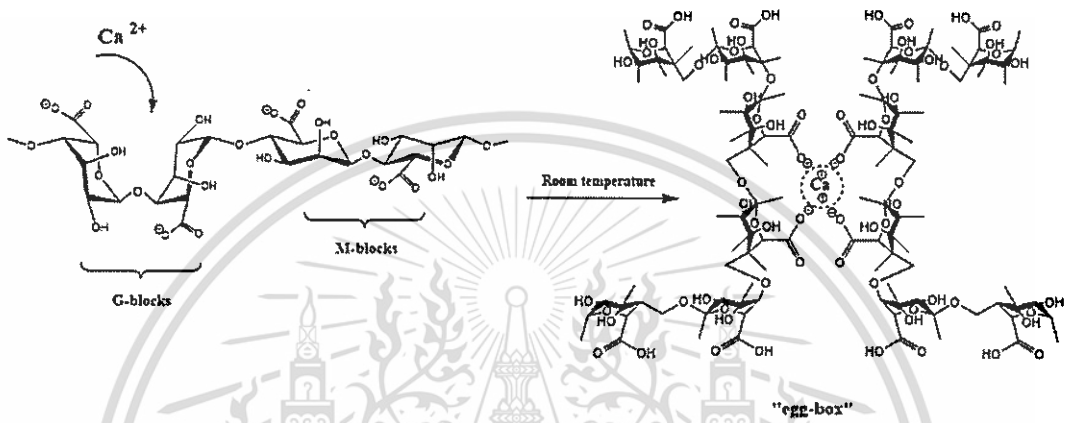

Figure 2.18 Schematic representation of the "egg-box" structure by major ionic interaction of carboxylate ions of alginate guluronate units and Ca^{2+} ions [164].

In addition, calcium ion can also bind to chitosan. J. Venkatesan et al. [179] proposed that there is a possibility to forms coordination bonds between $-NH_2$ of chitosan and Ca^{2+} of hydroxyapatite (Fig. 2.19). However, it has been reported that the introduction of Ca^{2+} ion did not directly influence the gelation behavior of chitosan. It was because chitosan has very limited affinity with alkaline-earth metals (e.g., Ca^{2+}) due to the absence of d and f unsaturated orbitals (unlike transition metals) [180].

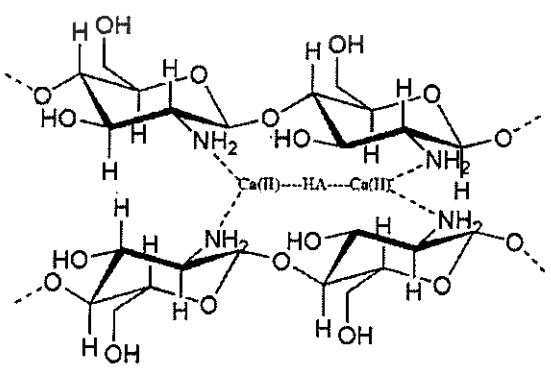

Figure 2.19 Interaction between $-NH_2$ of chitosan and Ca^{2+} of hydroxyapatite [179].

2.5.2 Zinc ion

Zinc ion has been used to crosslink alginate. M.O. Taha et al. [181] proposed that zinc ion can form coordinate covalent bonds with carboxylate groups of alginate (Fig. 2.20). In addition, it has been reported that zinc and calcium ions bind different sites of alginate [182]. While calcium ions bind only the G blocks, zinc ions are capable to crosslink G as well as M and MG blocks, allowing a more extensive three dimensional network. V. Pillay et al. [183] explained the different crosslinking mechanism of zinc and calcium ions on the basis of their different crystal structures and coordination numbers. In the case of Zn^{2+} ion, the peculiar crystal structure, together with the smaller atomic volume and ionic radius, results in a limited impedance to zinc ion diffusion into the alginate matrix and in higher cation content inside the polymeric binding sites. The higher content of zinc ions inhibits water molecules to permeate into the polymeric network, reducing the swelling. For this reason, zinc crosslinked alginate hydrogels have been for drug delivery applications to reduce the rate of release of encapsulated drugs.

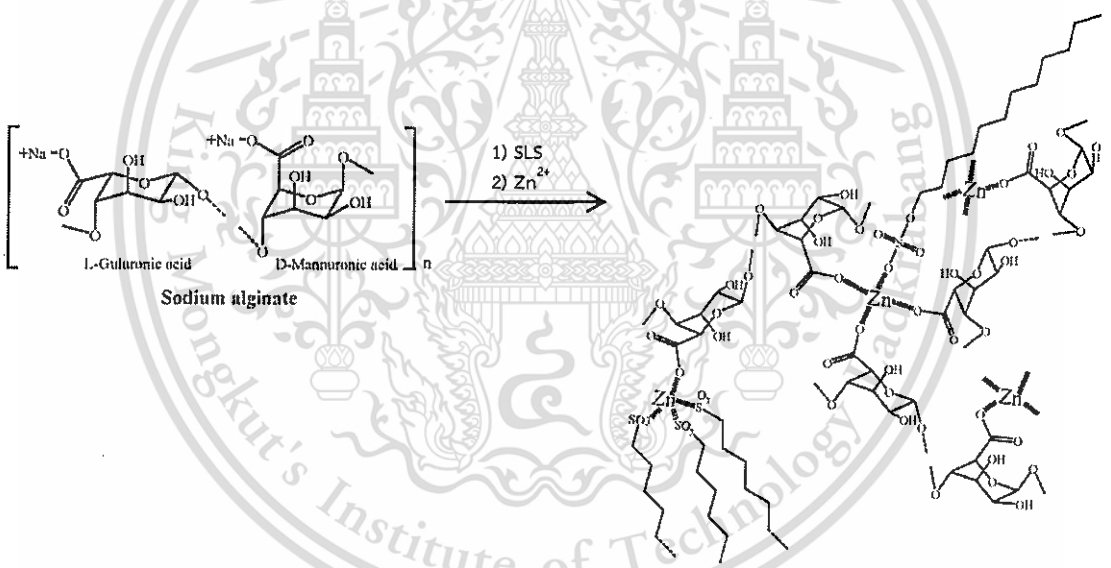

Figure 2.20 Representation of the formation of zinc crosslinked alginate-sodium lauryl sulfate (SLS) composite matrices [181].

Besides, zinc is one of the metal ions that are easiest to coordinate with chitosan. Chitosan binds Zinc ions through nitrogen, oxygen or a combination of them. X. Wang et al. [82] proposed the molecule structure of chitosan-Zn complexes with different chelate ratios as shown in Fig. 2.21. Fig. 2.21a corresponds to complexes with molar ratio of zinc and chitosan larger than 1:1, while Fig. 2.21b and 2.21c correspond to complexes with molar ratios equal to and fewer than 1:1, respectively.

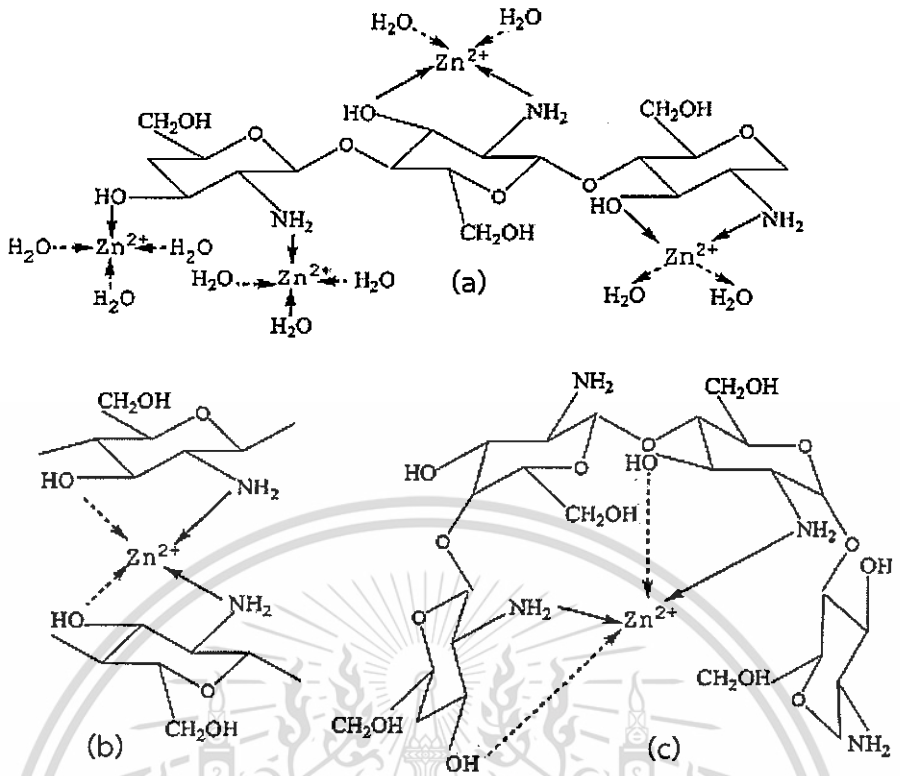

Figure 2.21 The reasonable structure of chitosan-Zn complexes [82].

2.5.3 Copper ion

Alginate has the ability to form gels in the presence of copper. Like zinc ions, copper ions were reported to be less selective in their binding to alginate. During crosslinking, the smaller ionic radii of Cu^{2+} (87×10^{-12} m) may translate to smaller impedance in their diffusion to the inner core of the alginate matrix as compared to Ca^{2+} (99×10^{-12} m) [184]. J.R. Rodrigues et al. [185] proposed the mechanism of copper ions binding to alginate as shown in Fig 2.22.

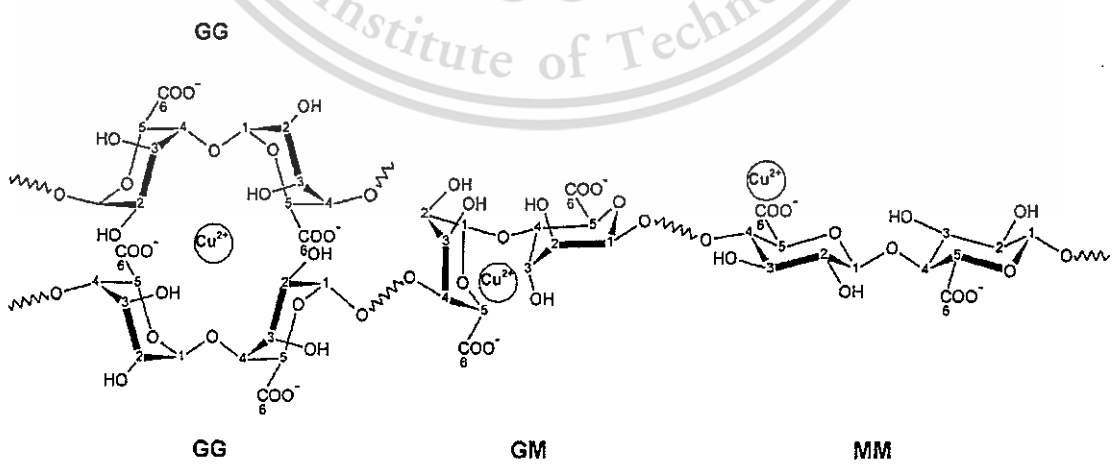

Figure 2.22 The probable interactions of the copper ions and alginate [185].

Furthermore, it is well known that chitosan has strong affinity to Cu^{2+} ions. Therefore, Cu^{2+} ions can also chelate with chitosan. Z. Modrzejewska et al. [81] proposed the structures chelate compounds of copper and chitosan as shown in Fig. 2.23. The proposed structure for the chitosan-Cu complex indicated that Cu^{2+} ions were likely to bond to three oxygen and one nitrogen ligands in a square-planar or a tetrahedral geometry.

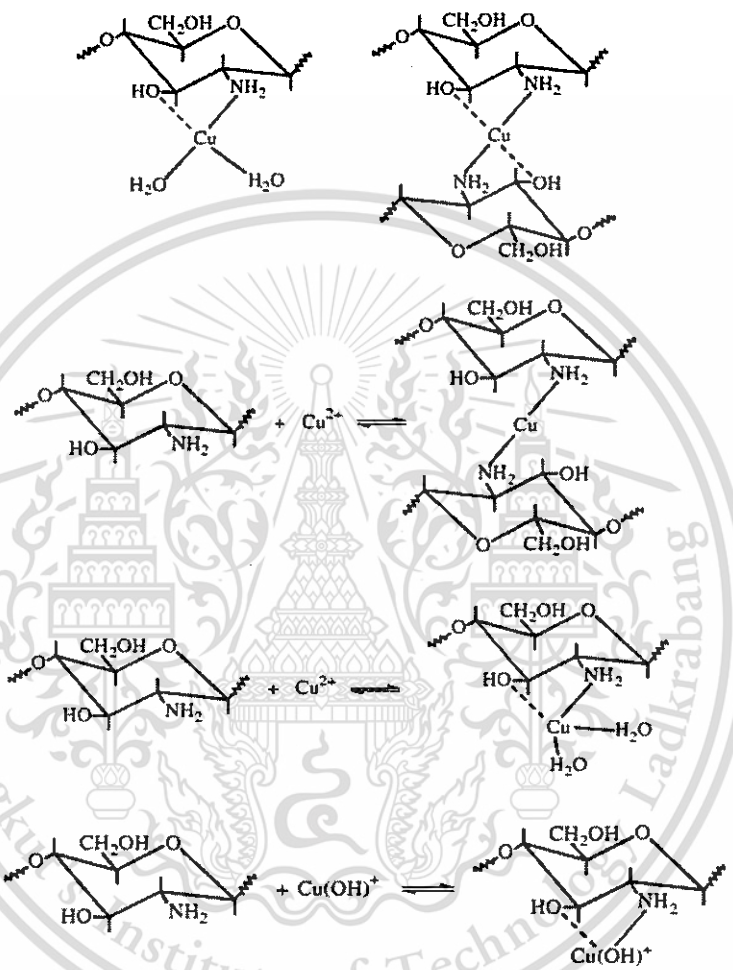

Figure 2.23 Structures chelate compounds of copper and chitosan [81].

Since capsule has been widely used to deliver a drug *via* the gastrointestinal tract, HC/SA capsules were prepared. The capsule is generally manufactured by dipping process. To achieve the desired shell distribution to manufacture capsule, it is necessary to ensure that the dipping composition adheres to the pin surface and quickly gels after withdrawing the pins from the dipping bath. Therefore, in this work, carrageenan as a gelling agent was added.

2.6 Carrageenan

2.6.1 Chemical structure of carrageenan [156]

Carrageenan is extracted from different species of Rhodophyta, e.g., Gigartina, Chondrus crispus, Eucheuma and Hypnea. Carrageenan is a mixture of linear polymers of sulfated galactans. Mostly, the chain is composed of alternating 3-linked β-*D*-galactopyranose (G-units) and 4-linked α-D-galactopyranose (D-units) or 4-linked 3,6-anhydrogalactose (DA-units). Other carbohydrate residues (e.g., xylose, glucose and uronic acid) and substituents (e.g., methyl ethers and pyruvic acid) are also present in carrageenan. There are three main types of carrageenan, which vary in their degree of sulfation, i.e., iota, kappa, and lambda carrageenans (Fig. 2.24). Kappa, iota and lambda carrageenans have one, two and three sulfate ester groups per disaccharide repeating unit, respectively.

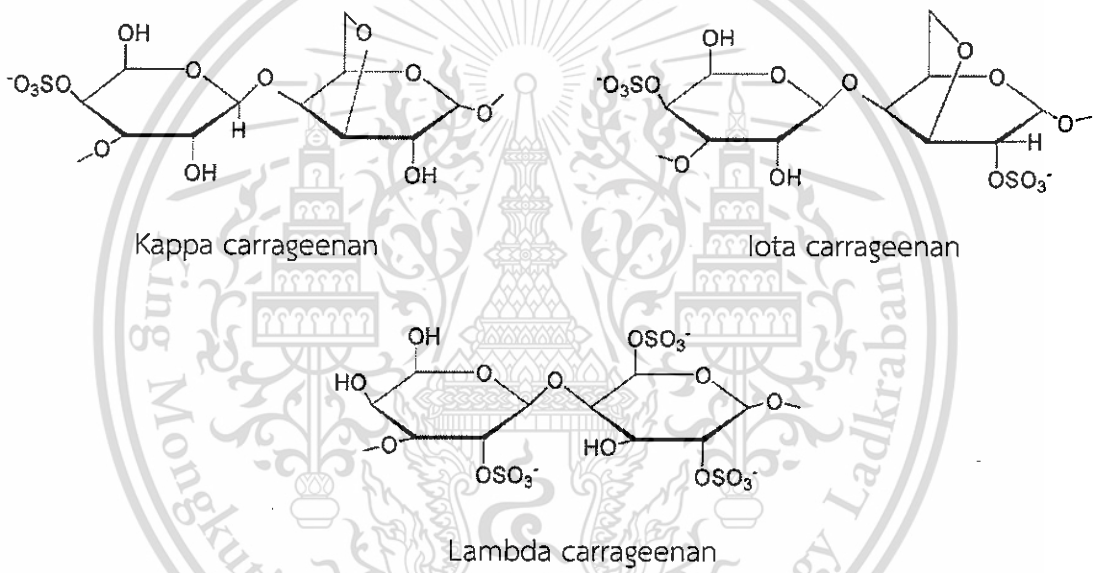

Figure 2.24 Chemical structures of kappa, iota and lambda carrageenans [186].

2.6.2 Properties of carrageenan

- Solubility [156]

Carrageenans are water-soluble, being insoluble in organic solvents, oil or fats. However, their solubility depends on the type of carrageenans, type and concentration of counter ions, temperature and pH. The most soluble carrageenan is lambda carrageenan, which lacks the more hydrophobic 3,6-anhydrogalactose and has three hydrophilic sulfate ester groups. Lambda carrageenan is readily water-soluble under most conditions. Kappa carrageenan is the most difficult carrageenan to dissolve. The sodium salt of kappa carrageenan is soluble in cold water, whereas, the potassium salt of kappa carrageenan is soluble only in hot solutions. Iota carrageenan has an intermediate solubility.

- Biological and toxicological properties [187]

Carrageenan shows several potential pharmaceutical properties including anticoagulant, anticancer, antihyperlipidemic, and immunomodulatory activities [188-189]. *In vitro* studies indicate that carrageenan has antiviral effects inhibiting the replication of hepatitis A viruses [190]. In addition, carrageenan is an extremely potent infection inhibitor for a broad range of sexually transmitted human papillomavirus [191]. Furthermore, carrageenan also exhibits antioxidant activity and free radical scavenging activity [192].

Because carrageenan is being used as food additive and pharmaceutical excipient, questions about its safety have been raised. Toxicological properties of carrageenan are as follows: LD_{50} (rat, oral) > 5 g/kg; LD_{50} (rabbit, skin) > 2 g/kg; 4 h LC_{50} (rat, inhalation) > 0.93 mg/L [193]. Carrageenan is nontoxic and nonirritating when used in nonparenteral pharmaceutical formulations [194]. However, due to sulfate groups, carrageenan shows adverse effects towards blood coagulations and immune system [195]. The presence of sulfate groups causes the strongest cytotoxicity [196]. The anticoagulant activity of carrageenans correlates with the contents of sulfate groups [197]. Therefore, extra care is required when formulating carrageenans into blood contact biomaterials, e.g., tissue recovery scaffolds or parental drug delivery vehicles.

2.6.3 Gelation

Only kappa and iota carrageenans are able to form gel. The former can form brittle gels and the latter forms soft gels. It is suggested that the presence of the anhydro bridges in kappa and iota carrageenan molecules are a key factor in gelation [198]. Carrageenan gels are thermally reversible. They start to form after cooling to about 50 °C and melt when heated [198]. At elevated temperatures, chains exist as random coils with a larger amount of conformational entropy. Upon cooling, entropy is reduced and chains re-orient into a more ordered conformation consisting of either double helix, aggregated mono-helices or aggregated helical dimers [199]. Kappa and iota carrageenans also exhibit gelation in the presence of mono- and di-valent cations. Several types of cations have different effects on the phase transitions and gelling of kappa and iota carrageenan gels. In case of iota carrageenan, the efficiency of cation ions in promoting the intermolecular association increases in the direction Na^+, K^+ and Ca^{2+} [200]. On the other hand, K^+ ions favor the gelation of kappa carrageenan.

Lambda carrageenan does not form gel. The 2-sulfate group of lambda carrageenan which is oriented towards the internal part of adjacent chains may prevent the formation of three-dimensional double helices [188].

From above mentions, kappa and iota carrageenans are typically used in gelling applications, whereas, lambda carrageenan is used in thickening applications [156].

Because capsule made from HC and SA was fragile and brittle, plasticizer was added. In this work, glycerol was selected.

2.7 Glycerol

Glycerol has a multitude of uses in pharmaceutical, cosmetic and food industries. As shown in Figure 2.25, glycerol is a simple polyol containing two primary and one secondary hydroxyl groups with a prostereogenic center at the C_2 position. It is a high boiling, viscous liquid that is colorless, odorless and hydroscopic [201]. It is completely soluble in water and alcohols, slightly soluble in ether and dioxane, but insoluble in hydrocarbon. In addition, glycerol is nontoxic to humans and the environment [202].

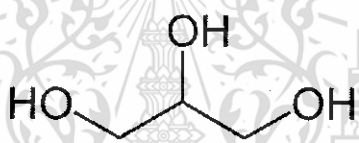

Figure 2.25 Structure of glycerol [201].

It has been reported that glycerol can be used as a plasticizer for polysaccharide film [203-205]. The low molecular size of glycerol allows it to occupy intermolecular spaces between polymer chains leading to the reduction of intermolecular forces among them. As a consequence, an increase in the free volume and, hence, in the molecular mobility is observed resulting in the lower values of glass transition temperature (T_g). A change in glycerol content affects the properties of the film. T_g of polysaccharide films strongly decreases with increasing glycerol content [206]. The literature reviews related about the glycerol plasticized polysaccharide film are shown as follows:

V. Epure et al. [203] developed glycerol-plasticized chitosan obtained by mechanical kneading. The glycerol-plasticized chitosan was ductile, whereas, the glycerol-free products are extremely brittle. It was found that the addition of glycerol resulted in a decrease of the tensile strength but a significant improvement in elongation properties is shown.

M. Altenhofen da Silva et al. [204] studied effects of the plasticizer concentration on the properties of alginate and pectin composite films crosslinked

with Ca^{2+} ions. The films were made by casting in two-stage crosslinking procedure. In the first stage a low reticulated film was prepared. After that, the obtained film was exposed for 30 min to 3% $CaCl_2 \cdot 2H_2O$ solutions containing glycerol. It was found that the increase in glycerol concentration in the finishing crosslinking solution decreased the tensile strength but increased the solubility in water, moisture content and elongation at break of the films. As a compromise between film mechanical resistance and flexibility, keeping low solubility and swelling in water, the use of 5-10% glycerol in the finishing crosslinking step is recommended. Concentrations lower than 3% glycerol produced brittle films and phase separation was observed on the film surface when concentrations higher than 12% glycerol were used.

P.V.A. Bergo et al. [205] studied the effect of glycerol contents on physical properties of cassava starch films. The increase in glycerol concentration caused a reduction on tensile strength and an increase of the elongation at break of films. These trends were probably due to the reduction in interactions between the biopolymers chains. The DSC results showed that the T_g of the prepared films decreased with increasing glycerol content. However, for samples with 30 and 45 g glycerol/100 g starch, two T_g curves were observed, probably due to a phase separation phenomenon.

2.8 Kinetic modeling of drug delivery

To describe the drug release rate from different drug delivery systems, a large numbers of kinetic models were developed. Some of important models are zero order, first order, Higuchi and Korsmeyer-Peppas model.

2.8.1 Zero order model [207]

This model describes the system that the release rate of drug is constant over a period of time and independent of its concentration. In its simplest form, zero order release can be represented as follows:

$$F = k_0 t \tag{2.3}$$

where F represents the fraction of drug released at time t and k_0 is the zero-order release constant.

To study of release kinetics, the graph is plotted between the cumulative percentage of drug released versus time.

2.8.2 First order model [207-208]

First order model is used to describe the absorption and/or elimination of some drugs. The release rate of this model is directly proportional to the amount of active agent load in the device. The drug release which follows the first order kinetic can be expressed by equation as follows:

$$\ln F = k_1 t \tag{2.4}$$

where F represents the fraction of drug released at time t and k_1 is the first-order release constant.

To study of release kinetics, the obtained data are plotted between log cumulative percentage of drug remaining versus time.

2.8.3 Higuchi model [207]

Higuchi model is suitable when the active agent has been dispersed in an insoluble matrix that can swell. This model assumes that the rate of dissolution of the active agent is faster than the rate of diffusion of active agent, which ensures the continuous release of active agent to the surrounding medium. The equation for this system is represented as follows:

$$F = k_H t^{0.5} \tag{2.5}$$

where F represents the fraction of drug released at time t and k_H is the Higuchi dissolution constant.

If a plot of the cumulative percentage of drug released versus the square root of time is linear, then drug release from the matrix is diffusion-controlled release.

2.8.4 Korsmeyer-Peppas model [208-209]

Korsemeyer–Peppas model describes drug release from a polymeric system. In order to find out the mechanism of drug release, an initial 60% drug release data can be fitted in this model. It is written in the form as follows:

$$F = kt^n \tag{2.6}$$

where F represents the fraction of drug released at time t, k is the rate constant and n is the release exponent indicating the drug release mechanism as given in Table 2.6.

Table 2.6 Release exponent and drug release mechanism from polymeric controlled delivery systems of different geometry [210].

Release exponent, n			Drug release mechanism
Thin film	Cylinder	Sphere	
0.50	0.45	0.43	Fickian diffusion
0.50 < n <1.00	0.45 < n <0.89	0.43 < n < 0.85	Anomalous diffusion
1.00	0.89	0.85	Case-II transport
n > 1.00	n > 0.89	n > 0.85	Super case-II transport

In case of thin film geometry, value of n = 0.5 indicates Fickian diffusion, or drug release that is diffusion-controlled, as in the Higuchi model. If the release exponent is in the range of 0.5 < n < 1, it indicates anomalous diffusion, or drug release that is both diffusion-controlled and swelling-controlled. If n = 1, it indicates case-II transport, or drug release that is zero-order, where the release rate is constant and controlled by polymer relaxation. Finally, when n > 1, it indicates super case-II transport, or drug release that is both swelling-controlled and erosion-controlled.

To study the release kinetics, the obtained data are plotted between log cumulative percentage of drug released versus log time.

Chapter 3
Research methodology

3.1 Materials

- Chitosan (CS; M_w 833,068 Daltons and DD = 94%), Eland Co., Ltd., Analytical grade
- Sodium alginate (SA; M_w 1,296,172 Daltons), Acros Organics Co., Ltd., Analytical grade
- Carrageenan, Union Chemical 1986 Co., Ltd., Food grade
- Hydroxyethylacrylate (HEA), Thai Mitsui Specialty Chemicals Co., Ltd., Commercial grade
- Acetic acid (CH_3COOH), Carlo Erba Reagents, Analytical grade
- Sodium hydroxide (NaOH), Laboratory Reagents & Fine Chemicals, Analytical grade
- Acetone (CH_3COCH_3), Zen Point, Commercial grade
- Glycerol, Carlo Erba Reagents, Analytical grade
- Calcium chloride dihydrate ($CaCl_2 \cdot 2H_2O$), Merck Millipore Ltd., Analytical grade
- Zinc sulfate heptahydrate ($ZnSO_4 \cdot 7H_2O$), Laboratory Reagents & Fine Chemicals, Analytical grade
- Copper(II) sulfate pentahydrate ($CuSO_4 \cdot 5H_2O$), Carlo Erba Reagents, Analytical grade
- Sodium chloride (NaCl), Laboratory Reagents & Fine Chemicals, Analytical grade
- Concentrated hydrochloric acid (HCl), Carlo Erba Reagents, Analytical grade
- 4'-Hydroxyacetanilide (Paracetamol), Merck Millipore Ltd., Analytical grade
- Phosphate buffered saline tablets, Merck Millipore Ltd., Analytical grade
- Sodium nitrate ($NaNO_3$), Carlo Erba Reagents, Analytical grade
- Acetate buffer, Sigma Aldrich Co., Ltd., Analytical grade
- Pullulan standard set, Sigma Aldrich Co., Ltd., Analytical grade
- Potassium bromide (KBr), Merck Millipore Ltd., Analytical grade
- Tetramethylsilane (TMS), Sigma Aldrich Co., Ltd., Analytical grade
- Acetic acid-d_4 (CD_3COOD), Sigma Aldrich Co., Ltd., Analytical grade
- Deuterium oxide (D_2O), Sigma Aldrich Co., Ltd., Analytical grade
- *Escherichia coli* (*E. coli*), Merck Millipore Ltd., Analytical grade
- *Staphylococcus aureus* (*S. aureus*), Merck Millipore Ltd., Analytical grade

- Dimethyl sulfoxide (DMSO), Sigma Aldrich Co., Ltd., Analytical grade
- Cation-adjusted Mueller-Hinton broth (CAMHB), Sigma Aldrich Co., Ltd., Analytical grade
- VERO Cell Line from African green monkey kidney, Sigma Aldrich Co., Ltd., Analytical grade
- Dulbecco's modified Eagle's medium (DMEM), Sigma Aldrich Co., Ltd., Analytical grade
- Fetal bovine serum (FBS), Sigma Aldrich Co., Ltd., Analytical grade
- Methylthiazolyldiphenyl-tetrazolium bromide (MTT), Sigma Aldrich Co., Ltd., Analytical grade
- Sodium dodecyl sulfate (SDS), Sigma Aldrich Co., Ltd., Analytical grade

3.2 Apparatus

- Nuclear magnetic resonance spectrometer (NMR), Bruker BioSpin AG, NMR 300 Ultra Shield
- Gel permeation chromatograph (GPC), Sithiporn Associates Co., Ltd., Waters 600E
- Fourier transform infrared spectrophotometer (FT-IR), PerkinElmer, Inc., Spectrum GX
- Scanning electron microscope-energy dispersive X-ray spectrometer (SEM-EDS), LEO Electron Microscopy Ltd., LEO1455VP
- Differential scanning calorimeter (DSC), Mettler-Toledo Ltd., DSC820
- X-ray diffractometer (XRD), Bruker BioSpin AG, D8 Advance
- Dynamic mechanical analyzer (DMA), UBM Co., E4000
- UV-Vis spectrophotometer (UV-Vis), BECTHAI Bangkok Equipment & Chemical Co., Ltd., Model Genesys los UV-Vis
- Microplate reader, Thermo Fisher Scientific Co., Ltd., Multiskan GO
- Universal Testing Machine (UTM), Lloyd Instruments Ltd., LR5K
- Water bath, Thermo Fisher Scientific Co., Ltd., Isotemp
- Ultrasonic Bath, Elma Electronic Inc., E30H
- Mechanical overhead stirrer, IKA® Works (Asia) Sdn Bhd, RW 20 Digital
- Propeller stirrer, IKA® Works (Asia) Sdn Bhd, R 1342 Propeller stirrer 4-bladed
- Hot plate, IKA® Works (Asia) Sdn Bhd, HS-5
- pH-meter, DKK-TOA Co., HM-20P
- Micropipette, Scilogex, LLC, Autoclavable Pipettor 200-1000 µL

- Thermostat, IKA® Works (Asia) Sdn Bhd, Euro-ST B
- Balance, Denver Instrument, TC-254
- Oven, Thermo Fisher Scientific Co., Ltd., Isotemp
- Vacuum oven, Thermo Fisher Scientific Co., Ltd., VT6060
- Halogen oven, Oxygen, KT-122
- Micrometer, Mitutoyo Europe GmbH, PK-0505SUE
- Hydraulic compression machine, Sang Thai Intertrade Co., BP1201
- Petri dish, Hycon, K1004
- Desiccator, Thai Pure Science Co., Ltd.
- Nylon 66 membrane (pore size 0.45 μm), Science Integration Co., Ltd.
- Capsule mold
- Magnetic bar
- Glassware

3.3 Experiment

3.3.1 Preparation of gastrointestinal fluids

3.3.1.1 Preparation of simulated gastric fluid (SGF, pH 1.2)

Simulated gastric fluid was composed of 7 mL concentrated HCl, 2 g NaCl and 1000 mL distilled water.

3.3.1.2. Preparation of simulated intestinal fluid (SIF, pH 7.4)

Simulated intestinal fluid was prepared by dissolving phosphate buffered saline tablets in 100 mL distilled water.

3.3.2 Preparation of hydroxyethylacryl chitosans (HCs)

Hydroxyethylacryl chitosans (HCs) were prepared by partially referring to the procedure of G. Ma et al. [12]. 1 g of CS was added into a solution of 100 mL of 1% w/v acetic acid. 4 g of hydroxyethylacrylate was then added to the solution. After that, the reaction was carried out with continuous stirring. The reaction temperature and the reaction time were varied from 60 to 90 °C and from 24 to 48 h, respectively, as followed in Table 3.1. After reaction, the solution was adjusted to a pH of 7 by using 10% w/v sodium hydroxide and then precipitated by dropping the solution into acetone. The precipitate was washed with plenty of acetone then dried under vacuum at ambient temperature to obtain HCs.

Table 3.1 Chemical ingredients for synthesis of HCs.

Sample	CS (g)	CH_3COOH 1% w/v (mL)	HEA (g)	Reaction time (h)	Reaction Temperature (°C)
HC1	1	100	4	48	60
HC2	1	100	4	48	80
HC3	1	100	4	24	90
HC4	1	100	4	48	90

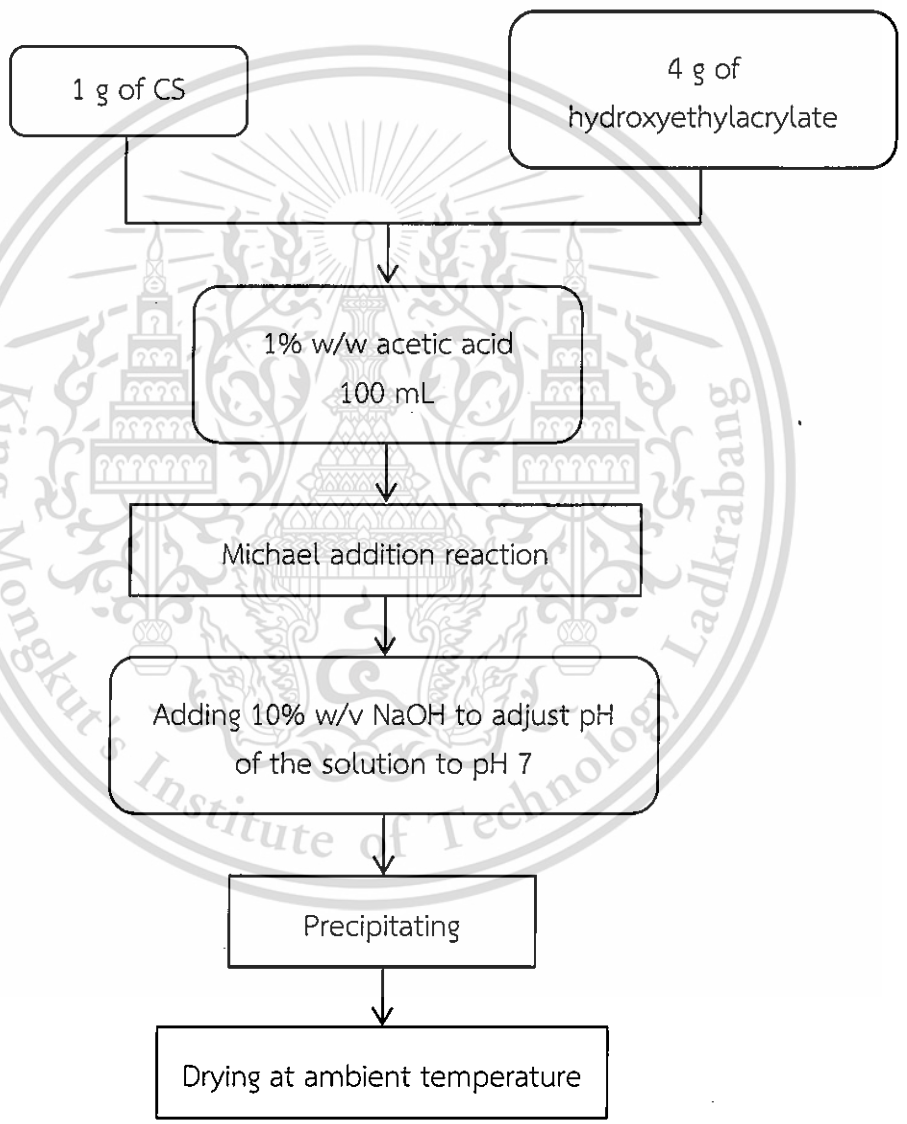

Figure 3.1 Schematic of preparation of HCs.

3.3.3 Testing and characterization of HCs

- Solubility test

Solubility of HCs in distilled water was evaluated at a concentration of 5 mg/mL at 70 °C. The resulting solutions were filtered through a nylon 66 membrane (pore size 0.45 μm) to ensure that the solutions were dissolved completely.

- GPC

The average molecular weights of HCs and CS were determined by GPC using pullulans as a standard. Samples (2 mg/mL) were dissolved in eluent (0.1 M sodium nitrate for HCs and acetate buffer for CS) and filtered using nylon 66 membrane (pore size 0.45 μm) before injection.

- FT-IR spectroscopy

FT-IR spectra were received using the potassium bromide pellet method. FT-IR spectra were collected over a range of 400-4,000 cm^{-1} with a resolution of 4.0 cm^{-1}.

- ^{1}H-NMR spectroscopy

^{1}H-NMR spectra were recorded using TMS as standard. CS was dissolved in a mixed solvent of CD_3COOD and D_2O, and HCs were dissolved in D_2O. Structure of CS and proposed structure of HCs are presented in Fig. 3.2.

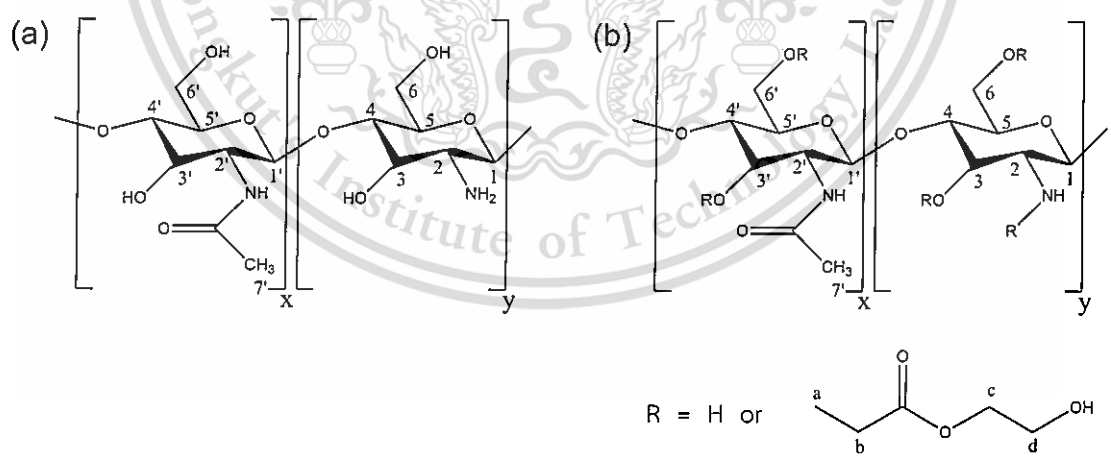

Figure 3.2 Structure of CS (a) and proposed structure of HCs (b).

The degree of deacetylation (DD) of CS was calculated with the method proposed by Hirai et al. [211] using Eq. 3.1. The degrees of substitution (DS) of HCs were calculated using Eq. 3.2.

$$DD = 1 - \left(\frac{1}{3}H_{7'}/\frac{1}{6}H_{2,2'-6,6'}\right) \quad (3.1)$$

where $H_{7'}$ is peak area for the signal from $-CH_3(7')-$ protons and $H_{2,2'-6,6'}$ is the summation of peak areas for the signal from –CH(2, 2', 3, 3', 4, 4', 5 and 5') protons and $-CH_2(6 \text{ and } 6')-$ protons.

$$DS = \frac{H_b/2}{H_{2,2'}} \quad (3.2)$$

Where H_b is peak area for the signal from $-CH_2(b)-$ protons and $H_{2,2'}$ is peak area for the signal from –CH(2 and 2')– protons.

- X-ray Diffraction

XRD patterns were studied using an X-ray diffractometer, starting from 2θ of 5–40° with a step size of 0.04° and a step time of 1 s.

- Antimicrobial test

Antibacterial activity against *Escherichia coli* (*E. coli*) and *Staphylococcus aureus* (*S. aureus*) was evaluated using broth microdilution method. Firstly, HCs were dissolved in DMSO to produce stock solution of 1280 µg/mL. After that, the stock solutions were diluted using CAMHB to obtain final concentrations ranging from 195-2500 µg/mL and added to 96-well plates. 100 µL of bacterial suspensions (adjusted to 5×10^5 CFU/mL) were added in each well. The plates were incubated at 37 °C for 24 h and examined for visible bacterial growth as evidenced by turbidity. The lowest concentration of antibiotic that prevented growth represented the minimal inhibitory concentration (MIC). Plates were examined in duplicate and the highest MIC value was recorded.

3.3.4 Preparation of HC/SA films

The HC was dissolved in distilled water under continuous stirring at 70 °C. After cooling to room temperature, SA was added to the HC solution with the weight ratios of (HC:SA) 100:0, 75:25, 50:50, 25:75, and 0:100 under continuous stirring to obtain an absolutely clear solution. The solutions were then poured into a Petri dish and dried at 40 °C to form HC/SA films with a thickness of 100±5 µm.

Table 3.2 Chemical ingredients for synthesis of HC/SA films.

Sample	Weight ratio	
	HC	SA
HC	100	0
HC75SA25	75	25
HC50SA50	50	50
HC25SA75	25	75
SA	0	100

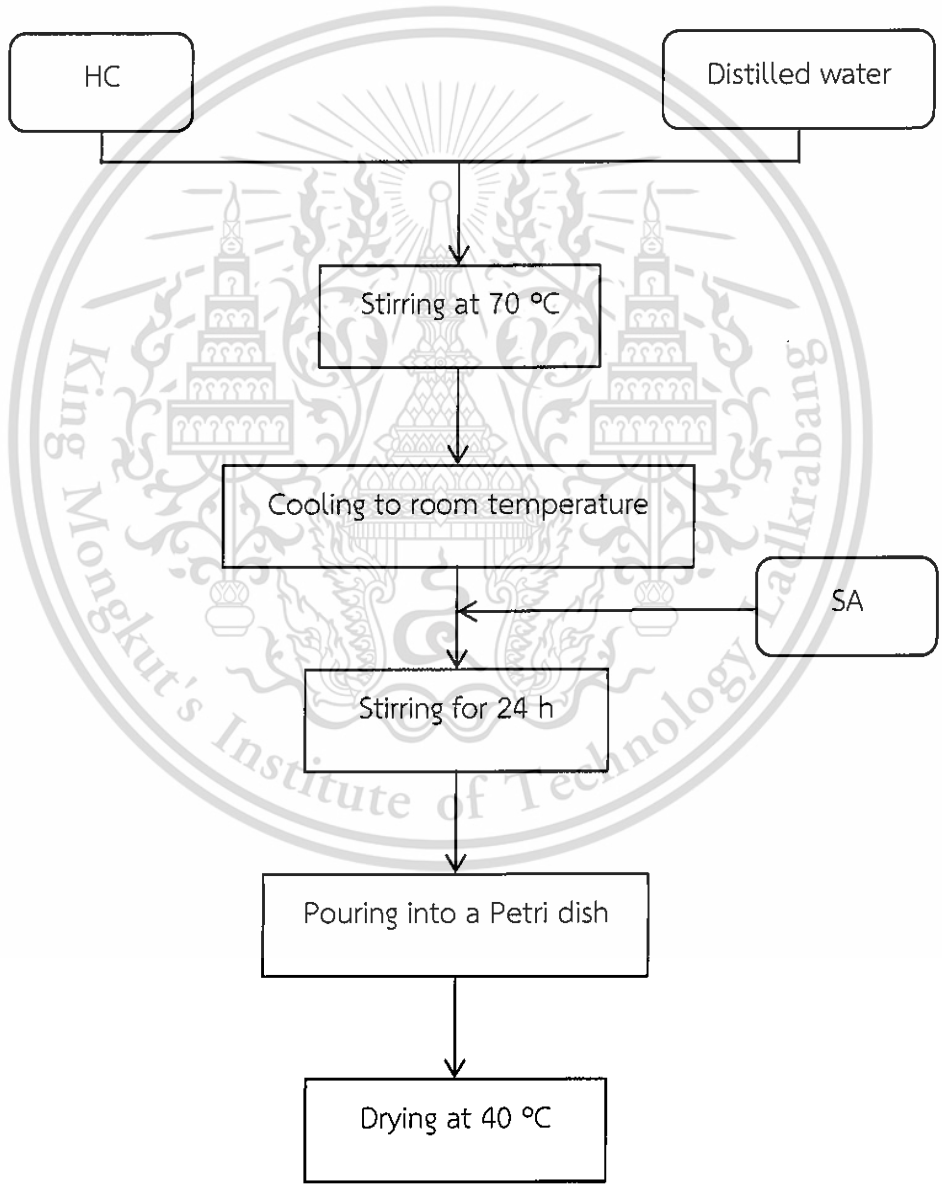

Figure 3.3 Schematic of preparation of HC/SA films.

3.3.5 Preparation of crosslinked HC/SA films

Firstly, the HC/SA films were cut into square pieces (1×1 inch^2). After that, they were soaked into 50 mL of metal ion solutions for 30 minutes. The concentrations of metal ion are listed below:

- 0.01, 0.05, 0.1, 0.25 and 0.5 M of calcium chloride solutions
- 0.5 M of zinc sulfate solution
- 0.5 M of copper(II) sulfate solution

The obtained films were immersed into distilled water for 30 seconds to purify and dried at 40 °C to obtain crosslinked HC/SA films.

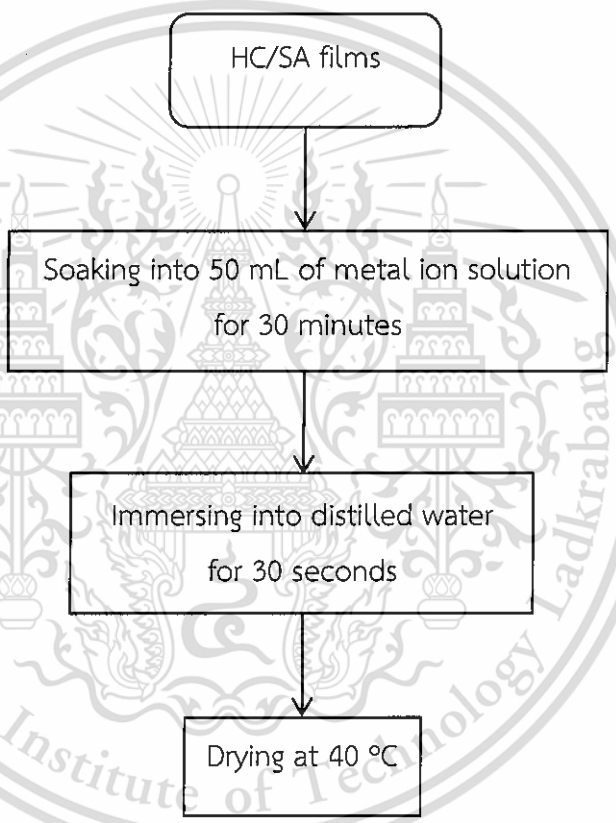

Figure 3.4 Schematic of preparation of HC/SA crosslinked films.

Table 3.3 Chemical ingredients for synthesis of HC/SA crosslinked films.

Sample	Weight ratio		Concentration of metal ions used (M)		
	HC	SA	Ca^{2+}	Zn^{2+}	Cu^{2+}
HC-Ca0.01	100	0	0.01	-	-
HC75SA25-Ca0.01	75	25			
HC50SA50-Ca0.01	50	50			
HC25SA75-Ca0.01	25	75			
SA-Ca0.01	0	100			
HC-Ca0.05	100	0	0.05	-	-
HC75SA25-Ca0.05	75	25			
HC50SA50-Ca0.05	50	50			
HC25SA75-Ca0.05	25	75			
SA-Ca0.05	0	100			
HC-Ca0.1	100	0	0.10	-	-
HC75SA25-Ca0.1	75	25			
HC50SA50-Ca0.1	50	50			
HC25SA75-Ca0.1	25	75			
SA-Ca0.1	0	100			
HC-Ca0.25	100	0	0.25	-	-
HC75SA25-Ca0.25	75	25			
HC50SA50-Ca0.25	50	50			
HC25SA75-Ca0.25	25	75			
SA-Ca0.25	0	100			
HC-Ca0.5	100	0	0.50	-	-
HC75SA25-Ca0.5	75	25			
HC50SA50-Ca0.5	50	50			
HC25SA75-Ca0.5	25	75			
SA-Ca0.5	0	100			
HC-Zn0.5	100	0	-	0.50	-
HC75SA25-Zn0.5	75	25			
HC50SA50-Zn0.5	50	50			
HC25SA75-Zn0.5	25	75			
SA-Zn0.5	0	100			

Table 3.3 Chemical ingredients for synthesis of HC/SA crosslinked films. (cont.)

Sample	Weight ratio		Concentration of metal ions used (M)		
	HC	SA	Ca^{2+}	Zn^{2+}	Cu^{2+}
HC-Cu0.5	100	0	-	-	0.50
HC75SA25-Cu0.5	75	25			
HC50SA50-Cu0.5	50	50			
HC25SA75-Cu0.5	25	75			
SA-Cu0.5	0	100			

3.3.6 Preparation of crosslinked HC/SA capsules

Firstly, size 0 capsule mold was made. Dimensions of the size 0 capsule are 7.650 mm in cap external diameter, 10.720 mm in cap length, 0.107 mm in cap thickness, 7.430 mm in body external diameter, 18.440 mm in body length and 0.104 mm in body thickness. A photograph of capsule mold is shown in Fig. 3.5.

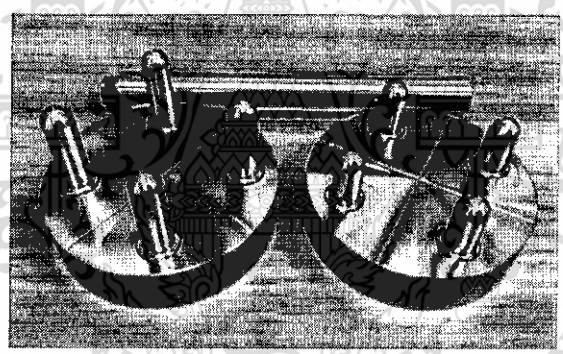

Figure 3.5 A photograph of capsule mold.

The mixtures with distinct HC:SA:carrageenan:glycerol weight ratios were prepared (Table 3.4). In detail, HC was dissolved in distilled water under continuous stirring at 70 °C. Subsequently, SA, carrageenan and glycerol were added to the HC solution to a final concentration of 6% w/v. The mixture was degassed and conditioned to 70 °C in a water sonication bath for 3 h. After that, the mixture was cooled to 50 °C. Then, the capsules were prepared by dipping a capsule mold into the mixture prepared above, followed by drying in halogen oven at room temperature for 12 h. The formed capsules were stripped and the rim of each shell was trimmed. After that, prepared capsules were soaked into 0.5 M of calcium chloride solutions for 30 min, subsequently immersed into distilled water for 30 seconds to purify and then dried at room temperature to obtain crosslinked HC/SA capsules.

Table 3.4 Chemical ingredients for synthesis of crosslinked HC/SA capsules.

Sample	Weight ratio				Concentration of calcium ions used (M)
	HC	SA	Carrageenan	Glycerol	
HC50SA50	21.25	21.25	42.50	15.00	-
HC50SA50Ca	21.25	21.25	42.50	15.00	0.50
SA	-	42.50	42.50	15.00	-
SACa	-	42.50	42.50	15.00	0.50

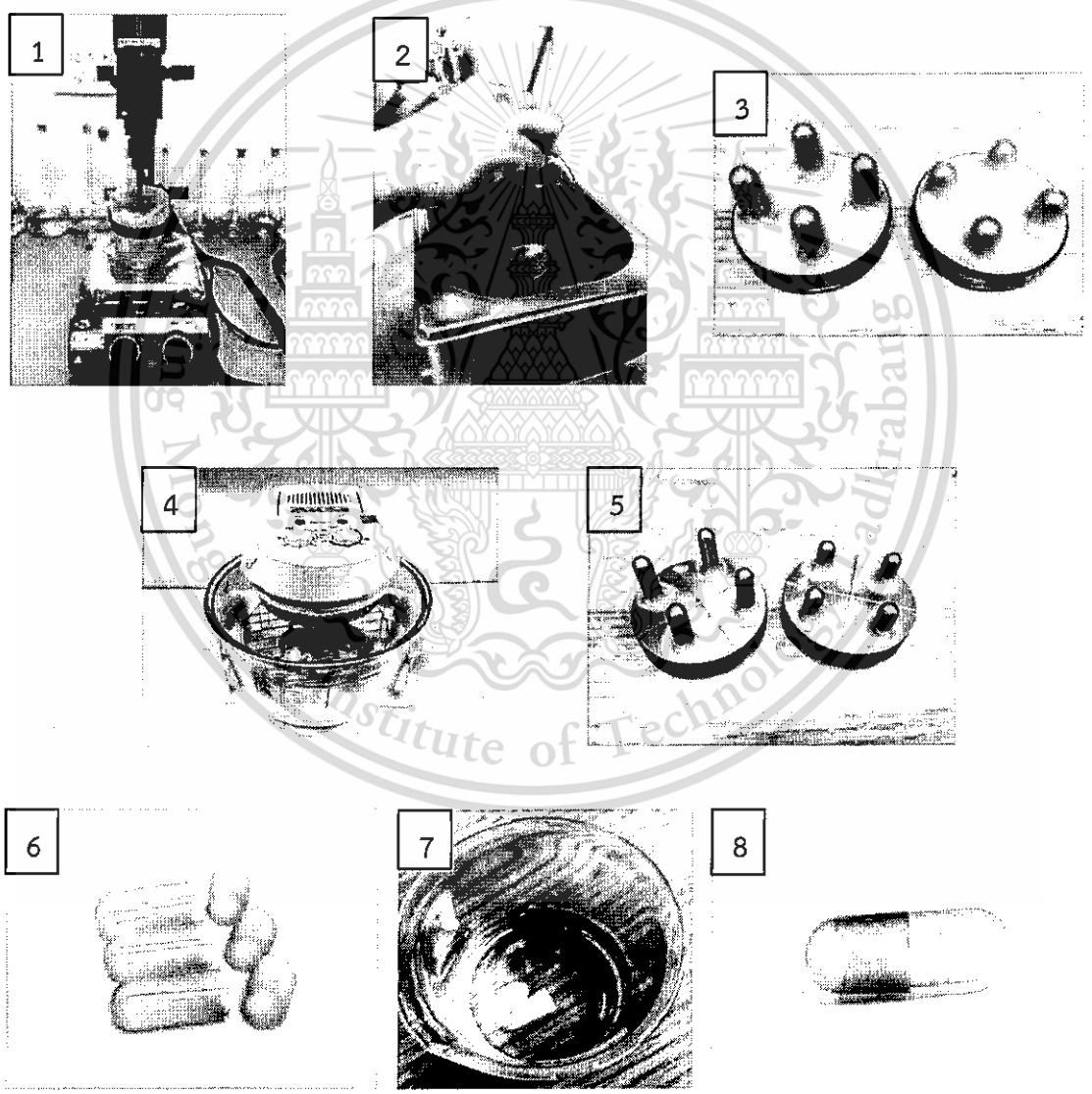

Figure 3.6 The process of preparation of crosslinked HC/SA capsules.

3.3.7 Testing and characterization of films and capsules

- DMA

The DMA experiments were carried out in the tension mode at a frequency of 1 Hz in a range of -30 to 200 °C at a heating rate of 2 °C/min.

- SEM-EDS

The surface morphology and distribution pattern of metal ions on the cross-sections of the films were examined by SEM-EDS. The films were fractured in liquid nitrogen, the sections of the films were coated with gold, then observed and photographed. The distribution pattern of metal ions was measured by EDS analysis.

- FT-IR spectroscopy

FT-IR spectra of the films were received using FT-IR. FT-IR spectra were collected over a range of 400-4,000 cm^{-1} with a resolution of 4.0 cm^{-1}.

- Swelling behavior

The degree of swelling and equilibrium value were determined gravimetrically. Dried samples of an appropriate size (1×1 $inch^2$) were weighed and then immersed into 100 mL of conditional fluids as follows:

- 0.01, 0.05, 0.1, 0.25, and 0.5 M of calcium chloride solutions at room temperature
- Distilled water at 37 °C
- Simulated gastric fluid (SGF, pH 1.2) at 37 °C
- Simulated intestinal fluid (SIF, pH 7.4) at 37 °C
- SGF for 2 h followed by SIF for 6 h at 37 °C

After an interval time, the swollen samples were taken from the fluids and the weights were measured. The swelling degree was calculated using Eq. 3.3. The samples were allowed to swell up within 24 h to ensure complete equilibrium swelling. The equilibrium swelling degree was calculated using Eq. 3.4.

$$\text{Swelling degree} = \frac{M_s - M_i}{M_i} \times 100 \quad (3.3)$$

$$\text{Equilibrium swelling degree (ESD)} = \frac{M'_s - M_i}{M_i} \times 100 \quad (3.4)$$

where M_s and M_i are the weights of the swollen wet sample and the initial dry sample, respectively. M'_s is the weight of the swollen wet sample at equilibrium swelling (24 h).

- Gel content

Dried samples of appropriate size (1×1 $inch^2$) were weighed and then immersed in 100 mL of conditional fluids as follows:

- Distilled water at 37 °C
- Simulated gastric fluid (SGF, pH 1.2) at 37 °C
- Simulated intestinal fluid (SIF, pH 7.4) at 37 °C
- SGF for 2 h followed by SIF for 6 h at 37 °C

After 24 h, the samples were then dried and weighed. The gel content was calculated using Eq. 3.5.

$$\%\text{Gel content} = \frac{M_d}{M_i} \times 100 \quad (3.5)$$

where M_i is the initial dry weight of the sample and M_d is the dry weight of the sample after immersion.

- DSC

DSC was used to study the state of water in the films. The swollen samples at the equilibrium state were frozen inside the DSC instrument chamber at −80°C, and then heated to 50 °C with a heating rate of 10°C/min. The equilibrium water content, freezing water content (including free and bound water) and non-freezing bound water content were calculated as follows:

$$\text{Equilibrium water content } (W_e) = \frac{M'_s - M_i}{M'_s} \times 100\% \quad (3.6)$$

where M_i is the weight of initial dry crosslinked film and M'_s is the weight of swollen wet crosslinked film at equilibrium swelling (24 h).

$$\text{Freezing water content } (W_f) = \frac{\Delta H_{endo}}{\Delta H_w} \times 100\% \quad (3.7)$$

where ΔH_{endo} is the area under the corresponding endothermic peak and ΔH_W is the heat of fusion of pure water (333.6 J/g) [212].

$$\text{Non -- freezing bound water content } (W_{nf}) = W_e - W_f \quad (3.8)$$

- MTT assay

Cytotoxicity of the films was assessed by Vero cell using an MTT assay. The films were immersed in PBS (pH 7.4) at 37 °C. After 24 h, each liquor stock was

obtained by filtering and then exposed in DMEM. Vero culture was cultured in a medium containing DMEM supplemented with 10% FBS and seeded in a 96-well plate at 100 µL/well and subsequently incubated at 37 °C for 24 h. Then, 100 µL of diluted liquor stock in DMEM was added to each plate and incubated at 37 °C for 24 h. Then, 10 µL of MTT solution (5 mg/mL) was added in each well and further incubated at 37 °C. After 4 h of incubation, the 9:1 mixture of DMSO:10% SDS was added in each well plate at a rate of 150 µL/well to dissolve the formazan crystals. Absorbance was measured at 570 nm using a microplate reader. The % cytotoxicity was calculated as follows:

$$\%\text{Cytotoxicity} = \frac{A-B}{A} \times 100 \quad (3.9)$$

Where A is the absorbance of the control and B is absorbance of the sample.

- *In vitro* drug release study

In vitro drug release profiles were studied using paracetamol as a soluble model drug. Before the drug release experiments, absorbance values of eight calibration solutions (0-0.02 mg/mL) were measured at 242 nm with a UV-Vis spectrophotometer. The specific absorbance was calculated from the slope of a standard calibration curve, obtained by plotting the concentration of the solutions against absorbance. To ensure that none of the other ingredients (HC, SA, carrageenan and glycerol) affected the UV absorption, 0.5% (w/w) solutions of HC, SA, carrageenan and glycerol were scanned between 200 and 600 nm, which yielded a flat spectrum with no absorption near the absorption maxima of paracetamol (242 nm).

Firstly, 0.15 g of paracetamol was loaded in to sealed bag formed by sealing HC/SA hydrogel film using aluminium adhesive tape and capsule. In case of sealed bag, paracetamol was compressed to a tablet (15 mm diameter x 1 mm thick) using hydraulic compression machine before loading. The photographs of drug-loaded sealed bag and capsule are shown in Fig. 3.7. The sealed bags and capsules were immersed in 100 mL of the SGF for 2 h, then removed and immediately immersed in 100 mL of the SIF for 6 h (37 °C). At selected time intervals, 0.2 mL of the fluid was examined and replaced by fresh fluid. The amount of released paracetamol from the sealed bag and capsules was determined the absorbance at 242 nm using a UV-Vis spectrophotometer. The percentage of released paracetamol was evaluated from standard calibration curve.

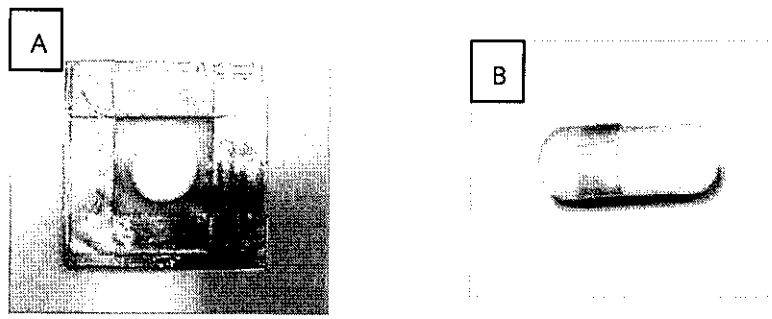

Figure 3.7 The photographs of drug-loaded sealed bag (a) and capsule (b).

- Analysis of *in vitro* drug release kinetics and mechanism

The *in vitro* drug release data were analyzed kinetically using various mathematical models, i.e., zero order, first order, Higuchi, and Korsmeyer-Peppas model.

$$\text{Zero order model: } F = k_0 t \tag{3.10}$$

where F represents the fraction of drug released at time t and k_0 is the zero-order release constant.

$$\text{First order model: } \ln F = k_1 t \tag{3.11}$$

where F represents the fraction of drug released at time t and k_1 is the first-order release constant.

$$\text{Higuchi model: } F = k_H t^{0.5} \tag{3.12}$$

where F represents the fraction of drug released at time t and k_H is the Higuchi dissolution constant.

$$\text{Korsmeyer} - \text{Peppas model: } F = kt^n \tag{3.13}$$

where F represents the fraction of drug released at time t, k is the rate constant and n is the release exponent indicating the drug release mechanism

The accuracy of these models was compared by calculation of squared correlation coefficient (R^2). In addition, the Korsmeyer-Peppas model is employed to characterize drug release mechanisms. When n is 0.5, it indicates Fickian diffusion. If n is in the range of $0.5 < n < 1$, it is defined as anomalous diffusion. If n is 1, it indicates case-II transport. Finally, when $n > 1$, it indicates super case-II transport [207-210].

Chapter 4
Results and discussion

4.1 Synthesis and characterization of hydroxyethylacryl chitosan (HC)

Chitosan (CS) has been widely used for biomaterials owing to its biocompatibility, non-toxicity, biodegradability and its antibacterial properties [8]. However, it is well known that CS cannot be dissolved in water above pH 6.5 because of its semicrystalline nature derived mainly from inter- and intramolecular hydrogen bonds, restricting its potential biomedical use. Chemical modification is helpful in improving the water solubility of CS. In this study, hydroxyethylacryl chitosan (HC) was synthesized by Michael addition reaction between CS and hydroxyethylacrylate (HEA). Mole ratio between CS and HEA used in the reaction was 1:6. The reaction temperatures were 60, 80 and 90 °C. Additionally, the reaction times were 24 and 48 h. The proposed route of HC synthesis is depicted in Figure 4.1.

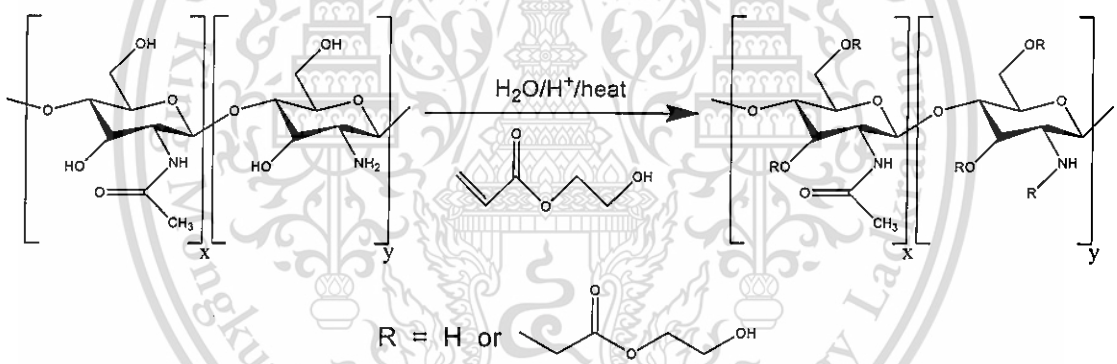

Figure 4.1 Proposed route of HC synthesis.

4.1.1 Degree of substitution (DS), weight average molecular weight (M_w), solubility and yield of HCs

Table 4.1 lists degree of substitution (DS), weight average molecular weight (M_w), solubility and yield of HCs synthesized by different reaction conditions. The DS was calculated from the peak area of ^{1}H-NMR spectrum. The method for calculating the DS is depicted in Appendix B. Generally, the amine group at C_2 position of CS can be easily alkylated. DS would be one when all amino groups were alkylated by Michael addition reaction. However, in some conditions, DS might be higher than one since two hydroxyl groups at C_3 and C_6 positions could also be alkylated. In this study, the DS values were 1.22-1.7, indicating that both amino groups and hydroxyl groups at C_3 and C_6 positions were alkylated. M_w of HCs was determined by GPC.

It was found that M_w of synthesized HCs were 46-62 kDa which was lower than unmodified CS (833 kDa). It was because acid hydrolysis could occur at β-(1-4) glycosidic bonds of the HC during Michael addition reaction. When increasing reaction temperature, the DS increased while M_w decreased. It was understandable that more reactants were activated at higher temperature resulting in increased reaction rate. However, at the reaction temperature of 90 °C, the reaction time showed no effect on DS. It might be because at high reaction temperature, the DS already reached the maximum value within 24 h.

The solubility of HCs in distilled water was evaluated at 70 °C using a concentration of 5 mg/mL. The results showed that all synthesized HCs could dissolve in water. As compared to CS, there was a report that CS with relatively low M_w (about 6500 Daltons) still could not dissolve in distilled water [213]. The solubility was directly related to their DS and M_w. It was found that it increased with increasing DS and decreasing M_w. It was because the presence of hydroxyethylacryl as side group disturbed the formation of ordered structure and the hydrogen bonding among CS chains. Another reason is that hydroxyethylacryl substituent is hydrophilic groups. Thus, the higher value of DS caused the higher hydroxyethylacryl group leading to improving the solubility. Moreover, the lower molecular weight also led to the lower intermolecular attraction forces resulting in increasing water solubility [214]. At the similar M_w (HC2 and HC4), HC4 (higher DS) could dissolve in water faster than HC2 (lower DS). Furthermore, compared to HC2, HC3 (higher M_w with higher DS) showed the better solubility in water. It could be concluded that the change of DS was the predominant factor affecting the solubility of modified CS in water.

The method for calculating yield of HCs is depicted in Appendix B. The HC1 exhibited the highest yield at about 80%. The results showed that the yield decreased with increasing solubility. It was because the higher solubility caused the higher dissolution during purification step.

In order to use the HC in biomedical applications, HC should dissolve in water without using acetic acid solution to allow its well mixing with other components and to avoid toxic to final product. However, in some applications, HC might contact with fluid during use. Thus, HC should not easily dissolve in water in order to stabilize its final shape. In addition, HC should be easily synthesized in high yield. From above mentions, HC1 was selected for the following studies. The structure of synthesized HC was characterized by FT-IR, ^{1}H-NMR and XRD. It will be discussed in detail in the following section.

Table 4.1 The DS, M_w, solubility and yield of HCs.

Formula	Reaction conditions	DS	M_w (Daltons)	Time used for dissolved at 70 °C (h)	Yield (%)
HC1	60 °C/48 h	1.22	62,700	72	80
HC2	80 °C/48 h	1.35	46,800	24	78
HC3	90 °C/24 h	1.70	57,900	12	59
HC4	90 °C/48 h	1.69	47,800	6	59

4.1.2 FT-IR analysis

FT-IR spectra of CS and HC are shown in Fig. 4.2. Compared to CS, HC showed excluding absorption peaks at 1,724 cm^{-1} indicating the C=O stretching of part of the hydroxyethylacryl group, and absorption peaks at 1,570 and 1,409 cm^{-1} due to the asymmetrical and symmetrical stretching of the –COO– groups [12, 215].

These additional peaks found in HC spectrum were the first evidence suggesting that HC were successfully prepared by Michael addition reaction. To confirm the results and obtain more details about structures, ^{1}H-NMR experiment was carried out.

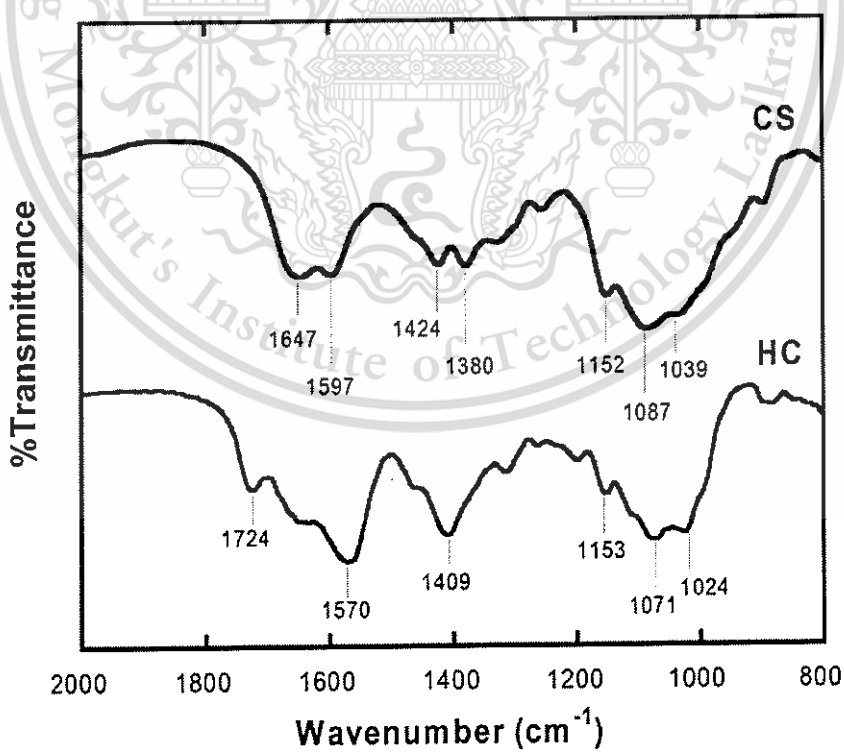

Figure 4.2 FT-IR spectra of CS and HC.

4.1.3 ^{1}H-NMR analysis

The ^{1}H-NMR spectra of CS in CD_3COOD/D_2O and HC in D_2O are shown in Fig. 4.3. After modification of CS, the peak corresponding to the $-CH_3$ (H7′) of *N*-acetylate was shifted from 1.79 to 1.89 ppm. The signals belonging to –CH(2 and 2′)– protons were also shifted from 2.90 to 2.83 ppm. New signals at δ = 2.45 and 3.15 ppm were assigned the to $-CH_2$(b)– proton and $-CH_2$(a)– proton, respectively. The multiplet signals from 3.6 to 4.0 ppm were attributed to –CH(3, 3′, 4, 4′, 5 and 5′)– and $-CH_2$(6, 6′, c and d)– protons. The DS values based on the amine position were calculated by the relative intensities from the peak area at about 2.45 ppm of the $-CH_2$(b)– proton against 2.8 ppm of the –CH(2 and 2′)– proton. The calculated DS data are shown in Table 4.1. Results confirmed that HC was successfully prepared *via* a Michael addition reaction of CS and hydroxyethylacrylate, corresponding to the FT-IR results.

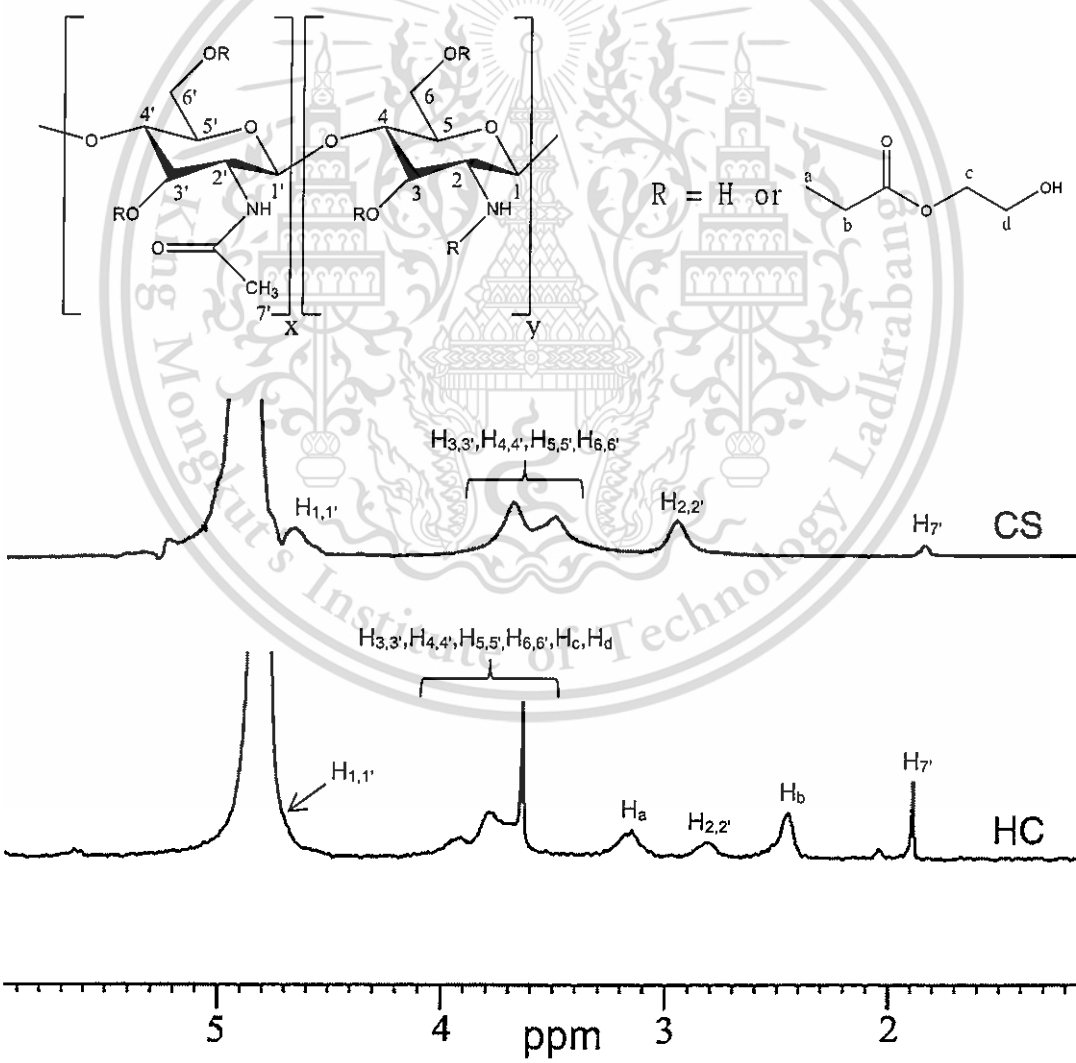

Figure 4.3 ^{1}H-NMR spectra of CS and HC.

4.1.4 XRD analysis

The structure of HC was also confirmed by X-ray diffraction studies. Fig. 4.4 shows the XRD patterns of CS and HC. CS showed two characteristic peaks around 2θ = 10.4° and 2θ = 19.76° assigned to crystal forms I and II, respectively [12]. HC, on the other hand, had a board halo pattern indicating lower crystallinity. It was ascribed to the presence of a bulky hydroxyethylacryl group that might hinder the formation of ordered structure and the hydrogen bonding among HC chains.

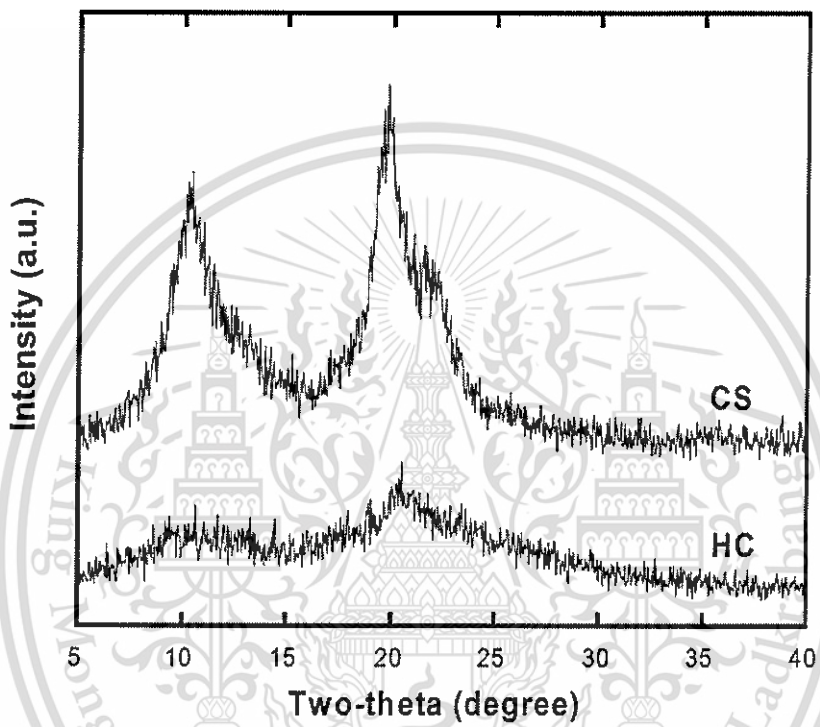

Figure 4.4 XRD patterns of CS and HC.

4.1.5 Antimicrobial analysis

The antibacterial activity of CS has been widely studied, and its practicability as an antimicrobial agent proven after many researches [125-126]. Generally, there is a strong association between antimicrobial activity of CS and its protonated amino group (NH^{+}_{3}). The protonated amino groups can interact with negatively charged groups at the surface of cells. This would prevent essential materials to enter the cells and/or lead to the leaking of fundamental solutes out of the cell. Furthermore, the binding of CS with the cell DNA (still *via* protonated amino groups) leads to the inhibition of the microbial RNA synthesis [111]. When HC has been prepared using the Michael addition reaction, there was a loss of partial amino groups, which led to low antimicrobial activity. Thus, in this study, the minimal inhibitory concentration (MIC) of HC was examined using broth microdilution method. HC showed antibacterial activity against *E. coli* and *S. aureus* with the MIC values of 6.250 and

3.125 mg/mL, respectively. The results proved that the synthesized HC still had antimicrobial ability against both *E. coli* (Gram-negative) and *S. aureus* (Gram-positive). Moreover, it was found that the action was more effective against *S. aureus* than *E. coli*. It is because the cell wall of *S. aureus* is fully composed of peptide polyglycogen. The peptidoglycan layer is composed of networks with plenty of pores, which allow foreign molecules to come into the cell easily. While the cell wall of *E. coli* is made up of a thin membrane of peptide polyglycogen and an outer membrane constituted of lipopolysaccharide, lipoprotein, and phospholipid. Because of the bilayer structure, the outer membrane is potential barrier against foreign molecules [216]. As mentioned above, the HC was difficult to penetrate into cell wall of *E. coli* than that of *S. aureus*. Therefore, HC was more effective against *S. aureus* than *E. coli*.

4.2 Characterization and properties of hydroxyethylacryl chitosan/ sodium alginate films (HC/SA films)

4.2.1 Miscibility

It is well known that blending is an effective method to enhance the performance of polymer. In this study, HC was blended with sodium alginate (SA). The miscibility is a very significant factor especially for a mechanical property of the blend. Polymer blends can be miscible when only one phase appeared after mixing of neat polymers. Therefore, only one glass transition temperature (T_g) should be recorded. The phase separation can be judged by the existence of two distinct T_g. For this reason a detailed analysis of the T_g of the prepared polymer blends is necessary to identify blend miscibility. In this study, the miscibility of HC/SA blends was estimated by DMA. Fig. 4.5 shows the temperature dependence of dynamic storage modulus (E'), dynamic loss modulus (E") and damping (tan δ), measured for films of HC, SA and HC/SA blends. It was found that the dynamic storage modulus of HC was lower than that of SA. It is because when the molecular structures of HC and SA are compared, HC has longer side chain than that of SA, hence it is difficult for molecules to arrange in close packing, thus allows the more free volume in the molecules, and therefore increases the mobility of the polymer chains. In HC film, one relaxation peak appeared at about 180 °C interpreting as motion of the side chain of HC. T_g of all the films were not clearly observed because both HC and SA have hydrogen bonding interactions between their molecules, restricting the chain motion. Therefore, the miscibility of HC and SA could not be proved by T_g of the film after blending. However, it was found that the dynamic storage moduli of the blends were located between those of the individual pure components in the order of the blend ratios (Fig 4.5a). These results might indicate that HC and SA were

compatible. It is reasonable because HC and SA have similar structure and hydrogen bonds can occur between HC and SA molecules. Moreover, appearance of all prepared films was transparent (Fig. 4.6). To confirm the results, FT-IR experiment was conducted.

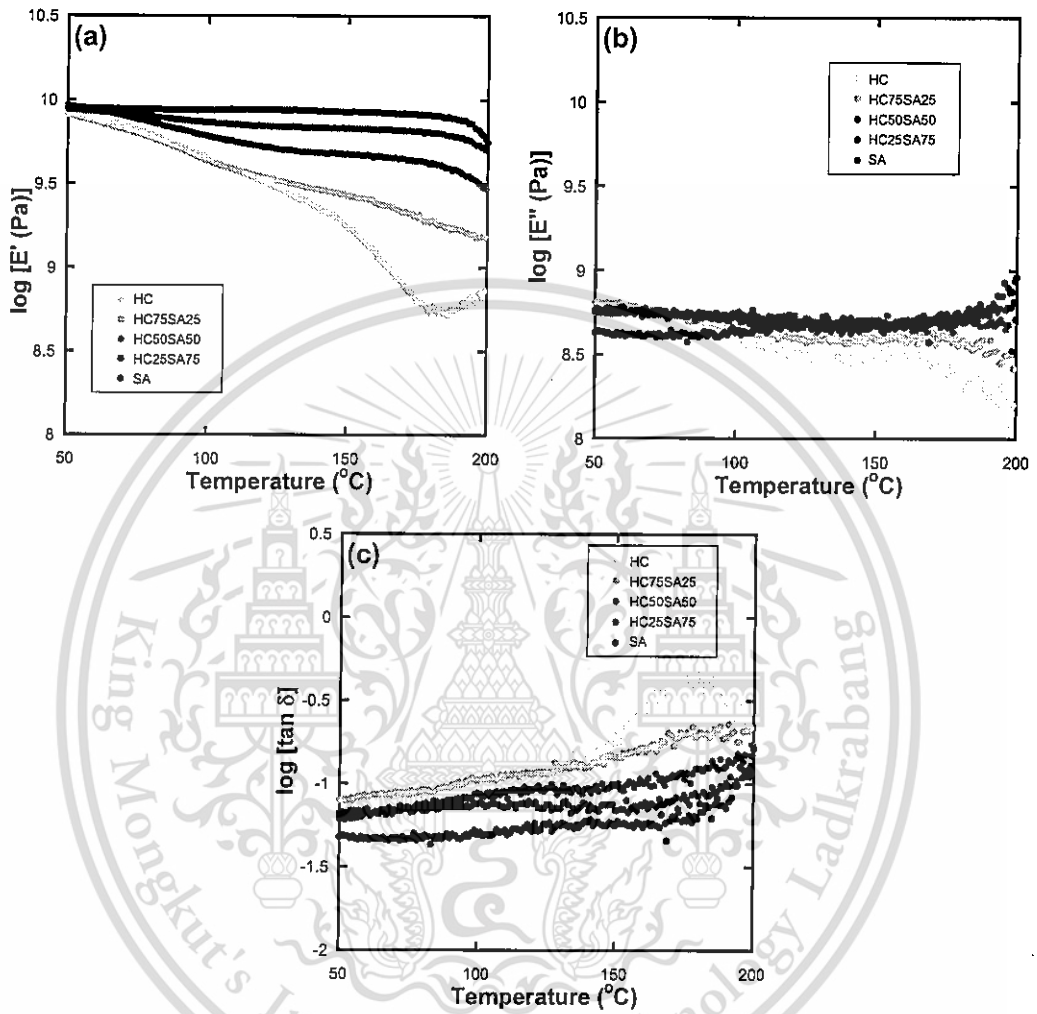

Figure 4.5 Temperature dependence of the E′ (a), E″ (b) and tan δ (c) of HC/SA films.

Fig. 4.7 represents the FT-IR spectra of HC, SA and HC/SA films. HC showed broad peak at 3367 cm^{-1} belonging to N–H and O–H stretching of HC molecules. The shoulder of peak at around 1724 cm^{-1} attributed to the C=O stretching part of the hydroxyethylacryl group of HC. The absorption peaks at 1574 and 1404 cm^{-1} assigned to asymmetrical and symmetrical stretching of the –COO– groups and characteristic peak at 1311 cm^{-1} assigned to N–H bending [217]. In the FTIR spectrum of SA, the characteristic peaks at 3392, 1607, 1416 and 1301 cm^{-1} corresponded to O–H stretching, $–COO^-$ asymmetric stretching, $–COO^-$ symmetric stretching and C–O stretching, respectively [20]. For HC/SA blended film (HC50SA50), the characteristic peaks were shifted from those of the neat HC and SA to be at 3376, 1603 and

1412 cm^{-1}, corresponding to the combination between HC and SA of O–H stretching, –COO– and $–COO^-$ asymmetric stretching, and –COO– and $–COO^-$ symmetric stretching, respectively. These evidences implied intermolecular interactions and good molecular compatibility between SA and HC, corresponding to the DMA results.

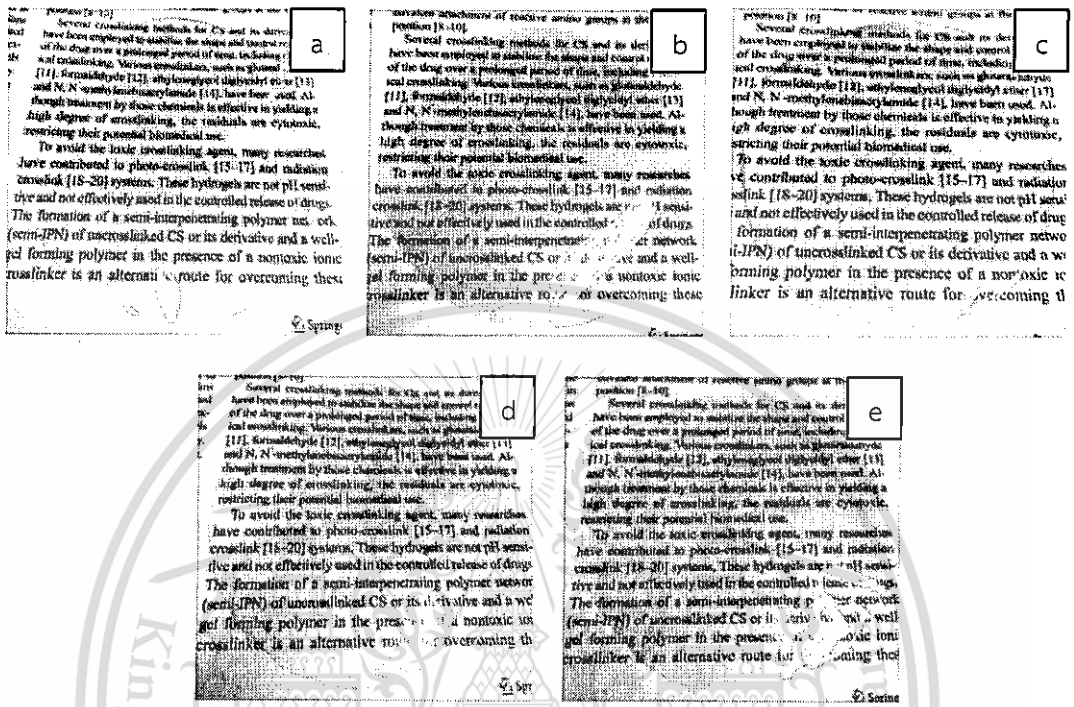

Figure 4.6 Photographs of different films: (a) HC film, (b) HC75SA25 film, (c) HC50SA50 film, (d) HC25SA75 film and (e) SA film.

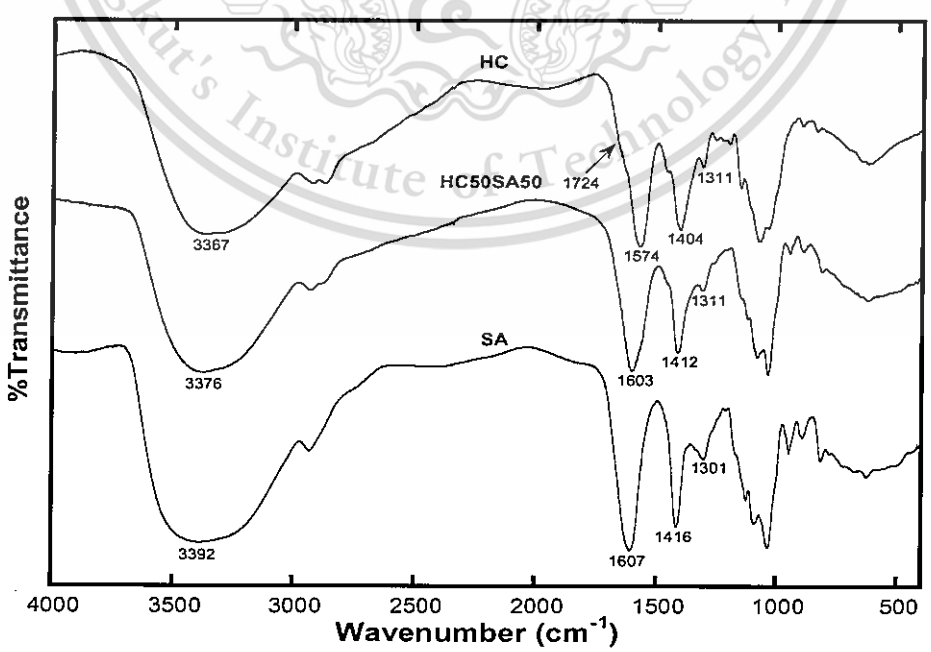

Figure 4.7 FT-IR spectra of HC/SA films.

4.2.2 Swelling behavior and gel content of HC/SA films in distilled water

Because the film might contact with water during use, the swelling behavior in distilled water at 37 °C was investigated. The dry films were exposed to the distilled water at 37 °C, the water penetrated into the films and then the swelling and the dissolution were occurred. Weight gain was calculated based on the initial dry weight of the film using Eq. 3.3. As seen in Fig. 4.8a, pure SA film was almost completely dissolved immediately after immersing in water. Similar result was reported by M.A. da Silva et al. [218]. While, the films containing HC tended to dissolve slower. These implied that the films with higher HC content exhibited higher stability than the lower one. Furthermore, the HC film did not show the decrease in swelling degree and its swelling degree reached 150 times. However, the initial shape of HC film could not be maintained in distilled water.

The gel content of the films after immersing in distilled water for one day is shown in Fig. 4.8b. It was found that the values of all prepared films were lower than 10% of their initial dry weights, therefore, the prepared films need to be crosslinked in order to improve their stability and stabilize their shape in water.

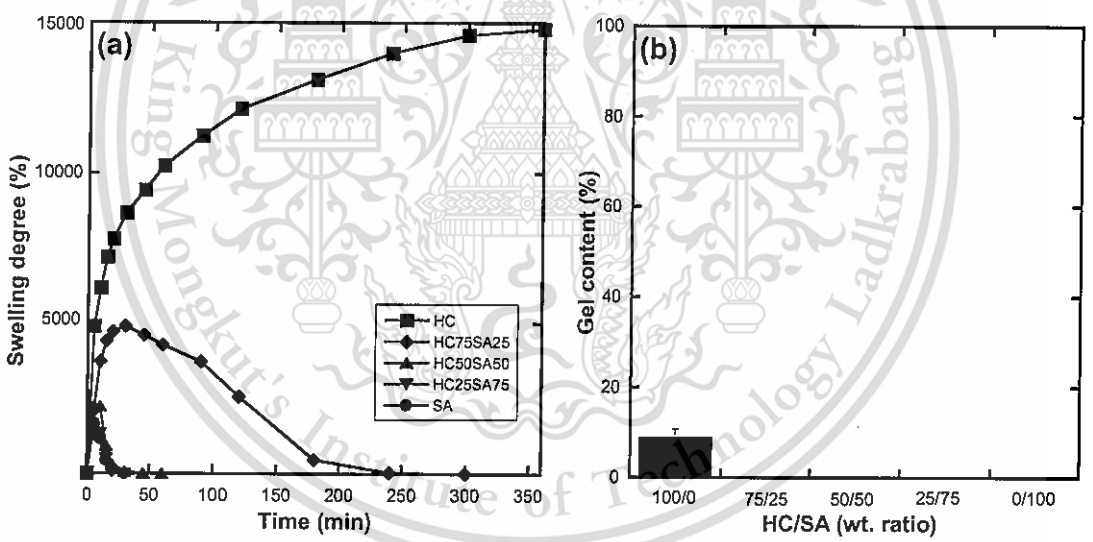

Figure 4.8 (a) Swelling degrees and (b) gel contents of the HC/SA films in distilled water at 37 °C.

4.2.3 *In vitro* swelling behavior and gel content of HC/SA films

The effects of the change in pH along the gastrointestinal (GI) tract from acidic in the stomach to basic in the small intestine on swelling behavior and gel content of the films have to be considered in order to predict the releasing behavior. Therefore, in this study, swelling behavior and gel content of the films in simulated gastric fluid (SGF), simulated intestinal fluid (SIF) and SGF followed by SIF were investigated.

4.2.3.1 Simulated gastric fluid (SGF, pH 1.2)

Swelling behavior of HC/SA films (with different weight ratio of HC/SA) in SGF at 37 °C was investigated. The results are shown in Fig. 4.9a. The HC film exhibited the highest degree of swelling at about 40 times and later decreased as partial dissolution occurred. The shape of HC film could not be maintained in SGF. This is because $-NHCH_2CH_2COOCH_2CH_2OH$ groups on HC can be protonated at pH 1.2 leading to the electrostatic repulsion among the ionized groups resulting in swelling and dissolution of HC film. While, the films containing SA showed higher stability than pure HC film in SGF. The decline in swelling degree of the films containing SA was not observed. In addition, the degree of swelling of the films decreased along with increasing the amount of SA. It is because $-COO^-$ groups on SA can turn to –COOH groups at low pH causing the strong hydrogen bond formations between carboxylic groups and hydroxyl groups resulting in a decrease in swelling degree. This phenomenon could be confirmed by FT-IR results. Fig. 4.10 represents FT-IR spectra of the films before and after immersing in SGF for 2 h. After immersing SA film in SGF (Fig. 4.10a), the intensity of the characteristic peaks at 1607 and 1416 cm^{-1} related to $-COO^-$ asymmetric and symmetric stretching, respectively, decreased. While, the new characteristic peaks observed at 1736 and 1242 cm^{-1} assigned to C=O stretching and C–OH vibrations (the combination between C–O stretching and C–O–H bending), respectively. In HC/SA blend films (Figs. 4.10b, 4.10c and 4.10d), the characteristic peaks around 1602 and 1412 cm^{-1} corresponded to the combination between HC and SA of –COO– and $-COO^-$ asymmetric stretching and –COO– and $-COO^-$ symmetric stretching, respectively. The intensity of these peaks decreased after immersing the films in SGF. The decrease in intensity related to the ratio between HC and SA. The intensity decreased along with increasing SA content because only $-COO^-$ group of SA changed form after immersing in SGF.

The gel content of the films after immersing in SGF for one day is shown in Fig. 4.9b. It was found that pure HC film mostly dissolved in SGF. The result suggested that HC film had low stability in SGF. Therefore, it could not be used alone as carrier for oral drug delivery in gastric environment. With increasing the amount of SA, the gel contents of the films increased significantly. Compared to the gel content in distilled water, the gel contents of the films containing SA in SGF were higher. It is due to the fact that $-COO^-$ groups on SA can turn to –COOH groups in SGF, as discussed earlier. The results implied that the films containing SA could be stable in SGF without using any external crosslinker.

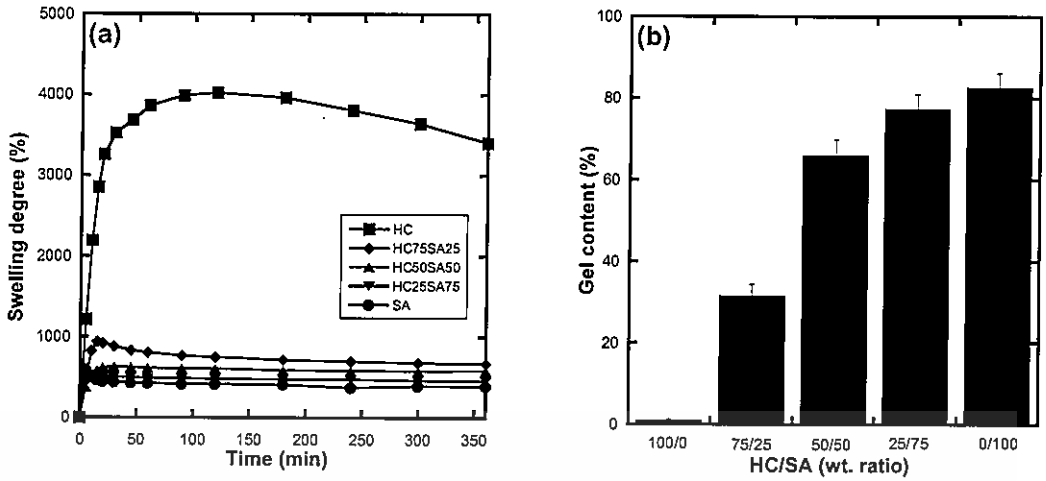

Figure 4.9 (a) swelling degrees and (b) gel contents of the HC/SA films in SGF at 37 °C.

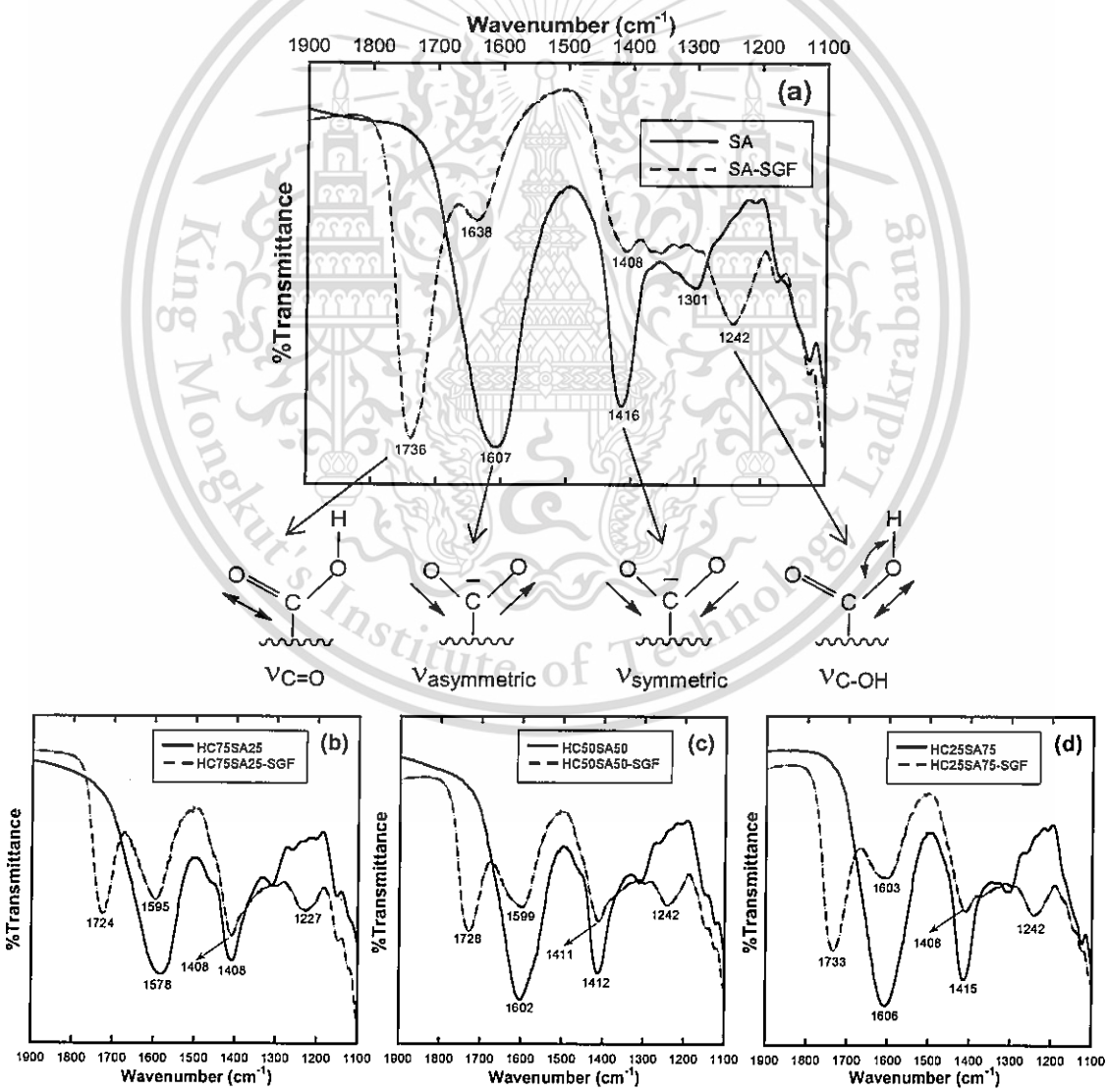

Figure 4.10 FT-IR spectra of (a) SA film, (b) HC75SA25 film, (c) HC50SA50 film and (d) HC25SA75 film before and after immersing in SGF for 2 h.

4.2.3.2 Simulated intestinal fluid (SIF, pH 7.4)

The swelling behavior of the films in SIF at 37 °C was investigated. The results (Fig. 4.11a) showed that HC/SA films rapidly absorbed the liquids and then disintegrated except HC film. It was found that the films with higher HC dissolved more slowly. The maximum swelling degree of HC film in SIF was approximately 37 times compared with that in distilled water at around 150 times. This phenomenon is due to the fact that pH of distilled water is approximately 6, while, pH of SIF is 7.4. Therefore, the swelling degree and dissolution rate of the films containing HC (pKa ~6.5) in SIF were lower than in distilled water [219].

The gel content of the films after immersing in SIF for one day is shown in Fig. 4.11b. All prepared films almost completely dissolved in SIF except HC film. The gel content of HC films in SIF was approximately 60% compared with that in distilled water at around 10%. This implied that HC film had quite high stability in SIF. However, the shape of the film could not be maintained.

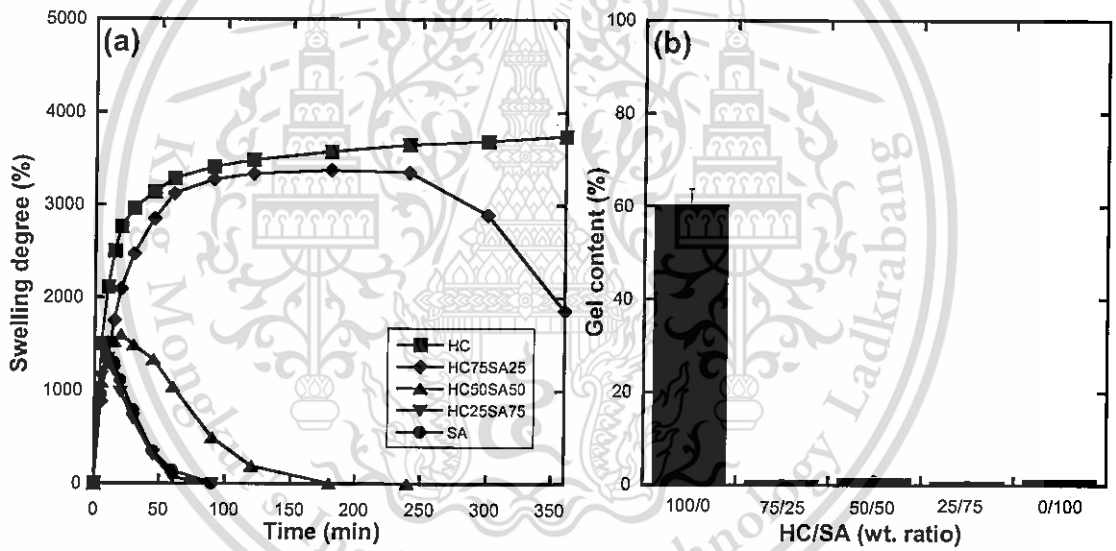

Figure 4.11 (a) swelling degrees and (b) gel contents of the HC/SA films in SIF at 37 °C.

4.2.3.3 Simulated gastrointestinal fluid (SGF followed by SIF)

The swelling behavior of the films in SGF (pH 1.2) for 2 h followed by in SIF (pH 7.4) for 6 h at 37 °C was investigated using simulated gastrointestinal fluid. Because the shape of HC film could not be maintained in SGF, it was not selected for the following studies. The results (Fig. 4.12) showed that the swelling degrees of all the films were quite stable in SGF within the first 2 h. When the films were transferred to SIF, the swelling degrees of the films containing HC decreased drastically. It could probably be explained by the formations of polyelectrolyte complexes between HC and SA as follows: In pH 1.2, HC was protonated

($-NH_2^+CH_2CH_2COOCH_2CH_2OH$), while SA was in its unionized form (–COOH), and there was less interaction between HC and SA. When the films were transferred to SIF, the $-NH_2^+CH_2CH_2COOCH_2CH_2OH$ on HC (pKa ~6.5) did not deprotonated immediately. Meanwhile, before the pH became greater than 6.5, –COOH on SA (pKa ~3.4-4.4) started to change to $-COO^-$, which could form polyelectrolyte complex with $-NH_2^+CH_2CH_2COOCH_2CH_2OH$ on HC, causing the elimination of some free water from the films. After the pH value reached 6.5, $-NH_2^+CH_2CH_2COOCH_2CH_2OH$ on HC started to deprotonated resulting in the partially destruction of polyelectrolyte complexes. Thus, the water was easily penetrated into the film and the swelling degree started to increase. This phenomenon was also found in chitosan-alginate. T. Zhang et al. reported that in situ chitosan-alginate polyelectrolyte complexation happened in gastrointestinal environment when physical mixtures of chitosan-alginate were employed as tablet matrix [220]. A schematic illustration of the formation of polyelectrolyte complexation of HC and SA in simulated gastrointestinal fluid was proposed in Fig. 4.13. On the contrary, the swelling degree of the SA film increased significantly after transferring to SIF. This was because carboxylic groups on SA were ionized in SIF causing hydrogen bond breaking. Without hydrogen bonds, the repulsive forces occurred between the ionized groups resulting in an increase of the swelling degree of the film. After reaching maximum value, the swelling degree of the SA film started to decline as dissolution occurred. The swelling degree of HC75SA25 film also decreased after reaching maximum value because this film had high HC which easily dissolve in SGF where almost 50% of its weight loss during immersion time as the result shown in Fig. 4.14a. Thus, after transferring to SIF, the film suffered from the dissolution in SGF was easily disintegrated in SIF. For HC50SA50 and HC25SA75 films, the decline in the swelling degree of the films was not observed. It suggested that the combination between HC and SA could delay the degradation rate of the films in SIF because of the formations of polyelectrolyte complexes between HC and SA during the transfer of the film from SGF to SIF. Unlike direct immersing of the HC/SA films in SIF, these films tended to degrade as there was no polyelectrolyte complex among HC and SA structures.

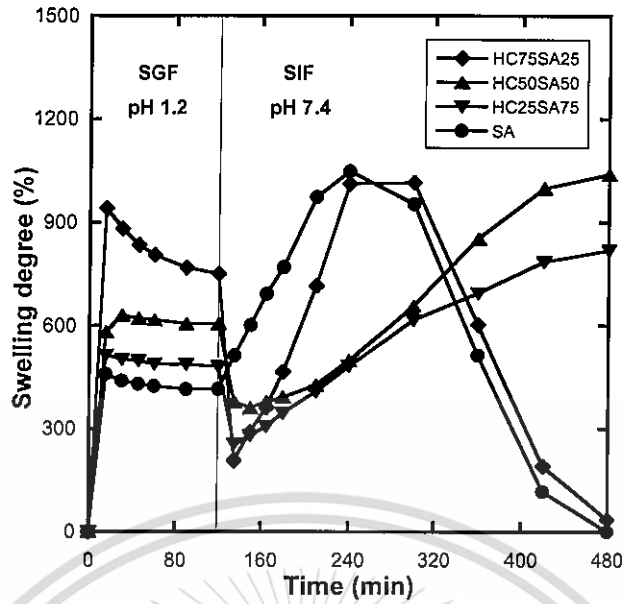

Figure 4.12 Swelling degrees of the HC/SA films in simulated gastrointestinal fluid at 37 °C.

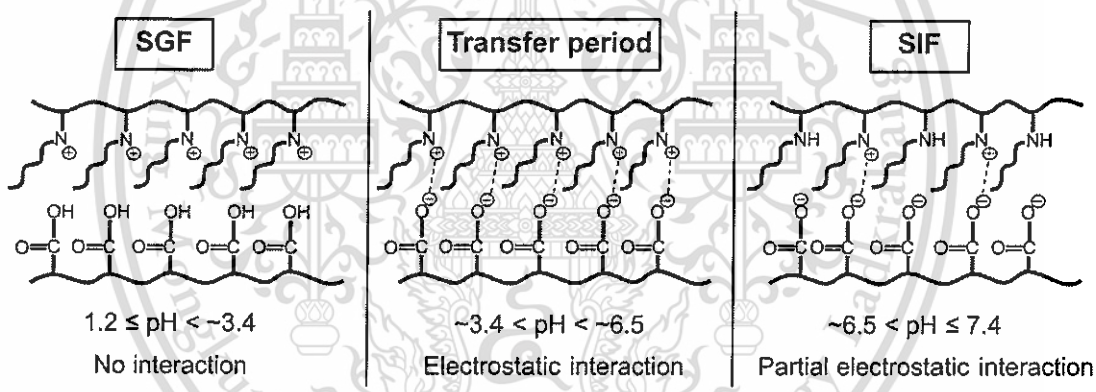

Figure 4.13 The proposed schematic illustration of the formation of polyelectrolyte complexation of HC and SA in simulated gastrointestinal fluid.

The gel contents of the HC/SA films after immersing in SGF for 2 h and in SGF for 2 h followed by SIF for 6 h were investigated to study stability of HC/SA films in simulated gastrointestinal fluid (Fig. 4.14). It was found that the gel contents of the films immersed in SGF for 2 h were relatively high (> 50%). After transferring to SIF for 6 h, the SA film was completely dissolved because there was no complexation between HC and SA. In case of HC75SA25 film, the gel content value was also relatively low because HC could be dissolved in SGF. While, the gel content values of HC50SA50 and HC25SA75 films were higher than 50%. This confirmed that HC could form polyelectrolyte complexation with SA during the transfer of the film from SGF to SIF.

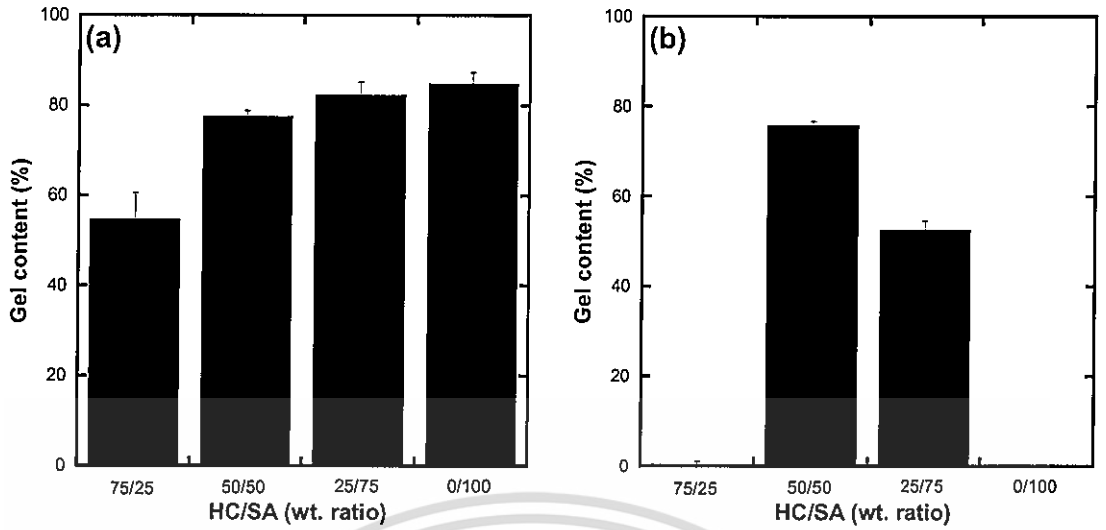

Figure 4.14 Gel contents of HC/SA films after immersing in SGF for 2 h (a) and after immersing in SGF for 2 h followed by SIF for 6 h (b) at 37 °C.

4.2.4 *In vitro* drug release studies

Paracetamol was used as a soluble model drug to study drug release behavior. The standard calibration curves of paracetamol in SGF and SIF are shown in Fig. 4.15a and Fig.4.15b, respectively.

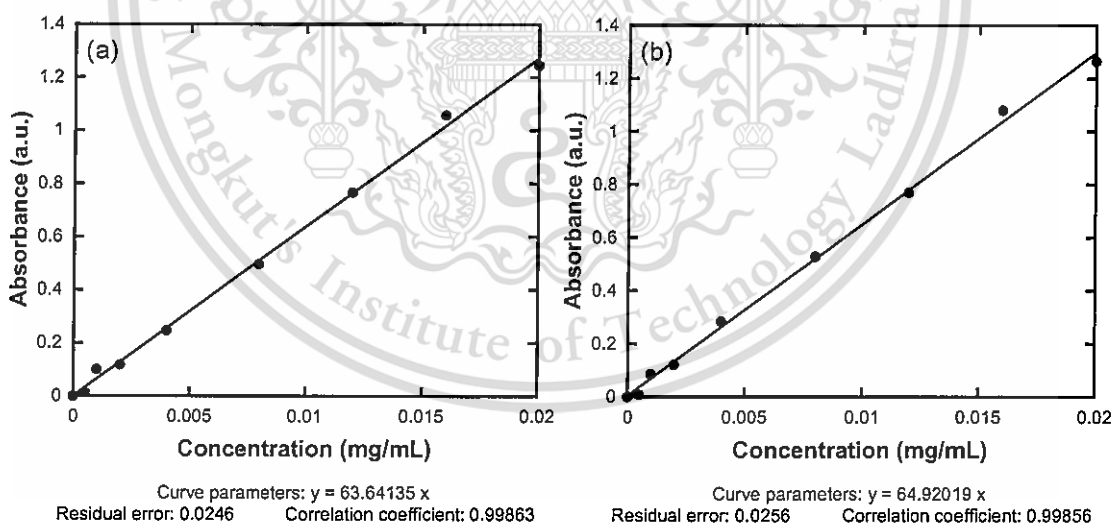

Figure 4.15 Standard calibration curves for paracetamol in (a) SGF and (b) SIF used for determining the release of paracetamol during drug release studies.

The percentage cumulative release profiles of paracetamol from the sealed bags formed by HC/SA films in SGF for 2 h followed by SIF 6 h are shown in Fig. 4.16. All the samples exhibited a very slight paracetamol release in SGF (< 20%). It was due to the low swelling degree and high stability of the films in SGF, as discussed

earlier. The results suggested that the HC/SA films could be used for oral delivery of drug to small intestine. In addition, they were also suitable for acid labile drugs. However, the release rate of paracetamol from the samples changed significantly after transferring into SIF. The HC50SA50, HC25SA75 and SA formulations failed to control the drug release for 8 h and burst release was observed within 7, 5 and 3 h, respectively. Meanwhile, there was no burst release for the HC75SA25 formulation. The results suggested that the burst release could occur in high SA samples. It is because SA is converted to insoluble alginic acid at low pH, which induces crack formation or lamination of SA matrix leading to the burst release [163]. This could be confirmed by SEM micrographs of cross-section of the films after immersing in SGF for 2 h (Fig. 4.17). The cracks were clearly observed on the cross-section of the SA film. It could be concluded that the SA alone was not stable in SIF, therefore, it needed to be combined with HC to delay the burst release time. The HC75SA25 formulation demonstrated the linearity of drug release profile and almost all paracetamol was released in SIF. These results suggested that the HC75SA25 formulation could be a good candidate to be used for controlling drug release in the small intestine.

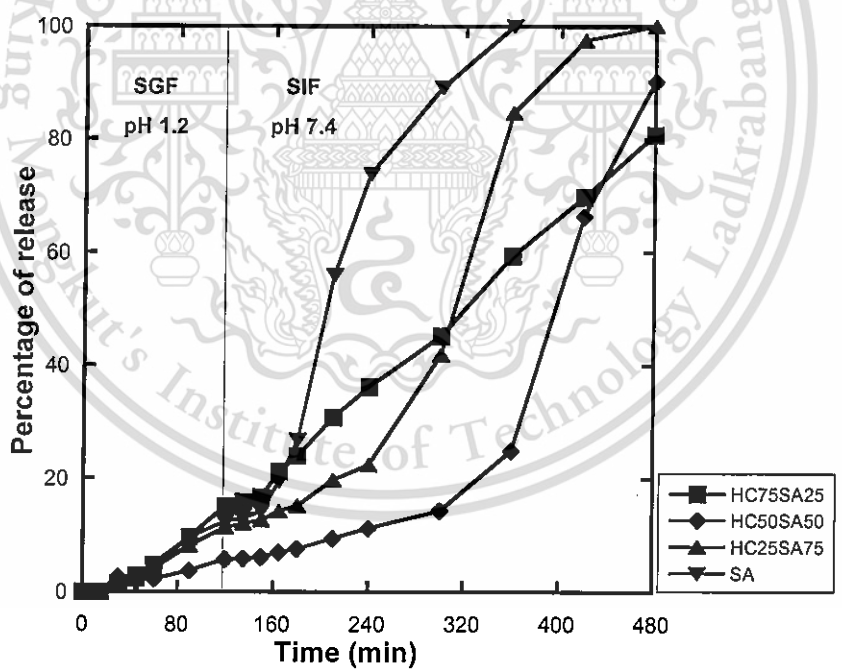

Figure 4.16 Percentages of paracetamol release from the HC/SA films after immersing in SGF for 2 h followed by SIF for 6 h at 37 °C.

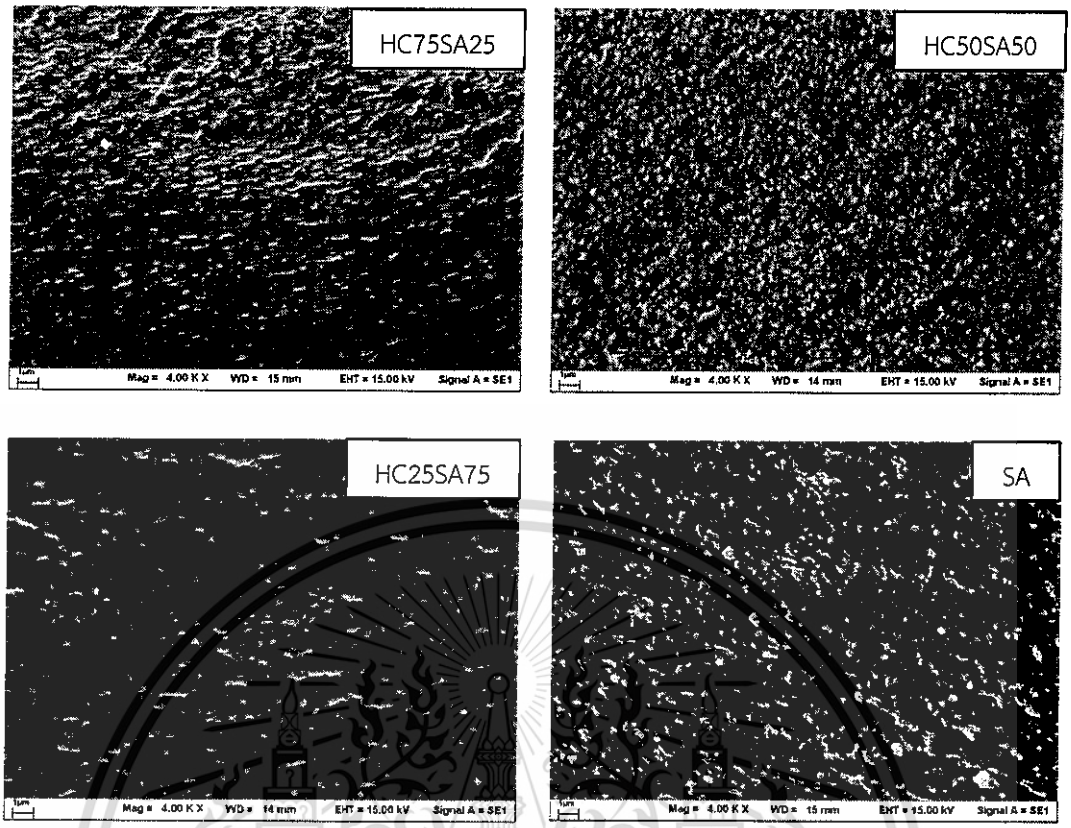

Figure 4.17 SEM micrographs (4000X) of cross-section of the HC/SA films after immersing in SGF for 2 h.

4.2.5 Drug release kinetics

The drug release kinetics mechanism of paracetamol from the HC/SA films was studied using various mathematical models, i.e., zero order, first order, Higuchi and Korsmeyer-Peppas model (Table 4.2). In SGF, the release profiles were found to follow Korsmeyer-Peppas model (R^2 = 0.9779-0.9998) except for HC50SA50 film. It might be because of the relatively low amount of paracetamol released from HC50SA50 film which usually does not fit to Korsmeyer-Peppas model. The values of release exponent (n) ranged from 1.5826-2.2316 indicating the drug release followed super case-II transport controlled by swelling and erosion of polymeric-blend matrix [221]. This could be attributed to the dissolution of HC in SGF. In SIF, due to the burst release of paracetamol from the films (not including HC75SA25), the results were not found suitable for fitting any equations. For the HC75SA25 film, the release profiles showed good fit for zero order model (R^2 = 0.9983) implying the independent of paracetamol concentration on drug release. In addition, its release profiles also showed good fit for Korsmeyer-Peppas model (R^2 = 0.9931) with n values of 1.3048 indicating super case-II transport. It was because high HC content caused the prevention of the burst release.

Table 4.2 Results of curve fitting into different mathematical models for paracetamol release profile from HC/SA films in SGF followed by SIF at 37 °C.

Formulation	Correlation coefficient, R^2				Release exponent, n (Korsmeyer-Peppas model)
	Zero order	First order	Higuchi model	Korsmeyer-Peppas model	
SGF					
HC75SA25	0.9555	0.9579	0.7491	0.9998	1.7084
HC50SA50	0.9059	0.8022	0.8125	0.6420	0.6579
HC25SA75	0.9604	0.8111	0.7607	0.9779	2.2316
SA	0.9677	0.9339	0.7849	0.9864	1.5826
SIF					
HC75SA25	0.9983	0.9499	0.9930	0.9931	1.3048
HC50SA50	0.8243	0.8243	0.7664	0.9100	2.0990
HC25SA75	0.9444	0.9629	0.9230	0.9620	1.9226
SA	0.9433	0.8470	0.9606	0.9221	2.3659

Consequently, the homogeneous HC/SA films were successfully prepared by using solvent casting method. These films possess pH-sensitive properties. It was found that the HC/SA films could be a good candidate to be used for controlling drug release in the small intestine. However, it was interesting to find an alternative drug delivery system with better prolonging drug release to colon environment. Therefore, the crosslinkers would be applied to improve properties of the films.

4.3 Characterization and properties of calcium crosslinked HC/SA films

4.3.1 Preparation of calcium crosslinked HC/SA films

Generally, several crosslinking methods for chitosan derivative have been employed to stabilize the shape and control drug release over a prolonged period of time, including chemical crosslinking. Various crosslinkers, such as glutaraldehyde [222], formaldehyde [223] and ethyleneglycol diglycidyl ether [224], have been used. Although the treatment by those chemicals is effective in yielding a high degree of crosslinking, the residuals are cytotoxicity, restricting their potential biomedical use. To avoid toxic crosslinking agent, many researches have contributed to photo-crosslink [135] and radiation crosslink [137] systems. However, these hydrogels were not pH sensitive and not effectively used as the controlled release of drugs. The formation of semi-interpenetrating polymer network (semi-IPN) of uncrosslinked

chitosan derivative and well-gel forming polymer with the presence of a nontoxic ionic crosslinker is an alternative route for overcoming these limitations. Semi-IPN is a way of blending two polymers where only one is crosslinked in the presence of another to produce an additional non-covalent interaction between the two polymers.

As mentioned above, in this study, the HC/SA films were crosslinked only SA part because SA is capable to form hydrogels under mild conditions in the absence of toxic reagents. In the presence of multivalent metal cations, SA easily forms three-dimensional networks due to the formation of ionic bridges between metal cations and its carboxylate groups of the same or different chains.

It was expected that the new type of crosslinked films could be developed *via* the effective combination of HC with SA using semi-IPN technique. Since HC did not easily dissolve in water at temperature approximating the human body, it was reasonable to modify the uncrosslinked part in order to stabilize its final shape and efficiently control delivery of drug. Calcium chloride ($CaCl_2$) was used as the ionic crosslinking agent for the SA part due to its low cost and non-toxic. The Ca^{2+} ions can interact with guluronate blocks of SA, resulting in the formation of an egg-box structure, as shown in Fig. 4.18. In addition, although, Ca^{2+} ions can interact with CS, it was reported that the introduction of Ca^{2+} ions did not directly influence the gelation behavior of CS due to its weak affinity with CS [180].

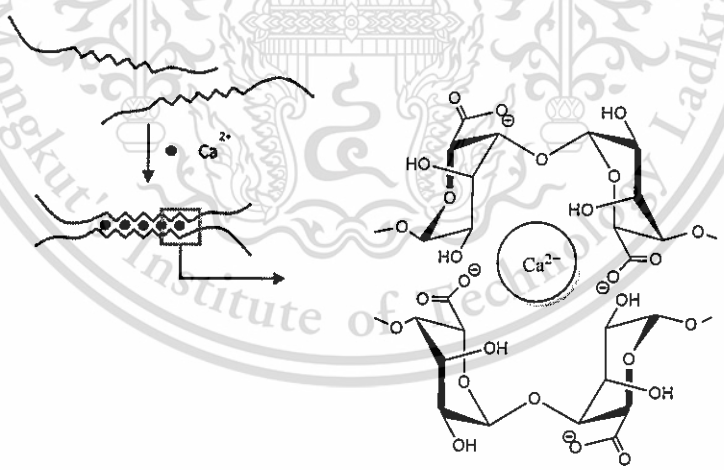

Figure 4.18 Formation of an SA hydrogel by calcium ions [168].

Two main methods for preparing crosslinked film are dipping in multivalent ion solutions and mixing with multivalent ions. However, it was reported that mixing method, in some cases, immediate gel formation could occur and no film could be cast [225]. Furthermore, the films created by dipping method showed higher stability in water than the film created by mixing method. Therefore, in this study, dipping method was used.

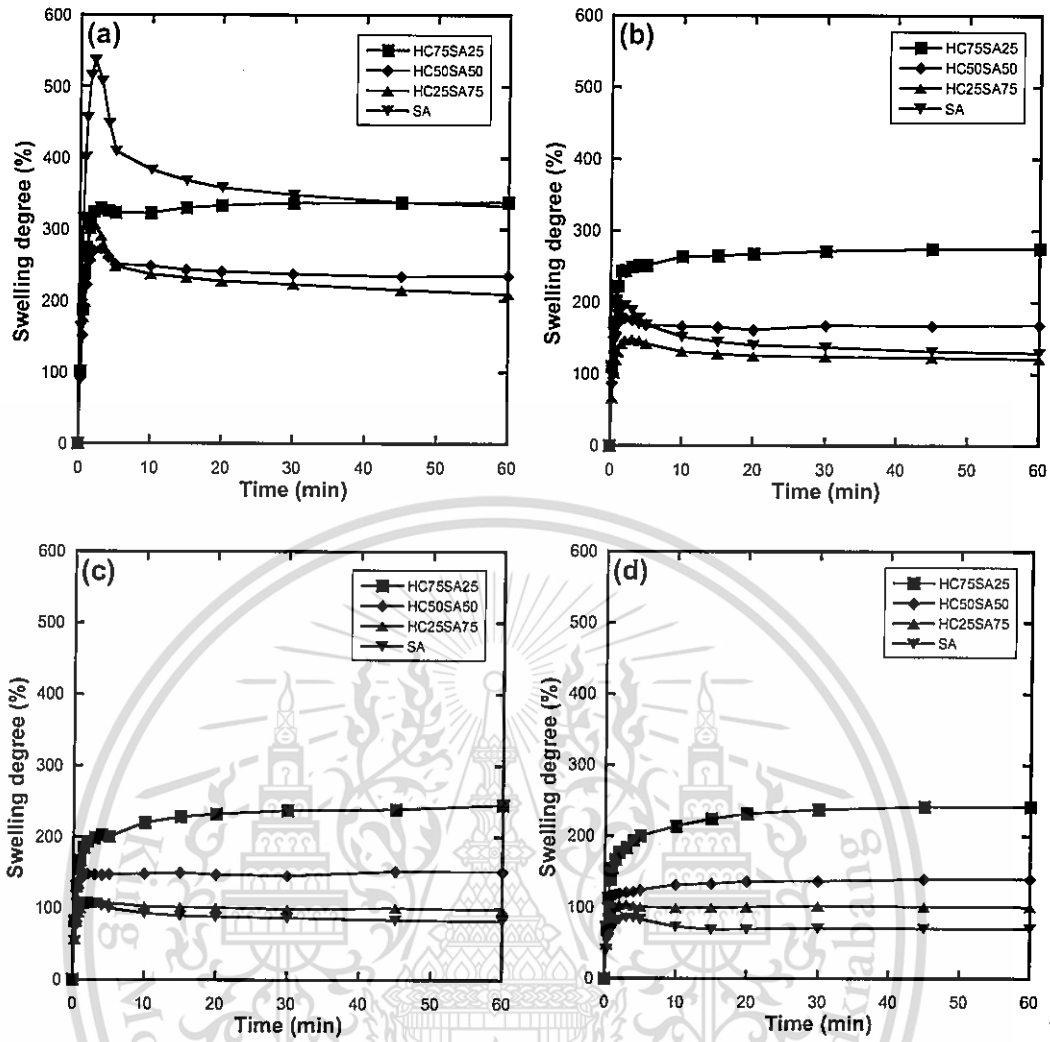

Figure 4.19 Swelling degrees of the HC/SA films in various $CaCl_2$ concentrations: (a) 0.05 M, (b) 0.1 M, (c) 0.25 M and (d) 0.5 M.

When the HC/SA films were dipped in $CaCl_2$ solutions, the crosslinking between $-COO^-$ groups of SA and Ca^{2+} ions lessened the solubility of the films. However, the crosslinking was not instantaneous throughout the film. It was a function of time and concentration. Therefore, in this study, swelling degrees of the films in different concentrations of $CaCl_2$ solutions from 0.01 M to 0.5 M as a function of time were investigated. In case of HC film, its shape could not be maintained when immersing in $CaCl_2$ solutions thus it was not used in following experiments. This indicated that HC could not be crosslinked by Ca^{2+} ions at given concentration. In addition, at concentrations of $CaCl_2$ of less than 0.05 M, the crosslink could not be properly formed. Hence, a minimum concentration of $CaCl_2$ used in subsequent experiments was 0.05 M. Swelling of the HC/SA films in various $CaCl_2$ concentrations is shown in Fig. 4.19. At low concentration of $CaCl_2$ especially at 0.05 M, the films with higher SA content tended to dissolve at the earlier stage of immersing time

while the film with higher HC did not. It was assumed that when the films were immersed in $CaCl_2$ solutions two competitive processes occurred. The dissolution of the SA part was very rapid while the diffusion of Ca^{2+} ions, which crosslinked the surface and reduced the rate of dissolution, was slower. When the concentration of $CaCl_2$ solutions was low, the first process, i.e., dissolution would be predominant. On the contrary, increasing $CaCl_2$ concentration would decrease the dissolution. In addition, it could be seen that all of the films reached swelling equilibrium within 30 min. Therefore, the appropriate time for crosslinking was 30 min.

In summary, the calcium crosslinked films composed of HC and SA were prepared by dipping the HC/SA films in $CaCl_2$ solution for 30 min. Several characteristics of semi-IPN hydrogel films were evaluated to assess their potential use for controlled drug release. These characteristics included their swelling behavior in various fluids, their gel content, the state of water in the gel, their drug release profile and their cytotoxicity.

4.3.2 Characterization of calcium crosslinked HC/SA films

4.3.2.1 FT-IR analysis

FT-IR experiment was carried out in order to study the structure of HC/SA network. Fig. 4.20 represents the FT-IR spectra of HC50SA50 and HC50SA50-Ca0.5 films. After crosslinking, the characteristic peaks for $-COO^-$ symmetric stretching of SA shifted from 1412 cm^{-1} to higher wavenumber at 1419 cm^{-1}. The changes demonstrated an evidence of the transformation of ionic bond of carboxylate ions between Na^+ and Ca^{2+} ions [20].

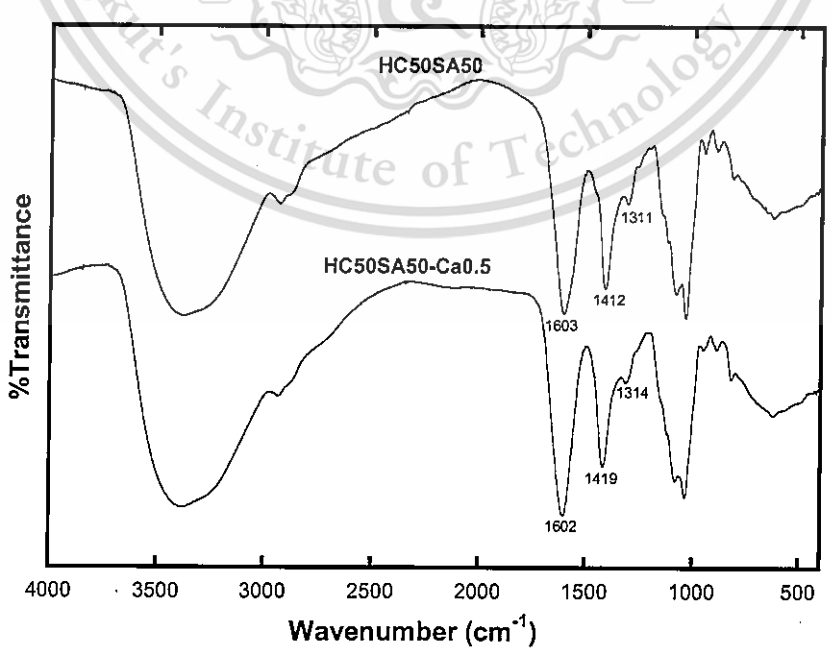

Figure 4.20 FT-IR spectra of HC50SA50 and HC50SA50-Ca0.5 films.

4.3.2.2 Distribution pattern of metal ions

Cross-sections of the calcium crosslinked HC/SA films were examined by SEM-EDS to investigate the distribution pattern of Ca^{2+} ions within the films. It could be seen in Fig. 4.21 that Ca^{2+} ions formed a uniform distribution throughout the films. The results suggested that the formation of calcium crosslinked SA at the surface of the films could not obstruct through diffusion of $CaCl_2$ (the Ca^{2+} ions) into the film matrix.

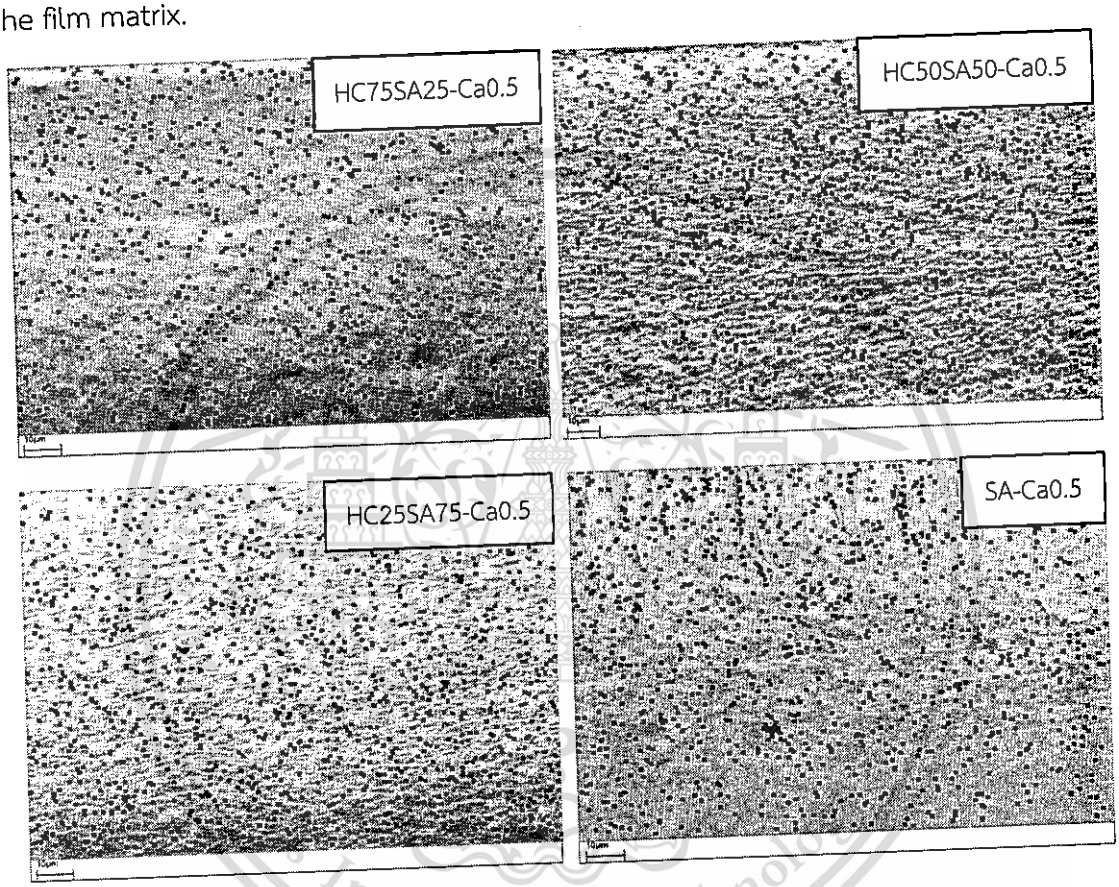

Figure 4.21 SEM-EDS micrographs of the entire film thickness showing two-dimensional distribution of Ca^{2+} ions on the cross-section of calcium crosslinked HC/SA films.

4.3.3 Swelling behavior and gel content of calcium crosslinked HC/SA films in distilled water

The influence of HC to SA ratios and concentration of crosslinking reagent on the swelling behavior of the crosslinked films was studied. As shown in Figs. 4.22a and 4.23b, all films could reach their equilibrium swelling in water within 30 min. Their equilibrium swelling degrees (ESD), which indicate the water retention ability of the films, are presented in Fig. 4.22c. The ESD of the films increased significantly when the HC to SA ratios were increased (Fig. 4.22a), but increased to a relatively lesser degree when the concentration of $CaCl_2$ was decreased (Fig. 4.22b).

The maximum value was reached at approximately 600% by HC75SA25-Ca0.05 (Fig. 4.22a). A lower ESD was obtained when a higher content of SA and/or a higher concentration of $CaCl_2$ were applied in the films. The introduction of SA and $CaCl_2$ with a mole ratio of 1:2 induced crosslinking *via* ionic interaction between the Ca^{2+} ions and SA at the carboxylate position. The high SA content and high concentration of $CaCl_2$ brought about high crosslinking density in the film, thus, hindering chain expansion during swelling.

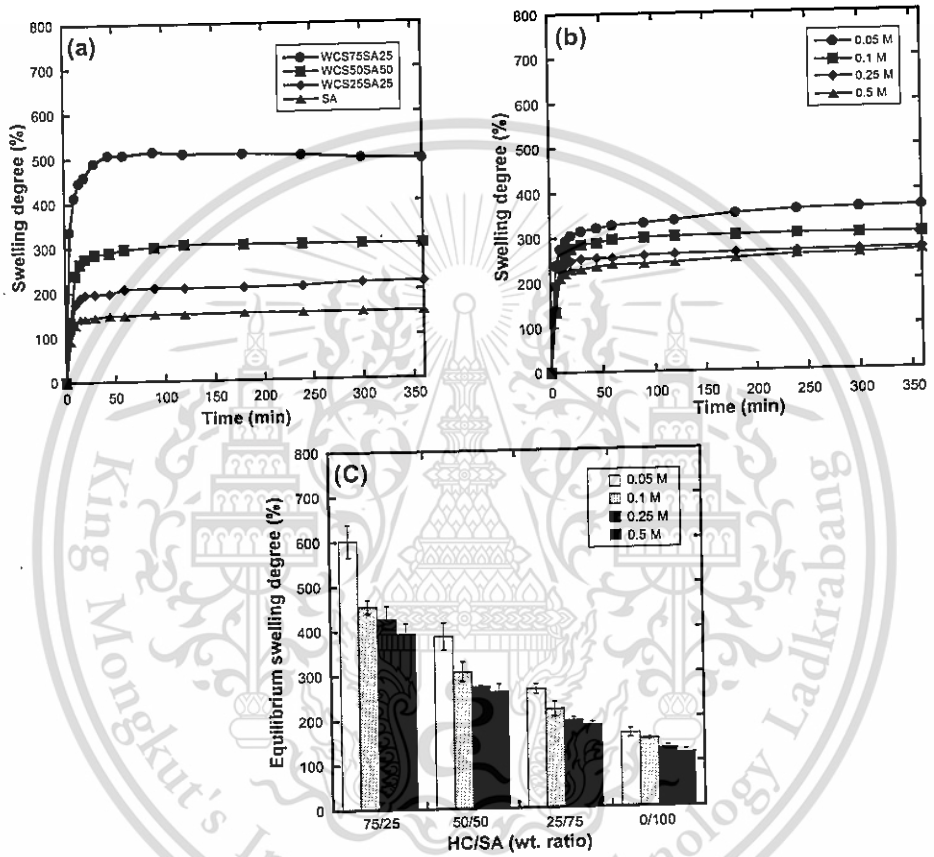

Figure 4.22 Swelling degrees of calcium crosslinked HC/SA films in distilled water at 37 °C: (a) varying ratios of HC to SA with 0.1 M $CaCl_2$, (b) HC50SA50 with varying concentrations of $CaCl_2$ and (c) at equilibrium.

Gel content with various ratios of HC to SA and concentrations of crosslinking agent in distilled water at 37 °C are displayed in Fig. 4.23. They were measured in order to imply the crosslinking degree of the polymer chains within the films. The values of all samples were higher than 60%, with the maximum values up to nearly 100%. Considering the various ratios of HC to SA, an increase in the content of SA caused an increase in the percentage of gel content because of the formation of crosslinks between Ca^{2+} ions and the carboxylate groups occurring only in SA. However, when the composition of HC to SA was fixed, the applied concentration of crosslinking agent (0.05-0.5 M of $CaCl_2$) showed less effect on gel content. Compered

to non-crosslinked films, gel content of crosslinked films increased significantly. Results suggested their potential to be used in applications requiring permanent contact with water.

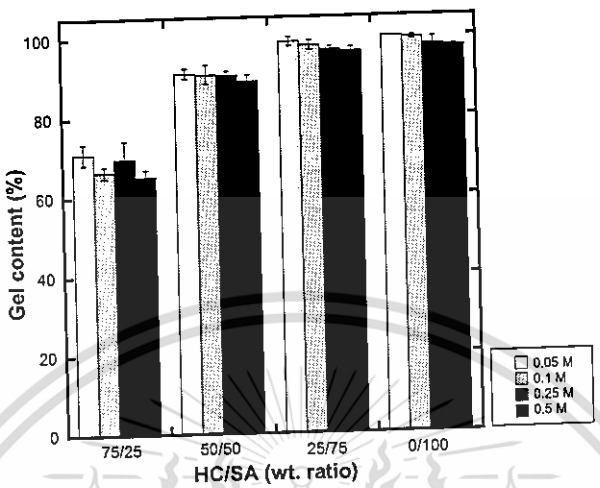

Figure 4.23 Gel contents of calcium crosslinked HC/SA films in distilled water at 37 °C.

To confirm that component dissolved out from the crosslinked film was HC, FT-IR experiment was carried out. After immersing the 0.5 M calcium crosslinked HC75SA25 film in water for 24 h, the remained water was evaporated. After that, the rest solid was characterized. As seen in Fig. 4.24, HC showed characteristic peak at 1076 cm^{-1} while characteristic peak of SA was at 1036 cm^{-1}. It was found that the characteristic peak of dissolved component was similar to HC. Therefore, it could be concluded that HC was the component that dissolved from crosslinked film.

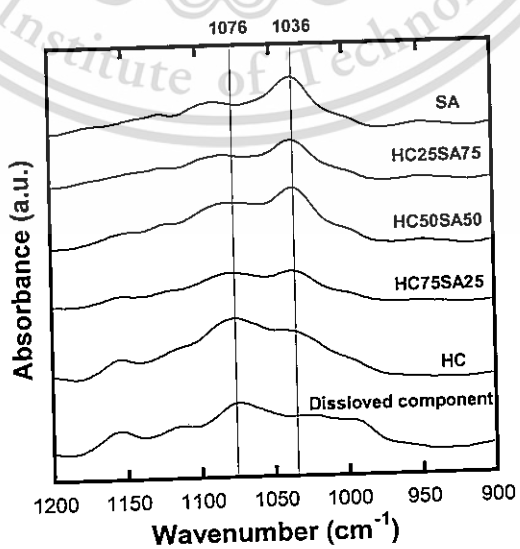

Figure 4.24 FT-IR spectra of HC/SA films and the rest solid from remained water after immersing the 0.5 M calcium crosslinked HC75SA25 film for 24 h.

At this point, all results proved that HC was successfully introduced into SA networks to form the semi-IPN structural hydrogels. Schematic illustration of this network structure is proposed in Fig. 4.25.

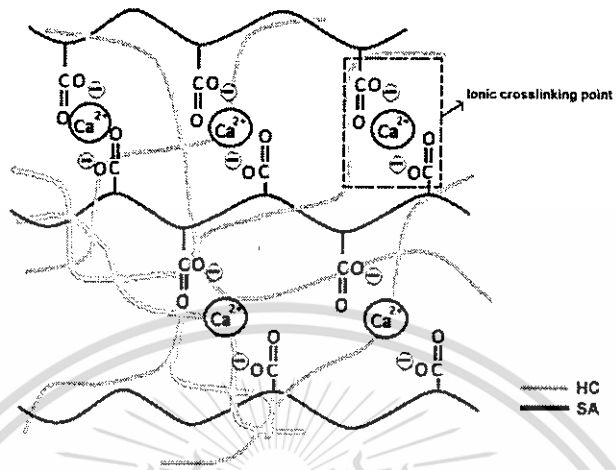

Figure 4.25 The proposed schematic illustration of HC/SA network structure.

4.3.4 State of water in calcium crosslinked HC/SA films

Although the water content affects the quality and functionality of the hydrogels since most applications of hydrogels are based on their water absorption, the biocompatibility is not definitely a simple function of water content. It is necessarily to investigate the state of water in the hydrogels

The state of water in water-swollen hydrogels has demonstrated by many researchers [96-98]. Three energetically distinct states of water have been identified as (i) free water which does not form hydrogen bonds with the polymer and can freeze or melt at the usual temperature of pure water, (ii) freezable bound water which interacts weakly with the polymer and freezes or melts at temperature shifted with respect to that of free water and (iii) non-freezable bound water which forms by the hydrogen bonds between water molecules and polar groups in the polymer and cannot freeze or melt at normal temperature range of pure water. Among these three states, it has been verified that the population of non-freezable bound water plays an important role in drug delivery behavior [99].

Recently, we investigated the state of water in calcium crosslinked HC/SA films by differential scanning calorimeter (DSC). Fig. 4.26 shows the DSC thermograms of the melting behavior of freezable water of the equilibrium swollen crosslinked HC/SA films at various ratios of HC to SA and at different concentration of $CaCl_2$ as a crosslinker. It could be seen that the endothermic peak around 0-20 °C separated into two peaks. The sharp one was remarked as freezable free water which undergoes similar thermal transitions to that of bulk water. It could be seen

from Fig. 4.26 that melting of water absorbed in all films started at a temperature slightly lower than that of pure water (dash line). It might be explained that the water in the films was not pure since there was some dissolution of low molecular weight polymers and $CaCl_2$. This was confirmed by the slightly decrease in gel content remaining of the films after swollen at equilibrium condition. Thus, the freezing point was depressed as the colligative properties of the solution.

On the other hand, the broad one was designed for freezable bound water which undergoes a thermal phase transition at a temperature shifted with respect to that of bulk water. In case of various ratios of HC to SA in the films, the observed DSC endotherms for the higher HC contents showed more broad and asymmetric peak than the lower one. This peak also moved to higher temperatures with higher HC contents in the films. This tendency could be explained that the higher water content in the films at equilibrium was obtained when the higher HC content was applied. Generally, for all studies on hydrogels of higher water content, the endothermic peaks are broad and structured [226]. It could be suggested that there were several states of water being bound with different binding sites of the HC and/or SA structures in different environments.

The state of water of the films using difference concentration of $CaCl_2$ as a crosslinker during film forming was also considered. As discussed in previous section, the lower concentration of $CaCl_2$ was applied, the higher water content in the film was obtained. However, the influence of concentration of $CaCl_2$ was not strong as of the ratios of HC to SA in the films. Thus, the broad endothermic peaks of the films crosslinked by the lower concentration of $CaCl_2$ showed slightly broader than those of the films crosslinked by the higher concentration of $CaCl_2$.

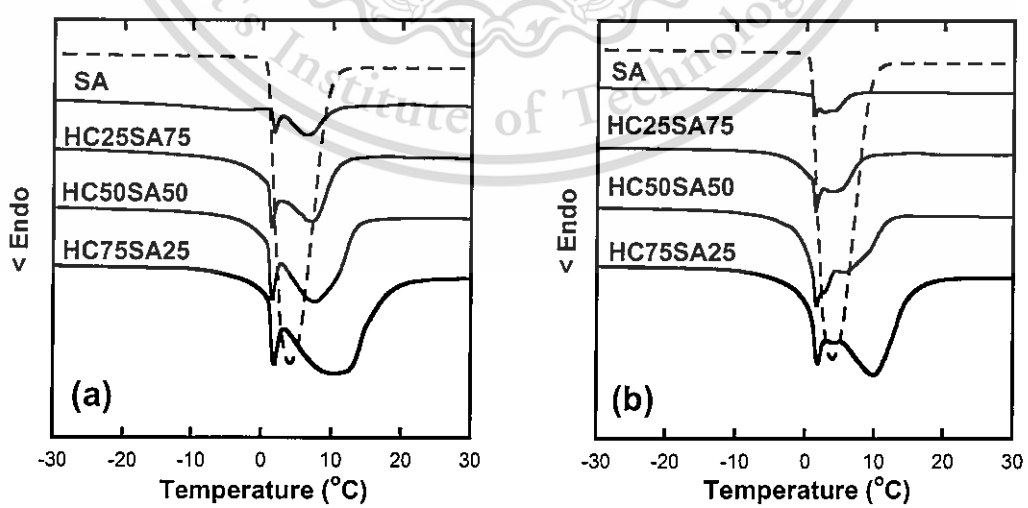

Figure 4.26 DSC thermograms of calcium crosslinked HC/SA films in swollen state with varying concentrations of $CaCl_2$: (a) 0.05 M $CaCl_2$ and (b) 0.5 M $CaCl_2$.

The freezable water content (free water and bound water) can be calculated from the area under the DSC peak represented the change in enthalpy using Eq. 3.7. The non-freezing bound water, however, cannot generally be observed by this technique. Alternatively, non-freezing bound water content can be obtained from Eq. 3.8. The freezable water and non-freezing bound water content are shown in Fig. 4.27. It could be seen that an increase in SA content brought about an increase in non-freezing bound water content. It is generally accepted that non-freezing bound water is formed by H-bonds between water molecules and polar groups in the polymer [97]. Alginate chains can be suggested to form H-bonding with water molecules better than the HC chains since it is known that interaction of water molecules with hydroxyl groups is stronger than with the amine groups [98]. Moreover, the structure of HC consists of the bulky hydroxyethylacryl group which might impede the formation of H-bonding between hydroxyl groups and water. In addition, the concentration of $CaCl_2$ used as crosslinker was not or less influent since non-freezable bound water was not strongly dependence on the mesh size of the polymer network [96].

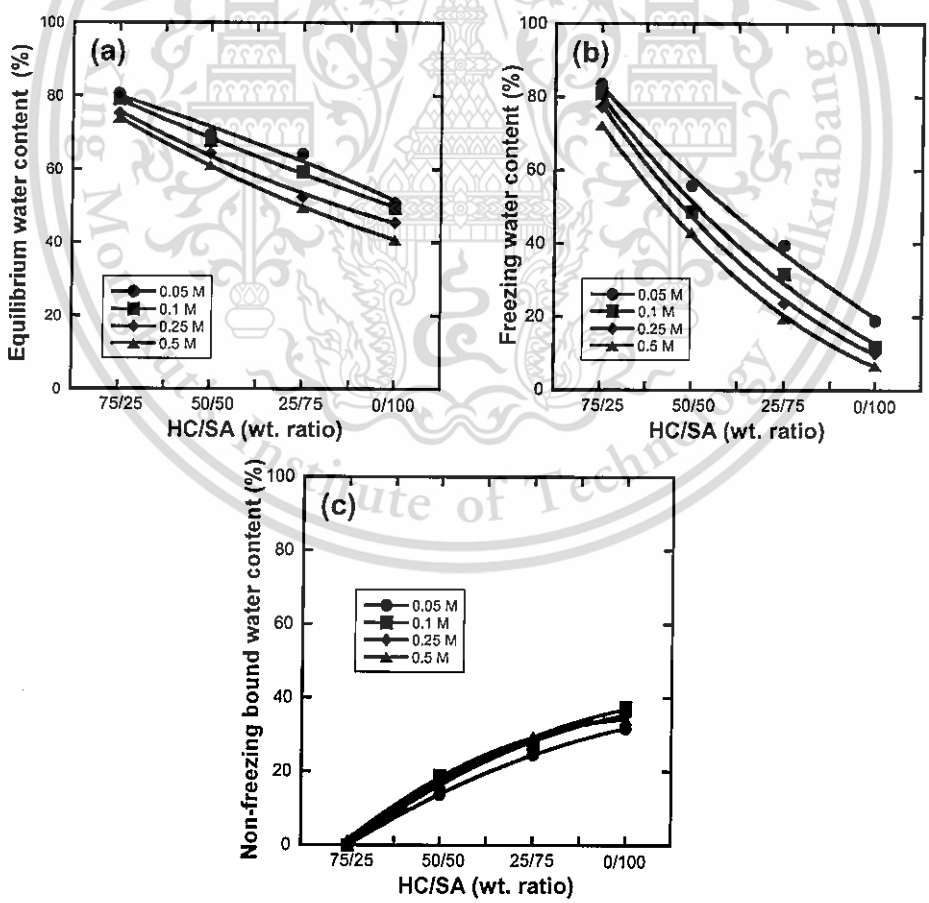

Figure 4.27 Water content of calcium crosslinked HC/SA films: (a) Equilibrium water content, (b) Freezing water content and (c) Non-freezing bound water content.

4.3.5 *In vitro* swelling behavior and gel content of calcium crosslinked HC/SA films

4.3.5.1 Simulated gastric fluid (SGF, pH 1.2)

Swelling behavior of the calcium crosslinked films in SGF at 37 °C was measured. The results are shown in Fig. 4.28. The HC75SA25 formulations exhibited the highest degree of swelling at about 10 times within 20 min and later declined as the dissolution occurred. For lower HC content formulations, HC50SA50, HC25SA75 and SA, the maximum degree of swelling decreased, respectively, and was maintained at the highest level. In addition, the degree of swelling of the films decreased with increasing concentration of crosslinking agent used. However, the differences in the values of swelling degree were relatively small. It was apparent that the change of HC to SA ratios was the predominant factor affecting the swelling degree of the hydrogels in SGF. Compared to the swelling degree of a film with the same formulation in distilled water at 37 °C, the hydrogels achieved a higher swelling degree in SGF than in distilled water, especially when high HC contents (HC75SA25 and HC50SA50) were used. This is because $-NHCH_2CH_2COOCH_2CH_2OH$ groups on HC can be protonated at pH 1.2 leading to the electrostatic repulsion among the ionized groups, as discussed earlier. However, in case of crosslinked SA film, the swelling degree in SGF also seemed slightly greater than that in distilled water. It was because Na^+ and H^+ ions presented in the SGF interfered and destroyed the interaction between Ca^{2+} ions and SA and brought about the collapse of partial crosslinking points.

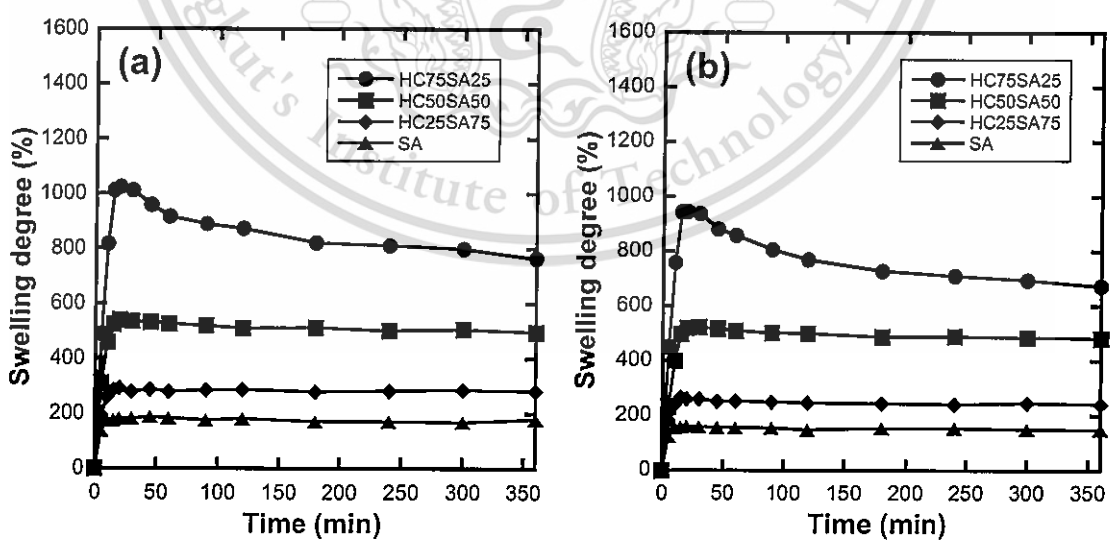

Figure 4.28 Swelling degrees of calcium crosslinked HC/SA films with varying concentration of $CaCl_2$ in SGF at 37 °C: (a) 0.1 M $CaCl_2$ and (b) 0.5 M $CaCl_2$.

Fig. 4.29 shows the gel contents of the calcium crosslinked HC/SA films in SGF. It was appointed to investigate the stability of the crosslinking point within the crosslinked films. Compared to the gel content in distilled water, the gel content of the crosslinked films in SGF was lower. It is due to the fact that HC and SA can be protonated or ion exchanged by appropriate positive charges presented in SGF. In case of HC, after protonating, the electrostatic repulsion among the ionized groups led to the dissolution of HC. In case of SA, although the crosslinked points between Ca^{2+} ions and the carboxylate groups were partially destroyed after ion exchange causing dissolution of the uncrosslinked SA, carboxylate groups in the SA after protonating could form hydrogen bonds which prevented the dissolution. Thus, the gel content of the hydrogels containing high SA content was still relatively high in SGF. Similar to the gel content of the hydrogels in distilled water, the gel content increased with an increase of SA, while the given concentration of crosslinking agent did not affect the gel content.

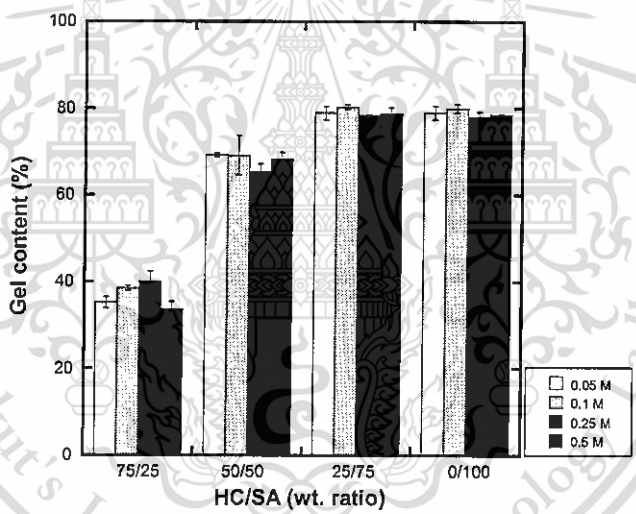

Figure 4.29 Gel contents of calcium crosslinked HC/SA films in SGF at 37 °C.

4.3.5.2 Simulated intestinal fluid (SIF, pH 7.4)

The swelling behavior of the calcium crosslinked HC/SA films in SIF at 37 °C was investigated. The results are shown in Fig. 4.30. It was clear from the results that the crosslinked films with a higher HC content could reach the higher maximum degree of swelling and degrade faster than the low one. It was because there was no crosslinking between HC and Ca^{2+} ion, therefore, HC could remarkably swell and later dissolve in SIF as inferred to carboxymethyl chitosan (CMCS), one of the water-soluble chitosans with a structure similar to HC [70]. Furthermore, in the crosslinked films with high SA content, the dissolution of the films also observed since the degradation of calcium crosslinked alginate could occur in SIF. It is due to the fact that the affinity of PO_4^{3-} ions presented in the SIF to Ca^{2+} ions is higher than

that of SA, resulting in breakage of the interaction between Ca^{2+} ions and the carboxylate groups of calcium crosslinked alginate [227]. This could be confirmed by the observation of some turbidity which appeared in SIF while doing an experiment. It might be because of the formation of calcium phosphate on the same analogy as mentioned by A.K. Nayak et al [18]. However, the results showed the effect of the presence of HC on the degradation of the films rather than the breakage of calcium crosslinked alginate. Moreover, it could be seen that the degradation time could be prolonged with increasing concentration of crosslinking agent used. It was because high concentration of $CaCl_2$ brought about high crosslinking density resulting in the slower degradation of the hydrogel films. In comparison with the swelling in SGF, the swelling of hydrogel films in SIF was higher, indicating their pH-sensitive swelling behavior.

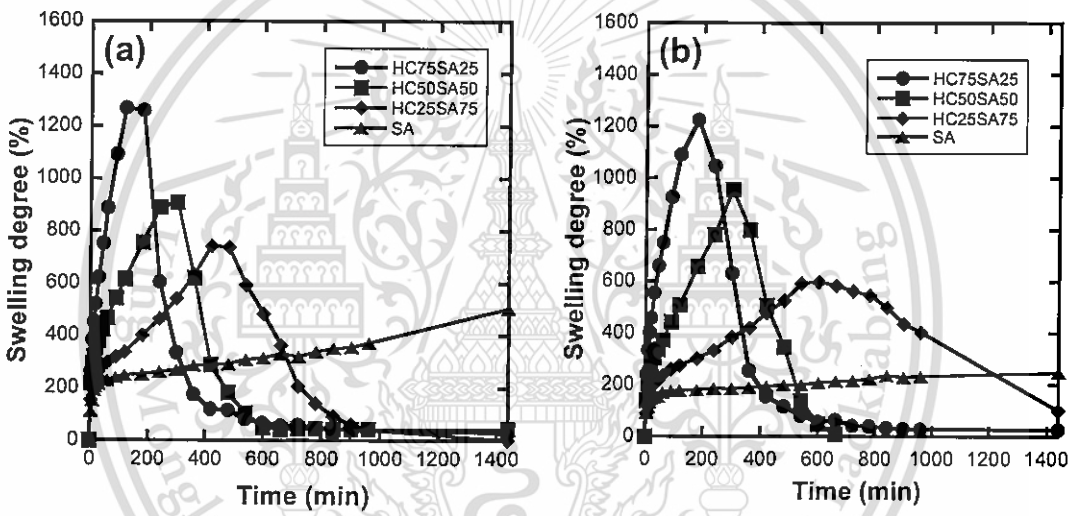

Figure 4.30 Swelling degrees of calcium crosslinked HC/SA films with varying concentration of $CaCl_2$ in SIF at 37 °C: (a) 0.1 M $CaCl_2$ and (b) 0.5 M $CaCl_2$.

4.3.5.3 Simulated gastrointestinal fluid (SGF followed by SIF)

The swelling degree of the calcium crosslinked HC/SA films in SGF (pH 1.2) for first 2 h and then, in SIF (pH 7.4) for next 6 h was investigated. The influences of HC to SA ratios and conditions of crosslinking on the swelling behavior of the films were examined. As seen in Fig. 4.31, the swelling degrees of all films were quite stable in SGF within the first 2 h. At the same conditions of crosslinking, the HC75SA25 formulations exhibited the highest degree of swelling. For the films with high SA content, the values of swelling degree of crosslinked films were lower than non-crosslinked films. It was suggested that the crosslinking with calcium ions became the dominant action for swelling behavior in SGF when SA content increased. However, the change of the concentrations of $CaCl_2$ (0.1 and 0.5 M) used

seemed no influence on the swelling of the films in SGF. When the films were transferred to SIF, the swelling degrees of the films containing HC decreased drastically because of the deprotonation of HC at neutral pH and the formation of polyelectrolyte complexes between HC and SA, as discussed in section 4.2.3.3. On the other hand, the swelling degree of the SA film increased after transferring to SIF since carboxylic groups on SA were ionized in SIF. In case of SA films, although the crosslinking was applied, the disintegration and the dissolution of the film after immersing in SGF followed by SIF still occurred. Unlike direct immersing of crosslinked SA films in SIF, the degradation of the films was not observed. (Fig. 4.30). It was because Ca^{2+} ions in the crosslinked calcium alginate could be replaced by the H^{+} ions in SGF and could interact with PO_4^{3-} ions in SIF, meanwhile, cationic ions presented in SIF could ionize at the –COOH of SA leading to degradation. In case of HC75SA25 formulation, the degradation time was prolonged when the concentrations of $CaCl_2$ increased. Although at low concentration of $CaCl_2$ the crosslinking was formed, the hydrogel was neither strong nor sufficient enough to delay the penetration of the fluid into the hydrogel. When the concentrations of $CaCl_2$ increased, the stronger hydrogel was obtained resulting in the delay of the penetration of the fluid into the hydrogel resulting in the slower degradation. For HC50SA50 and HC25SA75 formulations, the decline in the swelling degree of the films was not observed. It suggested that although some part of SA interacted with Ca^{2+} ions, the polyelectrolyte complexes between HC and SA during the transfer of the film from SGF to SIF could still be formed which delayed the degradation rate of the films. However, in HC50SA50 and HC25SA75 formulations, the concentrations of $CaCl_2$ used did not induce significant changes in the swelling degree of the hydrogel in SIF.

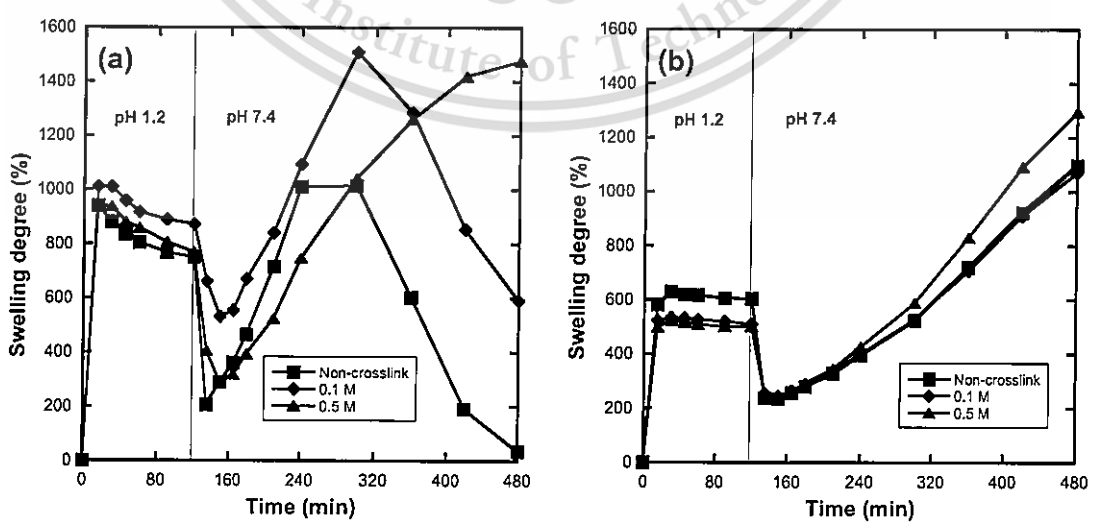

Figure 4.31 Swelling degrees of calcium crosslinked (a) HC75SA25, (b) HC50SA50, (c) HC75SA25 and (d) SA films in simulated gastrointestinal fluid at 37 °C.

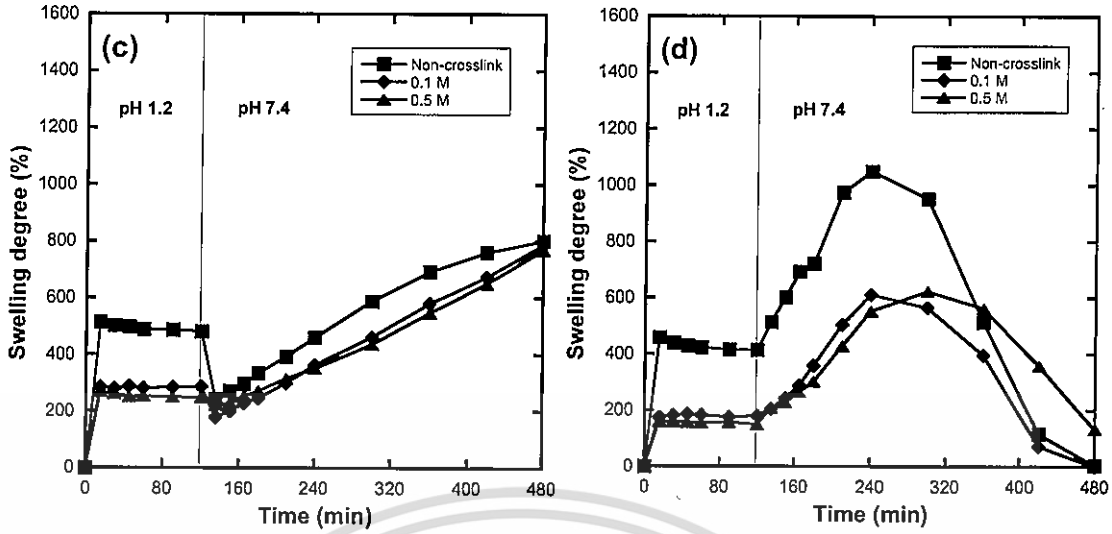

Figure 4.31 (cont.)

Stability of the hydrogels was established by observation in the gel content of the hydrogels after immersing in SGF for 2 h and in SGF for 2 h followed by SIF for 6 h. Fig. 4.32a shows the gel content of hydrogels in SGF for 2 h. It was found that the gel content of all of hydrogel films was relatively high in SGF (> 50%). The gel content of HC75SA25 formulation exhibited the lowest value. Furthermore, the change of the concentration of crosslinking agent had a non-significant effect on stability of hydrogel in SGF. However, the influence of the concentration of crosslinking agent could be observed when the hydrogel films were transferred to SIF. The gel contents of the hydrogels in SGF followed by SIF are displayed in Fig. 4.32b. The values of HC75SA25 and SA formulations were relatively low (< 15%). In case of SA formulation, it was because the interaction between Ca^{2+} ions and $-COO^{-}$ groups in the calcium crosslinked SA film could be destroyed by the H^{+} and Na^{+} ions in SGF and by PO_4^{3-} ions in SIF, as discussed earlier. In case of HC75SA25 formulation, the gel content values were also relatively low except for HC75SA25 film crosslinked with 0.5 M $CaCl_2$. It was because this formulation had high HC which easily dissolve in SGF. However, when crosslinking was applied, the higher concentration of crosslinking agent used provided the stronger hydrogel which prevented the film from dissolution. In addition, it was found that, at 0.5 M calcium chloride, the gel content of HC75SA25 film was higher than of SA film because there was polyelectrolyte complexation between HC and SA in HC75SA25 film. At this point, it could be concluded that two main factors that prevented the hydrogel from the disintegration in simulated gastrointestinal fluid were the crosslinking of SA part with Ca^{2+} ions and the formation of polyelectrolyte complexes between HC and SA. As seen in Fig. 4.32b, the change of concentration of $CaCl_2$ affected the gel content of HC25SA75 formulation but not HC50SA50 formulation. The results suggested that

the formation of polyelectrolyte complexes between HC and SA was a predominant factor influencing the stability of HC50SA50 formulation, while the crosslinking of SA part with Ca^{2+} ions was a predominant factor influencing the stability of HC25SA75 formulation.

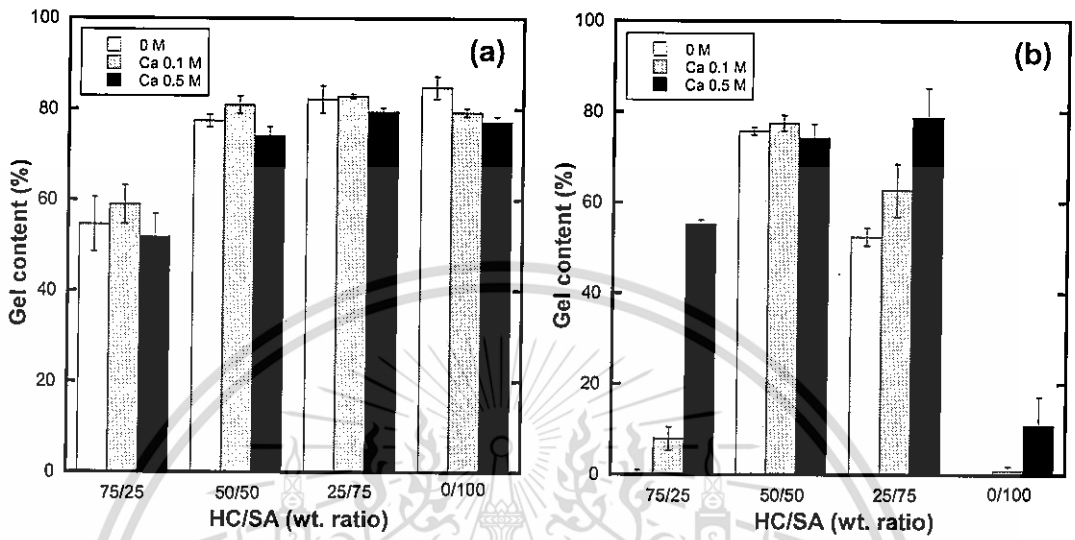

Figure 4.32 Gel contents of calcium crosslinked HC/SA films after immersing in SGF for 2 h (a) and after immersing in SGF for 2 h followed by SIF for 6 h (b) at 37 °C.

4.3.6 *In vitro* drug release studies

Fig. 4.33 shows the release profiles of paracetamol at 37 °C for 2 h in SGF followed by 6 h in SIF. All the hydrogels exhibited a very slight paracetamol release in SGF (< 20%) except for HC25SA75 and SA formulations crosslinked with 0.1 M $CaCl_2$. The amount of paracetamol released from these hydrogels was about 50% within 2 h. An explanation for this behavior was some part of SA in the films with high SA content could not be crosslinked when using low concentration of $CaCl_2$ leading to the unlike shrinkage resulting in an easy drug leakage from the hydrogel. When the hydrogels were transferred to SIF, the rate of paracetamol released increased as compared to that released in SGF. It was because the swelling of hydrogels in SIF was higher than that in SGF, as discussed earlier. It was found that the burst release of paracetamol in SIF occurred in the hydrogels containing high SA content. However, the crosslinking could depress the burst release of paracetamol effectively. The exception was for SA formulation because SA hydrogel crosslinked by Ca^{2+} ions could be transformed into insoluble alginic acid at low pH, as discussed in section 4.3.5.1, inducing crack formation or lamination of SA hydrogel matrix, leading to burst release of paracetamol from SA hydrogel. Furthermore, the higher degree of crosslinking by higher $CaCl_2$ concentration brought about the lower drug

release rate from the hydrogel. As discussed above, it could be concluded that high HC content and the crosslinking could prevent the burst release of paracetamol from hydrogel. Interestingly, the HC50SA50 formulation crosslinked with 0.5 M $CaCl_2$ exhibited the lowest amount of drug release in SIF (< 20%). This result suggested that 0.5 M calcium crosslinked HC50SA50 formulation could be a potential candidate for a site-specific drug delivery in the colon. However, other formulations could be used for delivering drugs to other parts of the body. The HC75SA25 and HC25SA75-Ca0.5 formulations were suitable to deliver the drug to the small intestine. The HC75SA25-Ca0.1, HC75SA25-Ca0.5 and HC50SA50-Ca0.1 formulations were good candidates for the sustained and targeted delivery of drug in both the small intestine and the colon.

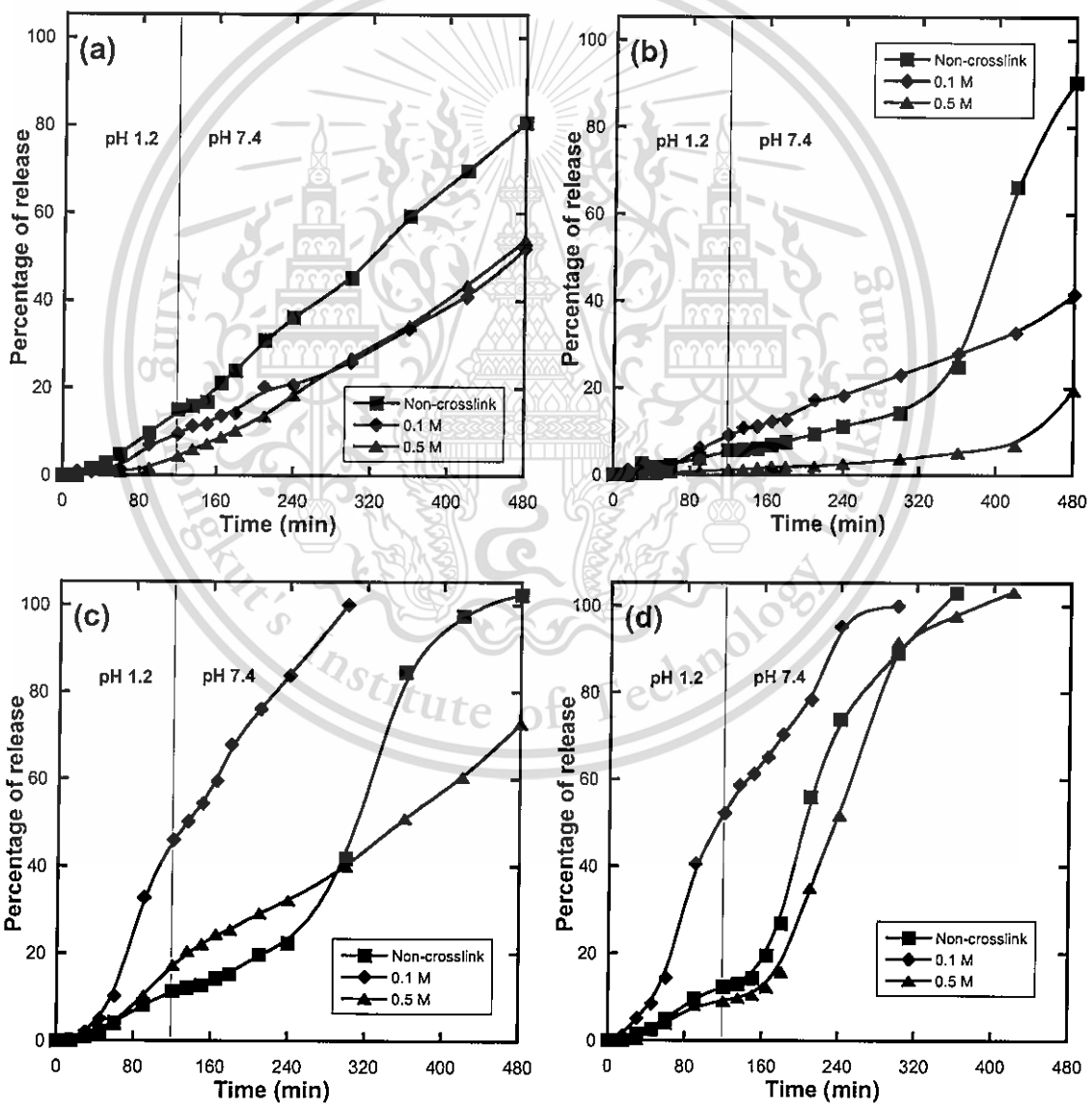

Figure 4.33 Percentages of paracetamol release from crosslinked (a) HC75SA25, (b) HC50SA50, (c) HC25SA75 and (d) SA films after immersing in SGF for 2 h followed by SIF for 6 h at 37 °C.

4.3.7 Drug release kinetics

The drug release kinetics mechanism of paracetamol from the HC/SA hydrogels was further analyzed using various mathematical models, i.e., zero order, first order, Higuchi and Korsmeyer-Peppas model. As seen in Table 4.3, the release profiles in SGF of HC25SA75 and SA formulations crosslinked with 0.1 M $CaCl_2$ were found to follow Korsmeyer-Peppas model (R^2 were 0.9908 and 0.9899, respectively). The values of release exponent (n) were 2.368 for HC25SA75 formulation and 1.9213 for SA formulation, indicating the drug release followed super case-II transport controlled by swelling and erosion of polymeric-blend matrix. This could be attributed to the unlike shrinkage of hydrogels containing high SA content in SGF resulting in the high release rate. On the contrary, HC75SA25-Ca0.1, HC50SA50-Ca0.1, HC75SA25-Ca0.5, HC50SA50-Ca0.5, HC25SA75-Ca0.5 and SA-Ca0.5 formulations did not fit for any equations owing to their low release rate.

Table 4.3 Results of curve fitting into different mathematical models for paracetamol release profile from calcium crosslinked HC/SA films in SGF at 37 °C.

Formulation	Correlation coefficient, R^2				Release exponent, n (Korsmeyer-Peppas model)
	Zero order	First order	Higuchi model	Korsmeyer-Peppas model	
HC75SA25-Ca0.1	0.8674	0.9107	0.6563	0.7487	1.2182
HC50SA50-Ca0.1	0.8241	0.7694	0.6065	0.5337	1.0754
HC25SA75-Ca0.1	0.9109	0.9362	0.6821	0.9908	2.3680
SA-Ca0.1	0.9342	0.8826	0.7292	0.9899	1.9213
HC75SA25-Ca0.5	0.7476	0.7153	0.6110	0.5387	0.6357
HC50SA50-Ca0.5	0.9248	0.7518	0.7184	0.8434	2.2573
HC25SA75-Ca0.5	0.8921	0.9544	0.6554	0.8886	1.8164
SA-Ca0.5	0.9419	0.7675	0.7753	0.8640	2.1700

In SIF (Table 4.4), HC75SA25-Ca0.1, HC50SA50-Ca0.1, HC25SA75-Ca0.1, SA-Ca0.1, HC75SA25-Ca0.5 and HC25SA75-Ca0.5 formulations showed good fit for Korsmeyer-Peppas model (R^2 = 0.9851-0.9965). The n values greater than 1 for HC75SA25 and HC50SA50 formulations indicated super case-II transport controlled by swelling and erosion and n values less than 1 for HC25SA75 and SA formulations indicated anomalous diffusion controlled by diffusion and swelling. For HC50SA50-Ca0.5 and SA-Ca0.5 formulations, the results were not found suitable for fitting any equations. In case of SA-Ca0.5 formulation, it was due to the burst release of

paracetamol from the hydrogel. For the HC50SA50-Ca0.5 formulation, it was because of the very low amount of paracetamol released in SIF. This indicated that this formulation could be a good candidate for a site-specific drug delivery in the colon, as discussed in release studies.

Table 4.4 Results of curve fitting into different mathematical models for paracetamol release profile from calcium crosslinked HC/SA films in SIF at 37 °C.

Formulation	Correlation coefficient, R^2				Release exponent, n (Korsmeyer-Peppas model)
	Zero order	First order	Higuchi model	Korsmeyer-Peppas model	
HC75SA25-Ca0.1	0.9838	0.9762	0.9635	0.9883	1.1915
HC50SA50-Ca0.1	0.9869	0.9792	0.9696	0.9890	1.0590
HC25SA75-Ca0.1	0.9900	0.9633	0.9957	0.9913	0.8780
SA-Ca0.1	0.9493	0.9433	0.9572	0.9851	0.7396
HC75SA25-Ca0.5	0.9962	0.9544	0.9811	0.9965	1.7484
HC50SA50-Ca0.5	0.7054	0.9470	0.6488	0.8888	1.7507
HC25SA75-Ca0.5	0.9894	0.9951	0.9679	0.9894	0.9833
SA-Ca0.5	0.9282	0.9382	0.9518	0.9367	2.4380

4.3.8 MTT assay

Cell viability of the synthesized hydrogels was determined following the MTT assay. The average percentages of cytotoxicity of HC75SA25, HC50SA50, HC25SA75 and SA hydrogel films crosslinked by 0.5 M $CaCl_2$ were 5.56±0.04, 10.27±8.17, 7.43±1.58 and 9.74±1.98, respectively. It could be concluded that the hydrogel films were not toxic to human cells. Hence, the results suggested potential application of these hydrogel films as biomaterials.

In summary, semi-IPN HC/SA hydrogel films were successfully prepared by using $CaCl_2$ as a crosslinker. The investigated systems indicated a significant reduction in swelling as the SA and crosslinking reagent content is increased. Hydrogel films with higher HC content degraded faster in SIF than those with lower HC content but all hydrogel films were stable in SGF. Compared to non-crosslinked system, the degradation time in simulated gastrointestinal fluid of crosslinked system was slow leading to the prolonged drug release. Moreover, all evaluated systems have been proven to be noncytotoxic. The comprehensive results of this study suggested their potential in controlled drug release in different parts of the body.

However, it was interesting to study an alternative drug delivery system with using different types of crosslinkers (zinc and copper ions). It was assumed that changing of the crosslinker types was possible to change the drug release profile.

4.4 Characterization and properties of zinc or copper crosslinked HC/SA films

In previous section, the HC/SA crosslinked film was prepared using calcium chloride as a crosslinker. The results indicated that calcium ions could crosslink only SA part. In order to study an alternative drug delivery system, in this section, zinc sulfate and copper(II) sulfate were used as crosslinkers. It was reported that zinc and copper ions can crosslink both CS and SA part [81-82, 181, 185]. It was, thus, expected that HC could form complexation with zinc and copper ions like CS. In addition, above results showed that the films crosslinked with 0.5 M calcium chloride had the lowest drug release. Therefore, the concentrations of zinc sulfate and copper(II) sulfate used in this study were 0.5 M. The effects of crosslinkers on swelling behavior, gel content and drug release profile were studied.

4.4.1 Characterization of zinc or copper crosslinked HC/SA films

4.4.1.1 FT-IR analysis

Fig. 4.34 represents the FT-IR spectra of zinc and copper crosslinked HC50SA50 films. The broader absorption peaks were observed in the range of 3600-3000 cm^{-1}. It indicated that the –NH– and –OH groups of HC and –OH groups of SA formed coordinate bonds with Cu^{2+} or Zn^{2+} ions. The characteristic peaks for asymmetrical and symmetrical stretching of the $-COO^{-}$ groups of SA also became broader, indicating the formation of complexes between carboxylate ions of SA and Cu^{2+} or Zn^{2+} ions. The possible types of the carboxylate binding were summarized in Fig. 4.35 [228]. The characteristic peak assigned to N–H bending of HC showed a significant shift from 1311 cm^{-1} to higher wavenumber at 1321 cm^{-1} for zinc crosslinked film and 1325 cm^{-1} for copper crosslinked film. It could be pointed that the –NH– groups of HC were involved in complexation [229]. According to all results, it could be concluded that both HC and SA could form complexation with zinc and copper ions. The reasonable structure chelate compounds between polymers (i.e., HC and SA) and zinc or copper ions are proposed in Fig. 4.36.

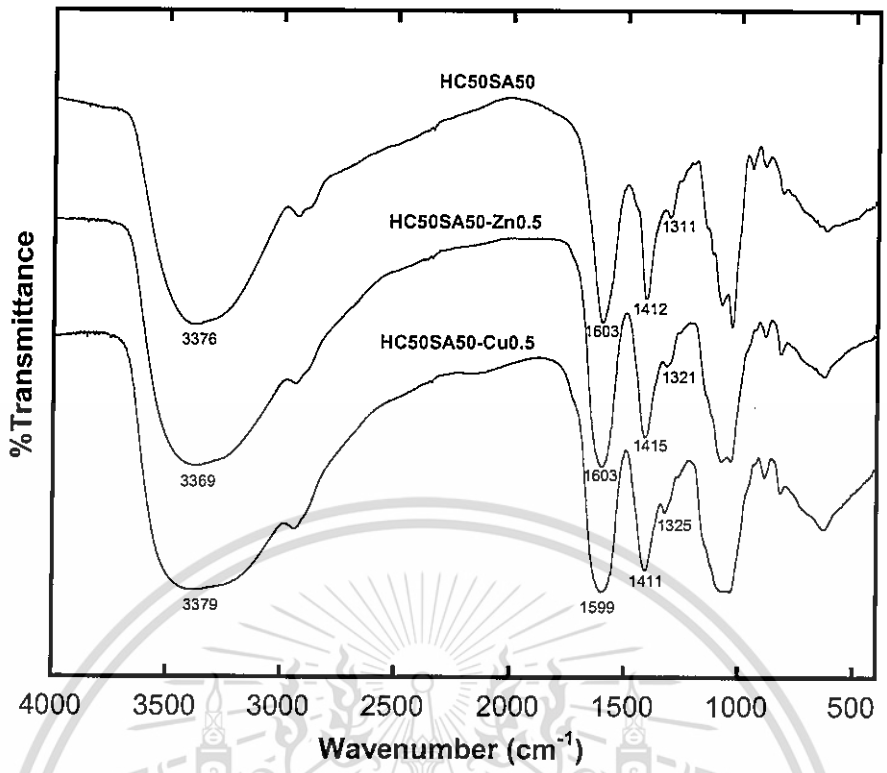

Figure 4.34 FT-IR spectra of zinc and copper crosslinked HC50SA50 films.

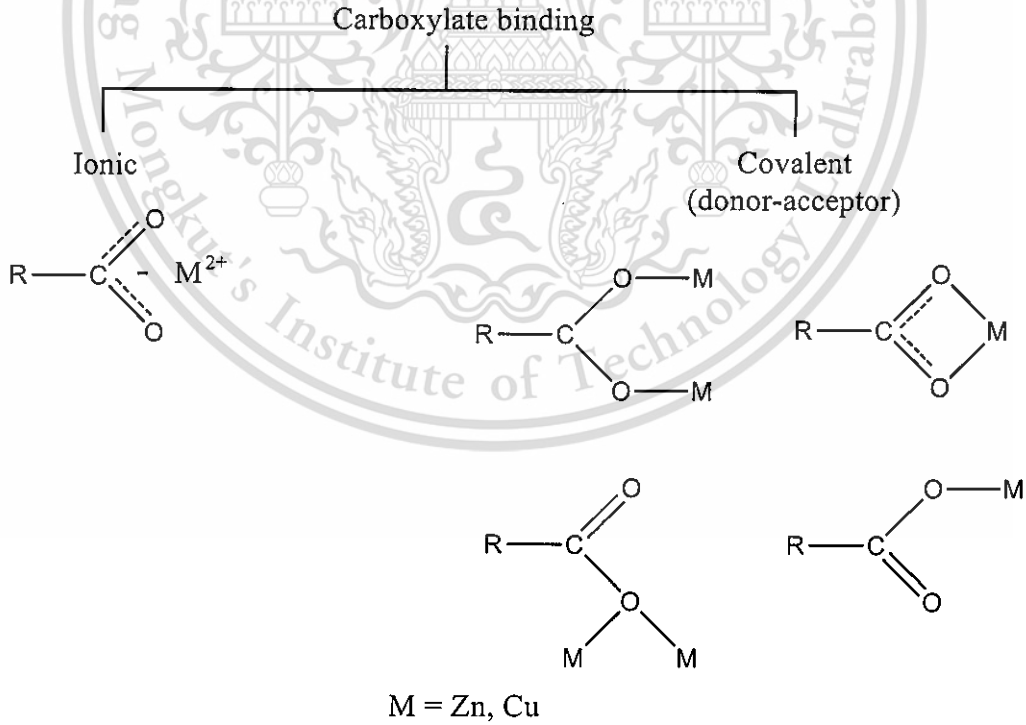

Figure 4.35 The possible types of the carboxylate binding. Adapted from Ref. [228].

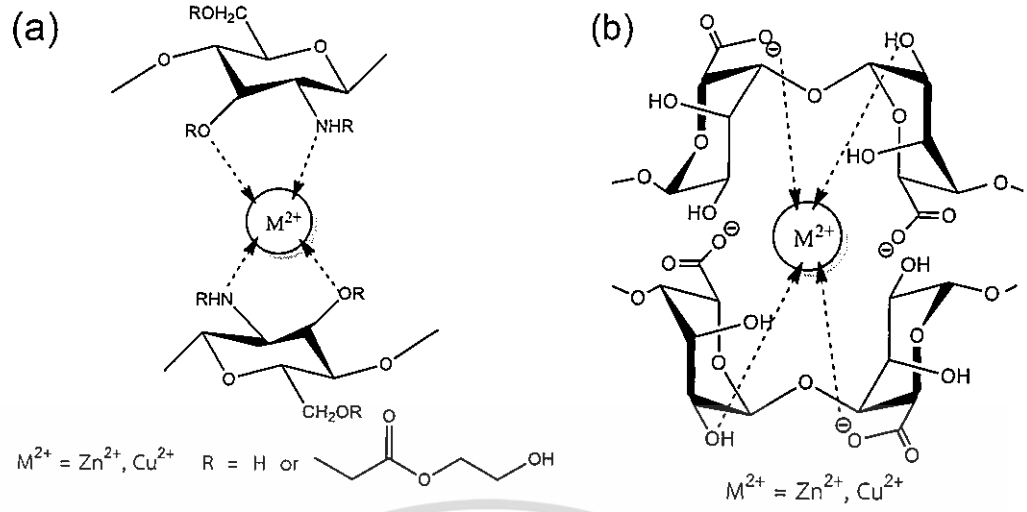

Figure 4.36 The proposed structure chelate compounds of HC (a) or SA (b) and zinc or copper ions.

4.4.1.2 Distribution pattern of metal ions

The distribution pattern of metal ions (i.e., Zn^{2+} and Cu^{2+}) within the films was examined by SEM-EDS. As shown in Fig. 4.37, the distribution patterns of all types of metal ions in the films were uniform.

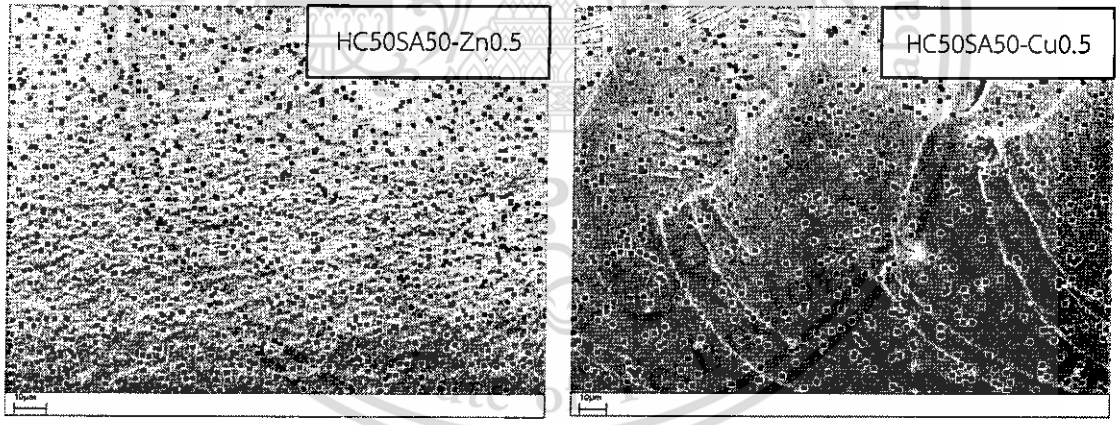

Figure 4.37 SEM-EDS micrographs of the entire film thickness showing two-dimensional distribution of Zn^{2+} and Cu^{2+} ions on the cross-section of crosslinked HC/SA films.

4.4.2 Swelling behavior and gel content of zinc or copper crosslinked HC/SA films in distilled water

To confirm crosslinked structure of the HC/SA hydrogels, swelling behavior and gel content in distilled water at 37 °C were measured. As seen in Fig. 4.38, compared to the equilibrium swelling degree of zinc or copper crosslinked films, the equilibrium swelling degree of calcium crosslinked films was higher. Since Ca^{2+} ions

could only crosslink with SA while Zn^{2+} and Cu^{2+} ions could crosslink both HC and SA resulting in relatively high crosslinking density in the corresponding films. Therefore, water was more difficult to be absorbed into zinc and copper crosslinked films leading to the relatively low degree of swelling. In addition, the films with high HC content exhibited higher equilibrium swelling degree. In case of calcium crosslinked films, it was because HC could not be crosslinked by Ca^{2+} ions. For zinc or copper crosslinked films, although both of HC and SA could be crosslinked, the films with high HC content still showed the higher equilibrium swelling degree. It is because structure of HC has longer side chain than that of SA hence it is difficult for molecules to arrange in close packing and thus allows the more free volume in the molecules where the water can easily penetrate into, resulting in relatively high degree of swelling.

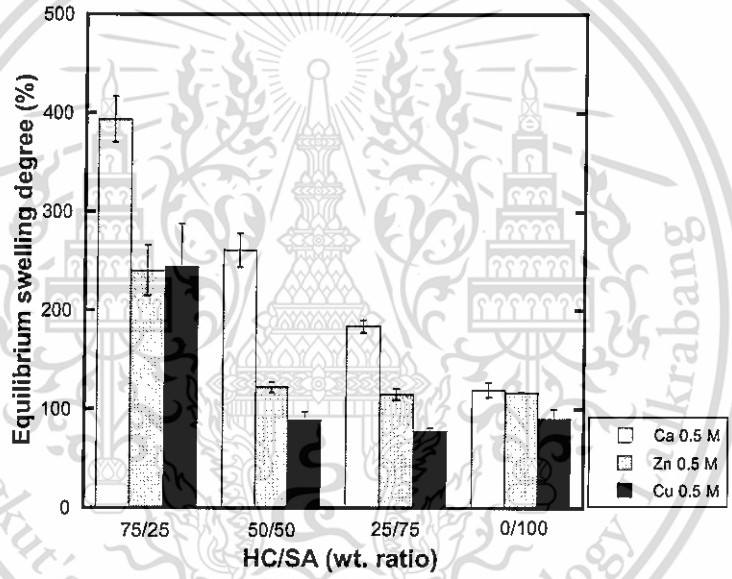

Figure 4.38 Equilibrium swelling degrees of crosslinked HC/SA films in distilled water at 37 °C.

Gel content with various ratios of HC to SA and kinds of crosslinking agents in distilled water at 37 °C are shown in Fig. 4.39. The values of gel content of crosslinked films were relatively high except for calcium crosslinked HC75SA25 film. It was because, in calcium crosslinking system, HC was not crosslinked causing in partially dissolution of the film.

At this point, all results proved that calcium ions could only crosslink with SA while zinc and copper ions could crosslink both HC and SA, corresponding to the FT-IR results. Schematic illustration of zinc or copper crosslinked HC/SA structure is proposed in Fig. 4.40.

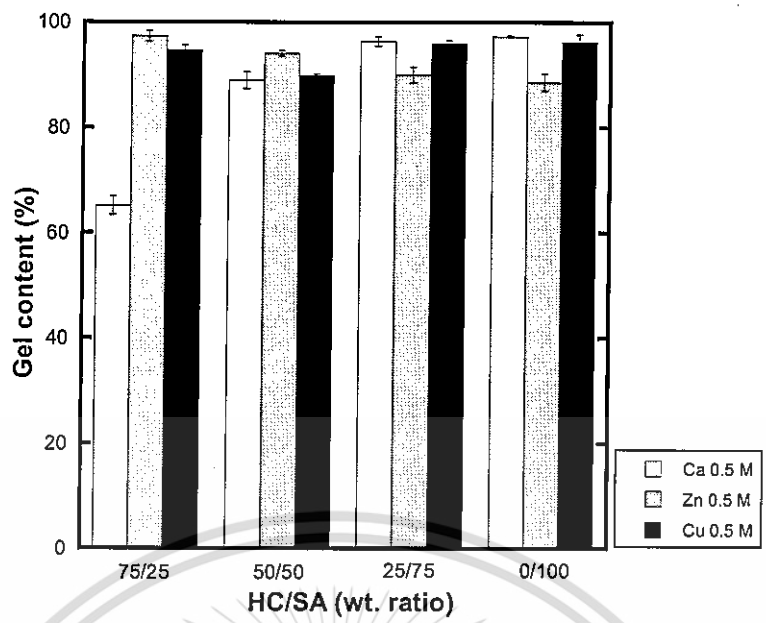

Figure 4.39 Gel contents of crosslinked HC/SA films in distilled water at 37 °C.

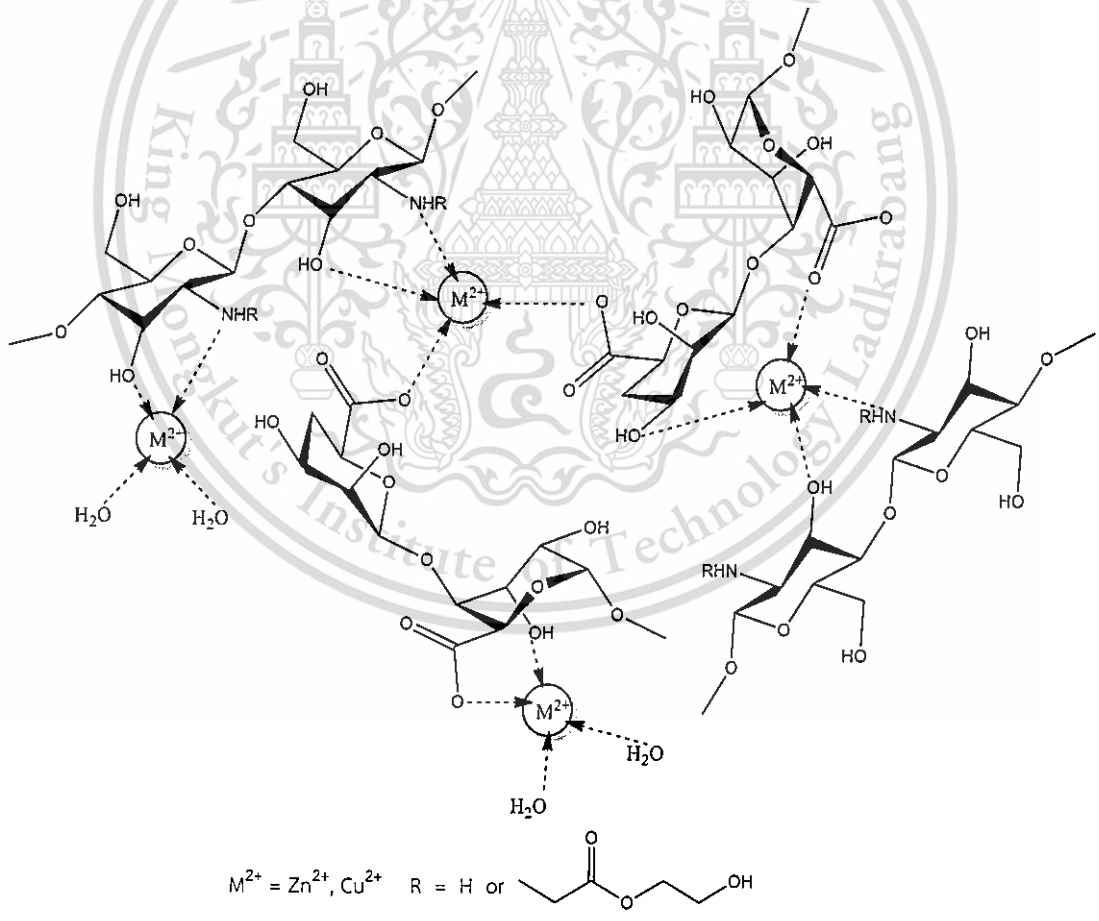

Figure 4.40 The proposed schematic illustration of zinc or copper crosslinked HC/SA structure.

4.4.3 *In vitro* swelling behavior and gel content of the crosslinked HC/SA films

4.4.3.1 Simulated gastric fluid (SGF, pH 1.2)

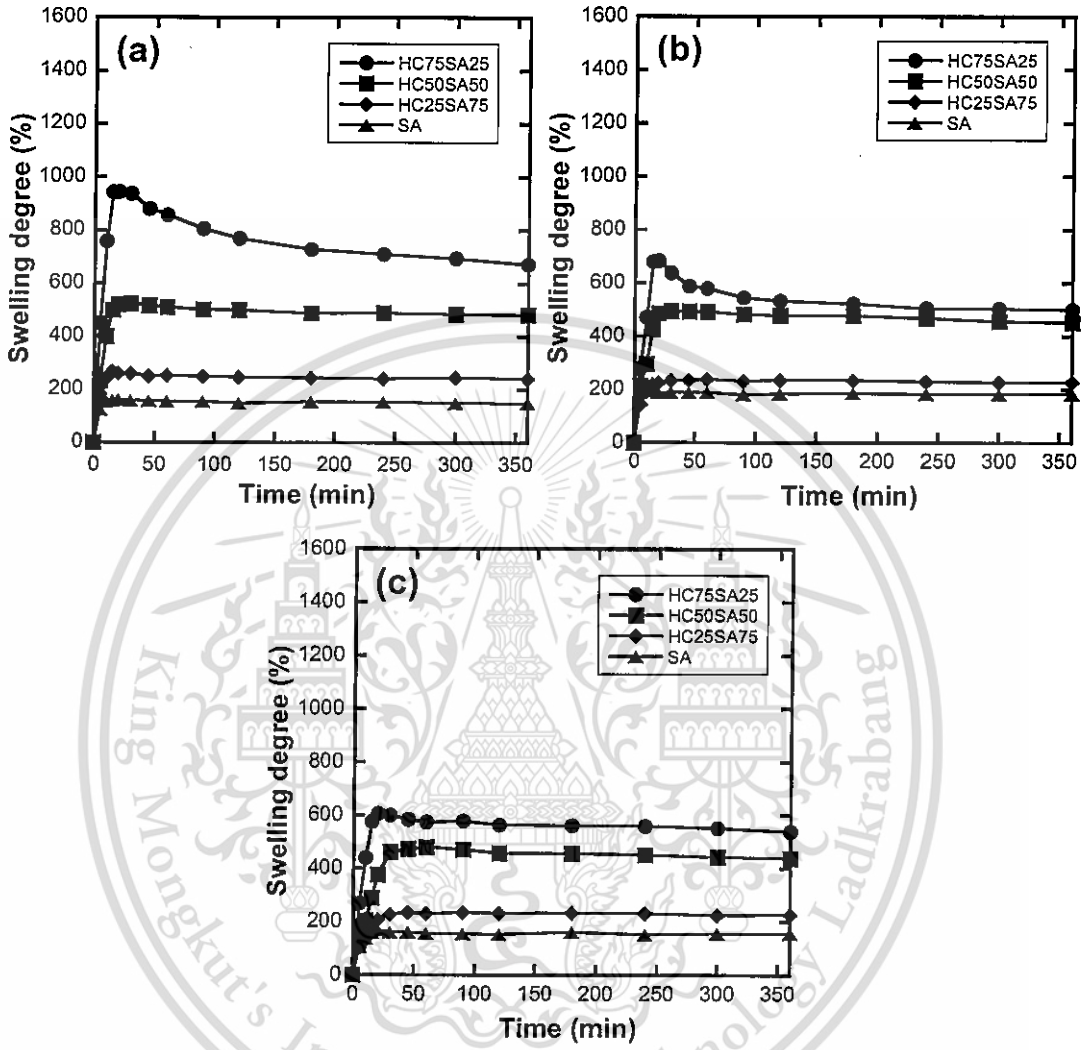

Figure 4.41 Swelling degrees of crosslinked HC/SA films with varying types of crosslinkers in SGF at 37 °C: (a) calcium chloride, (b) zinc sulfate and (c) copper(II) sulfate.

Swelling behavior of the crosslinked films in SGF at 37 °C was measured. The results are shown in Fig. 4.41. At the same type of crosslinkers, the HC75SA25 formulation exhibited the highest degree of swelling. This is because $-NHCH_2CH_2COOCH_2CH_2OH$ groups on HC can be protonated at pH 1.2, leading to the electrostatic repulsion among the ionized groups. In addition, the degree of swelling decreased along with increasing the amount of SA because $-COO^-$ groups on SA can turn to –COOH groups at low pH causing the strong hydrogen bond formations between carboxylic groups and hydroxyl groups. The types of crosslinker used (Ca^{2+},

Zn^{2+} and Cu^{2+}) had less significant effect on swelling degree of the crosslinked films, except for the HC75SA25 formulation. The swelling degree of zinc and copper crosslinked HC75SA25 films was lower than that of calcium crosslinked HC75SA25 film. It is because HC which is main component of the HC75SA25 film could be crosslinked by zinc or copper ions but not calcium ions resulting in the lower swelling degree of zinc or copper crosslinked HC75SA25 films.

Fig. 4.42 shows the gel content of the crosslinked films in SGF at 37 °C. In comparison with gel content in distilled water (Fig. 4.39), the gel content of the hydrogels in SGF was lower. It was because HC and SA became protonated in SGF resulting in the destruction of crosslinking points between metal ions (Ca^{2+}, Zn^{2+} and Cu^{2+}) and HC or SA causing dissolution of the uncrosslinked polymer from the hydrogels. Although the crosslinking points were destroyed, in case of SA, carboxylate groups in the SA after protonating could form hydrogen bonds which prevented the dissolution. Therefore, the gel content of the hydrogels with higher SA content was higher than the lower one. In HC75SA25 hydrogels, even though gel content values of zinc and copper crosslinked films were higher than that of calcium crosslinked films in distilled water, they were similar in SGF. These confirmed that crosslinking points between Zn^{2+} or Cu^{2+} ions and HC could be destroyed by H^{+} ions in SGF depending on the immersion time.

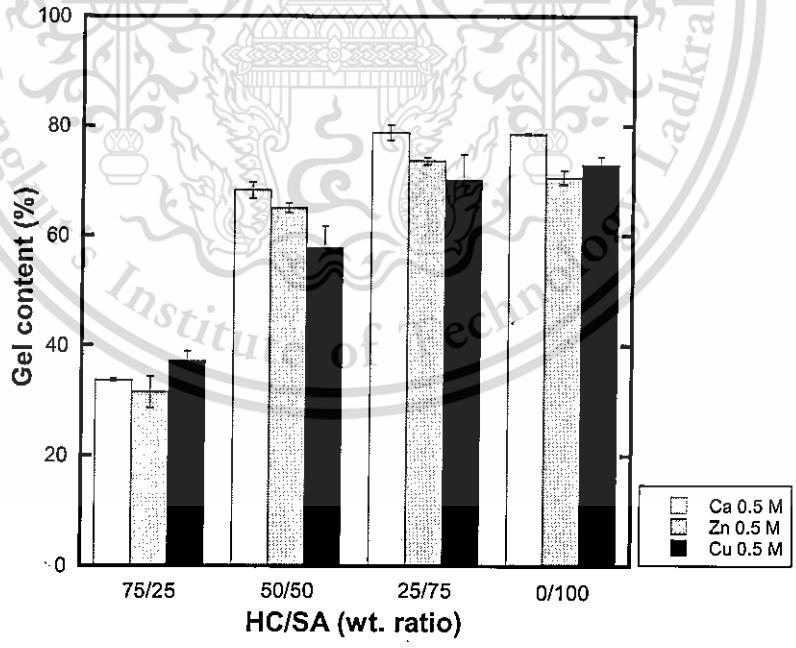

Figure 4.42 Gel contents of crosslinked HC/SA films in SGF at 37 °C.

4.4.3.2 Simulated intestinal fluid (SIF, pH 7.4)

The swelling behavior of the crosslinked HC/SA films in SIF at 37 °C was investigated. The results (Fig. 4.43) show that some of the hydrogel films degraded after a swelling period. The degradation occurred because of an exchange between PO_4^{3-} ions presented in SIF and metal ions in the crosslinked film leading to the lowering of crosslink density resulting in the dissolution of uncrosslink part. The degradation time significantly correlated to the hydrogel composition and crosslinker types. It is the fact that the stability of crosslinked films is dependent on the relative binding affinity of the metal ions for polymer. In case of calcium crosslinking system (Fig. 4.43a), the crosslinked films with higher ratio of HC to SA degraded faster than the lower one. The results indicated that the affinity of Ca^{2+} ion for HC was relatively low. Thus, Ca^{2+} ions could not crosslink HC at given concentration as discussed earlier. On the contrary, in case of zinc crosslinking system (Fig. 4.43b), the crosslinked films with higher ratio of SA to HC degraded faster than the others. It is because the binding affinity of Zn^{2+} ion for SA was lower than that of Ca^{2+} ions [184]. Thus, the less strongly bound Zn^{2+} ions were more easily displaced by the PO_4^{3-} ions presented in SIF. For copper crosslinking system (Fig. 4.43c), the degradation did not occur. Compared to calcium or zinc crosslinked films, the swelling degree of copper crosslinked film was the lowest. This could be attributed to the higher binding affinity of Cu^{2+} for HC and SA than Ca^{2+} and Zn^{2+}.

At this point, it could be concluded that the affinity of SA towards metal ions decreases in the following order: $Cu^{2+} > Ca^{2+} > Zn^{2+}$. Additionally, the affinity of HC for various metal ions is in the following order: $Cu^{2+} > Zn^{2+} > Ca^{2+}$. A similar trend was also observed in original CS [140].

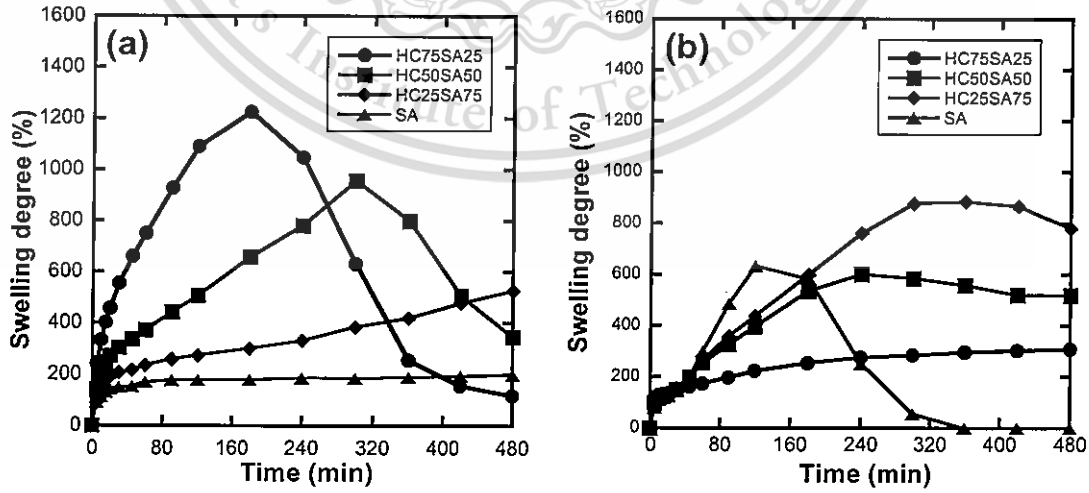

Figure 4.43 Swelling degrees of crosslinked HC/SA films with varying types of crosslinkers in SIF at 37 °C: (a) calcium chloride, (b) zinc sulfate and (c) copper(II) sulfate.

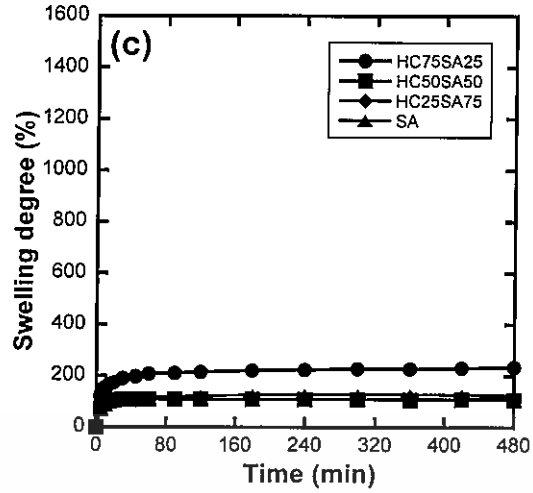

Figure 4.43 (cont.)

4.4.3.3 Simulated gastrointestinal fluid (SGF followed by SIF)

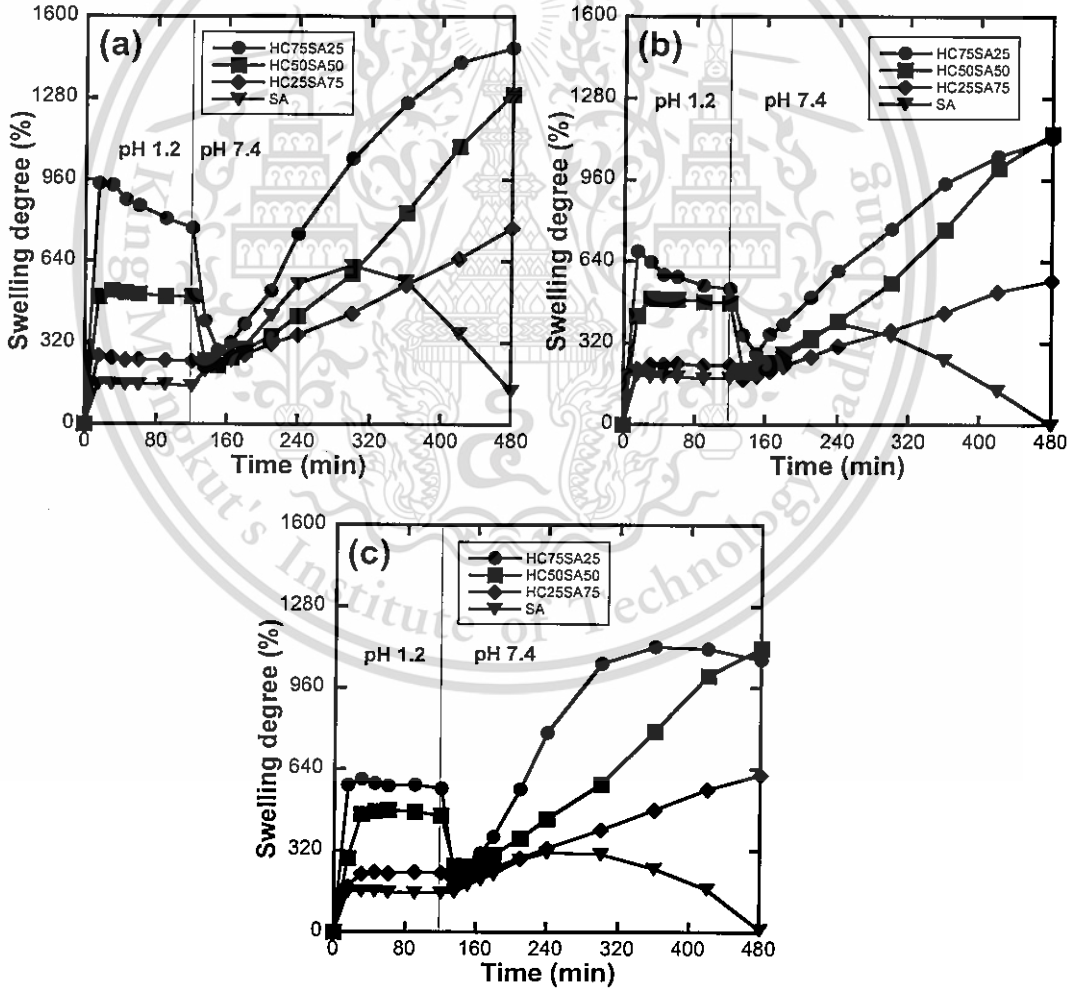

Figure 4.44 Swelling degrees of crosslinked HC/SA films with varying types of crosslinkers in simulated gastrointestinal fluid at 37 °C: (a) calcium chloride, (b) zinc sulfate and (c) copper(II) sulfate.

The swelling degree of the hydrogels in SGF (pH 1.2) for 2 h followed by in SIF (pH 7.4) for 6 h at 37 °C was determined. The results (Fig. 4.44) showed that the swelling degrees of all the hydrogels were quite stable in SGF within the first 2 h. When the hydrogels were transferred to SIF, the swelling degrees of the films containing HC decreased drastically because of the deprotonation of HC at neutral pH and the formation of polyelectrolyte complexes between HC and SA, as discussed in section 4.2.3.3 and 4.3.5.3. Compared to direct immersing in SIF, the behaviors of the films immersing in SGF followed by SIF changed significantly. In case of SA formulation, the degradation occurred in all samples (calcium, zinc and copper crosslinked films) after immersing in SGF followed by SIF unlike direct immersing in SIF (only zinc crosslinked SA film degraded). Additionally, the trend of swelling degree of the zinc crosslinked films changed. The swelling degrees of the zinc crosslinked films in SIF increased with increasing ratio of SA to HC. On the contrary, their swelling degrees in SGF followed by SIF increased with increasing ratio of HC to SA. Moreover, the swelling degrees of the copper crosslinked films in SGF followed by SIF were higher than that of the copper crosslinked films in directed SIF. All results suggested that metal ions in the crosslinked films could be partially replaced by H^+ ions in SGF leading to the reduction of crosslinking points resulting in the change of the behaviors of the crosslinked films. Because of the leaching of metal ions from the crosslinked films, the crosslinker types used did not induce significant changes in the swelling degree of the crosslinked films.

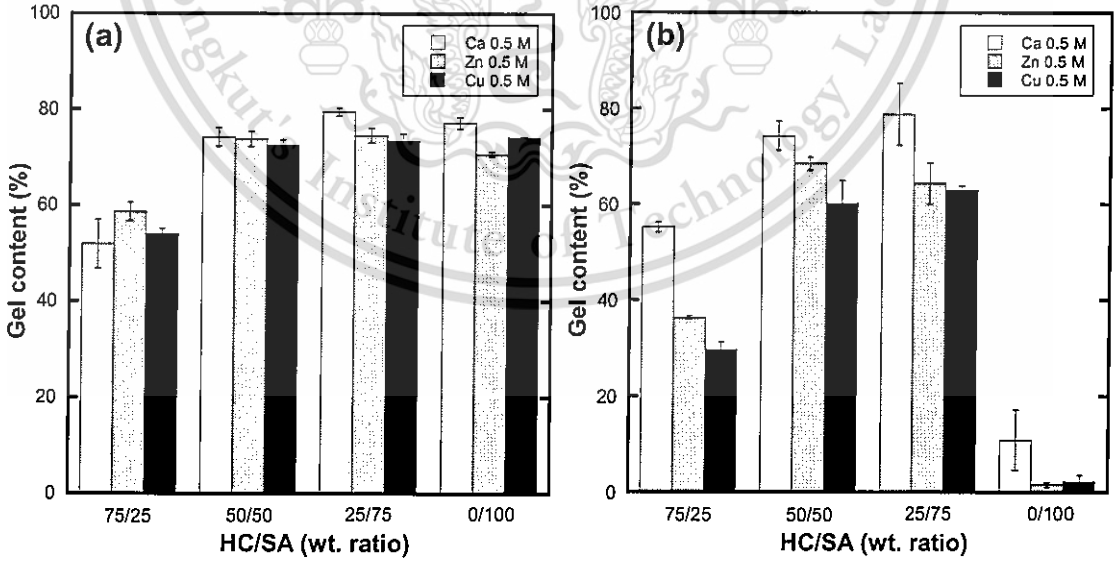

Figure 4.45 Gel contents of crosslinked HC/SA films after immersing in SGF for 2 h (a) and after immersing in SGF for 2 h followed by SIF for 6 h (b) at 37 °C.

Stability of the crosslinked films was established by observation in the gel content. Fig. 4.45a shows the gel content of crosslinked films in SGF for 2 h. It was found that the gel content of hydrogel films was relatively high in SGF (> 50%). There were no significant differences in gel content when changing crosslinker type. However, the influence of the types of crosslinkers could be observed when the hydrogel films were transferred to SIF. The gel contents of the hydrogel in SGF followed by SIF are displayed in Fig. 4.45b. The values of the hydrogel prepared from SA solely exhibited the lowest because there was no complexation between HC and SA in SA hydrogel as discussed earlier. At the same HC to SA ratio, the gel contents of calcium crosslinked films were higher compared to the others because the complexation of HC by zinc or copper ions reduced the number of $-NH_2^+CH_2CH_2COOCH_2CH_2OH$ groups available for interactions with $-COO^-$ groups of SA [230].

4.4.4 *In vitro* drug release studies

From the section 4.3.6, it was found that the HC50SA50 formulation crosslinked with 0.5 M $CaCl_2$ exhibited the lowest drug release rate. Therefore, the HC50SA50 formulation was selected to study an alternative drug delivery system with using different types of crosslinkers. Effect of crosslinker types on drug release was investigated as the results shown in Fig. 4.46. All the hydrogels exhibited a very slight paracetamol release in SGF (< 20%). The use of crosslinking procedures (Ca^{2+}, Zn^{2+}, and Cu^{2+}) showed no burst release in SIF. The rate of drug release from calcium crosslinking system was significant slower than that from zinc or copper crosslinking system, represented by gel content values.

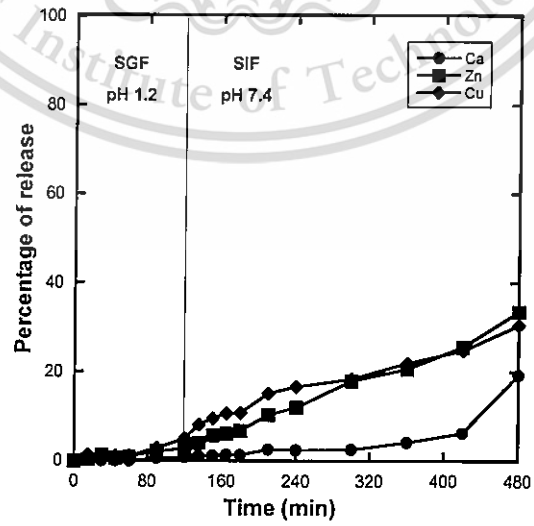

Figure 4.46 Percentages of paracetamol release from crosslinked films after immersing in SGF for 2 h followed by SIF for 6 h at 37 °C.

4.4.5 Drug release kinetics

The drug release kinetics mechanism of paracetamol from the HC/SA hydrogels with different types of crosslinkers was studied using various mathematical models, i.e., zero order, first order, Higuchi and Korsmeyer-Peppas model. The results of the curve fitting are given in Table 4.5. In SGF, the results did not fit for any equations. It was due to the relatively low amount of paracetamol release from the hydrogels. In SIF, in case of zinc and copper crosslinking systems, the release profiles showed good fit for zero order model (R^2 were 0.9897 for HC50SA50-Zn0.5 and 0.9811 for HC50SA50-Cu0.5) implying the independent of paracetamol concentration on drug release. However, the release profile of HC50SA50-Ca0.5 did not show fit for any equations due to the very low amount of paracetamol release in SIF, as discussed in release studies (section 4.4.4).

Table 4.5 Results of curve fitting into different mathematical models for paracetamol release profile from zinc or copper crosslinked HC/SA films in SGF followed by SIF at 37 °C.

Formulation	Correlation coefficient, R^2				Release exponent, n (Korsmeyer-Peppas model)
	Zero order	First order	Higuchi model	Korsmeyer-Peppas model	
SGF					
HC50SA50-Ca0.5	0.9248	0.7518	0.7184	0.8434	2.2573
HC50SA50-Zn0.5	0.8852	0.7474	0.7895	0.7693	0.9111
HC50SA50-Cu0.5	0.8401	0.7840	0.6865	0.5147	0.6131
SIF					
HC50SA50-Ca0.5	0.7054	0.9470	0.6488	0.8888	1.7507
HC50SA50-Zn0.5	0.9897	0.9419	0.9773	0.9874	1.5805
HC50SA50-Cu0.5	0.9811	0.9346	0.9802	0.9783	0.9794

In summary, the calcium crosslinked film showed the higher stability than that of zinc or copper crosslinked film in simulated gastrointestinal fluid because the complexation of HC by zinc or copper ions impeded the formation of polyelectrolyte complexes between HC and SA. The rate of drug release from calcium crosslinking system was the lowest compared to zinc and copper crosslinking system. Therefore, the crosslinking by calcium ions was selected for the following studies.

4.5 Characterization and properties of crosslinked HC/SA capsules

4.5.1 Preparation of crosslinked HC/SA capsules

The capsule has been widely used to deliver a drug *via* the gastrointestinal tract [231-233]. Initially drugs are usually filled into the capsule to provide a unit dose that effectively masks the bitter taste of drugs in an easy to swallow container. The capsule is generally manufactured by dipping metal pins in the gelling agent solution. To achieve the desired shell distribution to manufacture capsule, it is necessary to ensure that the dipping composition adheres to the pin surface and quickly gels after withdrawing the pins from the dipping bath. Therefore, it is hard to fabricate the capsule from HC/SA solution because HC/SA solution cannot form gel immediately after dipping process causing the flow of the composition on the pin surface. In order to overcome this problem, in this work, carrageenan was used. Carrageenan is a Rhodophyta-derived polysaccharide with side-chains of sulfonic groups [156]. Carrageenan gel is thermoreversible. It melts and has low viscosity at high temperature, meanwhile, it solidifies and forms gels at temperatures below 50 °C [198]. As previously mentioned, the addition of carrageenan made manufacture capsule from HC/SA solution easier because the solution could form gel with cooling preventing the flow of the composition on the pin surface. Another problem of manufacture capsule was difficult removing capsule shell from pin. It is because natural polymers used in this work are fragile and brittle. To make it easier to strip the capsule shells from the pins, plasticizer was added. In this work, glycerol was selected. It has been reported that glass transition temperature (T_g) of polysaccharide films strongly decreases with increasing glycerol content [206].

As mentioned above, in this study, HC/SA capsules were, therefore, prepared by dipping metal pins in the solution composed of HC, SA, carrageenan and glycerol. After drying, the shells were stripped of the pins and cut to desired length. The HC/SA capsules were prepared by using various weight ratios of HC:SA, i.e., 50:50 and 0:100. Carrageenan and glycerol contents were fixed at 42.5 and 15% w/w, respectively. It was because at carrageenan content less than 42.5% w/w, the gel could not be properly formed after dipping process causing the flow of the composition on the pin surface. In addition, at glycerol content less than 15% w/w, the capsule was not flexible enough for stripping from the pin. The crosslinked HC/SA capsule was prepared by dipping the HC/SA capsule into 0.5 M calcium chloride solution (selected from section 4.4). After dipping, the capsules became harder because the crosslinking occurred and glycerol was dissolved from the capsule. The photographs of the different capsules are given in Fig.4.47. The appearance of all prepared capsules was transparent. The capsule containing HC was yellow. The size of the different capsules is listed in Table 4.6. It was found

that the size of the capsule became smaller after crosslinking, especially the capsule with high SA content. This was due to the crosslinking reaction between SA and Ca^{2+} ions.

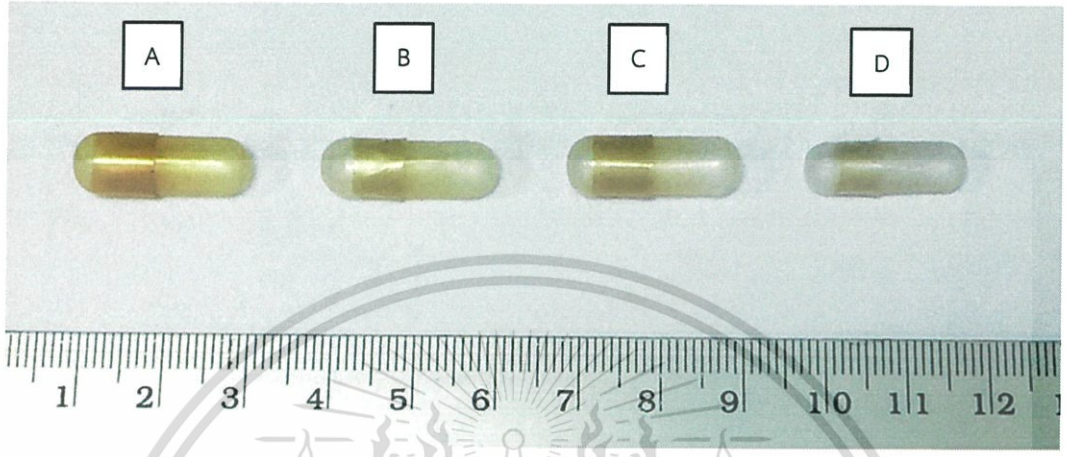

Figure 4.47 Photographs of different capsules: (a) HC50SA50 capsule, (b) HC50SA50Ca capsule, (c) SA capsule and (d) SACa capsule.

Table 4.6 The size of the different capsules.

Formulation	Cap			Body		
	External Diameter (mm)	Length (mm)	Thickness (mm)	External Diameter (mm)	Length (mm)	Thickness (mm)
H50S50	7.600 ±0.100	10.730 ±0.060	0.108 ±0.010	7.280 ±0.030	18.433 ±0.060	0.098 ±0.010
H50SA50Ca	7.470 ±0.120	10.220 ±0.030	0.102 ±0.010	7.270 ±0.060	17.830 ±0.060	0.100 ±0.010
SA	7.580 ±0.010	10.200 ±0.050	0.099 ±0.010	7.230 ±0.150	18.400 ±0.100	0.104 ±0.010
SACa	6.630 ±0.060	9.450 ±0.230	0.098 ±0.010	6.330 ±0.060	16.000 ±0.200	0.100 ±0.010

4.5.2 *In vitro* drug release studies

Fig. 4.48 shows the release profiles of paracetamol from the capsules after immersing in SGF for 2 h followed by SIF for 6 h at 37 °C. For gelatin capsule (commercial capsule), paracetamol was released completely within 15 min. On the contrary, the rate of paracetamol released from the prepared capsules was slower.

The amount of paracetamol released in SGF was lower than 40% for HC50SA50Ca capsule and 25% for SACa capsule. Paracetamol released lower from the capsule containing higher SA content because $-COO^-$ groups on SA could turn to –COOH groups at low pH causing the strong hydrogen bond formations between carboxylic groups and hydroxyl groups preventing the release of paracetamol. After transferring the capsules to SIF, it was found that the SACa capsule failed to control the drug release and burst release was observed within 3 h. It was because SA was converted to insoluble alginic acid at low pH (SGF), which induced crack formation or lamination of SA matrix, and later converted to soluble alginate form at SIF leading to the burst release. Meanwhile, there was no burst release for the HC50SA50Ca capsule. The HC50SA50Ca capsule showed the linearity of drug release profile and paracetamol was completely released in SIF. The results suggested that the HC50SA50Ca capsule could be a good candidate to be used for controlling drug release in the small intestine. However, it could be seen that the amount of paracetamol released from the capsules was higher than the sealed bags formed by HC/SA films (the results show in the section 4.4). This is because carrageenan added during capsule preparation can be ionized in both SGF and SIF (the pK_a value of the sulfate group on carrageenan is lower than 2) leading to the electrostatic repulsion among the ionized groups causing the increase in swelling degree resulting in the higher amount of paracetamol released [234]. In addition, glycerol in capsule could also be dissolved in both SGF and SIF allowing the formation of the voids in polymer matrix and leading to a fast release of paracetamol. Moreover, carrageenan used in this study was food-grade which is the mixture of iota, kappa, and lambda carrageenans. It was reported that lambda carrageenan is incapable of forming a double helix; therefore, it cannot form gel [198]. Because of this reason, when immersing capsule in tested fluid, uncrosslink part was easily dissolved from the capsule resulting in the higher amount of paracetamol released. Additionally, paracetamol loaded was in powder form for the capsule but in tablet form for the sealed bag. The former, thus, was easily dissolved in tested fluid causing the higher amount of paracetamol released comparing to the latter.

Fig. 4.49 shows the photographs of the capsules after releasing paracetamol. It was found that the shell of HC50SA50Ca capsule still maintained, meanwhile, the shell of the SACa capsule disintegrated. The results indicated that the predominant mechanisms for controlled release drug were the swelling mechanism for HC50SA50Ca capsule and erosion mechanism for SACa capsule.

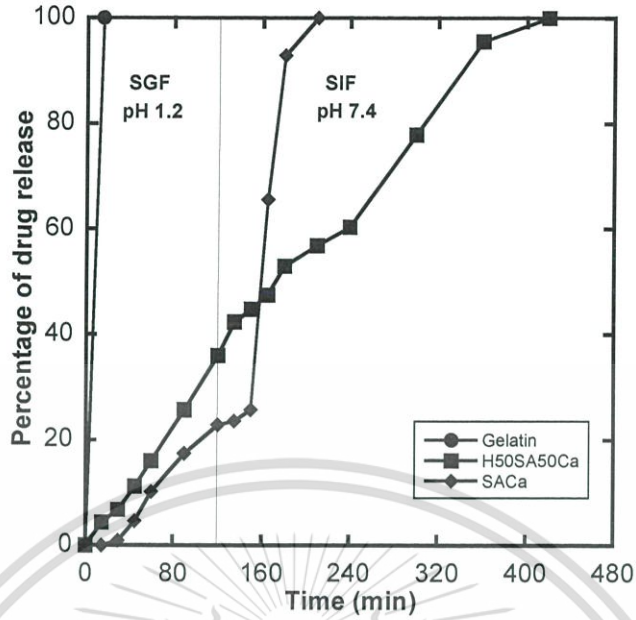

Figure 4.48 Percentages of paracetamol release from the capsules after immersing in SGF for 2 h followed by SIF for 6 h at 37 °C.

Figure 4.49 The photographs of the capsules after releasing paracetamol: (a) HC50SA50Ca capsule and (b) SACa capsule.

4.5.3 MTT assay

Cell viability of the synthesized capsules was determined following the MTT assay. The average percentages of cytotoxicity of HC50SA50 and SA capsules crosslinked by 0.5 M $CaCl_2$ were 9.73±3.22 and 8.72±1.46, respectively. It could be concluded that the prepared capsules were not toxic to human cells.

Consequently, the capsules formed by HC and SA were successfully prepared by using dipping process. Carrageenan and glycerol were added to manufacture the capsule. The HC50SA50Ca capsule showed the linearity of drug release profile and all paracetamol was released in SIF. Additionally, all the prepared capsules were noncytotoxic. The comprehensive results of this study suggested their potential in controlled drug release in small intestine.

Chapter 5
Conclusions and Recommendations

5.1 Conclusions

This research successfully prepared the novel pH-sensitive hydroxyethylacryl chitosan (HC)/ sodium alginate (SA) hydrogels using various metal ions (Ca^{2+}, Zn^{2+} and Cu^{2+}) as crosslinkers for a site-specific oral drug delivery. Firstly, HC was synthesized by Michael addition reaction of chitosan and hydroxyethylacrylate. The structure of synthesized HC was confirmed by FT-IR, ^{1}H-NMR, and XRD. It was found that the synthesized HC could dissolve in water at 70 °C. The optimum conditions to obtain the highest yield of HC were 60 °C of temperature and 48 h of time. The yield, DS and M_w of the synthesized HC were 80%, 1.22 and 62,700 Daltons, respectively.

The HC/SA films were prepared by using solvent casting method. The crosslinked HC/SA films were obtained by dipping the HC/SA films into various metal ions solution (Ca^{2+}, Zn^{2+} and Cu^{2+}). FT-IR results demonstrated that Ca^{2+} ions could crosslink only SA through the formation of ionic bonds while Zn^{2+} and Cu^{2+} ions could crosslink both HC through the formation of coordinate bonds and SA through the formation of partially ionic or coordinate bonds. It was found that these hydrogel films possessed pH-sensitive properties. The HC/SA hydrogel films were stable in simulated gastric fluid (SGF, pH 1.2) but degraded in simulated intestinal fluid (SIF, pH 7.4). In addition, the combination between HC and SA could delay the degradation rate of the hydrogel films in simulated gastrointestinal fluid (SGF followed by SIF) due to the formation of polyelectrolyte complexes between HC and SA during the transfer of the film from SGF to SIF. Furthermore, the calcium crosslinked film exhibited the higher stability in simulated gastrointestinal fluid than that of zinc or copper crosslinked film because the complexation of HC by zinc or copper ions impeded the formation of polyelectrolyte complexes between HC and SA. The release profiles of paracetamol from sealed bags formed by HC/SA hydrogel films in simulated gastrointestinal fluid were also investigated. The results showed that the amount of paracetamol released in SGF was relatively low (< 20%) and the burst release of paracetamol in SIF was depressed by increasing HC content and/or applying crosslinker. The rate of drug release from calcium crosslinking system was much slower than that from zinc or copper crosslinking system because of the higher stability in calcium crosslinking system. The sealed bag formed by the non-crosslinked HC75SA25 films demonstrated the linearity of drug release profile and almost all paracetamol was released in SIF. This formulation, thus, can be a good candidate to be used for controlling drug release in the small intestine.

Interestingly, the HC50SA50 formulation crosslinked with 0.5 M calcium chloride exhibited the relatively low drug release in simulated gastrointestinal fluid (< 20%). This indicated that this formulation could be a potential candidate for a site-specific drug delivery in the colon.

The HC/SA hydrogel capsules were also prepared by dipping process using carrageenan and glycerol as gelling agent and plasticizer, respectively. The HC50SA50 capsule crosslinked with 0.5 M calcium chloride showed the linearity of drug release profile and paracetamol was completely released in SIF. The results suggested that this formulation could be a potential candidate for controlled drug release in small intestine.

In summary, this development of HC/SA hydrogels using various metal ions as crosslinkers reported in this thesis showed their pH-sensitive behavior. This demonstrated that HC/SA hydrogels can be further tailored to expand the utilization of these systems in controlled drug release in different parts of the body.

5.2 Recommendations

1. Repeat some of the studies reported in this thesis using different drugs (hydrophobic and/or of higher molecular weight).

2. If the capsule with lowering drug release is required, the grade of carrageenan used (food grade carrageenan) should be changed to pure iota carrageenan and pure kappa carrageenan.

3. The processes of capsule preparation should be developed for larger production scale.

References

1. K.K. Jain. 2008. **Drug Delivery Systems**. New York: Humana Press.
2. M. Rizwan, R. Yahya, A. Hassan, M. Yar, A.D. Azzahari, V. Selvanathan, F. Sonsudin and C.N. Abouloul. 2017. "pH sensitive hydrogels in drug delivery: Brief history, properties, swelling, and release mechanism, material selection and applications." *Polymers*. 9: 1-37.
3. L.S. Liu, M.L. Fishman, J. Kost and K.B. Hicks. 2003. "Pectin-based systems for colon-specific drug delivery via oral route." *Biomaterials*. 24: 3333-3343.
4. M. D Kurkuri and T. M Aminabhavi. 2004. "Poly(vinyl alcohol) and poly(acrylic acid) sequential interpenetrating network pH-sensitive microspheres for the delivery of diclofenac sodium to the intestine." *Journal of Controlled Release*. 96: 9-20.
5. M. George and T.E. Abraham. 2007. "pH sensitive alginate-guar gum hydrogel for the controlled delivery of protein drugs." *International Journal of Pharmaceutics*. 335: 123-129.
6. Y. Luo and Q. Wang, 2014. "Recent development of chitosan-based polyelectrolyte complexes with natural polysaccharides for drug delivery." *International Journal of Biological Macromolecules*. 64: 353-367.
7. N. Bhattarai, J. Gunn and M. Zhang. 2010. "Chitosan-based hydrogels for controlled, localized drug delivery." *Advanced Drug Delivery Reviews*. 62: 83-99.
8. M. Dash, F. Chiellini, R.M. Ottenbrite and E. Chiellini. 2011. "Chitosan-A versatile semi-synthetic polymer in biomedical applications." *Progress in Polymer Science*. 36: 981-1014.
9. S. Jana, N. Maji, A.K. Nayak, K.K. Sen and S.K. Basu. 2013. "Development of chitosan-based nanoparticles through inter-polymeric complexation for oral drug delivery." *Carbohydrate Polymers*. 98: 870-876.
10. A. Kumar and M. Ahuja. 2013. "Carboxymethyl gum kondagogu-chitosan polyelectrolyte complex nanoparticles: Preparation and characterization." *International Journal of Biological Macromolecules*. 62: 80-84.
11. Y. Zhou, D. Yang, X. Gao, X. Chen, Q. Xu, F. Lu and J. Nie. 2009. "Semi-interpenetrating polymer network hydrogels based on water-soluble *N*-carboxylethyl chitosan and photopolymerized poly(2-hydroxyethyl methacrylate)." *Carbohydrate Polymers*. 75: 293-298.

12. G. Ma, D. Yang, Y. Zhou, M. Xiao, J.F. Kennedy and J. Nie. 2008. "Preparation and characterization of water-soluble *N*-alkylated chitosan." *Carbohydrate Polymers*. 74: 121-126.

13. X.Z. Shu, K.J. Zhu and W. Song. 2001. "Novel pH-sensitive citrate cross-linked chitosan film for drug controlled release." *International Journal of Pharmaceutics*. 212: 19-28.

14. B. Zeeb, A.H. Saberi, J. Weiss and D.J. McClements. 2015. "Formation and characterization of filled hydrogel beads based on calcium alginate: Factors influencing nanoemulsion retention and release." *Food Hydrocolloids*. 50: 27-36.

15. M.C. Straccia, G.G. d'Ayala, I. Romano and P. Laurienzo. 2015. "Novel zinc alginate hydrogels prepared by internal setting method with intrinsic antibacterial activity." *Carbohydrate Polymers*. 125: 103-112.

16. N.S. Heliopoulos, S.K. Papageorgiou, A. Galeou, E.P. Favvas, F.K. Katsaros and K. Stamatakis. 2013. "Effect of copper and copper alginate treatment on wool fabric. Study of textile and antibacterial properties." *Surface & Coatings Technology*. 235: 24-31.

17. S.N. Pawar and K.J. Edgar. 2012. "Alginate derivatization: A review of chemistry, properties and applications." *Biomaterials*. 33: 3279-3305.

18. A.K. Nayak, D. Pal and K. Santra. 2016. "Swelling and drug release behavior of metformin HCl-loaded tamarind seed polysaccharide-alginate beads." *International Journal of Biological Macromolecules*. 82: 1023-1027.

19. A.K. Nayak, B. Das and R. Maji. 2012. "Calcium alginate/gum Arabic beads containing glibenclamide: Development and *in vitro* characterization." *International Journal of Biological Macromolecules*. 51: 1070-1078.

20. S. Hua, H. Ma, X. Li, H. Yang and A. Wang. 2010. "pH-sensitive sodium alginate/poly(vinyl alcohol) hydrogel beads prepared by combined Ca^{2+} crosslinking and freeze-thawing cycles for controlled release of diclofenac sodium." *International Journal of Biological Macromolecules*. 46: 517-523.

21. P. Sinha, U. Ubaidulla, M.S. Hasnain, A.K. Nayak and B. Rama. 2015. "Alginate-okra gum blend beads of diclofenac sodium from aqueous template using $ZnSO_4$ as a cross-linker." *International Journal of Biological Macromolecules*. 79: 555-563.

22. S.S. Vaghani, M.M. Patel and C.S. Satish. 2012. "Synthesis and characterization of pH-sensitive hydrogel composed of carboxymethyl chitosan for colon targeted delivery of ornidazole." *Carbohydrate Research*. 347: 76-82.

23. I.M. El-Sherbiny. 2010. "Enhanced pH-responsive carrier system based on alginate and chemically modified carboxymethyl chitosan for oral delivery of protein drugs: Preparation and *in-vitro* assessment." *Carbohydrate Polymers*. 80: 1125-1136.

24. M. Tavakol, E. Vasheghani-Farahani, T. Dolatabadi-Farahani and S. Hashemi-Najafabadi. 2009. "Sulfasalazine release from alginate-*N,O*-carboxymethyl chitosan gel beads coated by chitosan." *Carbohydrate Polymers*. 77: 326-330.

25. J. Yang, J. Chen, D. Pan, Y. Wan and Z. Wang. 2013. "pH-sensitive interpenetrating network hydrogels based on chitosan derivatives and alginate for oral drug delivery." *Carbohydrate Polymers*. 92: 719-725.

26. R. Gong, C. Li, S. Zhu, Y. Zhang, Y. Du and J. Jiang. 2011. "A novel pH-sensitive hydrogel based on dual crosslinked alginate/ *N*-α-glutaric acid chitosan for oral delivery of protein." *Carbohydrate Polymers*. 85: 869-874.

27. A.F. Martins, P.V. Bueno, E.A. Almeida, F.H. Rodrigues, A.F. Rubira and E.C. Muniz. 2013. "Characterization of *N*-trimethyl chitosan/alginate complexes and curcumin release." *International Journal of Biological Macromolecules*. 57: 174-184.

28. L. Li, L. Wang, Y. Shao, R. Ni, T. Zhang and S. Mao. 2013. "Drug release characteristics from chitosan-alginate matrix tablets based on the theory of self-assembled film." *International Journal of Pharmaceutics*. 450: 197-207.

29. G.L. Amidon, H. Lennernas, P.V. Shah and J.R. Crison. "A theoretical basis for a biopharmaceutic drug classification: The correlation of *in vitro* drug product dissolution and *in vivo* bioavailability." *Pharmaceutical Research*. 12: 413-420.

30. B.D. Ratner, A.S. Hoffman, F.J. Schoen and J.E. Lemons. 1996. **Biomaterials Science: An Introduction to Materials in Medicine**. California: Academic Press.

31. A. Sood and R. Panchagnula. 2003. "Design of controlled release delivery systems using a modified pharmacokinetic approach: a case study for drugs having a short elimination half-life and a narrow therapeutic index." *International Journal of Pharmaceutics*. 261: 27-41.

32. R. Baker. 1987. **Controlled Release of Biologically Active Agents**. New York: John Wiley and Sons.

33. M. Alger. 1997. **Polymer Science Dictionary**. London: Chapman & Hall.

34. A.S. Hoffman. 2002. "Hydrogels for biomedical applications." *Advanced Drug Delivery Reviews*. 54. 3-12.

35. Y. Osada and K. Kajiwara. 2001. **Gels Handbook Volume 1: The Fundamentals**. California: Academic Press.

36. J.F. Künzler. 2003. **Hydrogel. In: Encyclopedia of Polymer Science and Technology**. New York: John Wiley and Sons.

37. A.V. Duflot, N.K. Kitaeva and V.R. Duflot. 2015. "Radiation-chemical preparation of poly(vinyl alcohol) hydrogels." *Radiation Physics and Chemistry*. 107: 1-6.

38. V. Ermatchkov, L. Ninni and urer. 2010. "Thermodynamics of phase equilibrium for systems containing *N*-isopropyl acrylamide hydrogels." *Fluid Phase Equilibria*. 296: 140-148.

39. L.D. Amer, A. Holtzinger, G. Keller, M.J. Mahoney and S.J. Bryant. 2015. "Enzymatically degradable poly(ethylene glycol) hydrogels for the 3D culture and release of human embryonic stem cell derived pancreatic precursor cell aggregates." *Acta Biomaterialia*. 22: 103-110.

40. R. Jin, L.S. Moreira Teixeira, P.J. Dijkstra, M. Karperien, C.A. van Blitterswijk, Z.Y. Zhong and J. Feijen. 2009. "Injectable chitosan-based hydrogels for cartilage tissue engineering." *Biomaterials*. 30: 2544-2551.

41. R. Pereira, A. Carvalho, D.C. Vaz, M.H. Gil, A. Mendes and P. Bártoloa. 2013. "Development of novel alginate based hydrogel films for wound healing applications." *International Journal of Biological Macromolecules*. 52: 221-230.

42. X. Zhang, Y. Wang, C. Lu and W. Zhang. 2014. "Cellulose hydrogels prepared from micron-sized bamboo cellulose fibers." *Carbohydrate Polymers*. 114: 166-169.

43. E.A. Kamoun, E.R.S. Kenawy, T.M. Tamer, M.A. El-Meligy and M.S.M. Eldin. 2015. "Poly(vinyl alcohol)-alginate physically crosslinked hydrogel membranes for wound dressing applications: Characterization and bio-evaluation." *Arabian Journal of Chemistry*. 8: 38-47.

44. D. Das and S. Pal. 2015. "Dextrin/poly(HEMA): pH responsive porous hydrogel for controlled release of ciprofloxacin." *International Journal of Biological Macromolecules*. 72: 171-178.

45. F.G. Thankam and J. Muthu. 2015. "Alginate-polyester comacromer based hydrogels as physiochemically and biologically favorable entities for cardiac tissue engineering." *Journal of Colloid and Interface Science*. 457: 52-61.

46. R.M. Ottenbrite, K. Park and T. Okano. 2010. **Biomedical Applications of Hydrogels Handbook**. New York: Springer.

47. E.M. Ahmed. 2015. "Hydrogel: Preparation, characterization, and applications: A review." *Journal of Advanced Research*. 6: 105-121.

48. N. Roshan and M. Rahul. 2013. "Photosensitive hydrogels for advanced drug delivery." *IJPI International Journal of pharmaceutical innovations*. 3: 11-16.

49. L Zhang, L. Wang, B. Guo, P.X. Ma. 2014. "Cytocompatible injectable carboxymethyl chitosan/*N*-isopropylacrylamide hydrogels for localized drug delivery." *Carbohydrate Polymers*. 103: 110-118.

50. Y. Kim, R. Iwatsuki, K. Kikuta, Y. Morita, T. Miyazaki and C. Ohtsuki. 2011. "Thermoreversible behavior of *K*-carrageenan and its apatite-forming ability in simulated body fluid." *Materials Science and Engineering*. 31: 1472-1476.

51. N. Bhattarai, F.A. Matsen and M. Zhang. 2005. "PEG-grafted chitosan as an injectable thermoreversible hydrogel." *Macromolecular Bioscience*. 5: 107-111.

52. P. Mukhopadhyay, K. Sarkar, S. Bhattacharya, A. Bhattacharyya, R. Mishra and P.P. Kundua. 2014. "pH sensitive *N*-succinyl chitosan grafted polyacrylamide hydrogel for oral insulin delivery." *Carbohydrate Polymers*. 112: 627-637.

53. M.A.A. El-Ghaffar, M.S. Hashem, M.K. El-Awady and A.M. Rabie. 2012. "pH-sensitive sodium alginate hydrogels for riboflavin controlled release." *Carbohydrate Polymers*. 89: 667-675.

54. G.R. Mahdavinia, H. Etemadi and F. Soleymani. 2015. "Magnetic/pH-responsive beads based on caboxymethyl chitosan and *K*-carrageenan and controlled drug release." *Carbohydrate Polymers*. 128: 112-121.

55. R. Hou, L. Nie, G. Du, X. Xiong and J. Fu. 2015. "Natural polysaccharides promote chondrocyte adhesion and proliferation on magnetic nanoparticle/PVA composite hydrogels." *Colloids and Surfaces B: Biointerfaces*. 132: 146-154.

56. C.Y. Chiang and C.C. Chu. 2015. "Synthesis of photoresponsive hybrid alginate hydrogel with photo-controlled release behavior" *Carbohydrate Polymers*. 119: 18-25.

57. J.Y. Wong and J.D. Bronzino. 2007. **Biomaterials**. New York: CRC Press.

58. L. Fan, Y. Du, B Zhang, J Yang, J. Zhou and J.F. Kennedy. 2006. "Preparation and properties of alginate/carboxymethyl chitosan blend fibers." *Carbohydrate Polymers*. 65: 447-452.

59. K. Möbus, J. Siepmann and R. Bodmeier. 2012. "Zinc-alginate microparticles for controlled pulmonary delivery of proteins prepared by spray-drying." *European Journal of Pharmaceutics and Biopharmaceutics*. 81: 121-130.

60. M.A. Azevedo, A.I. Bourbon, A.A. Vicente and M.A. Cerqueira. 2014. "Alginate/chitosan nanoparticles for encapsulation and controlled release of vitamin B_2." *International Journal of Biological Macromolecules*. 71: 141-146.

61. Z. Li, H.R. Ramay, K.D. Hauch, D. Xiao and M. Zhang. 2005. "Chitosan-alginate hybrid scaffolds for bone tissue engineering." *Biomaterials*. 26: 3919-3928.

62. S.J. Bidarra, C.C. Barrias and P.L. Granja. 2014. "Injectable alginate hydrogels for cell delivery in tissue engineering." *Acta Biomaterialia*. 10: 1646-1662.

63. H. Tan, C.R. Chu, K.A. Payne and K.G. Marra. 2009. "Injectable in situ forming biodegradable chitosan-hyaluronic acid based hydrogels for cartilage tissue engineering." *Biomaterials*. 30: 2499-2506.

64. A. Metters and J. Hubbell. 2005. "Network formation and degradation behavior of hydrogels formed by Michael-type addition reactions." *Biomacromolecules*. 6: 290-301.

65. K. Ono, Y. Saito, H. Yura, K. Ishikawa, A. Kurita, T. Akaike and M. Ishihara. 2000. "Photocrosslinkable chitosan as a biological adhesive." *Journal of Biomedical Materials Research*. 49: 289-295.

66. O. Jeon, J.E. Samorezov and E. Alsberg. 2014. "Single and dual crosslinked oxidized methacrylated alginate/PEG hydrogels for bioadhesive applications." *Acta Biomaterialia*. 10: 47-55.

67. G.T. Jeong, K.M. Lee, H.S. Yang, S.H. Park, J.H. Park, C. Sunwoo, H.W. Ryu, D. Kim, W.T. Lee, H.S. Kim, W.S. Cha and D.H. Park. 2007. "Synthesis of poly(sorbitan methacrylate) hydrogel by free-radical polymerization." *Applied Biochemistry and Biotechnology*. 137-140: 935-946.

68. C. Witthayaprapakorn, R. Somsunan and R. Molloy. 2011. "Preparation of hydrogels by redox initiation via free radical polymerisation for biomedical use as wound dressings." *The Journal of Industrial Technology*. 7: 57-63.

69. M.J. Afshari, N.Sheikh and H. Afarideh. 2015. "PVA/CM-chitosan/honey hydrogels prepared by using the combined technique of irradiation followed by freeze-thawing." *Radiation PhysicsandChemistry*. 113: 28-35.

70. C. Yang, L. Xu, Y. Zhou, X. Zhang, X. Huang, M. Wang, Y. Han, M. Zhai, S. Wei and J. Li. 2010. "A green fabrication approach of gelatin/CM-chitosan hybrid hydrogel for wound healing." *Carbohydrate Polymers*. 82: 1297-1305.

71. P. Ulanski and J.M. Rosiak. 1999. "The use of radiation technique in the synthesis of polymeric nanogels." *Nuclear Instruments and Methods in Physics Research B*. 151: 356-360.

72. T. Machiko, A. Haruyo, N. Naotsugu, Y. Toshiaki, K. Takamitsu, T. Shoji and T. Masao. 2007. "Preparation and properties of CMC gel." *Transactions of the Materials Research Society of Japan*. 32: 713-716.

73. S. Jin, M. Liu, F. Zhang, S. Chen and A. Niu. 2006. "Synthesis and characterization of pH-sensitivity semi-IPN hydrogel based on hydrogen bond between poly(*N*-vinylpyrrolidone) and poly(acrylic acid)." *Polymer*. 47: 1526-1532.

74. K. Deligkaris, T.S. Tadele, W. Olthuis and A. van den Berg. 2010. "Hydrogel-based devices for biomedical applications." *Sensors and Actuators B*. 147: 765-774.

75. K. Zhao, X. Zhang, J. Wei, J. Li, X. Zhou, D. Liu, Z. Liu and J. Li. 2015. "Calcium alginate hydrogel filtration membrane with excellent anti-fouling property and controlled separation performance." *Journal of Membrane Science*. 492: 536-546.

76. E.C. Shen, C. Wang, E. Fu, C.Y. Chiang, T.T. Chen and S. Nieh. 2008. "Tetracycline release from tripolyphosphate-chitosan cross-linked sponge: a preliminary *in vitro* study." *Journal of Periodontal Research*. 43: 642-648.

77. S.A. Soysal, P. Kofinas and Y.M. Lo. 2009. "Effect of complexation conditions on xanthan-chitosan polyelectrolyte complex gels." *Food Hydrocolloids*. 23: 202-209.

78. H.V. Sæther, H.K. Holme, G. Maurstad, O. Smidsrø and B.T. Stokke. 2008. "Polyelectrolyte complex formation using alginate and chitosan." *Carbohydrate Polymers*. 74: 813-821.

79. A. Kaur and G. Kaur. 2012. "Mucoadhesive buccal patches based on interpolymer complexes of chitosan-pectin for delivery of carvedilol." *Saudi Pharmaceutical Journal*. 20: 21-27.

80. S. Chen, G. Wu and H. Zeng. 2005. "Preparation of high antimicrobial activity thiourea chitosan-Ag^{+} complex." *Carbohydrate Polymers*. 60: 33-38.

81. Z. Modrzejewska, M. Dorabialska, R. Zarzycki and A. Wojtasz-Pająk. 2009. "The mechanism of sorption of Ag^{+} ions on chitosan microgranules: IR and NMR studies." *Progress on Chemistry and Application of Chitin and Its Derivatives*. 14: 49-64.

82. X. Wang, Y. Du and H. Liu. 2004. "Preparation, characterization and antimicrobial activity of chitosan-Zn complex." *Carbohydrate Polymers*. 56: 21-26.

83. S.C. Bhatia and N. Ravi. 2000. "A magnetic study of an Fe-chitosan complex and its relevance to other biomolecules." *Biomacromolecules*. 1: 413-417.

84. T. Funami, M. Hiroe, S. Noda, I. Asai, S. Ikeda and K. Nishinari. 2007. "Influence of molecular structure imaged with atomic force microscopy on the rheological behavior of carrageenan aqueous systems in the presence or absence of cations." *Food Hydrocolloids*. 21: 617-629.

85. N. Bhattarai, H.R. Ramay, J. Gunn, F.A. Matsen and M.Q. Zhang. 2005. PEG-grafted chitosan as an injectable thermosensitive hydrogel for sustained protein release." *Journal of Controlled Release*. 103, 609-624.

86. E.R. Kenawy, M.H. El-Newehy and S.S. Al-Deyab. 2010. "Controlled release of atenolol from freeze/thawed poly(vinyl alcohol) hydrogel." *Journal of Saudi Chemical Society*. 14: 237-240.

87. A.D. Jenkins, P. Kratochvil, R.F.T. Stepto and U.W. Suter. 1996. "Glossary of basic terms in polymer science." *Pure and Applied Chemistry*. 68: 2287-2311.

88. Y.S. Ye, J. Rick and B.J. Hwang. 2012. "Water soluble polymers as proton exchange membranes for fuel cells." *Polymers*. 4: 913-963.

89. Pietro Matricardi, Chiara Di Meo, Tommasina Coviello, Wim E. Hennink and Franco Alhaique. 2013. "Interpenetrating Polymer Networks polysaccharide hydrogels for drug delivery and tissue engineering." *Advanced Drug Delivery Reviews*. 65: 1172-1187.

90. M.D. Brigham, A. Bick, E. Lo, A. Bendali, J.A. Burdick and A. Khademhosseini. 2009. "Mechanically robust and bioadhesive collagen and photocrosslinkable hyaluronic acid semi-interpenetrating networks." *Tissue Engineering Part A*. 15: 1645-1653.

91. L. Weng, A. Gouldstone, Y. Wu and W. Chen. 2008. "Mechanically strong double network photo cross linked hydrogels from *N*, *N*-dimethylacrylamide and glycidyl methacrylated hyaluronan." *Biomaterials*. 29: 2153-2163.

92. W. Wu and D.S. Wang. 2010. "A fast pH-responsive IPN hydrogel: Synthesis and controlled drug delivery." *Reactive & Functional Polymers*. 70: 684-691.

93. C. Rodriguez-Tenreiro, L. Diez-Bueno, A. Concheiro, J.J. Torres-Labandeira and C. Alvarez-Lorenzo. 2007. "Cyclodextrin/carbopol micro-scale interpenetrating networks (ms-IPNs) for drug delivery." *Journal of Controlled Release*. 123: 56-66.

94. B.L. Guo and Q.Y. Gao. 2007. "Preparation and properties of a pH/temperature-responsive carboxymethyl chitosan/poly(*N*-isopropylacrylamide) semi-IPN hydrogel for oral delivery of drugs." *Carbohydrate Research*. 342: 2416-2422.

95. G. Li, L. Guo, X. Chang and M. Yang. 2012. "Thermo-sensitive chitosan based semi-IPN hydrogels for high loading and sustained release of anionic drugs." *International Journal of Biological Macromolecules*. 50: 899-904.

96. B. Cursaru, P.O. Stănescu and M. Teodorescu. 2010. "The states of water in hydrogels synthesized from diepoxy-terminated poly(ethylene glycol)s and aliphatic polyamines." *UPB Scientific Bulletin, Series B*. 72: 99-114.

97. W.G. Liu and K.D. Yao. 2001. "What causes the unfrozen water in polymers: hydrogen bonds between water and polymer chains?." *Polymer*. 42: 3943-3947.

98. D.R. Rueda, T. Secall and R.K. Bayer. 1999. "Differences in the interaction of water with starch and chitosan films as revealed by infrared spectroscopy and differential scanning calorimetry." *Carbohydrate Polymers*. 40: 49-56.

99. A.S. Hoffman, A. Afrassiabi and L.C. Dong. 1986. "Thermally reversible hydrogels: II. Delivery and selective removal of substances from aqueous solutions." *Journal of Controlled Release*. 4: 213-222.

100. Y. Qiu and K. Park. 2001. "Environment-sensitive hydrogels for drug delivery." *Advanced Drug Delivery Reviews*. 53: 321-339.

101. T.R. Hoare and D.S. Kohane. 2008. "Hydrogels in drug delivery: Progress and challenges." *Polymer*. 49: 1993-2007.

102. P. Gupta, K. Vermani and S. Garg. 2002. "Hydrogels: from controlled release to pH-responsive drug delivery." *Drug Discovery Today*. 7: 569-579.

103. M.E. Aulton. 2007. **Aulton's Pharmaceutics.** Amsterdam: Elsevier.

104. D.F. Evans, G. Pye, R. Bramley, A.G. Clark, T.J. Dyson and J.D. Hardcastle. 1998. "Measurement of gastrointestinal pH profiles in normal ambulant human-subjects." *Gut*. 29: 1035-1041.

105. E.L. McConnell, H.M. Fadda and A.W. Basit. 2008. "Gut instincts: explorations in intestinal physiology and drug delivery." *International Journal of Pharmaceutics*. 364: 213-226.

106. S. Hellmig, F. Von Schoning, C. Gadow, S. Katsoulis, J. Hedderich, U.R. Folsch and E. Stuber. 2006. "Gastric emptying time of fluids and solids in healthy subjects determined by 13C breath tests: influence of age, sex and body mass index." *Journal of Gastroenterology and Hepatology*. 21: 1832-1838.

107. M.T. Cook, G. Tzortzis, D. Charalampopoulos and V.V. Khutoryanskiy. 2012. "Microencapsulation of probiotics for gastrointestinal delivery." *Journal of Controlled Release*. 162: 56-67.

108. A.G. Press, I.A. Hauptmann, L. Hauptmann, B. Fuchs, M. Fuchs, K. Ewe and G. Ramadori. 1998. "Gastrointestinal pH profiles in patients with

inflammatory bowel disease." *Alimentary Pharmacology & Therapeutics*. 12: 673-678.

109. A. Coupe, S. Davis and I. Wilding. "Variation in gastrointestinal transit of pharmaceutical dosage forms in healthy subjects." *Pharmaceutical Research*. 8: 360-364.
110. X. Gao, C. He, C. Xiao, X. Zhuang and X. Chen. 2013. "Biodegradable pH-responsive polyacrylic acid derivative hydrogels with tunable swelling behavior for oral delivery of insulin." *Polymer*. 54: 1786-1793.
111. F. Croisier and C. Jérôme. 2013. "Chitosan-based biomaterials for tissue engineering." *European Polymer Journal*. 49: 780-792.
112. K.V. Harish Prashanth and R.N. Tharanathan. 2007. "Chitin/chitosan: modifications and their unlimited application potential-an overview." *Trends in Food Science & Technology*. 18: 117-131.
113. Y.W. Cho, J. Jang, C.R. Park and S.W. Ko. 2000. "Preparation and solubility in acid and water of partially deacetylated chitins." *Biomacromolecules*. 1: 609-614.
114. J.D. Schiffman and C.L. Schauer. 2007. "Cross-linking chitosan nanofibers." *Biomacromolecules*. 8: 594-601.
115. C. Chatelet, O. Damour and A. Domard. 2001. "Influence of the degree of acetylation on some biological properties of chitosan films." *Biomaterials*. 22: 261-268.
116. I. Aranaz, M. Mengíbar, R. Harris, I. Paños, B. Miralles, N. Acosta, G. Galed and Á. Heras. 2009. "Functional characterization of chitin and chitosan." *Current Chemical Biology*. 3: 203-230.
117. S.H. Pangburn, P.V. Trescony and J. Heller. 1982. "Lysozyme degradation of partially deacetylated chitin, its films and hydrogels." *Biomaterials*. 3: 105-108.
118. H. Zhang and S.H. Neau. 2001. "*in vitro* degradation of chitosan by a commercial enzyme preparation: effect of molecular weight and degree of deacetylation." *Biomaterials*. 22: 1653-1658.
119. P.B. Malafaya, G.A. Silva and R.L. Reis. 2007. "Natural-origin polymers as carriers and scaffolds for biomolecules and cell delivery in tissue engineering applications." *Advanced Drug Delivery Reviews*. 59: 207-233.
120. I. Wedmore, J.G. McManus, A.E. Pusateri and J.B. Holcomb. 2006. "A special report on the chitosan-based hemostatic dressing: experience in current combat operations." *Journal of Trauma and Acute Care Surgery*. 60: 655-658.

121. P. He, S.S. Davis and L. Illum. 1998. "*In vitro* evaluation of the mucoadhesive properties of chitosan microspheres." *International Journal of Pharmaceutics*. 166: 75-88.

122. P.J. Park, J.Y. Je, W.K. Jung, C.B. Ahn and S.K. Kim. 2004. "Anticoagulant activity of heterochitosans and their oligosaccharide sulfates." *European Food Research and Technolog*. 219: 529-533.

123. S.B. Rao and C.P. Sharma. 1997. "Use of chitosan as a biomaterial: studies on its safety and hemostatic potential." *Journal of Biomedical Materials Research*. 34: 21-28.

124. J. Smith, E. Wood and M. Dornish. 2004. "Effect of chitosan on epithelial cell tight junctions." *Pharmaceutical Research*. 21: 43-49.

125. N.R. Sudarshan, D.G. Hoover and D. Knorr. 1992. "Antibacterial action of chitosan." *Food Biotechnology*. 6: 257-272.

126. Y.C. Chung and C.Y. Chen. 2008. "Antibacterial characteristics and activity of acid-soluble chitosan." *Bioresource Technology*. 99: 2806-2814.

127. Y. Okamoto, K. Kawakami, K. Miyatake, M. Morimoto, Y. Shigemasa and S. Minami. 2002. "Analgesic effects of chitin and chitosan." *Carbohydrate Polymers*. 49: 249-252.

128. Q. Yanga, F. Doub, B. Lianga and Q. Shen. 2005. "Investigations of the effects of glyoxal cross-linking on the structure and properties of chitosan fiber." *Carbohydrate Polymers*. 61: 393-398.

129. K.C. Gupta and F.H. Jabrail. 2006. "Glutaraldehyde and glyoxal cross-linked chitosan microspheres for controlled delivery of centchroman." *Carbohydrate Research*. 341: 744-756.

130. O.A.C. Monteiro and C. Airoldi. 1999. "Some studies of crosslinking chitosan-glutaraldehyde interaction in a homogeneous system." *International Journal of Biological Macromolecules*. 26: 119-128.

131. R.O. Beauchamp, M.B. St Clair, T.R. Fennell, D.O. Clarke and K.T. Morgan. 1992. "A critical review of the toxicology of glutaraldehyde." *Critical Reviews in Toxicology*. 22: 143-174.

132. N.M. Kamiya, H. Kamiya, H. Kaji and H. Kasai. 1997. "Mutational specificity of glyoxal, a product of DNA oxidation, in the lacI gene of wild-type Escherichia coli W3110." *Mutation Research*. 377: 255-262.

133. F.L. Mi, Y.C. Tan, H.F. Liang and H.W. Sung. 2002. "*In vivo* biocompatibility and degradability of a novel injectable-chitosan-based implant." *Biomaterials*. 23: 181-191.

134. H.W. Sung, R.N. Huang, L.L. Huang and C.C. Tsai. 1999. "*In vitro* evaluation of cytotoxicity of a naturally occurring cross-linking reagent for biological

tissue fixation." *Journal of Biomaterials Science, Polymer Edition*. 10: 63-78.

135. X. Gao, Y. Zhou, G. Ma, S. Shi, D. Yang, F. Lu and J. Nie. 2010. "A water-soluble photocrosslinkable chitosan derivative prepared by Michael-addition reaction as a precursor for injectable hydrogel." *Carbohydrate Polymers*. 79: 507-512.
136. Y. Yi, S. Xu, H. Sun, D. Chang, Y. Yin, H. Zheng, H. Xu and Y. Lou. 2011. "Gelation of photocrosslinkable carboxymethyl chitosan and its application in controlled release of pesticide." *Carbohydrate Polymers*. 86: 1007-1013.
137. X. Yang, K. Yang, S. Wu, X. Chen, F. Yu, J. Li, M. Ma and Z. Zhu. 2010. "Cytotoxicity and wound healing properties of PVA/ws-chitosan/glycerol hydrogels made by irradiation followed by freeze-thawing." *Radiation Physics and Chemistry*. 79: 606-611.
138. X. Yang, Z. Zhu, Q. Liu, X. Chen and M. Ma. 2008. "Effects of PVA, agar contents, and irradiation doses on properties of PVA/ws-chitosan/glycerol hydrogels made by γ-irradiation followed by freeze-thawing." *Radiation Physics and Chemistry*. 77: 954-960.
139. H.P. Brack, S.A. Tirmizi and W.M. Risen. 1997. "Aspectroscopic and viscometric study of themetal ion-induced gelation of the biopolymer chitosan." *Polymer*. 38: 2351-2362.
140. M. Rinaudo. 2006. "Chitin and chitosan: Properties and applications." *Progress in Polymer Science*. 31: 603-632.
141. C. Qin, Y. Du, L. Xiao, Z. Li and X. Gao. 2002. "Enzymic preparation of water-soluble chitosan and their antitumor activity." *International Journal of Biological Macromolecules*. 31: 111-117.
142. J. Lia, Y. Du, J. Yang, T. Feng, A. Li and P. Chen. 2005. "Preparation and characterisation of low molecular weight chitosan and chito-oligomers by a commercial enzyme." *Polymer Degradation and Stability*. 87: 441-448.
143. J. Shao, Y. Yang and Q. Zhong. 2003. "Studies on preparation of oligoglucosamine by oxidative degradation under microwave irradiation." *Polymer Degradation and Stability*. 82: 395-398.
144. S. Wu, R. Cai and Y. Sun. 2012. "Degradation of curdlan using hydrogen peroxide." *Food Chemistry*. 135: 2436-2438.
145. Z. Xia, S. Wu and J. Chen. 2013. "Preparation of water soluble chitosan by hydrolysis using hydrogen peroxide." *International Journal of Biological Macromolecules*. 59: 242-245.

146. Y. Du, Y. Zhao, S. Dai and B. Yang. 2009. "Preparation of water-soluble chitosan from shrimp shell and its antibacterial activity." *Innovative Food Science and Emerging Technologies*. 10: 103-107.

147. H. Kang, Y. Cai, J. Deng, H. Zhang, Y. Tang and P. Liu. 2006. "Synthesis and aqueous solution behavior of phosphonate-functionalized chitosans." *European Polymer Journal*. 42: 2678-2685.

148. I.M. El-Sherbiny. 2009. "Synthesis, characterization and metal uptake capacity of a new carboxymethyl chitosan derivative." *European Polymer Journal*. 45: 199-210.

149. N. Vallapa, O. Wiarachai, N. Thongchul, J. Pand, V. Tangpasuthadol, S. Kiatkamjornwong and V.P. Hoven. 2011. "Enhancing antibacterial activity of chitosan surface by heterogeneous quaternization." *Carbohydrate Polymers*. 83: 868-875.

150. M. Jiang, K. Wang, J.F. Kennedy, J. Nie, Q. Yu and G. Ma. 2010. "Preparation and characterization of water-soluble chitosan derivative by Michael addition reaction." *International Journal of Biological Macromolecules*. 47: 696-699.

151. X.Z. Shu and K.J. Zhu. 2001. "Novel pH-sensitive citrate cross-linked chitosan film for drug controlled release." *International Journal of Pharmaceutics*. 212: 19-28.

152. S. Das, A. Chaudhury and K.Y. Ng. 2011. "Preparation and evaluation of zinc-pectin-chitosan composite particles for drug delivery to the colon: Role of chitosan in modifying *in vitro* and *in vivo* drug release." *International Journal of Pharmaceutics*. 406: 11-20.

153. L.N.M. Ribeiro, A.C.S. Alcântara, M. Darder, P. Aranda, F.M. Araújo-Moreira and E. Ruiz-Hitzkya. 2014. "Pectin-coated chitosan-LDH bionanocomposite beads as potential systems for colon-targeted drug delivery." *International Journal of Pharmaceutics*. 463: 1-9.

154. A. Islam, T. Yasin, I. Bano and M. Riaz. 2012. "Controlled release of aspirin from pH-sensitive chitosan/poly(vinyl alcohol) hydrogel." *Journal of Applied Polymer Science*. 124: 4184-4192.

155. Z. Liu, Y. Jiao and Z. Zhang. 2007. "Calcium-carboxymethyl chitosan hydrogel beads for protein drug delivery system." *Journal of Applied Polymer Science*. 103: 3164-3168.

156. A. Steinbüchel and R.H. Marchessault. 2005. **Biopolymers for Medical and Pharmaceutical Applications: Humic Substances, Polyisoprenoids, Polyesters, and Polysaccharides Volume 1**. New York: John Wiley and Sons.

157. S.N. Pawar and K.J. Edgar. 2012. "Alginate derivatization: A review of chemistry, properties and applications." *Biomaterials*. 33: 3279-3305.

158. R.L. Reis, N.M. Neves, J.F. Mano, M.E. Gomes, A.P. Marques and H.S. Azevedo. 2008. **Natural-Based Polymers for Biomedical Applications**, New York: CRC Press.

159. A.M. Stephen, G.O. Phillips and P.A. Williams. 2006. **Food Polysaccharides and Their Applications**. New York: CRC Press.

160. C.K. Kim and E.J. Lee. 1992. "The controlled release of blue dextran from alginate beads." *International Journal of Pharmaceutics*. 79: 11-19.

161. S. Sugawara, T. Imai and M. Otagiri. 1994. "The controlled release of prednisolone using alginate gel." *Pharmaceutical Research*. 11: 272-277.

162. S.C. Chen, Y.C. Wu, F.L. Mi, Y.H. Lin, L.C. Yu and H.W. Sung. 2004. "A novel pH-sensitive hydrogel composed of *N,O*-carboxymethyl chitosan and alginate cross-linked by genipin for protein drug delivery." *Journal of Controlled Release*. 96: 285-300.

163. A.L. Ching, C.V. Liew, L.W. Chan and P.W.S. Heng. 2008. "Modifying matrix micro-environmental pH to achieve sustained drug release from highly laminating alginate matrices." *European Journal of Pharmaceutical Sciences*. 33: 361-370.

164. L. Agüero, D. Zaldivar-Silva, L. Pena and M.L. Dias. 2017. "Alginate microparticles as oral colon drug delivery device: A review." *Carbohydrate Polymers*.168: 32-43.

165. M. George and T.E. Abraham. 2006. "Polyionic hydrocolloids for the intestinal delivery of protein drugs: Alginate and chitosan-a review." *Journal of Controlled Release*. 114: 1-14.

166. H. Chang, H. Park, P. Kelly and J. Robinson. 1985. "Bioadhesive polymers as platforms for oral controlled drug delivery. Synthesis and evaluation of some swelling, water-insoluble bioadhesive polymers." *Journal of Pharmaceutical Sciences*. 74: 399-405.

167. K.K. Kwok, M.J. Groves and D.J. Burgess. 1989. "Sterile microencapsulation of BCG in alginate-poly-L-lysine by an air spraying technique." *Proceedings International Symposium on Control Release Bioact Mater*. 16: 170-171.

168. J.P. Paques, E. van der Linden, C.J.M. van Rijn and L.M.C. Sagis. 2014. "Preparation methods of alginate nanoparticles." *Advances in Colloid and Interface Science*. 209: 163-171.

169. C.H. Goh, P.W. Sia Heng and L.W. Chan. 2012. "Alginates as a useful natural polymer for microencapsulation and therapeutic applications." *Carbohydrate Polymers*. 88: 1-12.

170. C.M. DeRamos, A.E. Irwin, J.L. Nauss and B. E. Stout. 1997. "^{13}C NMR and molecular modeling studies of alginic acid binding with alkaline earth and lanthanidemetal ions." *Inorganica Chimica Acta*. 256: 69-75.

171. A.H. Clark and S.B. Ross-Murphy. 1987. "Structural and mechanical properties of biopolymer gels." *Advances in Polymer Science*. 83: 57-192.

172. A. Haug. 1961. "Fractionation of alginate and some properties of alginate fractions." *Colloques Internationaux du Centre National de la Recherche Scientifique*. 103: 163-172.

173. K.Y. Lee and D.J. Mooney. 2012. "Alginate: properties and biomedical applications." *Progress in Polymer Science*. 37: 106-126.

174. A. Haug and O. Smidsrød. 1965. "Fractionation of alginates by precipitation with calcium and magnesium ions." *Acta Chemica Scandinavica*. 19: 1221-1226.

175. K.I. Draget, G. Skjåk Bræk and O. Smidsrød. 1994. "Alginic acid gels: the effect of alginate chemical composition and molecular weight." *Carbohydrate Polymers*. 25: 31-38.

176. T. Agarwala, S.N.G.H. Narayana, K. Pal, K. Pramanik, S. Giri and I. Banerjee, 2015. "Calcium alginate-carboxymethyl cellulose beads for colon-targeted drug delivery." *International Journal of Biological Macromolecules*. 75: 409-417.

177. Y.H. Lin, H.F. Liang, C.K. Chung, M.C. Chen and H.W. Sung. 2005. "Physically crosslinked alginate/*N,O*-carboxymethyl chitosan hydrogels with calcium for oral delivery of protein drugs." *Biomaterials*. 26: 2105-2113.

178. L.W. Chan, Y. Jin and P.W.S. Heng. 2002. "Cross-linking mechanisms of calcium and zinc in production of alginate microspheres." *International Journal of Pharmaceutics*. 242: 255-258.

179. J. Venkatesan and S.K. Kim. 2010. "Chitosan composites for bone tissue engineering-an overview." *Marine Drugs*. 8: 2252-2266.

180. J. Nie, Z. Wang and Q. Hu. 2016. "Chitosan hydrogel structure modulated by metal ions." *Scientific Reports*. 6: 1-8.

181. M.O. Taha, W. Nasser, A. Ardakani and H.S. Alkhatib. 2008. "Sodium lauryl sulfate impedes drug release from zinc-crosslinked alginate beads: switching from enteric coating release into biphasic profiles." *International Journal of Pharmaceutics*. 350: 291-300.

182. M.C. Straccia, I. Romano, A. Oliva, G. Santagata and P. Laurienzo. 2014. "Crosslinker effects on functional properties ofalginate/*N*-succinylchitosan based hydrogels." *Carbohydrate Polymers*. 108: 321-330.

183. V. Pillay and R. Fassihi. 2005. "Novel modulation of drug delivery using binary zinc-alginate-pectinate polyspheres for zero-order kinetics over several days: Experimental design strategy to elucidate the crosslinking mechanism." *Drug Development and Industrial Pharmacy*. 31: 191-207.

184. C.H. Goh, P.W.S. Heng and L.W. Chan. 2012. "Cross-linker and non-gelling Na^+ effects on multi-functional alginate dressings." *Carbohydrate Polymers*. 87: 1796-1802.

185. J.R. Rodrigues and R. Lagoa. 2006. "Copper Ions Binding in Cu-Alginate Gelation." *Journal of Carbohydrate Chemistry*. 25: 219-232.

186. K.M. Zia, S. Tabasum, M. Nasif, N. Sultan, N. Aslam, A. Noreen and M. Zuber. 2017. "A review on synthesis, properties and applications of natural polymer based carrageenan blends and composites." *International Journal of Biological Macromolecules*. 96: 282-301.

187. L. Li, R. Ni, Y. Shao and S. Mao. 2014. "Carrageenan and its applications in drug delivery." *Carbohydrate Polymers*. 103: 1-11.

188. V.L. Campo, D.F. Kawano, D.B. da Silva Jr. and I. Carvalho. 2009. "Carrageenans: Biological properties, chemical modifications and structural analysis-A review." *Carbohydrate Polymers*. 77: 167-180.

189. I. Wijesekara, R. Pangestuti and S.K. Kim. 2011. "Biological activities and potential health benefits of sulfated polysaccharides derived from marine algae." *Carbohydrate Polymers*. 84: 14-21.

190. S. Girond, J.M. Crance, H. Van Cuyck-Gandre, J. Renaudet and R. Deloince. 1991. "Antiviral activity of carrageenan on hepatitis A virus replication in cell culture." *Research in Virology*. 142: 261-270.

191. C.B. Buck, C.D. Thompson, J.N. Roberts, M. Mueller, D.R. Lowy and J.T. Schiller. 2006. "Carrageenan is a potent inhibitor of papillomavirus infection." *PLOS Pathogens*. 2: 671-680.

192. M.C. Rocha de Souza, C.T. Marques, C.M. Guerra Dore, F.R. Ferreira da Silva, H.A. Oliveira Rocha and E.L. Leite. 2007. "Antioxidant activities of sulfated polysaccharides from brown and red seaweeds." *Journal of Applied Phycology*. 19: 153-160.

193. M.L. Weiner. 1991. "Toxicological properties of carrageenan." *Inflammation Research*. 32: 46-51.

194. R.C. Rowe, P.J. Sheskey and M.E. Quinn. 2009. **Handbook of pharmaceutical excipients.** London: Pharmaceutical Press.

195. W. Liang, X. Mao, X. Peng and S. Tang. 2014. "Effects of sulfate group in red seaweed polysaccharides on anticoagulant activity and cytotoxicity." *Carbohydrate Polymers*. 101: 776-785.

196. K. Reddy, G. Krishna Mohan, S. Satla and S. Gaikwad. 2011. "Natural polysaccharides: Versatile excipients for controlled drug delivery systems." *Asian Journal of Pharmaceutical Sciences*. 6: 275-286.

197. F.R.F. Silva, C.M.P.G. Dore, C.T. Marques, M.S. Nascimento, N.M.B. Benevides, H.A.O. Rocha, S.F. Chavante and E.L. Leite. 2010. "Anticoagulant activity, paw edema and pleurisy induced carrageenan: Action of major types of commercial carrageenans." *Carbohydrate Polymers*. 79: 26-33.

198. J. Liu, X. Zhan, J. Wan, Y. Wang and C. Wang. 2015. "Review for carrageenan-based pharmaceutical biomaterials: Favourable physical features versus adverse biological effects." *Carbohydrate Polymers*. 121: 27-36.

199. A.K. Stone and M.T. Nickerson. 2012. "Formation and functionality of whey protein isolate-(kappa-, iota-, and lambda-type) carrageenan electrostatic complexes." *Food Hydrocolloids*. 27: 271-277.

200. K. te Nijenhuis. 1997. **Thermoreversible Networks**. Berlin: Springer.

201. H. Zhang and M.W. Grinstaff. 2014. "Recent advances in glycerol polymers: Chemistry and biomedical applications." ***Macromolecular Rapid Communications***. 35: 1906-1924.

202. H.W. Tan, A.R. Abdul Aziz and M.K. Aroua. 2013. "Glycerol production and its applications as a raw material: A review." *Renewable and Sustainable Energy Reviews*. 27: 118-127.

203. V. Epure, M. Griffon, E. Pollet and L. Avérous. 2011. "Structure and properties of glycerol-plasticized chitosan obtained by mechanical kneading." *Carbohydrate Polymers*. 83: 947-952.

204. M.A. da Silva, A.C.K. Bierhalz and T.G. Kieckbusch. 2009. "Alginate and pectin composite films crosslinked with Ca^{2+} ions: Effect of the plasticizer concentration." *Carbohydrate Polymers*. 77: 736-742.

205. P.V.A. Bergo, R.A. Carvalho, P.J.A. Sobral, R.M.C. dos Santos, F.B.R. da Silva, J.M. Prison, J. Solorza-Feria and A.M.Q.B. Habitante. 2008. "Physical properties of edible films based on cassava starch as affected by the plasticizer concentration." *Packaging Technology and Science*. 21: 85-89.

206. M. Avella, E.D. Pace, B. Immirzi, G. Impallomeni, M. Malinconico and G. Santagata. 2007. "Addition of glycerol plasticizer to seaweeds derived alginates: Influence of microstructure on chemical-physical properties." *Carbohydrate Polymers*. 69: 503-511.

207. S. Kasapis, I. Norton and J. Ubbink. 2009. **Modern Biopolymer Science**. California: Academic Press.

208. A. De, R. Bose, A. Kumar and S. Mozumdar. 2014. **Targeted Delivery of Pesticides Using Biodegradable Polymeric Nanoparticles**. New Delhi: Springer.

209. E. Holowka and S.K. Bhatia. 2014. **Drug Delivery**. New York: Springer

210. J. Siepmann and F. Siepmann. 2008. "Mathematical modeling of drug delivery." *International Journal of Pharmaceutics*. 364: 328-343.

211. A. Hirai, H. Odani and A. Nakajima. 1991. "Determination of degree of deacetylation of chitosan by ^{1}H NMR spectroscopy." *Polymer Bulletin*. 26: 87-94.

212. D.R. Lide. 2003. **CRC Handbook of Chemistry and Physics**. New York: CRC Press.

213. C. Kaemkit. 2012. "Preparation of water-soluble chitosan/montmorillonite nanoclay for dye absorption application." M.Sc. dissertation, King Mongkut's Institute of Technology Ladkrabang.

214. K. Braeckman, R. Labeque, H. Emmerson and A. Brooker. **Cleaning composition for use in a laundry or dishwashing machine**. United States. US 2004/0259749 A1. 23 December 2004.

215. D.L. Pavia, G.M. Lampman, G.S. Kriz and J.R. VyVyan. 2009. **Introduction to spectroscopy**. California: Brooks/Cole.

216. S.K. Kim. 2010. **Chitin, chitosan, oligosaccharides and their derivatives: Biological activities and applications**. New York: CRC Press.

217. P. Treenate, P. Monvisade and M. Yamaguchi. 2014. "Development of hydroxyethylacryl chitosan/alginate hydrogel films for biomedical application." *Journal of Polymer Research*. 21: 1-12.

218. M.A. da Silva, A.C.K. Bierhalz and T.G. Kieckbusch. 2009. "Alginate and pectin composite films crosslinked with Ca^{2+} ions: Effect of the plasticizer concentration." *Carbohydrate Polymers*. 77: 736-742.

219. P. Treenate and P. Monvisade. 2015. "Controlled release of paracetamol from pH-sensitive hydroxyethylacryl chitosan/sodium alginate films for oral drug delivery." 825-830. in **Burapha University International Conference 2015**. Chonburi: Burapha University.

220. T. Zhang, S. Mao and W. Sun. 2010. "Design and *in vitro* evaluation of a film-controlled dosage form self-converted from monolithic tablet in gastrointestinal environment." *Journal of Pharmaceutical Sciences*. 99: 4678-4690.

221. B. Das, S. Dutta, A.K. Nayak and U. Nanda. 2014. "Zinc alginate-carboxymethyl cashew gum microbeads for prolonged drug release: development and

optimization." *International Journal of Biological Macromolecules*. 70: 506-515.

222. Q. Yu, Y. Song, X. Shi, C. Xu and Y. Bin. 2011. "Preparation and properties of chitosan derivative/poly(vinyl alcohol) blend film crosslinked with glutaraldehyde." *Carbohydrate Polymers*. 84: 465-470.
223. B.S. Rao and K.V. Murthy. 2000. "Preparation and *in vitro* evaluation of chitosan matrices cross-linked by formaldehyde vapors." *Drug Development and Industrial Pharmacy*. 26: 1085-1090.
224. E. Marsano, E. Bianchi, S. Vicini, L. Compagnino, A. Sionkowska, J. Skopińska and M. Wiśniewski. 2005. "Stimuli responsive gels based on interpenetrating network of chitosan and poly(vinylpyrrolidone)." *Polymer*. 46: 1595-1600.
225. A.E. Pavlath, C. Gossett, W. Camirand, and G.H. Robertson. 1999. "Ionomeric films of alginic acid." *Journal of Food Science*. 64: 61-63.
226. J. Ostrowska-Czubenko and M. Gierszewska-Drużyńska. 2009. "Effect of ionic crosslinking on the water state in hydrogel chitosan membranes." *Carbohydrate Polymers*. 77: 590-598.
227. L.S. Liu, S.Q. Liu, S.Y. Ng, M. Froix, T. Ohno and J. Heller. 1997. "Controlled release of interleukin-2 for tumour immunotherapy using alginate/chitosan porous microspheres." *Journal of Controlled Release*. 43: 65-74.
228. V. Zeleňák, Z. Vargová and K. Györyová. 2007. "Correlation of infrared spectra of zinc(II) carboxylates with their structures." *Spectrochimica Acta Part A: Molecular and Biomolecular Spectroscopy*. 66: 262-272.
229. R.L. Patale and V.B. Patravale. 2011. "*O,N*-carboxymethyl chitosan-zinc complex: A novel chitosan complex with enhanced antimicrobial activity." *Carbohydrate Polymers*. 85: 105-110.
230. F. Reynaud, N. Tsapis, S.S. Guterres, A.R. Pohlmann and E. Fattal. 2015. "Pectin beads loaded with chitosan-iron microspheres for specific colonic adsorption of ciprofloxacin." *Journal of Drug Delivery Science and Technology*. 30: 494-500.
231. M.J. Wang, Y.L. Xie, Q.D. Zheng and S.J. Yao. 2009. "A novel, potential microflora-activated carrier for a colon-specific drug delivery system and its characteristics." *Industrial & Engineering Chemistry Research*. 48: 5276-5284.
232. T. Phaechamud and W. Darunkaisorn. 2016. "Drug release behavior of polymeric matrix filled in capsule." *Saudi Pharmaceutical Journal*. 24: 627-634.
233. B. Bhatt and V. Kumar. 2016. "Regenerated cellulose capsules for controlled drug delivery: Part III. Developing a fabrication method and evaluating

extemporaneous utility for controlled-release." *European Journal of Pharmaceutical Sciences*. 91: 40-49.

234. A.C. Pinheiro, A.I. Bourbon, M.A.C. Quintas, b, M.A. Coimbra, A.A. Vicente. 2012. "*K*-carrageenan/chitosan nanolayered coating for controlled release of a model bioactive compound." *Innovative Food Science and Emerging Technologies*. 16: 227-232.

Appendices

Appendix A: Characterization of HCs

A.1 FT-IR

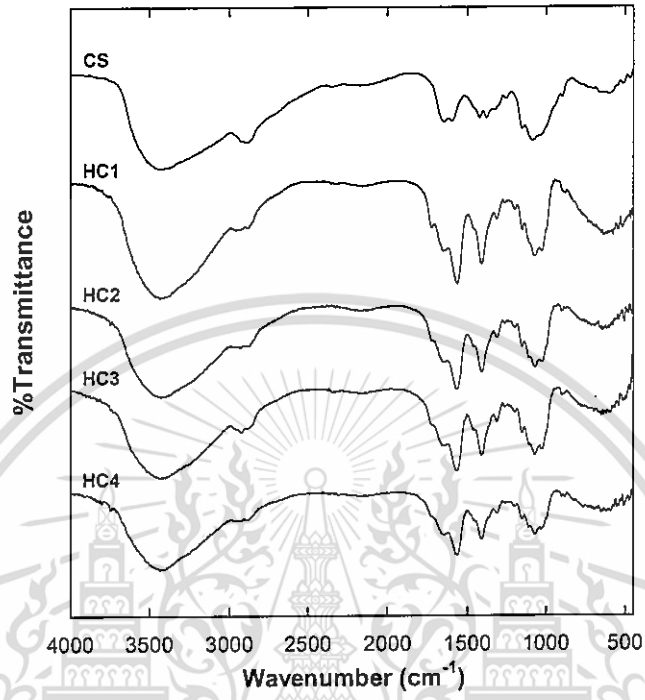

Figure A-1 FT-IR spectra of CS and HCs.

A.2 XRD

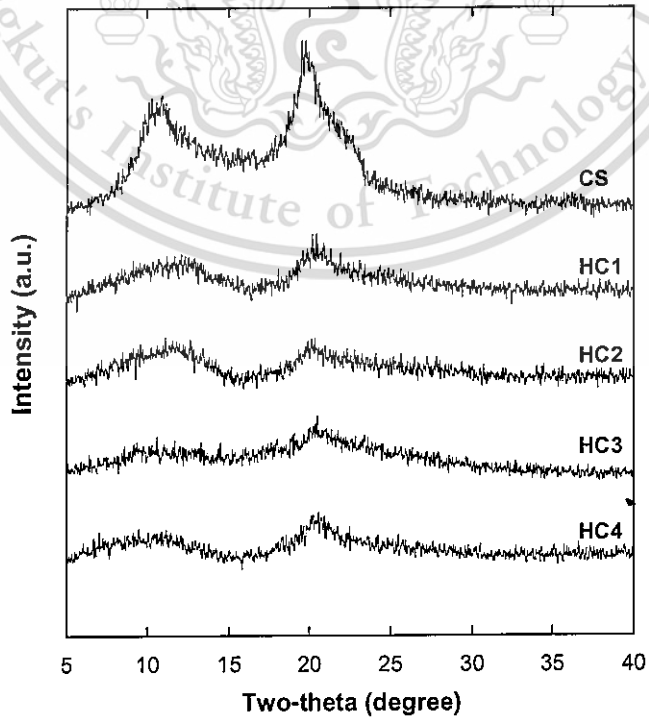

Figure A-2 XRD patterns of CS and HCs.

A.3 ^{1}H-NMR

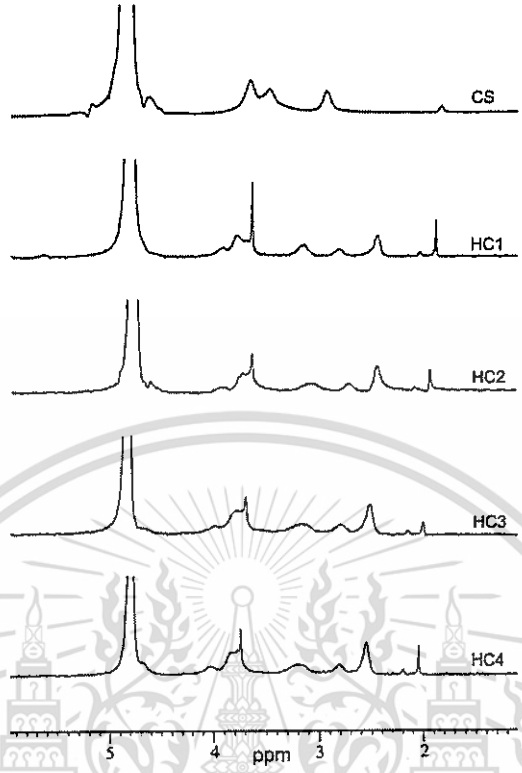

Figure A-3 ^{1}H-NMR spectra of CS and HCs.

A.4 GPC

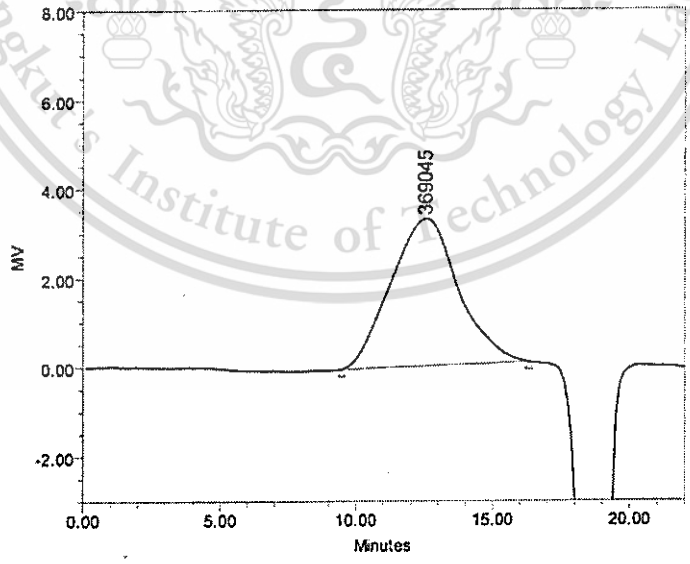

	Mn (Daltons)	Mw (Daltons)	MP (Daltons)	Mz (Daltons)	Mz+1 (Daltons)	Polydispersity
1	141512	833068	369045	2614411	4708139	5.886889

Figure A-4 GPC chromatogram of CS.

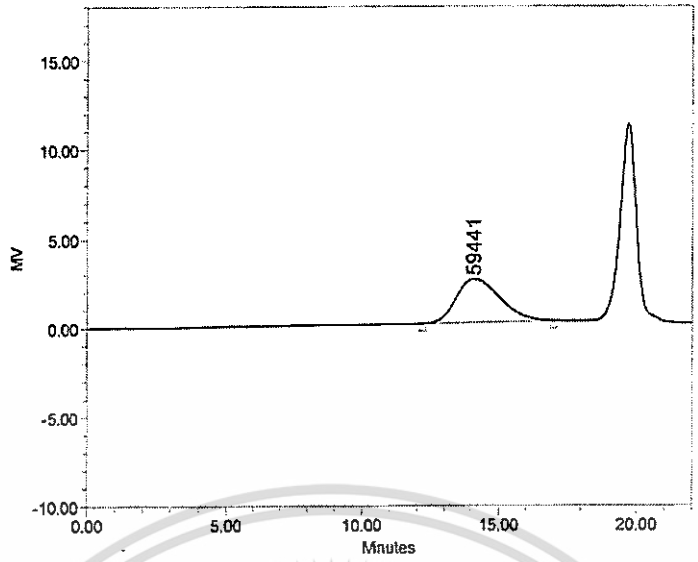

	Mn (Daltons)	Mw (Daltons)	MP (Daltons)	Mz (Daltons)	Mz+1 (Daltons)	Polydispersity
1	28689	62722	59441	108338	160374	2.186264

Figure A-5 GPC chromatogram of HC1.

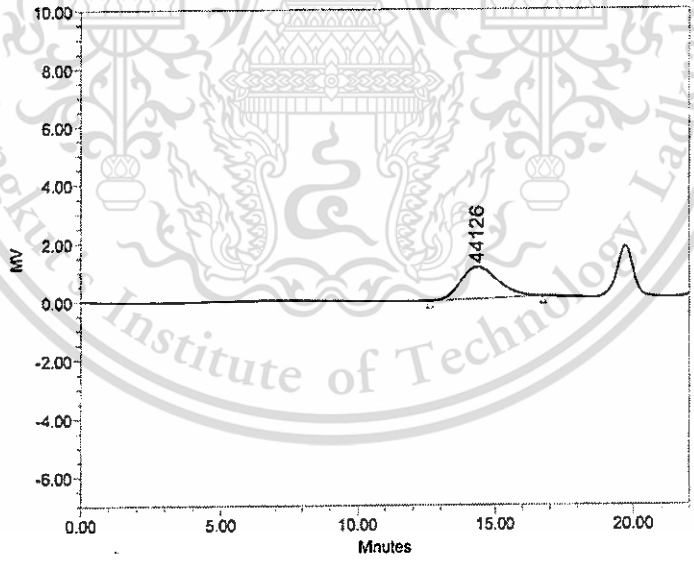

	Mn (Daltons)	Mw (Daltons)	MP (Daltons)	Mz (Daltons)	Mz+1 (Daltons)	Polydispersity
1	26383	46836	44126	71857	99043	1.775220

Figure A-6 GPC chromatogram of HC2.

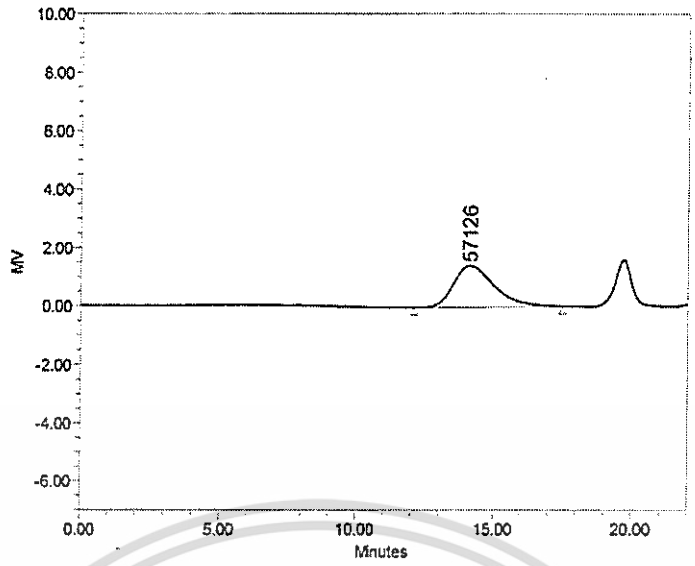

	Mn (Daltons)	Mw (Daltons)	MP (Daltons)	Mz (Daltons)	Mz+1 (Daltons)	Polydispersity
1	24252	57926	57126	96911	142944	2.388484

Figure A-7 GPC chromatogram of HC3.

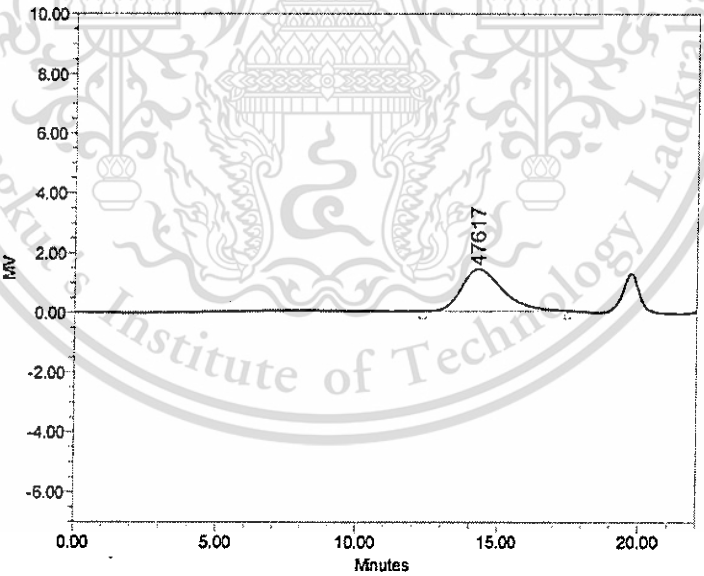

	Mn (Daltons)	Mw (Daltons)	MP (Daltons)	Mz (Daltons)	Mz+1 (Daltons)	Polydispersity
1	20927	47842	47617	78809	113672	2.286117

Figure A-8 GPC chromatogram of HC4.

Appendix B: Calculation

B.1 Degree of deacetylation of CS

The degree of deacetylation (DD) of CS was calculated with the method proposed by Hirai et al. [171] using equation as follows:

$$DD = 1 - \left(\frac{1}{3}H_{7'}/\frac{1}{6}H_{2,2'-6,6'}\right) \quad \text{(B-1)}$$

where $H_{7'}$ is peak area for the signal from $-CH_3(7')-$ protons and $H_{2,2'-6,6'}$ is the summation of peak areas for the signal from –CH(2, 2', 3, 3', 4, 4', 5 and 5') protons and $-CH_2(6 \text{ and } 6')-$ protons.

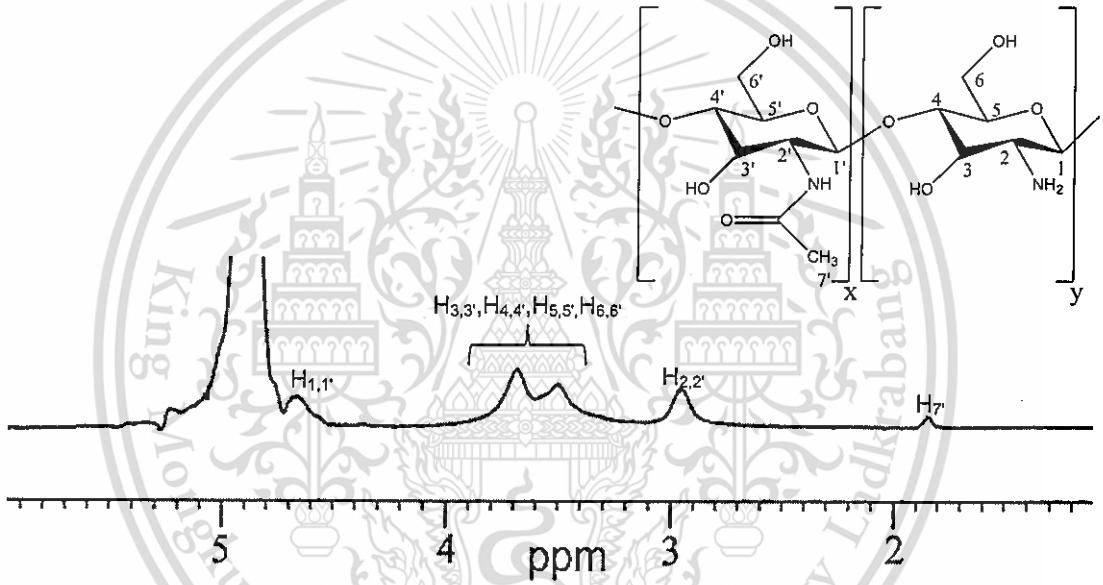

Figure B-1 ^{1}H-NMR spectra of CS.

The peak areas of each signals was obtained by ImageJ program. $H_{7'}$ and $H_{2,2'-6,6'}$ were 96 and 3173, respectively.

$$DD = 1 - (\frac{1}{3}96/\frac{1}{6}3173)$$

$$= 0.94$$

Therefore, the degree of deacetylation of CS was 0.94.

B.2 Degrees of substitution of HCs

The proposed structure of HCs is shown in Fig. B-2.

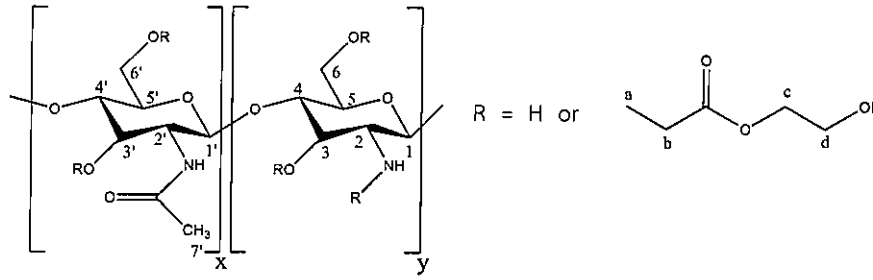

Figure B-2 Proposed structure of HCs.

The degrees of substitution (DS) of HCs were calculated using equation as follows:

$$DS = \frac{H_b/2}{H_{2,2'}} \qquad \text{(B-2)}$$

Where H_b is peak area for the signal from $-CH_2$(b)– protons and $H_{2,2'}$ is peak area for the signal from –CH(2 and 2')– protons.

For example,

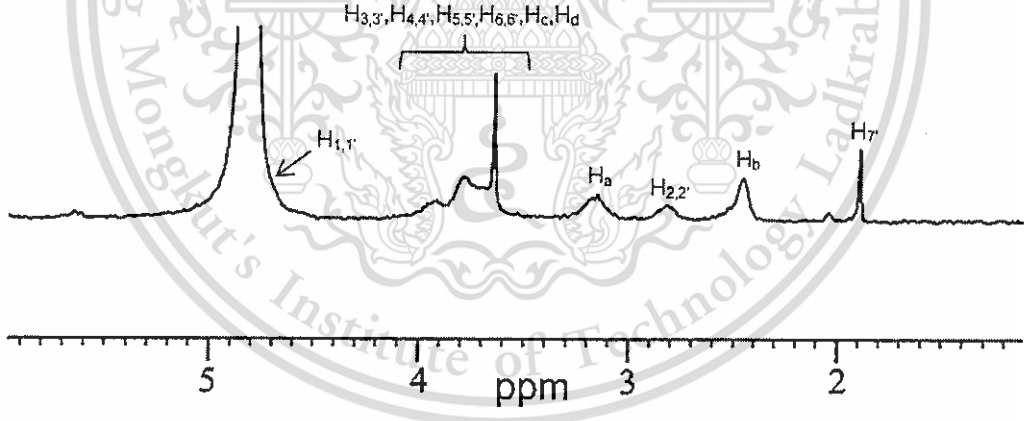

Figure B-3 ^{1}H-NMR spectra of HC1.

The peak areas of each signals was obtained by ImageJ program. H_b and $H_{2,2'}$ were 815 and 334, respectively.

$$DS = \frac{815/2}{334}$$

$$= 1.22$$

Therefore, the degree of substitution of HC1 was 1.22.

B.3 Average molecular weight per repeating unit

Before calculating average molecular weight per repeating unit (Mw_{unit}) of HCs, average molecular weight per repeating unit of CS used in the reaction was needed to be firstly determined. It should be mentioned again that CS is the product from deacetylation of chitin as illustrated in Figure B-4.

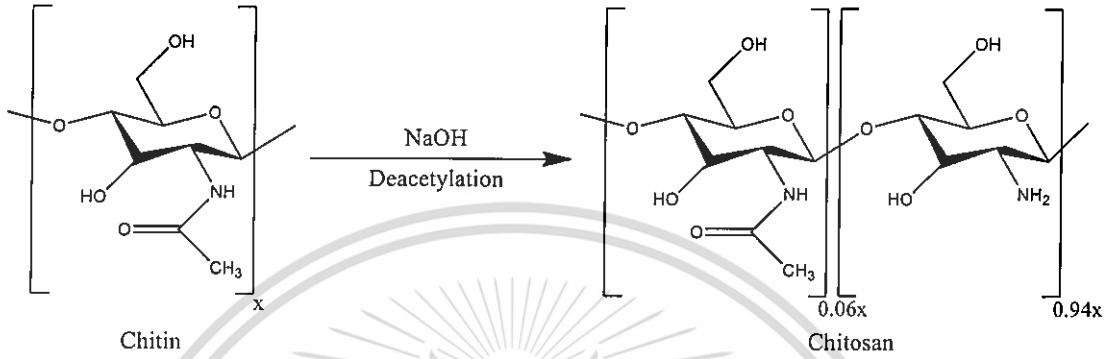

Figure B-4 Deacetylation reaction of chitin.

Therefore, average molecular weight per repeating unit of CS could be determined as following equation:

$$\text{Mw}_{\text{unit}}\text{ of CS} = \left(\text{Mw}_{\text{unit}}\text{ of chitin} - \left(\text{Mw}_{\text{acetyl}} \times \text{DD}_{\text{CS}}\right)\right) + \left(\text{Mw}_{\text{H}} \times \text{DD}_{\text{CS}}\right) \quad \text{(B-3)}$$

$$= (203 - (43 \times 0.94)) + (1 \times 0.94)$$

$$= 163.52$$

Therefore, average molecular weight per repeating unit of CS was 163.52.

Thereafter, average molecular weight per repeating unit of HCs was calculated using equation as follows:

$$\text{Mw}_{\text{unit}}\text{ of HC} = \left(\text{Mw}_{\text{unit}}\text{ of CS} - \left(\text{Mw}_{\text{H}} \times \text{DS}_{\text{HC}}\right)\right) + \left(\text{Mw}_{\text{HEA}} \times \text{DS}_{\text{HC}}\right) \quad \text{(B-4)}$$

For example,

From the section B.2, DS of HC1 was 1.22.

$$\text{Mw}_{\text{unit}}\text{ of HC1} = (163.52 - (1 \times 1.22)) + (117 \times 1.22)$$

$$= 305.04$$

Therefore, average molecular weight per repeating unit of HC1 was 305.04.

B.4 Percent yield

Theoretical weight of HCs was calculated using equation as follows:

$$\text{Theoretical weight of HC} = \frac{\text{weight of CS}}{\text{Mw}_{\text{unit}} \text{ of CS}} \times \text{Mw}_{\text{unit}} \text{ of HC} \quad \text{(B-5)}$$

For example,

Weight of CS used in the reaction was 3 g. From the section B.3, average molecular weight per repeating unit of CS and HC1 were 163.52 and 305.04, respectively.

$$\text{Theoretical weight of HC1} = \frac{3}{163.52} \times 305.04$$

$$= 5.6 \text{ g}$$

Therefore, theoretical weight of HC1 was 5.6 g.

Percent yield of products could be calculated using equation as follows:

$$\%\text{Yield} = \frac{\text{Actual weight}}{\text{Theroretical weight}} \text{x } 100 \quad \text{(B-6)}$$

For example,

After the reaction, 4.48 g of HC1 (product) was obtained. Therefore,

$$\%\text{Yield} = \frac{4.48}{5.6} \text{x } 100$$

$$= 80\%$$

Therefore, percent yield of HC1 was 80%.

Appendix C: Characterization of HC/SA films

C.1 FT-IR

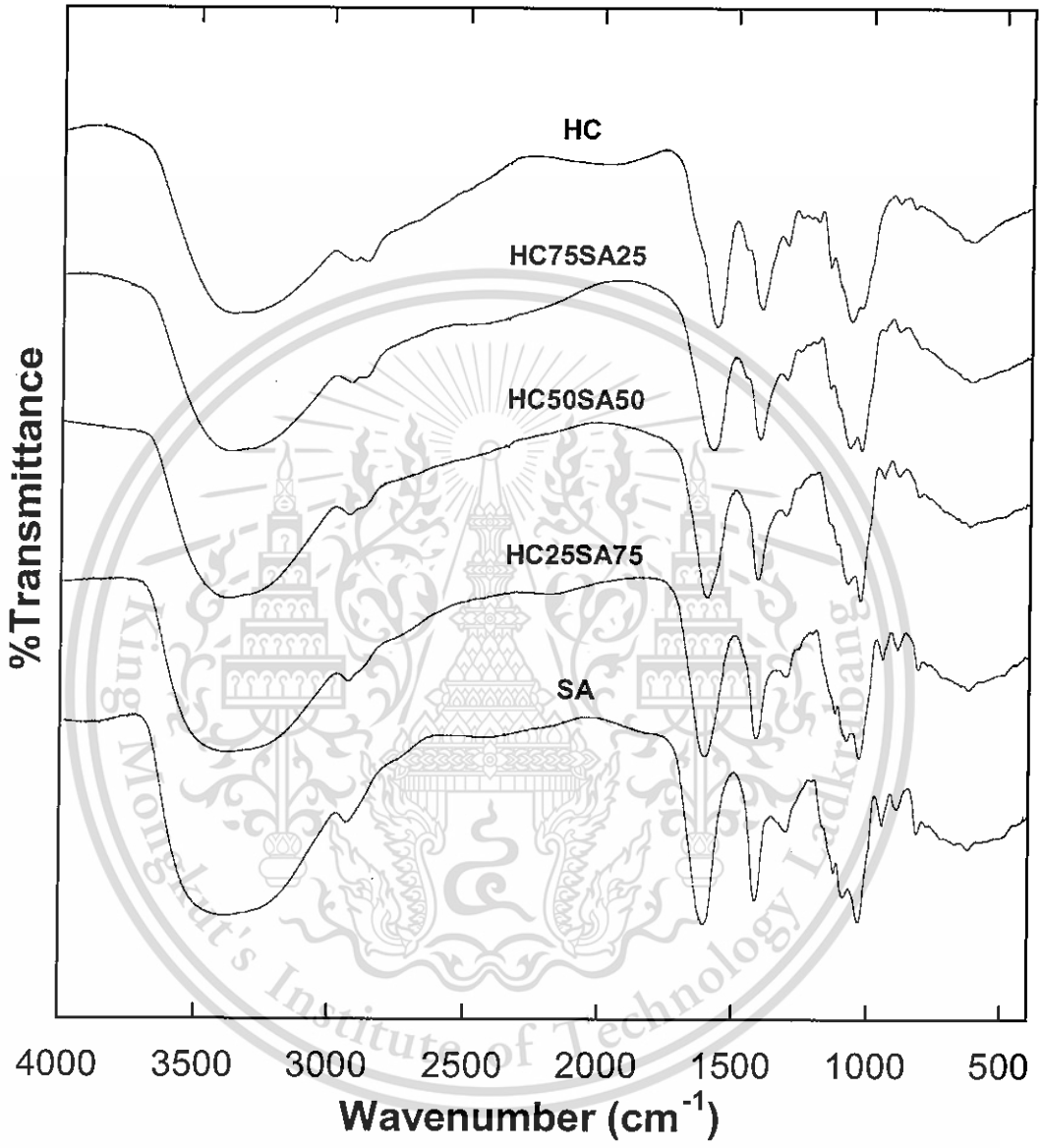

Figure C-1 FT-IR spectra of HC/SA films.

C.2 SEM

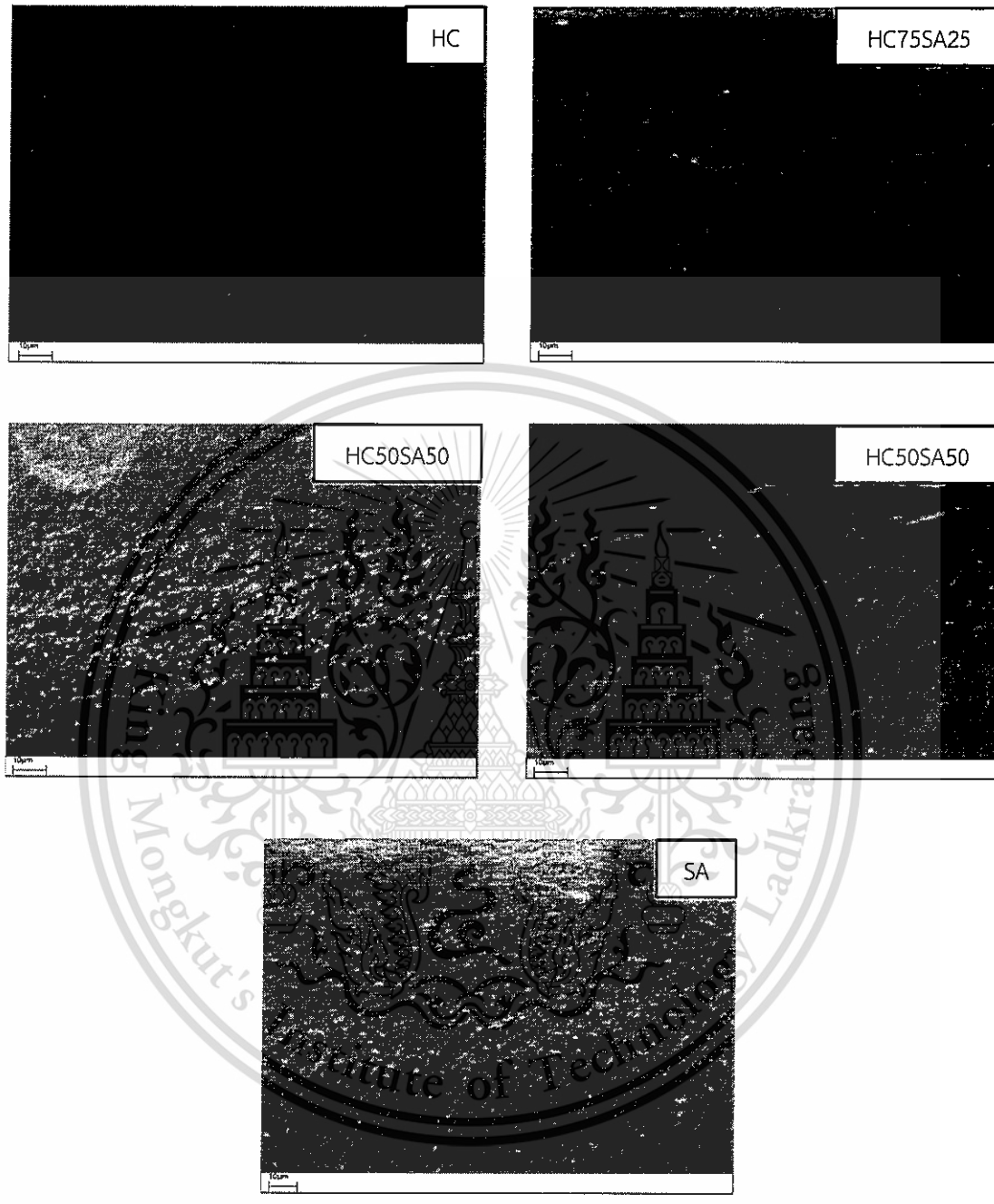

Figure C-2 SEM micrographs (800X) of cross-section of the HC/SA films.

Appendix D: Characterization of crosslinked HC/SA films

D.1 FT-IR

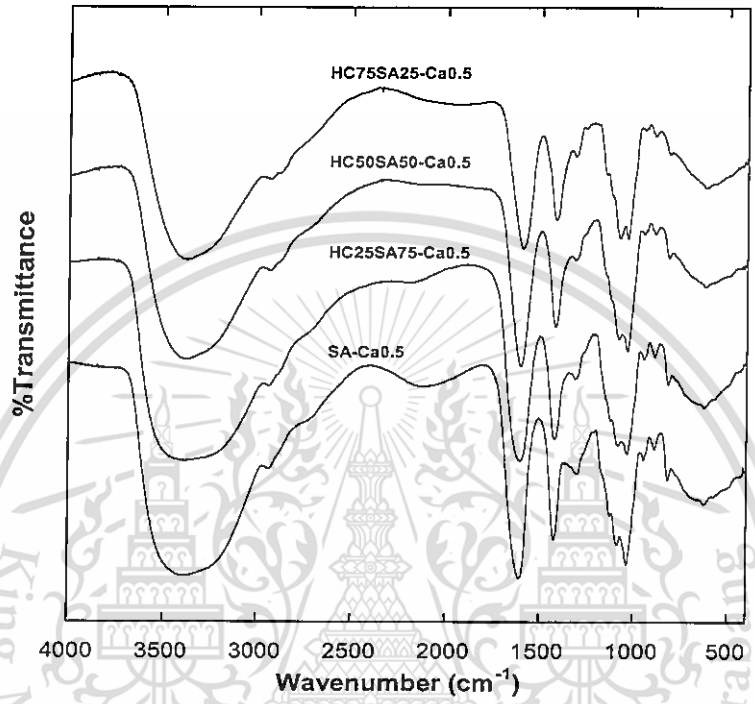

Figure D-1 FT-IR spectra of calcium crosslinked HC/SA films.

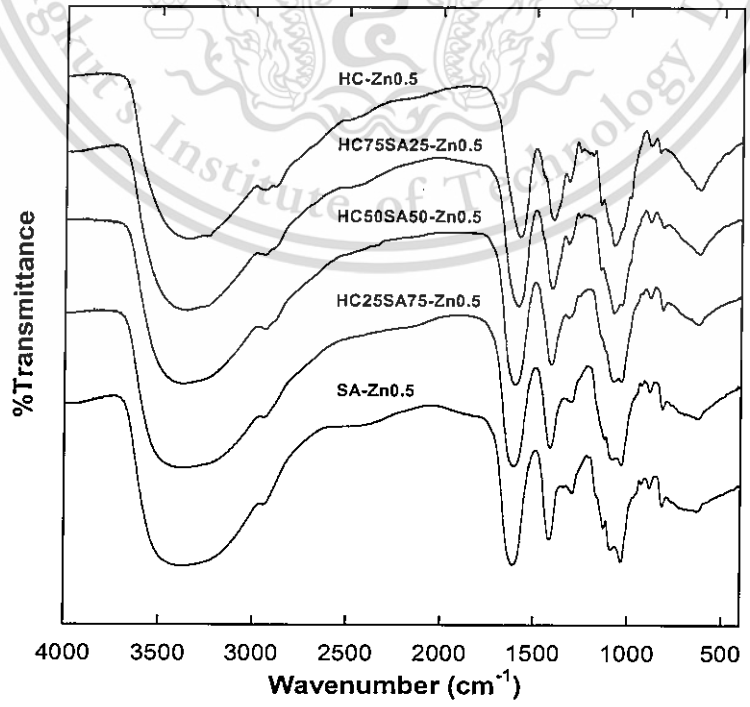

Figure D-2 FT-IR spectra of zinc crosslinked HC/SA films.

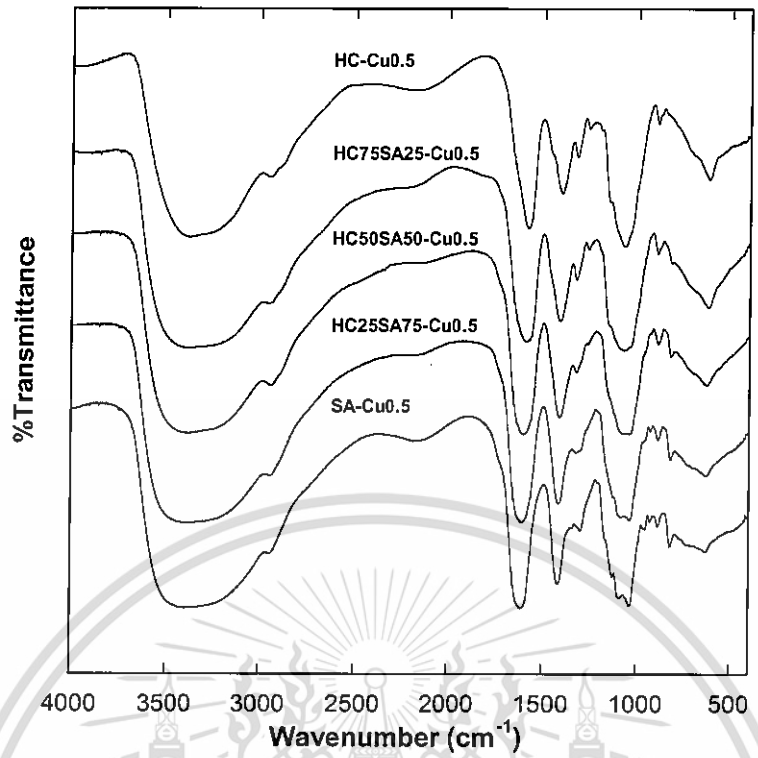

Figure D-3 FT-IR spectra of copper crosslinked HC/SA films.

D.2 SEM-EDS

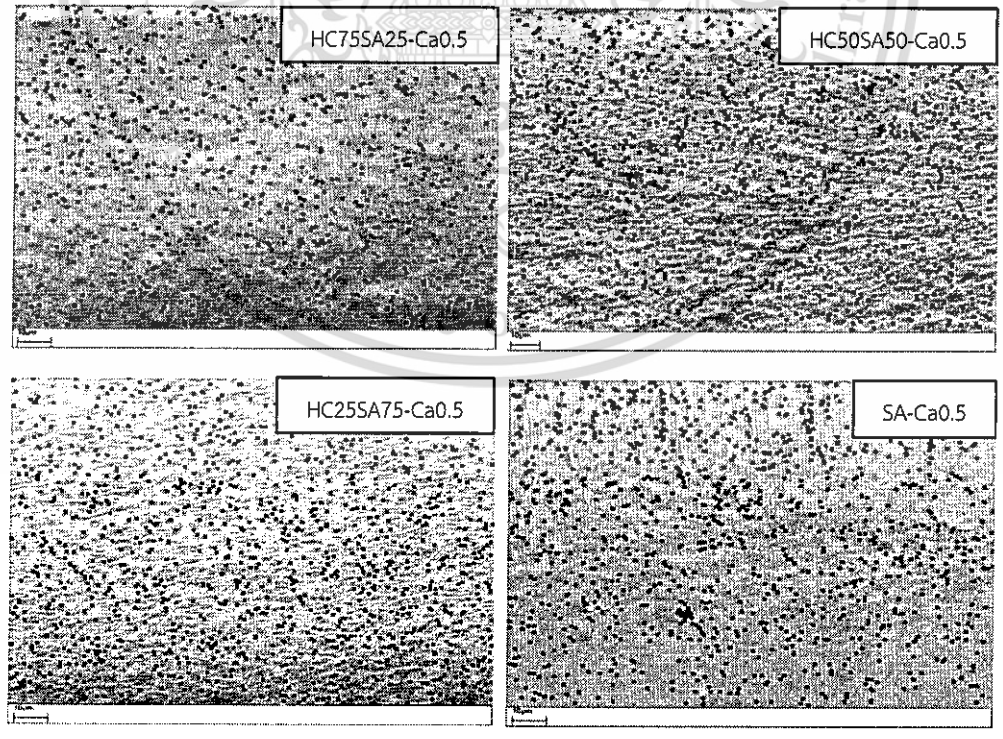

Figure D-4 SEM-EDS micrographs of the entire film thickness showing two-dimensional distribution of Ca^{2+} ions on the cross-section of calcium crosslinked HC/SA films.

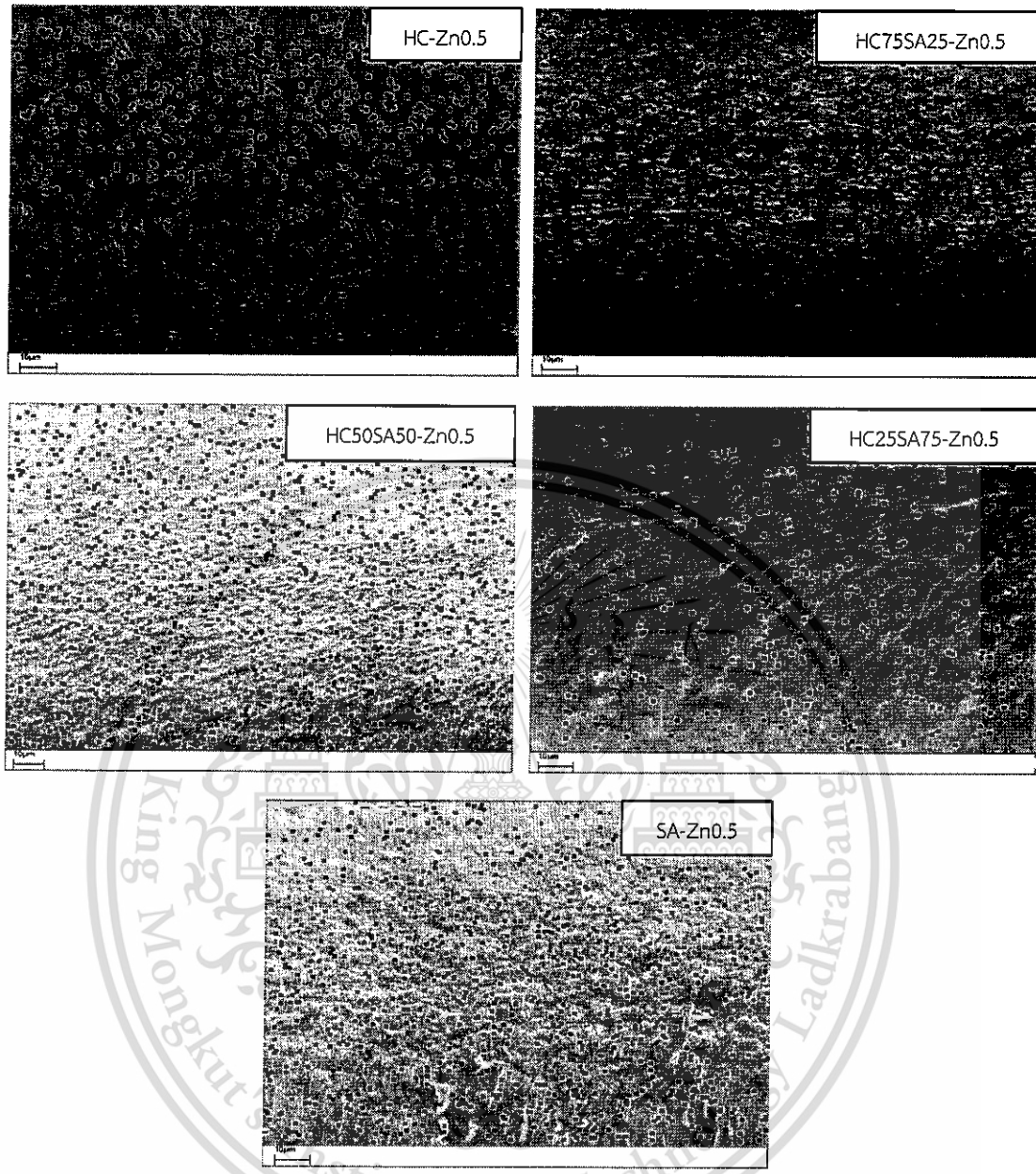

Figure D-5 SEM-EDS micrographs of the entire film thickness showing two-dimensional distribution of Zn^{2+} ions on the cross-section of zinc crosslinked HC/SA films.

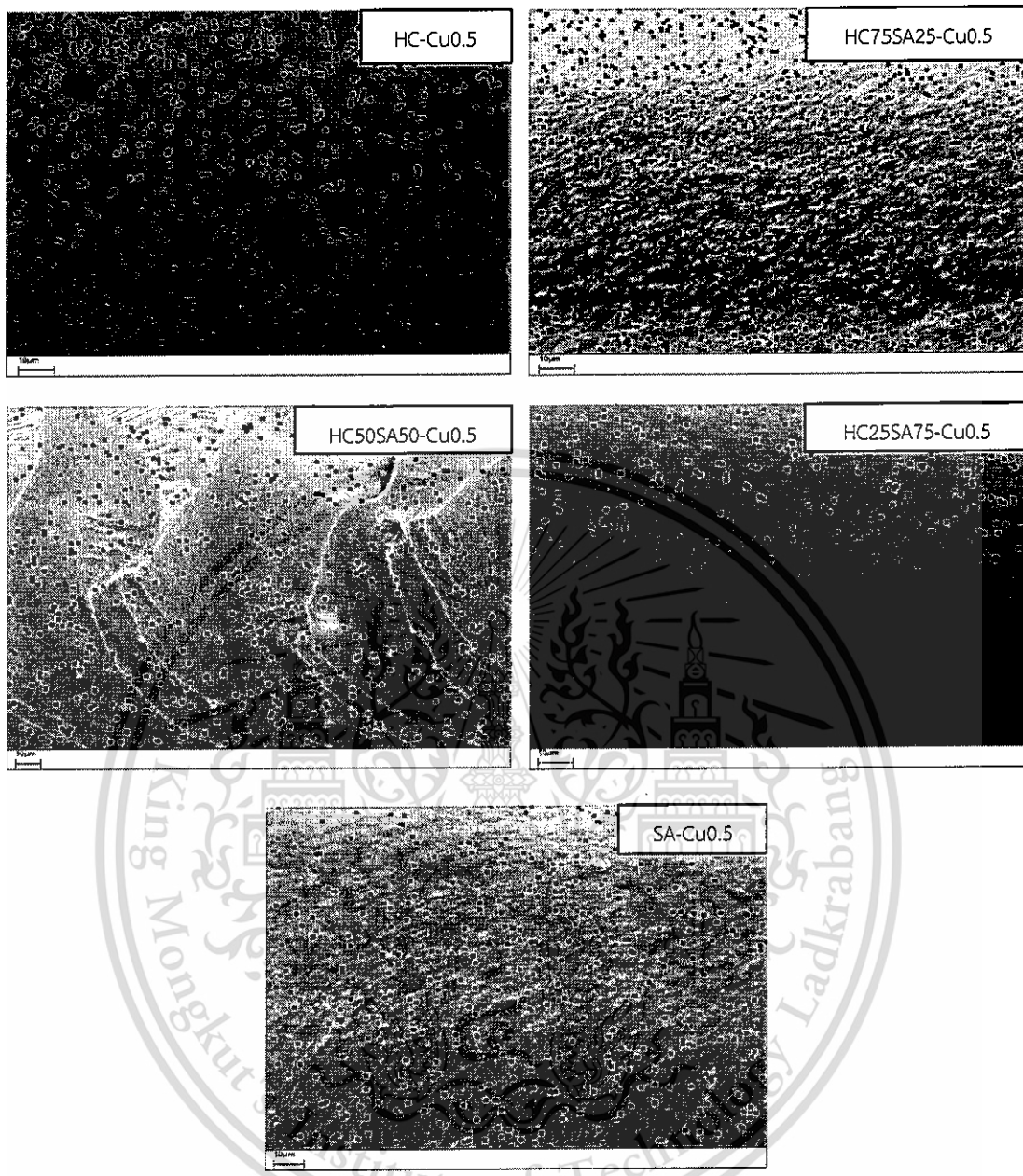

Figure D-6 SEM-EDS micrographs of the entire film thickness showing two-dimensional distribution of Cu^{2+} ions on the cross-section of copper crosslinked HC/SA films.

Appendix E: Swelling behavior

E.1 Distilled water

Table E-1 Swelling behavior of the HC/SA films in distilled water at 37 °C.

Time (min)	Swelling degree (%)				
	HC	HC75SA25	HC50SA50	HC25SA75	SA
0	0	0	0	0	0
5	4890±104	2083±129	2201±231	1490±24	1683±74
10	6175±49	3734±362	2244±202	1334±336	1164±139
15	7192±238	4407±308	922±59	505±71	443±111
20	7804±140	4710±159	307±90	72±42	126±31
30	8660±274	4901±145	67±11	0	0
45	9425±358	4606±34	6±3		
60	10235±345	4284±170	0		
90	11245±372	3719±183			
120	12134±495	2555±75			
180	13113±464	472±342			
240	14000±1894	38±35			
300	14600±460	0			
360	14809±459				
1440	2466±640				

Table E-2 Swelling behavior of the 0.05 M calcium crosslinked HC/SA films in distilled water at 37 °C.

Time (min)	Swelling degree (%)			
	HC75SA25-Ca0.05	HC50SA50-Ca0.05	HC25SA75-Ca0.05	SA-Ca0.05
0	0	0	0	0
5	354±20	238±24	161±21	91±4
10	423±36	275±23	196±11	124±8
15	441±38	293±26	211±17	140±14
20	456±49	306±31	216±8	143±6
30	475±44	315±24	228±3	159±11
45	495±47	322±28	228±7	161±9
60	513±52	328±33	242±5	157±10
90	535±57	333±27	237±6	159±5
120	540±58	339±24	247±8	169±5
180	559±53	352±27	243±15	167±2
240	564±56	359±23	259±5	171±6
300	592±61	362±24	259±10	168±10
360	602±53	363±33	254±16	162±3
1440	602±37	387±30	266±11	164±10

Table E-3 Swelling behavior of the 0.1 M calcium crosslinked HC/SA films in distilled water at 37 °C.

Time (min)	Swelling degree (%)			
	HC75SA25-Ca0.1	HC50SA50-Ca0.1	HC25SA75-Ca0.1	SA-Ca0.1
0	0	0	0	0
5	337±23	134±66	112±35	92±31
10	414±18	240±18	175±17	127±15
15	447±27	264±16	189±18	142±6
20	458±18	276±11	195±18	150±7
30	490±24	285±12	202±9	155±3
45	508±27	289±2	198±14	148±9
60	508±24	297±3	207±18	148±5
90	514±12	292±10	210±17	152±5
120	509±27	306±10	214±12	150±3
180	524±21	300±2	210±5	145±6
240	508±22	305±6	211±12	152±4
300	497±13	304±10	217±14	147±5
360	494±7	304±5	218±12	152±5
1440	455±16	307±22	221±17	152±2

Table E-4 Swelling behavior of the 0.25 M calcium crosslinked HC/SA films in distilled water at 37 °C.

Time (min)	Swelling degree (%)			
	HC75SA25-Ca0.25	HC50SA50-Ca0.25	HC25SA75-Ca0.25	SA-Ca0.25
0	0	0	0	0
5	209±55	191±15	89±8	92±14
10	324±20	228±7	160±7	126±7
15	368±4	243±10	171±9	131±2
20	385±1	249±3	177±2	137±12
30	400±13	253±4	174±3	132±1
45	409±12	256±5	182±4	130±7
60	412±29	255±1	179±1	131±5
90	431±23	268±14	180±1	131±9
120	433±28	263±6	187±10	124±9
180	439±26	265±9	181±3	143±8
240	444±13	274±16	183±3	125±8
300	442±19	266±11	192±9	132±5
360	447±3	270±3	183±7	134±8
1440	426±30	273±3	195±6	130±7

Table E-5 Swelling behavior of the 0.5 M calcium crosslinked HC/SA films in distilled water at 37 °C.

Time (min)	Swelling degree (%)			
	HC75SA25-Ca0.5	HC50SA50-Ca0.5	HC25SA75-Ca0.5	SA-Ca0.5
0	0	0	0	0
5	192±9	148±20	151±8	89±3
10	283±20	209±26	176±16	115±14
15	346±21	219±11	182±11	109±3
20	362±23	229±17	176±21	109±8
30	370±20	224±17	174±9	108±4
45	391±12	236±12	178±5	117±5
60	410±13	247±6	184±7	119±9
90	413±31	241±14	179±10	113±11
120	424±6	244±12	187±7	122±14
180	436±15	251±22	185±7	122±11
240	420±3	258±10	188±7	122±7
300	438±18	259±23	200±8	127±6
360	429±30	263±20	194±8	123±11
1440	394±6	261±17	184±6	120±7

Table E-6 Swelling behavior of the 0.5 M zinc crosslinked HC/SA films in distilled water at 37 °C.

Time (min)	Swelling degree (%)			
	HC75SA25-Zn0.5	HC50SA50-Zn0.5	HC25SA75-Zn0.5	SA-Zn0.5
0	0	0	0	0
5	128±7	90±6	89±4	86±6
10	195±10	122±6	122±4	120±13
15	221±12	136±12	135±2	127±6
20	232±14	141±9	136±1	131±1
30	229±21	132±5	130±3	128±3
45	233±17	136±3	126±7	130±4
60	238±19	130±4	123±4	125±3
90	244±26	133±3	123±2	117±4
120	245±25	130±7	125±5	125±1
180	249±32	132±10	125±5	126±0
240	251±35	132±9	123±4	123±5
300	255±38	132±6	123±2	123±2
360	256±43	128±3	118±7	119±6
1440	241±25	123±5	115±6	117±1

Table E-7 Swelling behavior of the 0.5 M copper crosslinked HC/SA films in distilled water at 37 °C.

Time (min)	Swelling degree (%)			
	HC75SA25-Cu0.5	HC50SA50-Cu0.5	HC25SA75-Cu0.5	SA-Cu0.5
0	0	0	0	0
5	135±7	93±14	52±12	66±11
10	153±14	87±7	70±11	89±9
15	174±5	107±11	86±5	100±8
20	188±11	98±9	94±14	95±12
30	190±10	112±21	100±12	96±8
45	207±13	103±10	96±6	101±4
60	220±19	103±17	88±8	93±5
90	237±26	104±9	83±6	101±2
120	233±25	103±13	81±6	99±9
180	234±39	103±9	86±2	99±14
240	237±39	94±9	80±7	86±4
300	244±39	83±12	89±6	100±7
360	239±41	86±5	84±2	95±12
1440	244±44	89±9	78±3	90±10

E.2 Calcium chloride solutions

Table E-8 Swelling behavior of the HC/SA films in 0.05 M calcium chloride solution.

Time (min)	Swelling degree (%)			
	HC75SA25	HC50SA50	HC25SA75	SA
0	0	0	0	0
0.25	101±3	92±4	101±7	163±2
0.5	187±3	152±4	177±6	316±2
0.75	238±4	192±4	230±5	401±10
1	274±5	223±5	263±5	456±13
1.5	311±4	257±3	300±5	515±16
2	324±7	270±2	307±4	537±14
3	329±2	273±7	290±6	507±17
4	326±3	262±6	265±7	448±17
5	323±3	251±8	248±7	409±18
10	323±5	249±9	237±6	383±5
15	330±6	243±1	232±6	368±5
20	333±4	241±4	227±4	358±6
30	337±5	238±4	223±4	349±6
45	338±8	234±5	216±4	338±6
60	338±7	235±5	209±2	332±2

Table E-9 Swelling behavior of the HC/SA films in 0.1 M calcium chloride solution.

Time (min)	Swelling degree (%)			
	HC75SA25	HC50SA50	HC25SA75	SA
0	0	0	0	0
0.25	110±3	87±4	66±2	99±3
0.5	172±3	131±4	101±2	146±3
0.75	202±3	157±4	119±2	172±3
1	223±6	171±6	131±2	184±5
1.5	243±5	178±7	142±3	189±5
2	244±7	178±9	147±1	196±2
3	249±8	175±2	149±4	189±1
4	251±3	172±3	147±4	179±5
5	252±3	169±1	142±2	169±6
10	264±3	167±1	131±2	152±8
15	265±2	166±2	128±3	145±7
20	268±5	162±5	125±5	140±3
30	272±5	168±5	124±6	137±2
45	275±4	167±6	123±4	132±4
60	275±5	168±7	121±4	129±4

Table E-10 Swelling behavior of the HC/SA films in 0.25 M calcium chloride solution.

Time (min)	Swelling degree (%)			
	HC75SA25	HC50SA50	HC25SA75	SA
0	0	0	0	0
0.25	82±2	81±3	57±2	54±4
0.5	131±2	113±3	81±1	76±5
0.75	155±2	129±4	94±2	89±3
1	168±4	140±5	100±3	97±2
1.5	185±5	147±5	106±3	107±4
2	194±1	148±4	108±2	108±5
3	199±2	148±4	108±2	108±5
4	203±3	147±2	109±2	104±6
5	201±3	148±2	107±1	100±2
10	220±4	149±5	103±5	93±2
15	228±4	150±5	102±5	90±3
20	232±4	148±5	101±4	88±4
30	238±6	146±4	99±2	87±4
45	239±6	153±4	101±2	84±1
60	245±7	152±4	98±3	83±1

Table E-11 Swelling behavior of the HC/SA films in 0.5 M calcium chloride solution.

Time (min)	Swelling degree (%)			
	HC75SA25	HC50SA50	HC25SA75	SA
0	0	0	0	0
0.25	72±2	62±2	48±1	41±2
0.5	113±2	90±1	70±1	56±2
0.75	138±3	105±2	84±2	66±4
1	155±1	116±3	93±2	71±5
1.5	167±4	119±2	101±1	78±5
2	177±5	120±1	104±3	83±5
3	184±3	121±4	105±2	86±6
4	195±6	122±3	103±2	86±3
5	201±7	125±3	101±2	84±2
10	214±6	132±3	100±4	73±3
15	225±6	133±5	100±3	69±3
20	231±7	137±1	101±3	70±4
30	238±9	137±2	102±4	71±4
45	242±10	140±3	101±5	71±1
60	242±10	140±4	101±1	70±3

E.3 Simulated gastric fluid (SGF, pH 1.2)

Table E-12 Swelling behavior of the HC/SA films in SGF at 37 °C.

Time (min)	Swelling degree (%)				
	HC	HC75SA25	HC50SA50	HC25SA75	SA
0	0	0	0	0	0
5	1217±139	458±3	378±6	550±48	591±27
10	2193±222	827±35	509±7	525±32	501±21
15	2858±230	940±16	582±13	514±25	459±21
20	3263±259	924±14	620±6	507±30	447±19
30	3527±144	882±16	630±6	502±24	440±18
45	3684±206	834±16	620±5	498±28	430±20
60	3866±177	805±15	616±10	489±29	424±13
90	3992±58	768±22	605±11	487±22	415±10
120	4025±53	750±11	605±14	481±25	415±26
180	3966±18	714±20	586±1	476±23	409±9
240	3809±96	697±14	582±5	474±25	372±24
300	3640±167	676±17	576±7	461±20	390±24
360	3406±115	669±25	580±11	455±19	386±25
1440	177±31	617±15	549±12	453±26	381±11

Table E-13 Swelling behavior of the 0.05 M calcium crosslinked HC/SA films in SGF at 37 °C.

Time (min)	Swelling degree (%)			
	HC75SA25-Ca0.05	HC50SA50-Ca0.05	HC25SA75-Ca0.05	SA-Ca0.05
0	0	0	0	0
5	577±34	338±12	208±19	118±24
10	960±37	445±122	273±4	153±10
15	1034±24	541±70	294±4	175±13
20	1033±6	564±44	298±3	175±10
30	998±11	572±50	293±11	183±9
45	940±17	564±44	288±6	176±8
60	905±14	566±32	297±7	175±2
90	871±29	550±33	288±6	186±9
120	857±26	547±27	284±2	186±11
180	819±32	548±33	293±4	185±11
240	775±9	555±30	297±7	172±13
300	754±7	544±23	294±4	183±8
360	730±15	535±33	283±6	175±10
1440	659±16	519±21	293±11	172±7

Table E-14 Swelling behavior of the 0.1 M calcium crosslinked HC/SA films in SGF at 37 °C.

Time (min)	Swelling degree (%)			
	HC75SA25-Ca0.1	HC50SA50-Ca0.1	HC25SA75-Ca0.1	SA-Ca0.1
0	0	0	0	0
5	489±30	310±25	194±9	136±12
10	817±66	458±36	260±13	174±8
15	1011±31	524±14	285±7	175±15
20	1024±30	540±18	293±12	182±5
30	1011±27	535±18	280±9	183±8
45	959±51	532±25	288±24	187±4
60	916±57	527±22	281±8	183±1
90	890±60	520±19	285±12	176±4
120	872±51	510±14	287±9	181±7
180	821±41	513±16	279±5	171±9
240	811±46	502±24	284±6	171±7
300	799±38	506±23	285±9	168±9
360	764±47	496±24	282±18	179±3
1440	717±33	489±26	276±17	176±8

Table E-15 Swelling behavior of the 0.25 M calcium crosslinked HC/SA films in SGF at 37 °C.

Time (min)	Swelling degree (%)			
	HC75SA25-Ca0.25	HC50SA50-Ca0.25	HC25SA75-Ca0.25	SA-Ca0.25
0	0	0	0	0
5	425±54	292±29	193±8	128±32
10	760±22	440±41	253±11	159±27
15	941±73	499±45	267±17	178±15
20	951±79	502±46	265±22	177±6
30	933±74	499±46	273±5	175±20
45	910±62	493±51	267±16	172±16
60	889±52	497±45	269±16	167±8
90	848±47	476±40	259±18	175±6
120	832±50	474±51	255±18	169±5
180	795±35	469±41	258±16	169±8
240	775±32	461±48	259±17	172±13
300	751±33	447±46	264±13	174±11
360	753±33	459±43	255±15	174±12
1440	686±40	440±37	254±23	169±14

Table E-16 Swelling behavior of the 0.5 M calcium crosslinked HC/SA films in SGF at 37 °C.

Time (min)	Swelling degree (%)			
	HC75SA25-Ca0.5	HC50SA50-Ca0.5	HC25SA75-Ca0.5	SA-Ca0.5
0	0	0	0	0
5	451±17	233±2	183±12	123±7
10	759±55	400±64	242±9	156±2
15	943±21	499±28	268±6	158±10
20	945±9	520±11	261±12	162±9
30	938±16	523±4	262±4	159±4
45	881±27	517±5	251±2	157±12
60	858±24	510±4	253±5	156±4
90	806±23	502±4	251±7	157±8
120	770±23	501±3	248±3	149±8
180	728±39	487±9	245±3	154±6
240	711±22	489±12	242±3	154±10
300	695±23	486±12	246±14	150±3
360	673±32	482±14	242±6	148±11
1440	596±30	465±9	246±6	157±5

Table E-17 Swelling behavior of the 0.5 M zinc crosslinked HC/SA films in SGF at 37 °C.

Time (min)	Swelling degree (%)				
	HC-Zn0.5	HC75SA25-Zn0.5	HC50SA50-Zn0.5	HC25SA75-Zn0.5	SA-Zn0.5
0	0	0	0	0	0
5	596±79	278±6	210±10	144±10	161±4
10	1196±390	471±12	304±18	193±20	197±1
15	2344±255	679±17	455±11	219±15	195±4
20	2871±177	684±32	528±3	225±6	187±7
30	3072±100	638±30	537±6	235±5	189±3
45	3109±290	588±16	539±10	236±6	189±4
60	3101±215	580±24	542±8	239±6	190±3
90	3070±178	545±27	531±14	232±11	181±9
120	3080±182	532±24	527±12	235±12	184±6
180	2945±258	523±19	527±17	236±10	186±6
240	2500±134	506±10	519±13	231±10	184±8
300	2231±169	493±24	509±15	229±8	184±6
360	1756±130	500±17	503±13	229±12	183±9
1440	504±47	449±21	487±12	221±15	178±6

Table E-18 Swelling behavior of the 0.5 M copper crosslinked HC/SA films in SGF at 37 °C.

Time (min)	Swelling degree (%)				
	HC-Cu0.5	HC75SA25-Cu0.5	HC50SA50-Cu0.5	HC25SA75-Cu0.5	SA-Cu0.5
0	0	0	0	0	0
5	409±118	268±19	142±35	103±23	105±16
10	1096±261	440±44	204±37	132±8	138±6
15	1735±452	576±22	290±63	177±15	159±2
20	2215±431	606±25	377±61	207±13	168±10
30	2661±133	600±33	461±20	228±16	162±9
45	2881±169	583±22	474±1	236±15	161±10
60	3009±69	574±23	480±14	231±10	157±10
90	2874±93	579±26	470±23	235±12	155±11
120	2606±270	563±25	457±8	232±13	153±8
180	2193±363	561±25	457±19	233±5	161±3
240	1342±363	559±11	452±16	232±12	153±10
300	787±128	552±8	444±12	225±14	156±10
360	329±92	539±12	439±18	226±12	156±4
1440	16±2	521±8	412±16	216±14	152±11

E.4 Simulated intestinal fluid (SIF, pH 7.4)

Table E-19 Swelling behavior of the HC/SA films in SIF at 37 °C.

Time (min)	Swelling degree (%)				
	HC	HC75SA25	HC50SA50	HC25SA75	SA
0	0	0	0	0	0
5	1501±201	881±10	794±185	1099±87	957±126
10	2114±68	1363±73	1344±214	1292±92	1338±178
15	2499±46	1756±106	1524±67	1224±55	1300±199
20	2763±57	2094±138	1600±3	1056±128	1109±214
30	2964±42	2471±137	1490±38	860±18	791±74
45	3139±60	2851±113	1334±44	543±49	346±33
60	3286±55	3121±154	1041±42	276±18	142±25
90	3409±82	3275±134	494±113	28±4	1±0
120	3487±109	3337±92	186±60	0	0
180	3575±92	3374±137	4±1		
240	3651±84	3353±209	0		
300	3690±88	2895±404			
360	3744±104	1862±310			
1440	3636±51	0			

Table E-20 Swelling behavior of the 0.05 M calcium crosslinked HC/SA films in SIF at 37 °C.

Time (min)	Swelling degree (%)			
	HC75SA25-Ca0.05	HC50SA50-Ca0.05	HC25SA75-Ca0.05	SA-Ca0.05
0	0	0	0	0
5	344±83	273±16	177±31	104±25
10	463±55	358±27	257±46	153±4
15	531±56	400±25	307±46	201±12
20	597±66	419±14	337±55	236±17
30	689±71	451±34	364±47	279±9
45	829±102	491±33	386±46	314±18
60	942±71	532±43	401±44	321±15
90	1089±45	597±44	431±54	362±15
120	1225±109	696±20	482±74	381±22
180	1401±85	870±46	553±121	419±14
240	718±197	1023±46	636±158	451±25
300	413±87	1162±7	743±241	493±36
360	219±99	952±77	795±179	542±41
420	164±65	435±94	704±106	599±51
480	134±50	286±52	561±142	637±64
540	125±45	120±25	482±93	702±60
600	110±39	87±24	442±70	777±79
660	108±37	58±16	369±60	806±41
720	100±40	59±17	334±51	845±73
780	86±25	58±17	259±66	950±30
840	77±10	47±11	193±20	928±60
900	76±20	41±10	131±34	952±10
960	69±24	40±10	61±13	782±51
1440	33±11	39±16	51±10	125±57

Table E-21 Swelling behavior of the 0.1 M calcium crosslinked HC/SA films in SIF at 37 °C.

Time (min)	Swelling degree (%)			
	HC75SA25-Ca0.1	HC50SA50-Ca0.1	HC25SA75-Ca0.1	SA-Ca0.1
0	0	0	0	0
5	265±66	219±12	154±25	111±15
10	385±45	294±20	199±14	153±1
15	454±41	318±3	227±21	192±4
20	521±51	352±14	239±15	205±8
30	624±62	381±13	262±31	215±7
45	753±108	423±14	285±26	229±16
60	888±92	467±5	298±9	231±2
90	1093±83	543±3	321±24	241±13
120	1270±223	617±17	337±29	250±14
180	1260±23	756±11	401±70	253±12
240	605±32	890±23	466±89	262±15
300	336±77	909±44	542±98	270±6
360	177±19	621±63	632±88	286±3
420	119±17	289±88	743±47	289±23
480	117±28	182±27	738±86	292±28
540	81±33	104±44	595±44	309±29
600	66±24	50±11	485±47	314±17
660	57±26	43±14	365±79	331±17
720	59±12	46±4	209±89	320±7
780	46±6	46±16	141±61	340±15
840	48±12	41±18	92±27	351±9
900	39±11	42±20	60±10	356±24
960	41±3	42±11	40±15	373±36
1440	29±12	44±16	2±1	504±36

Table E-22 Swelling behavior of the 0.25 M calcium crosslinked HC/SA films in SIF at 37 °C.

Time (min)	Swelling degree (%)			
	HC75SA25-Ca0.25	HC50SA50-Ca0.25	HC25SA75-Ca0.25	SA-Ca0.25
0	0	0	0	0
5	289±35	226±41	134±36	111±10
10	393±41	285±36	161±32	147±11
15	486±64	328±41	202±24	165±7
20	554±68	356±44	228±16	168±21
30	657±80	397±60	236±26	186±5
45	816±25	440±88	267±61	194±14
60	979±98	496±111	298±2	199±2
90	1137±165	596±142	300±11	202±15
120	1214±157	716±15	342±1	205±11
180	1291±25	894±59	407±20	210±3
240	298±24	816±39	506±65	216±13
300	172±15	483±67	626±71	218±7
360	80±7	201±22	711±152	233±4
420	65±3	90±25	742±19	236±1
480	50±7	30±7	786±72	235±8
540	44±6	29±3	648±40	241±13
600	36±12	24±12	438±96	254±31
660	23±3	22±4	259±13	256±20
720	17±2	33±5	110±33	257±17
780	16±2	26±5	35±5	268±26
840	8±1	16±2	29±6	263±15
900	7±2	9±1	17±2	273±12
960	5±2	9±3	11±1	277±22
1440	5±1	5±1	10±3	333±28

Table E-23 Swelling behavior of the 0.5 M calcium crosslinked HC/SA films in SIF at 37 °C.

Time (min)	Swelling degree (%)			
	HC75SA25-Ca0. 5	HC50SA50-Ca0.5	HC25SA75-Ca0.5	SA-Ca0.5
0	0	0	0	0
5	242±11	139±61	90±16	91±12
10	334±3	203±32	154±40	114±12
15	404±1	245±30	175±44	131±15
20	458±4	272±28	191±42	143±15
30	556±23	304±26	208±46	150±10
45	661±38	337±26	217±43	154±20
60	751±30	372±33	236±49	170±13
90	927±23	444±36	260±45	176±13
120	1092±130	507±48	274±54	178±8
180	1225±277	658±58	302±54	179±2
240	1047±22	781±54	333±60	187±11
300	632±55	956±63	385±88	186±1
360	255±60	799±28	421±86	189±4
420	156±58	508±13	478±82	194±1
480	117±49	346±64	527±94	199±15
540	82±12	140±16	594±99	200±9
600	59±26	48±13	599±94	208±4
660	63±16	31±8	584±63	213±9
720	42±15	29±9	563±76	216±6
780	40±11	11±5	546±70	224±15
840	34±9	10±2	500±56	235±23
900	30±5	10±1	436±54	229±8
960	28±5	5±1	404±33	233±9
1440	27±6	1±1	101±34	247±17

Table E-24 Swelling behavior of the 0.5 M zinc crosslinked HC/SA films in SIF at 37 °C.

Time (min)	Swelling degree (%)				
	HC-Zn0.5	HC75SA25-Zn0.5	HC50SA50-Zn0.5	HC25SA75-Zn0.5	SA-Zn0.5
0	0	0	0	0	0
5	200±6	115±14	98±9	101±1	80±2
10	236±13	130±7	118±12	131±2	111±5
15	253±7	133±8	128±8	128±5	119±2
20	271±4	135±8	130±12	129±3	125±7
30	282±3	146±9	149±11	156±12	143±3
45	319±4	161±16	200±1	200±36	200±7
60	346±18	175±5	254±1	265±34	298±8
90	369±2	198±2	327±2	360±43	486±25
120	400±2	224±12	396±16	437±41	634±15
180	446±12	254±8	535±51	599±84	583±87
240	491±5	276±16	600±22	761±21	251±73
300	561±3	285±26	586±3	879±29	56±15
360	657±8	296±39	557±8	885±36	0
420	711±4	303±23	519±2	867±35	
480	794±20	309±26	519±5	780±48	

Table E-25 Swelling behavior of the 0.5 M copper crosslinked HC/SA films in SIF at 37 °C.

Time (min)	Swelling degree (%)				
	HC-Cu0.5	HC75SA25-Cu0.5	HC50SA50-Cu0.5	HC25SA75-Cu0.5	SA-Cu0.5
0	0	0	0	0	0
5	146±3	121±14	71±7	76±3	83±3
10	184±4	153±9	104±6	103±8	101±10
15	209±9	167±10	102±5	109±5	109±12
20	226±11	172±18	102±2	106±7	110±6
30	248±12	190±14	109±4	108±6	116±1
45	281±17	192±23	105±12	103±2	120±5
60	309±16	208±13	107±7	109±1	117±3
90	336±23	206±17	109±5	110±5	119±5
120	363±20	215±16	109±5	108±2	123±2
180	409±16	221±17	103±6	107±7	125±4
240	441±25	224±16	104±19	106±6	119±9
300	477±27	229±15	102±5	106±1	129±8
360	511±39	228±18	105±5	112±4	128±8
420	539±49	237±23	103±12	111±12	127±3
480	579±53	235±21	108±2	117±8	125±2

E.5 Simulated gastrointestinal fluid (SGF followed by SIF)

Table E-26 Swelling behavior of the HC/SA films in simulated gastrointestinal fluid at 37 °C.

Time (min)	Swelling degree (%)			
	HC75SA25	HC50SA50	HC255A75	SA
0	0	0	0	0
15	673±32	357±28	297±19	469±88
30	757±31	439±11	305±21	503±36
45	713±30	456±18	304±26	482±30
60	695±38	450±15	306±25	472±34
90	670±36	448±10	300±22	452±38
120	651±25	449±8	295±27	455±35
135	207±32	238±4	243±27	513±34
150	291±15	235±9	271±19	601±53
165	361±7	256±16	297±25	693±70
180	465±20	281±10	333±25	721±82
210	716±63	330±13	393±36	974±95
240	1013±83	397±31	459±46	1049±71
300	1015±30	524±44	588±49	953±37
360	603±133	720±106	693±2	514±46
420	192±114	923±90	760±43	117±38
480	40±35	1098±59	801±47	5±1

Table E-27 Swelling behavior of the 0.1 M calcium crosslinked HC/SA films in simulated gastrointestinal fluid at 37 °C.

Time (min)	Swelling degree (%)			
	HC75SA25-Ca0.1	HC50SA50-Ca0.1	HC25SA75-Ca0.1	SA-Ca0.1
0	0	0	0	0
15	961±49	375±27	200±23	183±8
30	1014±21	444±6	219±20	187±10
45	966±16	449±6	226±13	191±8
60	936±22	437±4	223±9	186±8
90	883±14	445±3	222±9	183±7
120	881±33	437±6	230±19	187±10
135	661±31	254±11	179±18	204±15
150	533±38	245±7	200±14	243±20
165	555±39	265±1	228±15	287±34
180	670±51	288±1	246±18	359±38
210	841±88	331±5	300±38	504±26
240	1094±92	400±6	361±52	611±88
300	1509±212	528±36	462±51	566±58
360	1286±153	706±70	580±44	397±35
420	853±90	910±61	673±93	73±10
480	591±33	1069±53	787±84	0

Table E-28 Swelling behavior of the 0.5 M calcium crosslinked HC/SA films in simulated gastrointestinal fluid at 37 °C.

Time (min)	Swelling degree (%)			
	HC75SA25-Ca0.5	HC50SA50-Ca0.5	HC25SA75-Ca0.5	SA-Ca0.5
0	0	0	0	0
15	794±54	407±53	235±10	187±18
30	843±8	454±51	257±10	193±15
45	837±14	458±56	265±13	196±15
60	819±9	458±55	259±8	199±8
90	797±8	445±46	254±10	192±16
120	786±6	441±46	256±17	185±9
135	406±49	252±45	221±13	208±12
150	290±40	230±31	229±18	229±17
165	319±42	261±42	254±10	265±23
180	393±46	292±49	272±29	301±35
210	524±48	345±58	315±37	428±80
240	747±94	426±92	351±32	552±90
300	1043±165	589±87	436±52	624±70
360	1261±228	830±86	547±89	562±57
420	1420±316	1091±91	651±70	358±21
480	1477±300	1294±136	769±56	132±33

Table E-29 Swelling behavior of the 0.5 M zinc crosslinked HC/SA films in simulated gastrointestinal fluid at 37 °C.

Time (min)	Swelling degree (%)			
	HC75SA25-Zn0.5	HC50SA50-Zn0.5	HC25SA75-Zn0.5	SA-Zn0.5
0	0	0	0	0
15	686±13	368±37	220±6	177±14
30	788±9	416±8	224±2	178±12
45	772±12	409±10	227±1	176±9
60	770±4	409±14	221±6	173±12
90	730±11	400±11	223±9	175±13
120	733±2	401±5	220±6	168±7
135	352±10	213±17	179±8	187±12
150	277±2	222±2	192±1	221±19
165	354±14	244±11	209±3	245±27
180	392±3	263±5	229±15	283±38
210	499±60	334±13	267±13	349±51
240	603±89	406±24	309±15	399±50
300	768±71	556±40	369±15	349±41
360	947±55	765±73	440±29	255±46
420	1053±46	1005±67	521±55	135±33
480	1121±58	1141±63	564±63	0

Table E-30 Swelling behavior of the 0.5 M copper crosslinked HC/SA films in simulated gastrointestinal fluid at 37 °C.

Time (min)	Swelling degree (%)			
	HC75SA25-Cu0.5	HC50SA50-Cu0.5	HC25SA75-Cu0.5	SA-Cu0.5
0	0	0	0	0
15	695±77	395±37	213±15	165±5
30	704±76	492±16	230±11	156±1
45	693±68	490±10	238±7	151±2
60	683±64	484±6	231±7	147±4
90	661±66	476±6	228±4	141±8
120	656±65	480±13	223±9	145±9
135	227±47	260±22	186±10	157±9
150	237±37	257±40	204±6	183±13
165	308±48	269±34	224±11	207±5
180	373±73	303±31	253±20	226±29
210	561±21	366±46	288±29	284±39
240	782±34	444±49	328±31	311±47
300	1054±166	581±68	400±24	306±44
360	1121±113	788±66	480±26	249±59
420	1113±134	1007±39	559±33	168±54
480	1069±111	1114±86	617±41	10±17

Appendix F: Gel content

Table F-1 Gel contents of the films in distilled water for 24 h at 37 °C.

Sample	Gel content (%)
HC	8.94±1.76
HC75SA25	0
HC50SA50	0
HC25SA75	0
SA	0
HC75SA25-Ca0.05	71.01±2.64
HC50SA50-Ca0.05	91.03±1.31
HC25SA75-Ca0.05	98.83±1.13
SA-Ca0.05	99.90±0.01
HC75SA25-Ca0.1	66.39±1.44
HC50SA50-Ca0.1	90.76±2.33
HC25SA75-Ca0.1	97.84±1.22
SA-Ca0.1	99.44±0.46
HC75SA25-Ca0.25	69.68±4.59
HC50SA50-Ca0.25	90.58±0.95
HC25SA75-Ca0.25	96.65±0.85
SA-Ca0.25	97.71±1.70
HC75SA25-Ca0.5	65.15±1.76
HC50SA50-Ca0.5	89.01±1.60
HC25SA75-Ca0.5	96.35±0.92
SA-Ca0.5	97.26±0.16
HC-Zn0.5	98.11±0.59
HC75SA25-Zn0.5	97.35±1.08
HC50SA50-Zn0.5	94.09±0.52
HC25SA75-Zn0.5	89.99±1.49
SA-Zn0.5	88.56±1.63
HC-Cu0.5	95.70±0.94
HC75SA25-Cu0.5	94.70±0.95
HC50SA50-Cu0.5	89.76±0.39
HC25SA75-Cu0.5	95.87±0.65
SA-Cu0.5	96.20±1.50

Table F-2 Gel contents of the films in SGF for 24 h at 37 °C.

Sample	Gel content (%)
HC	0.99±0.34
HC75SA25	31.57±2.82
HC50SA50	65.95±3.83
HC25SA75	77.33±3.69
SA	82.54±3.61
HC75SA25-Ca0.05	35.21±1.34
HC50SA50-Ca0.05	69.30±0.51
HC25SA75-Ca0.05	78.96±1.57
SA-Ca0.05	78.95±1.59
HC75SA25-Ca0.1	38.58±0.55
HC50SA50-Ca0.1	69.21±4.57
HC25SA75-Ca0.1	80.33±0.51
SA-Ca0.1	80.02±0.93
HC75SA25-Ca0.25	40.09±2.32
HC50SA50-Ca0.25	65.39±1.81
HC25SA75-Ca0.25	78.42±0.18
SA-Ca0.25	78.05±1.15
HC75SA25-Ca0.5	33.70±1.83
HC50SA50-Ca0.5	68.31±1.55
HC25SA75-Ca0.5	78.80±1.39
SA-Ca0.5	78.55±0.24
HC-Zn0.5	2.60±1.36
HC75SA25-Zn0.5	31.57±2.82
HC50SA50-Zn0.5	65.09±0.86
HC25SA75-Zn0.5	73.68±0.67
SA-Zn0.5	70.69±1.23
HC-Cu0.5	0.1±0.01
HC75SA25-Cu0.5	37.21±1.81
HC50SA50-Cu0.5	57.81±3.92
HC25SA75-Cu0.5	70.23±4.64
SA-Cu0.5	72.93±1.44

Table F-3 Gel contents of the films in SGF for 2 h at 37 °C.

Sample	Gel content (%)
HC75SA25	54.63±5.99
HC50SA50	77.51±1.39
HC25SA75	82.26±2.92
SA	84.84±2.49
HC75SA25-Ca0.1	59.03±4.27
HC50SA50-Ca0.1	81.00±1.95
HC25SA75-Ca0.1	82.93±0.49
SA-Ca0.1	79.34±0.86
HC75SA25-Ca0.5	51.98±5.07
HC50SA50-Ca0.5	74.23±1.95
HC25SA75-Ca0.5	79.52±0.76
SA-Ca0.5	77.21±1.20
HC75SA25-Zn0.5	58.68±1.91
HC50SA50-Zn0.5	73.83±1.57
HC25SA75-Zn0.5	74.62±1.50
SA-Zn0.5	70.65±0.47
HC75SA25-Cu0.5	54.06±1.10
HC50SA50-Cu0.5	72.50±1.24
HC25SA75-Cu0.5	73.42±1.54
SA-Cu0.5	74.16±0.25

Table F-4 Gel contents of the films after immersing in SGF for 2 h followed by SIF for 6 h at 37 °C.

Sample	Gel content (%)
HC75SA25	0.36±0.62
HC50SA50	75.75±0.84
HC25SA75	52.52±1.96
SA	0
HC75SA25-Ca0.1	7.98±2.60
HC50SA50-Ca0.1	77.52±1.71
HC25SA75-Ca0.1	62.80±5.84
SA-Ca0.1	0.92±0.88
HC75SA25-Ca0.5	55.18±1.03
HC50SA50-Ca0.5	74.27±3.02
HC25SA75-Ca0.5	78.79±6.50
SA-Ca0.5	10.89±6.26
HC75SA25-Zn0.5	36.30±0.32
HC50SA50-Zn0.5	68.51±1.39
HC25SA75-Zn0.5	64.36±4.31
SA-Zn0.5	1.56±0.49
HC75SA25-Cu0.5	29.68±1.55
HC50SA50-Cu0.5	60.18±4.76
HC25SA75-Cu0.5	62.90±0.89
SA-Cu0.5	2.26±1.27

Appendix G: *In vitro* drug release behavior

Table G-1 Percentages of paracetamol release from sealed bags formed by non-crosslinked films in simulated gastrointestinal fluid at 37 °C.

Time (min)	Percentages of paracetamol release			
	HC75SA25	HC50SA50	HC25SA75	SA
0	0	0	0	0
15	0	0	0.11±0.19	0
30	1.44±1.34	2.53±3.56	0.88±1.01	1.55±1.02
45	2.87±2.32	1.87±1.69	2.10±2.15	2.54±2.49
60	4.75±2.77	2.20±1.37	4.08±1.88	4.87±2.13
90	9.61±5.32	3.74±2.12	8.16±4.30	9.61±4.28
120	15.13±4.83	5.72±1.81	11.36±2.98	12.38±4.47
135	15.90±4.29	5.83±1.62	12.13±3.64	12.93±4.66
150	16.79±5.66	6.16±2.01	12.68±4.20	14.27±5.73
165	21.21±5.97	6.93±2.81	14.23±4.37	19.49±2.39
180	23.97±6.13	7.59±2.61	15.23±4.59	26.90±6.20
210	30.81±9.11	9.46±4.29	19.75±5.00	55.98±12.61
240	36.12±8.11	11.22±3.7	22.40±4.56	73.88±5.04
300	45.17±12.75	14.30±7.4	41.82±7.97	89.15±2.04
360	59.31±16.01	24.86±8.54	84.62±16.96	100.00
420	69.70±10.44	66.28±16.81	97.49±5.15	
480	80.75±8.62	90.23±5.61	100.00	

Table G-2 Percentages of paracetamol release from sealed bags formed by 0.1 M calcium crosslinked films in simulated gastrointestinal fluid at 37 °C.

Time (min)	Percentages of paracetamol release			
	HC75SA25-Ca0.1	HC50SA50-Ca0.1	HC25SA75-Ca0.1	SA-Ca0.1
0	0	0	0	0
15	0.88±0.19	1.07±0.46	0	0.99±0.24
30	0.88±0.19	0.86±0.17	1.98±0.58	5.05±0.25
45	1.32±0.01	0.86±0.55	4.95±1.16	8.45±0.67
60	1.32±0.01	0.79±0.66	10.23±2.91	14.37±2.52
90	7.05±0.76	6.19±2.50	32.77±11.63	40.59±7.80
120	9.46±2.48	9.16±0.53	45.96±15.38	52.22±13.35
135	11.34±2.66	10.85±1.07	50.25±17.03	58.69±16.82
150	11.78±3.03	11.21±0.63	54.32±17.90	61.33±13.55
165	13.65±3.49	12.35±0.48	59.48±17.65	65.06±12.15
180	14.20±3.68	12.75±0.65	67.83±18.49	70.33±12.60
210	20.25±4.34	17.32±2.43	76.08±19.02	78.33±11.42
240	20.69±4.80	18.24±2.01	83.77±20.67	95.22±8.60
300	25.97±6.99	23.10±3.69	100.00	100.00
360	33.68±6.59	27.90±5.19		
420	40.94±7.36	32.75±5.2		
480	51.95±9.23	41.62±6.27		

Table G-3 Percentages of paracetamol release from sealed bags formed by 0.5 M calcium crosslinked films in simulated gastrointestinal fluid at 37 °C.

Time (min)	Percentages of paracetamol release			
	HC75SA25-Ca0.5	HC50SA50-Ca0.5	HC25SA75-Ca0.5	SA-Ca0.5
0	0	0	0	0
15	0.73±0.76	0	0.57±0.09	0.19±0.03
30	1.39±1.34	0	0.57±0.10	0.19±0.02
45	0.95±0.83	0.11±0.01	1.36±0.51	2.82±0.31
60	0.84±0.77	0.55±0.09	3.62±1.24	3.80±0.44
90	1.64±0.87	0.88±0.11	10.34±3.03	8.10±1.04
120	4.35±1.22	1.21±0.12	17.23±4.38	9.01±1.26
135	5.93±2.56	1.21±0.12	20.47±6.89	9.78±2.15
150	7.22±4.02	1.66±0.10	22.13±7.46	10.40±2.61
165	8.76±3.35	1.99±0.09	24.44±6.88	12.16±3.53
180	10.21±3.51	1.99±0.12	25.38±7.66	15.71±7.61
210	13.49±5.96	1.99±0.22	29.19±7.96	34.99±19.90
240	18.36±7.35	2.54±0.35	32.17±10.76	51.75±21.8
300	26.96±8.97	3.64±0.44	40.04±9.48	91.66±19.10
360	34.28±7.33	5.19±0.29	50.94±7.17	97.78±11.63
420	43.60±8.37	6.87±0.95	60.44±7.05	100.00
480	53.85±10.59	19.53±1.26	72.73±5.34	

Table G-4 Percentages of paracetamol release from sealed bags formed by 0.5 M zinc or 0.5 M copper crosslinked films in simulated gastrointestinal fluid at 37 °C.

Time (min)	Percentages of paracetamol release	
	HC50SA50-Zn0.5	HC50SA50-Cu0.5
0	0	0
15	0.33±0.03	1.32±0.14
30	0.31±0.08	1.10±0.95
45	0.66±0.12	1.11±0.23
60	0.98±0.11	1.12±0.96
90	2.14±0.49	2.85±0.49
120	2.80±0.47	5.04±0.47
135	4.12±0.88	8.11±2.88
150	5.76±0.15	9.53±1.15
165	6.10±00.54	10.63±3.54
180	6.76±0.36	10.74±3.36
210	10.40±2.15	15.13±5.15
240	12.05±5.13	16.67±.13
300	17.98±6.99	18.42±6.99
360	20.64±5.92	21.94±5.92
420	25.58±6.42	24.79±6.42
480	33.53±7.24	30.50±7.24

Table G-5 Percentages of paracetamol release from capsules in simulated gastrointestinal fluid at 37 °C.

Time (min)	Percentages of paracetamol release		
	Gelatin	H50SA50Ca	SACa
0	0	0.00	0.00
15	100.00	4.39±0.41	0.00
30		6.81±1.03	0.88±0.01
45		11.20±2.93	4.62±1.31
60		16.02±1.59	10.12±2.01
90		25.69±3.82	17.38±4.23
120		36.02±7.22	22.89±4.04
135		42.38±7.61	23.55±4.97
150		44.80±7.99	25.72±4.62
165		47.43±8.47	65.58±17.33
180		52.92±8.77	92.87±2.13
210		56.87±8.79	100.00
240		60.38±9.54	
300		77.92±5.68	
360		95.58±4.58	
420		100.00	

Author Biography

Name	Miss Pitchaya Treenate
Date of Birth	10 March 1987
Address	411/24 Jaransanitwong Road, Bangkunsri, Bangkoknoi, Bangkok 10700, Thailand
E-mail	ptreenate@hotmail.com

Education

2005 - 2009	King Mongkut's Institute of Technology Ladkrabang, Thailand B.Sc. in Industrial Chemistry, Faculty of Science, GPA: 3.50 Special Project Topic: Modification of high strength polyethylene fiber surface with calcium silicate for medical application
2009 - 2017	King Mongkut's Institute of Technology Ladkrabang, Thailand Ph.D. in Applied Chemistry, Faculty of Science, GPA: 4.00 Thesis Topic: Novel pH-sensitive hydrogels from hydroxyethylacryl chitosan/sodium alginate for site-specific drug delivery

Scholarships

2009 - 2017	Scholarship from the Royal Golden Jubilee Ph.D Program, Thailand research fund

Publications

[1] P. Treenate, P. Monvisade and M. Yamaguchi. 2014. "Development of hydroxyethylacryl chitosan/alginate hydrogel films for biomedical application." *Journal of Polymer Research*. 21: 1-12.

[2] P. Treenate, P. Monvisade and M. Yamaguchi. 2015. "The effect of glycerol/water and sorbitol/water on the plasticization of hydroxyethylacryl chitosan/sodium alginate films." *MATEC Web of Conferences*. 30: 1-4.

[3] P. Treenate and P. Monvisade. 2017. "*In vitro* drug release profiles of pH-sensitive hydroxyethylacryl chitosan/sodium alginate hydrogels using paracetamol as a soluble model drug." *International Journal of Biological Macromolecules*. 99: 71-18.

[4] P. Treenate and P. Monvisade. 2017. "Crosslinker effects on properties of hydroxyethylacryl chitosan/sodium alginate hydrogel films." *Macromolecular Symposia*. 372: 147-153.

Conferences

[1] P. Treenate, P. Monvisade and M. Yamaguchi. 2013. "Characterization and swelling behavior of WCS/SA hydrogel film using $CaCl_2$ as a crosslinker." in **14th RGJ-Ph.D. Congress**. Pattaya: Thailand.

[2] P. Treenate, P. Monvisade and M. Yamaguchi. 2013. "Characterization and swelling behavior of water-soluble chitosan/sodium alginate hydrogel film as a potential wound dressing." in **3rd International Symposium on Technology for Sustainability**. Hong Kong: China.

[3] P. Treenate and P. Monvisade. 2015. "Controlled release of paracetamol from pH-sensitive hydroxyethylacryl chitosan/sodium alginate films for oral drug delivery." in **Burapha University International Conference 2015**. Chonburi: Thailand.

[4] P. Treenate, P. Monvisade and M. Yamaguchi. 2015. "The effect of glycerol/water and sorbitol/water on the plasticization of hydroxyethylacryl chitosan/sodium alginate films." in **2015 4th International Conference on Material Science and Engineering Technology**. Singapore.

[5] P. Treenate and P. Monvisade. 2016. "Crosslinker effects on properties of hydroxyethylacryl chitosan/sodium alginate hydrogel films." in **Polymer Networks Group meeting 2016**. Stockholm: Sweden.

[6] P. Monvisade and P. Treenate. 2016. "Biological properties of calcium-silver crosslinked hydroxyethylacryl chitosan/sodium alginate film as a potential wound dressing." in **The 14th International Symposium on Biocontrol and Biotechnology**. Saint-Petersburg: Russian Federation.

Experience

Apr 2008 - May 2008	Trainee at Toyota Motor Thailand Co., Ltd.
Sep 2012 - Dec 2012	Research abroad at School of Materials Science, Japan Advanced Institute of Science and Technology
Feb 2014 - Aug 2014	Research abroad at School of Materials Science, Japan Advanced Institute of Science and Technology
Dec 2015 - Jun 2016	Research assistant for the development project of Plastics Institute of Thailand